UNIVERSITY OF CALIFORNIA

Santa Barbara

# Socioeconomic challenges and opportunities in the low-carbon transition of the energy system

A dissertation submitted in partial satisfaction of the

requirements for the degree Doctor of Philosophy

in Environmental Science and Management

by

Haozhe Yang

Committee in charge:

Professor Ranjit Deshmukh, Chair

Professor Gang He

Professor Kyle C. Meng

Professor Eric Masnet

June 2024

The dissertation of Haozhe Yang is approved.

_____

Gang He

_____

Kyle C. Meng

_____

Eric Masanet

_____

Ranjit Deshmukh, Committee Chair

June 2024

Socioeconomic challenges and opportunities in the low-carbon transition of the energy system



by

Haozhe Yang

ACKNOWLEDGEMENTS

It is still hard to accept the fact that my journey in Santa Barbara is ending. I want to acknowledge lots of people, but the space for writing is limited. I will try my best to express my feelings with a few words, and may the force be with me.

The first names that appear in my mind are my advisors, Ranjit Deshmukh and Sangwon Suh. I always felt I made more trouble for my advisors than the papers I wrote with them. They must be very lenient to keep working with a troublemaker like me for five years.

Ranjit, I will never forget how you grilled me in every detail of our papers, and how many extra cases I ran to test the robustness of our results. I sometimes feel I am the least lucky person in Bren for having an advisor with the highest standard. However, at the end of my PhD life, when looking at our accomplishments, I believe I am the luckiest person for having the most helpful advisor. Thank you for accompanying me during the hardest time of my PhD career. I hope our CETLAB can grow to a “too-big-to-fall” lab, and make more appearances at conferences.

Sangwon, I am always grateful to you for bringing me here from China. I still remember your ambitious statement in our first phone call: “Let’s work on some big ideas together”. You tortured me in every graph, every sentence, and every word of my paper. However, you allowed me to drink half a bottle of wine and a quarter of your precious liquor “Wuliang Ye”, in our first lab gathering party. In the end, thank you for shepherding me to what I am. I am also grateful to my PhD committee members, Kyle Meng, Gang He, and

Eric Masanet. My first two chapters received great help from Kyle, and my last two chapters cannot be made without the advice from Gang and Eric.

I must thank the two big sisters, to whom I always resort to when the reckless me makes trouble. Jing Meng is the person who has been facilitating my academic career since 2015. I always called her when I was frustrated or puzzled, and she always gave me the most professional advice. Jiajia Zheng is always the most reliable big sister in our lab, who has a warm heart disguised by her cold face. She is the first person I thought of when I crashed a car in North Carolina, or had a dead battery in Goleta. Her husband, John, offered much help with all the drama I met, and more importantly, he taught me how to be a grill master.

I am indebted to my friends in Santa Barbara here. I would like to thank my labmates, my co-commentator of Korean and Taiwan TV shows, and my companion in drinking wine, tea, and coffee, Wen-tien Wang. You saved my PhD life from a daily routine in home-office-gym-home. I want to thank Yang Qiu and Qian Gao. You are my labmates, but also my friends. I am grateful to my cohort Flavio Malagutti, who helped during the darkest time of my PhD career. Thank you for teaching me how to be a collaborator with professors, and the importance of watering flowers. I appreciated Liliana Sierra Castillo, who hosted the coffee hour with me, which is the most challenging task in Bren. She also gave me the nickname “Bearpaw”. I am thankful to my roommates, Huiyu Jiang and Hanmo Li: one teaches me how to cook, while the other teaches me how to drive. Together, they taught me how to live a decent life in the US. I want to thank the little brother in my house, Jiayi Mei. He joined us in the last year, but brought us lots of joy. More importantly, he revived our memory of being a naive kid.

I appreciate my friends in Bren. My PhD cohorts, Kaili Brande, Annette Hilton, Brian Lee, Cori Lopazanski, Liviu Iancu, Sandy Sum, Flavio Malagutti, Liliana Sierra Castillo and Linus Blomqvist. I appreciate the Aoyun Xue and Enze Jin. I often chat with them every Friday. Weiwei Li, thank you for sharing so much information with me. Thank for you ending the Peking-Tsinghua rivalry, and developing a new area for collaboration. I also want to thank my other friends in Bren: Seonghoon Kim, Mauricio Collado, Nakoa Farrant, Trace Martin, Bonnie Basnett, Tina Fang and Flora He. The staff in Bren are always helpful. I want to thank Satie Airame, Sage Davis, Kristine Duarte, Kimberly Yom, the compute team, the financial team, and all the other Bren staff who helped me.

The last two paragraphs must belong to my partner and parents.

I don't know how to use words to express the support from my partner Xiaodong Zhang. You gave up a comfortable life in China, and came to the U.S. with me. I will never forget the moment when you got on the plane to the U.S. with her Rowlet. I cannot forget how many times we flew between Santa Barbara and Durham. Thank you for your care and tolerance, while I only care about working with my papers. Thank you for being a patient listener, as I cannot stop talking with you. This whole dissertation is for you.

Lastly, I want to give the greatest acknowledgment to my parents. They don't have the opportunity to go to universities, and thus put all their fantasies about university life on me. My mom (胡锐) supported me all the way from elementary school to Ph.D. I don't know how I can pay her back. My dad (杨春林) is a quiet person, and he is not good at expressing his feelings. However, I do know he cares about me in his way. They cannot attend my ceremony here, so I must express my deepest feelings here.

VITA OF Haozhe Yang
June 2024

## EDUCATION

Bachelor of Science, Environmental Science, Peking University, June 2016
Bachelor of Science, Economy, Peking University, June 2016
Master of Science, Environmental Science, Peking University, June 2019
Doctor of Philosophy, Environmental Science, University of California, Santa Barbara, June 2024 (expected)

## PROFESSIONAL EMPLOYMENT

2021-2024: Teaching Assistant, Bren School of Environmental Science and Management, University of California, Santa Barbara

## PUBLICATIONS

(23) **Yang, H**., Luo, Q., He, G., Lin, J., Johnson, J.X., Garcia-Menendez, F., Deschenes, O., Mileva, A. and Deshmukh, R., 2024. Regional disparities in health and employment outcomes of China's transition to a low-carbon electricity system. **Environmental Research: Energy**, 1(2), 025001.
(22) **Yang, H.**, Deshmukh, R., Suh, S., 2023, Global transcontinental power pools for low-carbon electricity, **Nature Communications**, 14(1), 8350
(21) Wu, H., **Yang, H.**, Hu, X., Zheng, L., Li, J., Li, Y., Wang, X., Ge, W., Zhou, Y., Liu, Y. and Liu, J., 2024. Complementing carbon tax with renewable energy investment to decarbonize the energy system in China. **Renewable and Sustainable Energy Reviews**, 189, p.113997.
(20) **Yang, H.**, Meng, K.C. and Suh, S., 2023. Spatial distributions of stranded fossil asset costs and benefits from climate change mitigation. **Environmental Research Communications**, 5(6), p.061001.
(19) Luo, Q., Garcia-Menendez, F., **Yang, H.**, Deshmukh, R., He, G., Lin, J. and Johnson, J.X., 2023. The health and climate benefits of economic dispatch in China's power system. **Environmental science & technology**, 57(7), pp.2898-2906.
(18) Wang, Y., Liu, J., Guan, D., Meng, J., Liu, Z., Xiang, S., **Yang, H.**, Fu, X., Hu, X., Yang, Q. and Yi, K., 2022. The volume of trade-induced cross-border freight transportation has doubled and led to 1.14 gigatons CO2 emissions in 2015. **One Earth**, 5(10), pp.1165-1177.
(17) Liu, H., Liu, J., Liu, Y., Yi, K., **Yang, H.**, Xiang, S., Ma, J. and Tao, S., 2021. Spatiotemporal variability and driving factors of ground-level summertime ozone pollution over eastern China. **Atmospheric Environment**, 265, p.118686.
(16) **Yang, H.** and Suh, S., 2021. Economic disparity among generations under the Paris Agreement. **Nature Communications**, 12(1), 5663
(15) Zhang, Y., Liu, J., Tao, W., Xiang, S., Liu, H., Yi, K., **Yang, H.**, Xu, J., Wang, Y., Ma, J. and Wang, X., 2021. Impacts of chlorine emissions on secondary pollutants in China. **Atmospheric Environment**, 246, p.118177.

(14) Hu, X., Liu, J., **Yang, H.**, Meng, J., Wang, X., Ma, J. and Tao, S., 2020. Impacts of potential China's environmental protection tax reforms on provincial air pollution emissions and economy. **Earth's Future**, 8(4), p.e2019EF001467.
(13) Xiang, S., Liu, J., Tao, W., Yi, K., Xu, J., Hu, X., Liu, H., Wang, Y., Zhang, Y., **Yang, H.** and Hu, J., 2020. Control of both PM2. 5 and O3 in Beijing-Tianjin-Hebei and the surrounding areas. **Atmospheric Environment**, 224, p.117259.
(12) Wang, Y.‖, **Yang, H.**‖, Liu, J., Xu, Y., Wang, X., Ma, J., Xu, J., Yi, K. and Tao, S., 2020. Analysis of multiple drivers of air pollution emissions in China via interregional trade. **Journal of Cleaner Production**, 244, p.118507 (‖ equal contribution).
(11) **Yang, H.**, Tao, W., Wang, Y., Liu, Y., Liu, J., Zhang, Y. and Tao, S., 2019. Air quality and health impacts from the updated industrial emission standards in China. **Environmental Research Letters**, 14(12), p.124058.
(10) Meng, J., **Yang, H.**, Yi, K., Liu, J., Guan, D., Liu, Z., Mi, Z., Coffman, D.M., Wang, X., Zhong, Q. and Huang, T., 2019. The slowdown in global air-pollutant emission growth and driving factors. **One Earth**, 1(1), pp.138-148.
(9) Yi, K., Meng, J., **Yang, H.**, He, C., Henze, D.K., Liu, J., Guan, D., Liu, Z., Zhang, L., Zhu, X. and Cheng, Y., 2019. The cascade of global trade to large climate forcing over the Tibetan Plateau glaciers. **Nature Communications**, 10(1), pp.1-9.
(8) **Yang, H.**, Liu, Y., Liu, J., Meng, J., Hu, X. and Tao, S., 2019. Improving the imbalanced global supply Chain of phosphorus fertilizers. **Earth's Future**, 7(6), pp.638-651.
(7) Hu, X., Sun, Y., Liu, J., Meng, J., Wang, X., **Yang, H.**, Xu, J., Yi, K., Xiang, S., Li, Y. and Yun, X., 2019. The impact of environmental protection tax on sectoral and spatial distribution of air pollution emissions in China. **Environmental Research Letters**, 14(5), p.054013.
(6) Yi, K., Liu, J., Wang, X., Ma, J., Hu, J., Wan, Y., Xu J., **Yang H.**, Liu H., Xiang, S., Tao, S., 2018. A combined Arctic-tropical climate pattern controlling the inter-annual climate variability of wintertime PM2.5 over the North China Plain. **Environmental Pollution**, 245, 607-615.
(5) **Yang, H.**, Tao, W., Liu, Y., Qiu, M., Liu, J., Jiang, Ke., Yi, K., Xiao, Y., Tao, S., 2019. The contribution of the Beijing, Tianjin and Hebei region's iron and steel industry to local air pollution in winter. **Environmental Pollution**, 245, 1095-1106.
(4) **Yang, H.**, Liu, Y., Liu, J., Wang, Y., & Tao, S., 2018. The roles of the metallurgy, nonmetal products and chemical industry sectors in air pollutant emissions in China. **Environmental Research Letters**, 13(8), 084013.
(3) **Yang, H.**, Liu, J., Jiang, K., Meng, J., Guan, D., Xu, Y., & Tao, S., 2018. Multi-objective analysis of the co-mitigation of CO2 and PM2.5 pollution by China's iron and steel industry. **Journal of Cleaner Production**, 185, 331-341.
(2) Meng, J., Liu, J., Yi, K., **Yang, H.**, Guan, D., Liu, Z., Zhang, J., Ou, J., Dorling, S., Mi, Z., 2018. Origin and radiative forcing of black carbon aerosol: production and consumption perspectives. **Environmental Science & Technology** 52(11).
(1) Meng, J., Mi, Z., **Yang, H.**, Shan, Y., Guan, D., & Liu, J., 2017. The consumption-based black carbon emissions of China's megacities. **Journal of Cleaner Production**, 161, 1275-1282.

## CONFERENCES

2023
Institute for Operations Research and the Management Sciences Annual Meeting, Phoenix (oral)
41st International Energy Workshop, Golden (oral)
14th Annual Interdisciplinary Ph.D. Workshop in Sustainable Development, Columbia University (oral)
2022
America Geophysical Union Fall Meeting, Chicago (poster)
INFORMS Annual Meeting, Indianapolis (oral)
Industrial Ecology, Gorden Research Conference, Newry (poster)

## AWARDS

Chancellor Fellowship, University of California, Santa Barbara, 2019
National Scholarship, Ministry of Education in China, 2018
Merit Student, Peking University, 2018

## FIELDS OF STUDY

Power system modeling with Professor Ranjit Deshmukh
Climate change mitigation with Professor Sangwon Suh

ABSTRACT

Socioeconomic challenges and opportunities in the low-carbon transition of the energy system

by

Haozhe Yang

The actions to mitigate climate change lag behind the ambitions to limit the increase of the global average temperature by 2ºC. Socioeconomic challenges play an important role in slowing the progress of the low-carbon transition. However, while socioeconomic factors are pivotal in the low-carbon transition of the energy system, it is unclear how these factors quantitatively change the benefits and costs at national, organizational and individual levels. Here, I quantify the distribution of costs and benefits across time and space, and explore how the allocation of costs and benefits shape different stances toward the low-carbon transition. To address the socioeconomic challenges, I further examine how innovations in policy and technology enable politically and economically feasible pathways towards a low-carbon energy system. In the first chapter, I quantify the spatial distribution of stranded asset costs together with that of the GDP benefits stemming from climate change mitigation. To limit the average global temperature increase within 2°C, 95% of the global net benefits are shouldered by low and lower-middle income countries, while 90% of the stranded assets costs are borne by higher income countries. In the second chapter, I analyze the lifetime

costs and benefits of climate change mitigation by age cohorts across countries under the Paris Agreement. My results show that the age cohorts born prior to 1960 generally experience a net reduction in lifetime net benefits. Age cohorts born after 1990 will gain net benefits from climate change mitigation in most lower income countries, while no age cohorts enjoy net benefits regardless of the birth year in many higher income countries. In the third chapter, I examine whether global transcontinental power pools address the unequal distribution of benefits and costs caused by heterogeneous resource endowments of renewable energy across countries. Employing an electricity planning model with hourly supply-demand projections and high-resolution renewable resource maps, I assess whether transcontinental power pools reliably meet the growing global demand for renewable electricity and concurrently reduce system costs. I find that transcontinental power pools enable renewables to meet 100% of future electricity demand, while also reducing costs by up to 23% across power pools. Transitioning to the next two chapters, I dissect socioeconomic barriers at the regional level, focusing on China. The fourth chapter quantifies the spatial distribution of health and employment outcomes of low-carbon electricity pathways in China. I integrate an electricity system planning model (GridPath), a health impact model (InMAP), and a multiregional input-output model to quantify China's provincial-level impacts of electricity system decarbonization on costs, health outcomes, employment, and labor compensation. I find that disparities in health impacts across provinces narrow as fossil fuels are phased out, whereas disparities in labor compensation widen. Wealthier East Coast provinces reap the greatest benefits in labor compensation because of materials and equipment manufacturing, and offshore wind deployment. In the last chapter, I investigate whether the innovation of the hydrogen technology enables an

economically feasible pathway in the low-carbon transition. I leverage an electricity planning model, GridPath, to quantify the cost implications of hydrogen penetrations, and further demonstrate how hydrogen interplay with other zero-carbon technologies and hard-to-abate sectors. I find that hydrogen reduces the cost of a zero-carbon electricity system by 16%, compared with a scenario without hydrogen. Apart from the role of long-term storage, hydrogen from the zero-carbon electricity system can be used to meet hydrogen demand in hard-to-abate sectors, while incurring a marginal decrease in the unit cost of energy demand. My dissertation reveals the socioeconomic barriers inherent in the low-carbon transition of the energy system, and calls for more actions to address the socioeconomic issues towards a sustainable energy system.

To my beloved mother Rui Hu and father Chunlin Yang

献给我的母亲胡锐和父亲杨春林！

TABLE OF CONTENTS

## I. Introduction

Climate change caused by greenhouse gas emissions is threatening the future of human beings[1]. To avoid the substantial damage from climate change, by the end of the 21st century, the average of global temperature increase relative to the pre-industry should be limited by well below 2ºC, and even further to 1.5ºC [2]. Carbon dioxide ($CO_2$) emissions from the energy system account for over 70% of annual greenhouse gas emissions[3]. The $CO_2$ emissions from the energy system are required to reach net zero by 2070 to achieve the 2ºC target, and by 2050 to achieve the 1.5ºC target[4,5].

The economic costs to achieve a net-zero energy system are high[6]. Global GDP in 2050 is estimated to decline by 1.3-2.7% to limit global temperature rise to 2ºC with a 67% probability, and by 1.6-2.8% to the 1.5ºC target with a 50% probability[5]. However, when monetizing the economic value of averting climate damage, the benefits of transitioning to a low-carbon energy system far outweigh the costs[7–9].

Despite the economic benefits of the low-carbon transition, the window to limit the temperature increase is rapidly narrowing[10,11]. Current climate actions lag behind the ambition to limit the temperature increase by 2ºC[12]. The United Nation's Emission Gap Report finds that global warming will be limited to 2.9°C above pre-industrial levels by 2100 if countries fully implement the unconditional National Determined Contributions (NDC) committed in the Paris Agreement[13].

The lukewarm response to climate ambitions despite the substantial economic benefits begs the question: what are the underlying factors that are hindering the transition to a low-carbon energy system?

Social factors, which are rarely represented in quantitative analysis of the low-carbon transition of the energy system, are playing increasingly important roles[14]. By integrating the social and economic considerations, I aim to explain the lukewarm response of the low-carbon transition. I analyze how the spatiotemporal distribution of benefits and costs shapes disparate stances among countries, organizations, and individuals toward the low-carbon transition[15,16]. This entails examining factors such as stranded assets, employment, health, and GDP, which contribute to both economic and social dimensions of the transition.

While socioeconomic factors often act as barriers in the low-carbon transition, a carefully-crafted climate policy also advances climate solutions by mitigating these socioeconomic obstacles.[17] Benefiting every single stakeholder of the low-carbon transition is crucial to encouraging collaboration among countries. For example, while abundant land is available to achieve a net-zero emission energy system, socioeconomic factors, including the constraints in biodiversity conservation, financial, and engineering, limit the use for renewable energy[18,19]. To tackle the land availability issue, building a global or regional power pool enables countries to optimize land use by tapping into the most cost-effective renewable resources[20,21].

Technology innovations also play an important role in addressing the socioeconomic concerns towards a net-zero energy system. Hydrogen, when produced by renewable electricity, is a zero-carbon fuel with the capacity to replace fossil fuels in hard-to-abate sectors[22]. Currently, fossil fuel reserves are distributed in a few countries, thereby incurring energy security problems in many countries with scarce fossil fuel resources[23]. The emergence of hydrogen allows countries with scarce fossil fuel reserves to enhance energy security while promoting the expansion of renewable energy[24]. In Europe and the United

States, governments are subsidizing hydrogen to accelerate the low-carbon transition, with energy security serving as a major motivator[25,26].

In our research, we delve into the socioeconomic challenges and opportunities in five chapters. The first chapter explains the lack of ambition in climate policy by quantifying the spatiotemporal distribution of costs and benefits for climate change mitigation. In the second chapter, I elucidate the challenges of climate change mitigation by exposing the economic disparity among generations. In the third chapter, I explore how a global transcontinental power pool facilitates an electricity system with 100% renewable energy. In the fourth chapter, taking China as an example, I reveal the unequal distribution of employment and health outcomes across regions in the low-carbon transformation of the electricity system. In the fifth chapter, I highlight the role of hydrogen in a zero-carbon electricity system.

## II. Spatial distributions of stranded fossil asset costs and benefits from climate change mitigation

Material from: Yang, H., Meng, K. C. & Suh, S. Spatial distributions of stranded fossil asset costs and benefits from climate change mitigation. Environ. Res. Commun. 5, 061001 (2023). https://doi.org/10.1088/2515-7620/acd514

**Abstract**

A global 2°C climate target is projected to generate significant economic benefits. However, the presence of fossil fuel assets that are stranded as a consequence of climate change mitigation could complicate cost-benefit considerations at the country level. Here, we quantify the spatial distribution of stranded asset costs (SAC) together with that of the GDP benefits of climate mitigation (BCM). Under a 2°C scenario, global total SAC is $19 trillion while global BCM is $63 trillion by 2050. At the country level, the sign of a country's net benefit, the difference between BCM and SAC, is largely determined by the sign of its BCM. Net benefits are broadly positive across subtropical and tropical countries where high baseline temperatures imply GDP damage from climate change and negative across temperate countries where low baseline temperatures imply GDP gains. Notably, even major fossil fuel producers such as India, China, USA, and Saudi Arabia are projected to receive positive net benefits from a 2°C scenario by 2050. Overall, 95% of global net benefit will be borne by low and lower-middle income countries. These results could inform the geopolitics of global climate change cooperation in the decades to come.

### *A. Introduction*

Climate change mitigation will yield substantial global benefits. Avoided losses in global gross domestic product (GDP), a component of total potential benefits, is estimated to range from $100 to $400 trillion by 2100 under the 2°C global climate target compared to a business-as-usual scenario before the Paris Agreement[27,28]. At the same time, the dramatic decarbonization required to achieve such a target will incur a variety of costs[29], prompting trade-offs across other economic and social priorities. One class of cost for many countries is the lost value of their fossil fuel assets[30,31], estimated to be $4 trillion between 2016-2035[32] and $12 trillion between 2011-2100[33]. These "stranded asset" costs (SAC) have received increasing attention, as exemplified in the political opposition against language to "phase down" fossil fuels during the Glasgow meetings under the United Nations Framework Convention on Climate Change [34,35].

SACs are unevenly distributed across countries, and depend on a country's endowment of fossil fuel reserves and extraction costs[36–38.] The GDP benefits of climate mitigation (BCM) may also be highly heterogeneous in part because the nonlinear GDP-temperature relationship implies economic losses in hotter locations while colder locations experience economic gains[39,40]. This prompts a series of questions. Are the same countries with high SAC also those with high BCM? For which countries do BCM exceed SAC? How do these spatial patterns change over time horizons as country-level SAC and BCM evolve dynamically? Such dynamics are of interest as fossil fuel reserves deplete over time and marginal GDP losses grow for hotter locations as temperatures increase. We address these questions by conducting a joint analysis of country-level SAC and BCM. While SAC and BCM are incomplete measures of total climate policy costs and benefits, which itself may not fully explain climate

policy adoption, our analysis may nonetheless shed light on existing barriers to international climate policy cooperation and how they could evolve in the decades to come.

This study quantifies SACs associated with the value of fossil fuels that a country forgoes from reduced fossil fuel production under a global 2°C target[41]. Following van der Ploeg et al[42], we define SAC as the foregone discounted net present profits from fossil fuel production for a country under a 2°C target relative to a pre-Paris Agreement business-as-usual (BAU) scenario between 2020-2050. Country-level BCM is the country-level avoided GDP loss of a 2°C global target, based on an econometrically estimated GDP-temperature damage function[43]. We combine these two measures, showing how the net benefit from these two measures are distributed across countries and according to countries' income groups. To examine how net benefits evolve over time, we present net present values for both 2020-2030 and 2020-2050 time horizons as well as show payback periods.

### *B. Methods and Materials*

Temperature projections follow Representative Concentration Pathways (RCPs), and GDP and population trajectories come from the Shared Socioeconomic pathways (SSPs)[44]. RCP6.0 is used as our "business-as-usual" or pre-Paris Agreement scenario (i.e., BAU scenario)[45,46], while RCP 2.6 is used as the scenario (i.e., 2°C scenario) whereby global mean temperature increase is capped below 2°C (Table S1). Socioeconomic assumptions follow SSP2.

The total cost of climate change mitigation is composed of (a) the change in profits for producers and (b) the change in welfare for consumers due to climate policy. Producers

include both firms in sectors that use fossil fuels and those in sectors that use non-fossil (e.g., renewable) fuels. In this paper, we focus on the forgone profits of fossil fuel producers, calculated as the forgone net present profits from fossil fuel production under a global 2°C relative to business-as-usual. As such, we consider an incomplete measure of the total cost of climate policy while omitting profit changes to non-fossil fuel production and welfare changes in consumers, both of which may play a role in determining support for climate policy. As is standard in non-renewable resource settings, a country's stranded asset profit is the sum of resource rents across its fossil fuel deposits. A deposit's resource rents, in turn, are determined by its resource grade and scarcity[47,48]. The stranded asset costs are only those associated with forgone profits for fossil fuel extraction and not any resulting local environmental changes due to lowered fossil fuel extraction.

Our analysis of fossil fuel profits is at the country-level. This implicitly assumes countries own property rights to their fossil fuel resources, which indeed is the case for 90% of global fossil fuel reserves[49]. Furthermore, we assume either (a) countries are also fossil fuel extractors or (b) the global market to extract fossil fuel resources is perfectly competitive, as a country receives all profits in either case. In particular, under perfect competition, profits are zero for the fossil fuel extractor, such that revenue less extraction cost for an extracting firm equals the royalty lease paid to the country. Failure of either assumptions would not affect our estimate of forgone profits but rather how that profit is split between countries that own the fossil fuel reserve and the fossil fuel extractor. In that case, one could view our forgone profit estimate as that associated with fossil fuel reserves owned by a particular country rather than that actually received by the country.

Forgone profits are calculated using projected fossil fuel prices and production generated by Integrated Assessment Models (IAMs) in the ADVANCE database under SSP2[50,51]. We obtain projected country-level fossil fuel price and production for each scenario and IAM (i.e., AIM/CGE, IMAGE, POLES, WITCH) from the IPCC AR6 library[52] in the ADVANCE database (Table S2). We use ADVANCE's 'Reference' and '2020 WB2C' scenarios as our BAU and 2°C scenarios, respectively. All projected price and production data are normalized to observed 2018 values from the World Bank[53] and the U.S. Energy Information Agency[54], respectively, to ensure continuous time series trajectories. Data on fossil fuel reserves come from the Federal Institute for Geosciences and Natural Resources (BGR)[55]. Data on reserve-level extraction cost for oil and natural gas come from the Rystad database[56,57], and for coal from Welsby et al.[37]. We perform analyses for the following 12 countries/regions: Brazil, China, India, Japan, Russia, USA, European Union, Latin America, Middle East and Africa, rest-of-Asia, rest-of-OECD, rest-of-Reforming Economies. For multi-country regions, we assume that countries in that region follow the same fossil fuel price and production path. We classify countries into high, upper-middle, lower-middle and low income groups, following definitions provided by the World Bank[58].

The benefits of climate change mitigation are measured in terms of avoided GDP losses using a historically-estimated econometric relationship between GDP and temperature from Burke et al.[43]. This too is an incomplete measure of climate policy benefits, notably missing non-market benefits such as health impacts. In the main text, we use a 3% discount rate to calculate values, presented in 2018 dollars. Our main focus is the 2020-2050 time horizon, though we also present net present values for the 2020-2030 horizon.

### 1. Calculating SAC

The global carbon budget is estimated to be 980−1420 gigaton (Gt) of CO2 if the global economy is to limit the global mean temperature increase to below 2°C with at a two-thirds probability[59]. By contrast, global total economic reserves of fossil energy resources would emit 2900−3500 Gt of CO2e if combusted[36]. Thus, in the absence of large-scale carbon capture and storage, a substantial share global fossil fuel reserves must remain underground[36,51]. We translate this reduced global demand for fossil fuel onto country-level fossil fuel production using established mitigation scenarios from IAMs. To calculate country-level foregone profit, or SAC, we construct country-level fossil fuel supply curves using deposit-level extraction cost data (Table S5-S7), and determine the change in country-level profits between BAU (or pre-Paris Agreement) and 2°C scenarios due to loss in production from marginal deposits according to extraction cost.

Specifically, for each country/region i, fossil fuel k, year t, and scenario s ∈{BAU, 2C}, each IAM model generates endogenous fossil fuel price, $p^s_{ikt}$, and total production, $q^s_{ikt}$. Each country has deposit d for fossil fuel k with heterogeneous reserves, $r_{ikdt}$, and constant extraction costs, $c_{ikdt}$. Deposits enter production in the order from low to high extraction cost until total production, $q^s_{ikt}$, is met. Denote the set of deposits in production for country i, fuel k, in year t as $D^s_{ikt}$. We define the deposit-weighted country-level extraction cost as

$$c^s{}_{ikt} = \frac{\sum_{d \epsilon D^s{}_{ikt}} c_{ikdt} \times r_{ikdt}}{\sum_{d \epsilon D^s{}_{ikt}} r_{ikdt}}$$

The discounted profit between 2020-2050 from extracting fuel k for country i is

$$A^{s}{}_{ik} = \sum_{t=2020}^{2050} \frac{(p^{s}{}_{ikt} - c^{s}{}_{ikt}) \times q^{s}{}_{ikt}}{(1+\delta)^{t-2020}}$$

where δ=0.03 is the discount rate. Finally, we define SAC for country i as the difference in discounted profit, summed across fuels, between the BAU and 2ºC scenarios

$$SAC_i = \sum_k A^{BAU}{}_{ik} - \sum_k A^{2C}{}_{ik}$$

In a few countries, the domestic fossil fuel production may increase slightly to offset increased global fossil fuel price increases as large fossil fuel producers decrease production. For these countries, the SAC may be negative, which occurs for 3 out of the 169 countries analyzed (Table S8). Our benchmark country-level SAC is the median value across AIM/CGE, IMAGE, POLES, and WITCH IAMs. We also present SAC values for each IAM.

**2. Calculating BCM**

Following Burke et al.[43] the functional relationship between country i's growth rate in Gross Domestic Product (GDP) per capita and its average surface temperature in year t is

$$h(temp^{s}{}_{it}) = \beta_1 temp^{s}{}_{it} + \beta_2 temp^{s}{}_{it}{}^{2}$$

where the parameters $\beta_1$ and $\beta_2$ are econometrically estimated using historical data by Burke et al.[43] and $temp^{s}{}_{it}$ is projected population-weighted country-year temperature under scenario s, also obtained from Burke et al.[27]. Next, define $\Delta_{it}$ as the additional effect of warming on GDP per capita growth in country i and year *t* compared to that country's average historical temperature, $\overline{temp_i}$

$$\Delta^{s}{}_{it} = h(temp^{s}{}_{it}) - h(\overline{temp_i})$$

Let $\eta_{it}$ be the baseline growth rate of GDP per capita and $pop_{it}$ be the population under SSP2, obtained from the International Institute for Applied System Analysis[60]. GDP under climate change is then

$$G^s{}_{it} = G^s{}_{i,t-1}(1 + \eta_{it} + \Delta^s{}_{it})$$

$$GDP^s{}_{it} = G^s{}_{it} \times pop_{it}$$

As with SAC, BCM is defined as the discounted net present GDP between the two scenarios

$$BCM_i = \sum_{t=2020}^{2050} \frac{(GDP^{2C}{}_{it} - GDP^{BAU}{}_{it})}{(1+\delta)^{t-2020}}$$

**3. Robustness**

Our main results are calculated over the 2020-2050 horizon. We also present results for the 2020-2030 horizon to examine how impacts over a longer horizon affects SAC and BCM values. We further conduct several robustness checks. First, calculate SAC by including the value of stranded fossil fuel infrastructure. Second, we replace our baseline 3% discount rate with a 5% discount rate. Third, we present SAC values under separate IAM projections. Fourth, we calculate BCM under alternative SSP scenarios. Fifth, we calculate the net benefits on a per capita basis.

### *C. Results*

For the 2020-2030 time horizon, the median value of total global SAC under a 2°C target across IAMs is $3.8 trillion (in 2018 dollars), with a range of $2.3 trillion (AIM/CGE) to $13 trillion (WITCH) (Fig. 1a). This is on par in magnitude with the global BCM under SSP2 with a value of $4.8 trillion (Fig. 1c). There is little variation in global BCM across SSP scenarios due to the limited temperature variation across the scenarios by 2030 (Fig. 1c).

The difference between global total BCM and SAC becomes more pronounced over the 2020-2050 horizon as marginal GDP damages increase with higher temperatures because of the nonlinear GDP-temperature damage function. Between 2020-2050, the median total SAC across IAMs is $19 trillion (in 2018 dollars), with a range of $13 trillion (AIM/CGE model) to $32 trillion (WITCH model) (Fig. 1b). By contrast, the global BCM under SSP2 is over three times larger at $63 trillion (Fig. 1d). There is now also greater variation in global BCM across SSP scenarios with a range of $52 trillion (SSP3) to $92 trillion (SSP5) (Fig. 1d).

Half of the 2020-2050 median global SAC comes from stranded oil reserves ($9 trillion), followed by stranded coal reserves ($6 trillion) and then stranded natural gas reserves ($4 trillion). When adding the cost of stranded fossil fuel infrastructure, the median 2020-2050 global SAC increase to $22 trillion (Figs. S1-S2). When we replace our benchmark 3% discount rate with a 5% discount rate, the range of global SAC across IAMs is $10-24 trillion (Figs. S3- S4). By comparison, Bauer et al.[23]estimates a global SAC of $12 trillion using the REMIND model and a 5% discount rate.

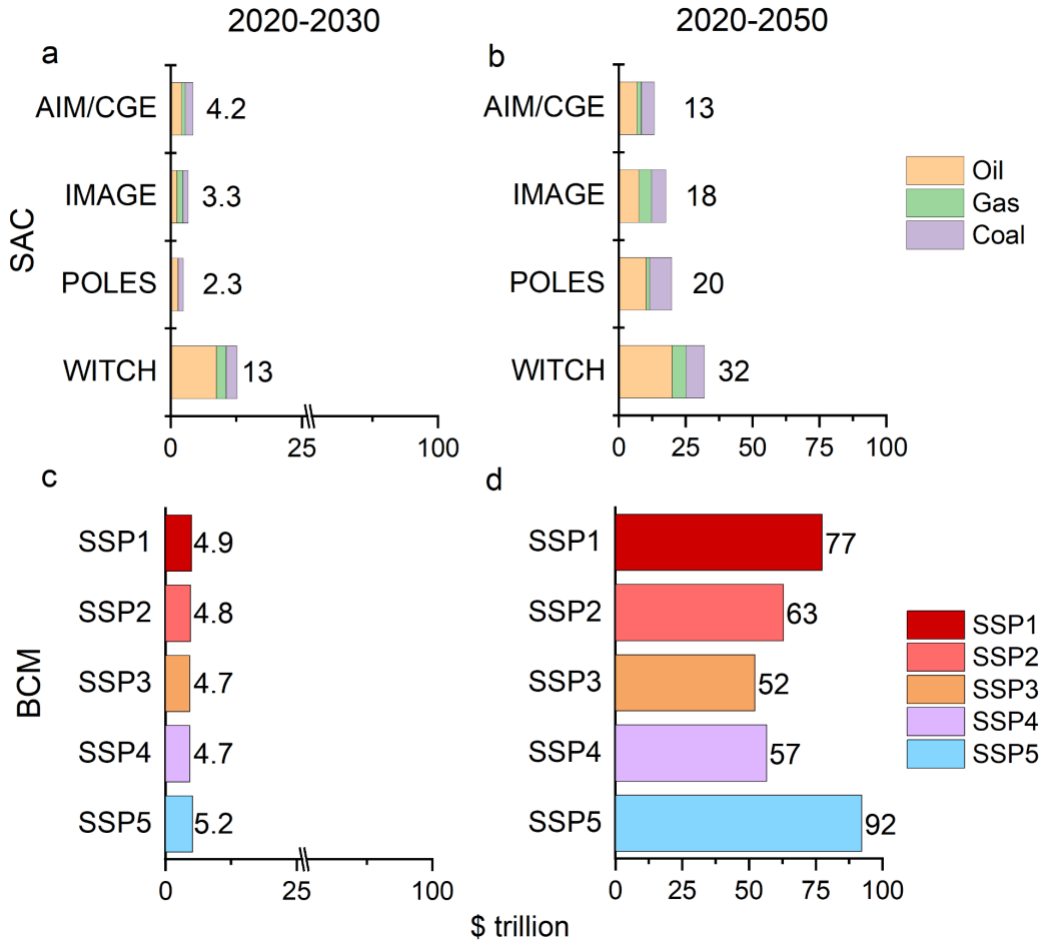


**Figure 1: Global Stranded Asset Costs (SAC) and Benefits from Carbon Mitigation (BCM). (a)** Global SAC across Integrated Assessment Models (IAMs) by fossil fuel for the 2020-2030 horizon. (**b)** Same as (a) for the 2020-2050 horizon. (**c)** Global GDP-based BCM across Shared Socioeconomic Pathways (SSP) for the 2020-2030 horizon. (**d)** Same as (c) for the 2020-2050 horizon.

SACs are highly heterogeneous across countries and regions. Regionally, North America, Asia and Eastern Europe experience the largest SACs, while Western European, Latin American and Sub-Saharan African countries generally incur lower values (Fig. 2a and 2b). At the country level, Russia incurs the largest SAC ($2.6 trillion), closely followed by

China ($2.6 trillion) and Saudi Arabia ($2.4 trillion) over 2020-2050. Iran incurs over $1 trillion in SAC while USA, Iraq, India, Canada, Qatar and Australia will experience over $0.5 trillion of SAC (Table S3) over 2020-2050.

Likewise, there is considerable heterogeneity in BCM across countries and years. Tropical and subtropical countries generally benefit from climate change mitigation. By contrast some temperate countries incur smaller or even negative BCM because the quadratic GDP-temperature damage function exhibits a global optimum with temperate countries located on the cooler side of the optimum. This dispersion widens as the time horizon lengthens from 2020-2030 to 2020-2050 as marginal temperature-induced GDP losses become larger (Fig. 2c and 2d). Between 2020-2050, India is expected to receive the highest BCM at $24 trillion, while Russia incurs the lowest BCM at -$6 trillion (Table S4).

Turning to net benefits, as measured by BCM minus SAC, countries typically fall in three categories, broadly defined by whether BCM or SAC determines the sign of a country's net benefit and why. The first category are countries with large positive BCMs and small SACs and thus positive net benefits. These countries tend to be in subtropical and tropical regions where baseline high temperatures imply large avoided GDP losses from climate policy but have few fossil fuel reserves. Between 2020-2030, net benefits of climate change mitigation are positive in many countries across Latin America, Africa, South Asia and Southeastern Asia (Fig. 2e). Net benefits become positive across almost all countries in these regions by 2050 (Fig. 2f).

The second category are countries with large negative BCMs which reinforces positive SAC values, resulting in negative net benefits. For these countries, primarily consisting of Europe, Canada, and Russia, net benefits are negative across both 2020-2030 and 2020-2050

horizons, largely because higher temperatures can increase economic activity in these colder locations[39,43]. SAC values exacerbate the economic burden of climate change mitigation for these countries. Between 2020-2050, net benefits are -$9 trillion for Russia and -$3 trillion for Canada (Fig. 2f).

The last category consists of countries with large SACs but which an even larger BCM still determines the sign of net benefits. These countries include India, China, USA, and Saudi Arabia, which are projected to experience net benefits of $23, $6, $2, and $0.4 trillion by 2050, respectively. A common feature unifies the countries across these three groups: the sign of their net benefit by 2050 is primarily determined by their BCM, not their SAC. There are three notable exceptions to this: Australia, Iran, and Iraq all experience negative net benefits because sizable fossil reserves imply a higher SAC and BCM.

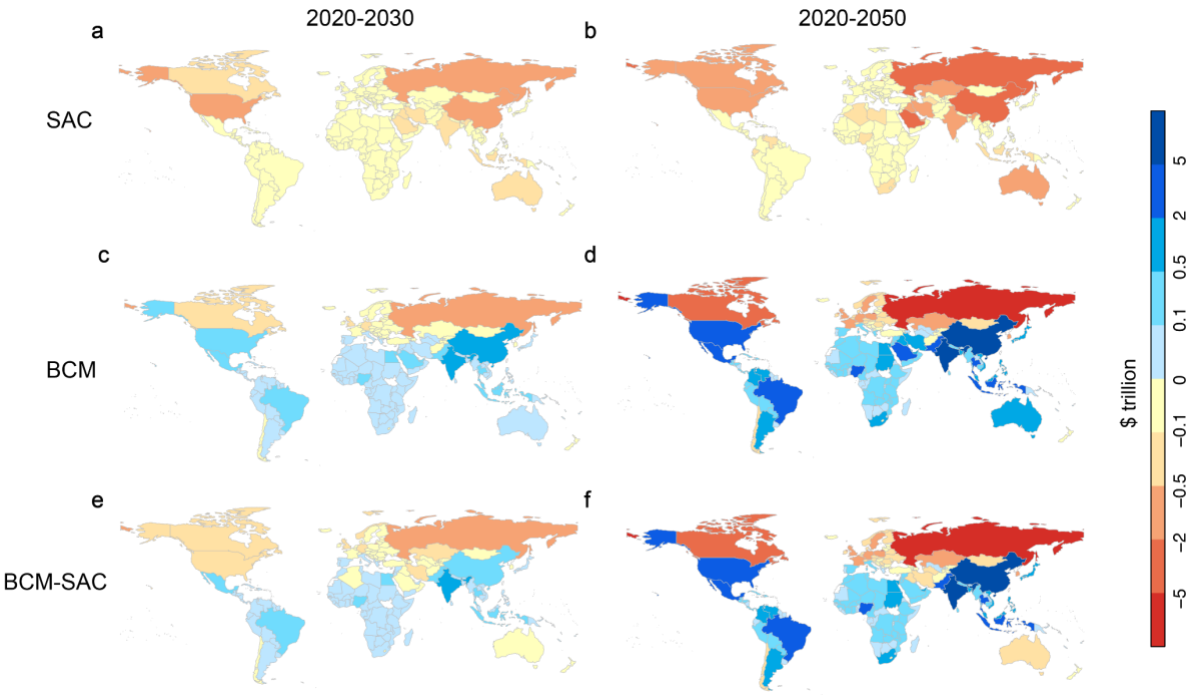


**Figure 2: Distribution of SACs and BCMs across countries.**

**(a)** Country-level median SAC across IAM models for the 2020-2030 horizon. (**c)** Country-level BCM under SSP2 for the 2020-2030 horizon. (**e)** Country-level BCM (b) minus SAC (a) for the 2020-2030 horizon. (**b,d,f).** Same as panels (a,c,e) for the 2020-2050 horizon.

We next consider total SAC, BCM, and BCM minus SAC by income group. In general, higher income countries experience larger SACs while lower income countries experience higher BCMs. Specifically, high and upper-middle income countries are projected to experience 88% and 89% of the global SAC by 2030 and 2050, respectively (Fig. 3a and 3b). It is notable that, except for India ($0.9 trillion), the countries that bear the top ten highest SACs over 2020-2050 are all high- and upper-middle-income countries (Table S3). The total SAC share borne by low income countries is under 1% for both 2030 and 2050 time horizons. By contrast, for BCM, about two-thirds of the global BCM is borne by low and lower-middle income countries by both 2030 and 2050 (Fig. 3c and 3e). Combining SAC and BCM values, by 2050, 95% of global net benefits of a 2ºC global target are projected to be experienced by low and lower-middle income countries, with largest values for lower-middle income countries at $40 trillion. By contrast, total net benefit by 2050 is negative for high-income countries -$5.7 trillion.

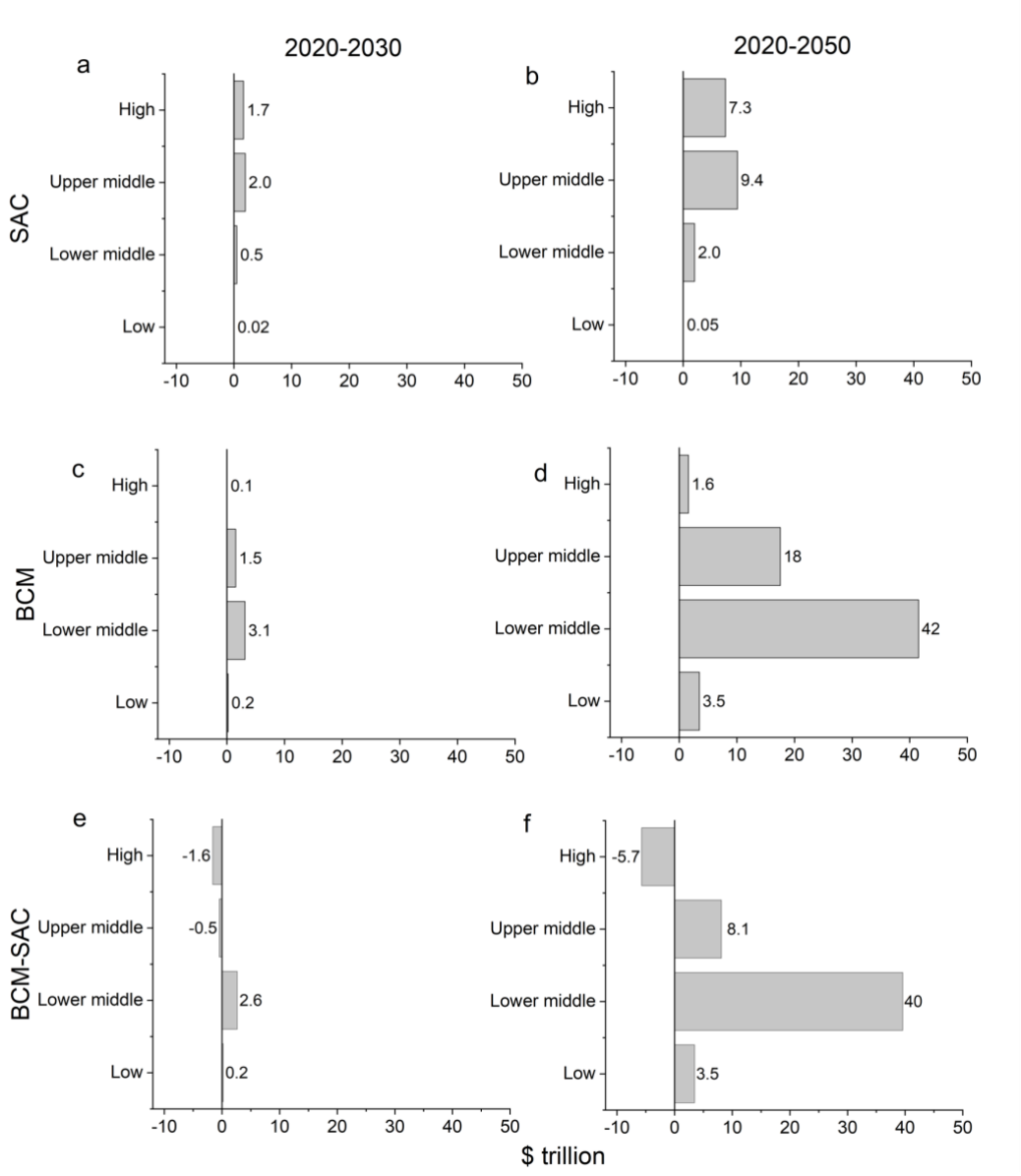


**Figure 3: SACs and BCMs by income groups.**

**(a)** Income group-level total median SAC across IAM models for the 2020-2030 horizon. (**c)** Income group-level total BCM under SSP2 for the 2020-2030 horizon. (**e)** Income group-level total BCM (b) minus SAC (a) for the 2020-2030 horizon. (**b,d,f).** Same as panels (a,c,e) for the 2020-2050 horizon.

Finally, we examine when contemporaneous annual (non-discounted) net benefits become positive over the 2020-2050 horizon, or the payback period. At the global level, the payback period for total net benefit is 5 years (Fig. 4a). Payback periods, however, vary substantially by income groups, consistent with income heterogeneity in total discounted net benefits. For lower-middle and low income countries, the payback period is 1 year (Fig. 4d and 4c). For upper-middle income countries, the payback period is 11 years. While for high income countries, payback never occurs (Fig. 4b).

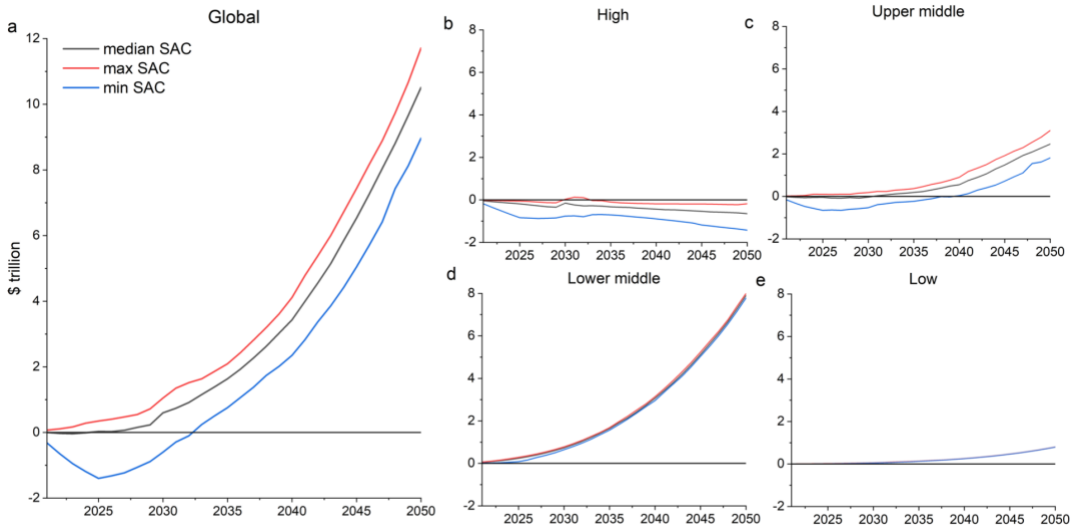


**Figure 4: Payback periods**

**(a)** Annual (undiscounted) net benefit under median, minimum, and maximum SAC across IAM models and SSP2. **(b,c,d,e)** Reproduces panel (a) but separately for high, upper-middle, lower-middle, and low income country groups.

We subject our results to various additional sensitivity analyses by further adding the cost of stranded fossil fuel infrastructure (Figs. S1-S2); replacing our 3% discount rate with a 5% discount rate (Fig. S3-S4); examining specific IAM outputs that differ, among other features,

by their endogenous fossil fuel price paths (Figs. S5-S10), considering different SSPs (Figs S11-S12). We also analyze the distribution of net benefits on a per capita basis (Fig. S12). These analyses reaffirm our main conclusions: while important in the next decade, BCMs, not SACs, largely determine the sign of a country's net benefit over a 2020-2050 horizon.

### *D. Discussion*

Although SAC is only a component of a country's total climate policy costs, which themselves may not reflect the particular concentration of political interests that influence a country's climate policy, a large SAC may partly explain the reluctance to support climate policy by countries with substantial fossil fuel reserves. The unequal distribution of costs from stranded assets and climate mitigation benefits may also speak to arguments for climate policy based on historical cumulative GHG emissions and the fairness principle. Higher income countries are responsible for nearly 90% of historical cumulative emissions (Fig. S13). However, compared to lower income countries, higher income countries may also receive lower net benefits from joining a global 2°C target. For example, the SAC for Iran, Russia, and Australia overweighs their BCM. It is notable that the NDCs of these nations also fall short in meeting the 2°C target under the Paris Agreement[61], despite their large cumulative historical emissions. By contrast, the NDCs submitted by Morocco, Ethiopia, Kenya and Philippines reflect more ambitious goals in greenhouse gas emissions despite their smaller historical cumulative emissions.

Future work can extend our analysis along several dimensions. First, our analysis assumes all fossil profits accrue to a country. While 90% of reserves are indeed owned by countries, some of the total profits from fossil fuels may accrue to foreign operating companies

that extract the fuel, affecting the distribution of SAC across countries[62]. Second, our SAC measure does not include the cost of stranded fossil fuel infrastructure, provided that this cost is not sunk. Although there are studies that quantify the stranded infrastructure cost of coal power plants[63–65], it is unknown how much of the other fossil fuel infrastructure (e.g., oil wells, refineries, and pipelines) will be stranded globally under a global 2ºC target. As a robustness check, we added stranded infrastructure cost into our SAC measure by assuming energy companies lose all their infrastructure assets (Figs. S1-S2). We find that adding infrastructure cost does not qualitatively change the overall spatial pattern of net benefits across countries.

Finally, as noted already, many other political and social determinants affect a country's adoption of climate policy besides economic costs and benefits. For example, decarbonization policies that target new capital stocks in the energy sector may help offset stranded asset costs, reshaping the influence of fossil fuels in global climate negotiations[66]. Likewise, policies that alter political access should also be considered as fossil fuel companies with high SACs may be more effective in lobbying over climate policies, undermining such policies benefits to society[67]. Other social impacts of the climate policy, e.g., the unemployment from the stranded fossil fuel reserves, also play an important role in the design of a climate policy[68].

Even within an economic perspective, our measure of SAC and BCM misses important components of total costs and benefits. On the cost side, this includes how climate policy alters profits for non-fossil fuel producers and welfare for consumers. On the benefits side, this includes everything omitted from GDP, which notably includes potential health benefits of climate policy[69]. Furthermore, even within our narrow SAC measure, there are nuances to whether a high SAC necessarily implies opposition to particular forms of climate policy. For

example, a fossil fuel rich country with high benefits from climate policy may nonetheless support climate policy that favors carbon capture and storage technology which enables reduced net GHG emissions with continued fossil fuel production. Future research should incorporate how the results from this study along with these other considerations alter the prospects of international climate policy cooperation.

## *E. Appendix*

### 1. Code and Data availability

Our code is deposited https://github.com/climate-change-ucsb/Stranded-fossil-fuel. The original code for calculating the benefits of climate change is from Ricke et al.[70]. The projected temperature data under RCPs is from Burke[27]. The SSP[60] and ADVANCE[52] database is hosted by IIASA. The deposit-level data for oil and gas is from the Rystad database in Mercure et al.[31], and the data for coal is from Welsby et al.[37]. The database of country-level benefits with uncertainty levels under all scenarios, damage functions and discounting schemes is available via https://climate-change.shinyapps.io/generation_gap/.

## 2. Supplementary Tables

**Table S1.** Global temperature increase (°C) by 2100 relative to 1985-2005 mean under different RCP scenarios from CMIP5 [71]. In our calculations, we add 0.8°C[72] to obtain current temperature levels.

| | mean | 5% | 95% |
|---|---|---|---|
| RCP2.6 | 1.8 | 1.2 | 2.6 |
| RCP4.5 | 2.7 | 2.0 | 3.5 |
| RCP6.0 | 3.1 | 2.5 | 4.1 |
| RCP8.5 | 4.7 | 3.6 | 5.8 |

**Table S2**. IAMs contained in the ADVANCE database[52]. We select IAMs that project ~6 $W/m^2$ in global average radiative forcing by 2100 under a 'Reference' scenario, consistent with RCP6.0.

| Model | Forcing ($W/m^2$) | Price ($/GJ) | Primary consumption (GJ) | Trade volume (GJ) | Time horizon |
|---|---|---|---|---|---|
| AIM/CGE V.2 | 6.1 | YES | YES | YES | 2020-2100 |
| IMACLIM V1.1 | NA | YES | YES | YES | 2020-2050 |
| IMAGE 3.0 | 5.6 | YES | YES | YES | 2020-2100 |
| MESSAGE-GLOBIOM_1.0 | 5.0 | YES | YES | YES | 2020-2100 |
| POLES ADVANCE | NA | YES | YES | YES | 2020-2100 |
| REMIND V1.7 | 5.9 | YES | YES | NO | 2020-2100 |
| WITCH2016 | 5.6 | YES | YES | YES | 2020-2100 |

**Table S3.** Countries with top 10 highest SAC between 2020-2050 using calculations based on a 3% discount rate.

| | SAC ($ trillion) |
|---|---|
| Russia | 2.6 |
| China | 2.6 |
| Saudi Arabia | 2.4 |
| Iran | 1.1 |
| USA | 1.0 |
| Iraq | 0.9 |
| India | 0.9 |
| Canada | 0.8 |
| Qatar | 0.7 |
| United Arab Emirates | 0.7 |
| Other | 5.0 |
| Total | 18.8 |

**Table S4. Countries with the top 5 highest and bottom 5 lowest** BCM values at the 10%, 25%, 50%, 75%, and 90% percentiles (via bootstrapping) between 2020-2050. Calculations based on a 3% discount rate.

| Country | 10% | 25% | 50% | 75% | 90% |
|---|---|---|---|---|---|
| India | 16.0 | 19.3 | 23.7 | 27.6 | 31.2 |
| China | -4.0 | 2.2 | 8.3 | 15.2 | 20.0 |
| Indonesia | 2.9 | 3.5 | 4.3 | 5.1 | 5.8 |
| Brazil | 2.4 | 3.1 | 3.9 | 4.7 | 5.3 |
| United States | -4.5 | -0.6 | 3.2 | 7.5 | 10.3 |
| Rest | 7.3 | 19.6 | 32.8 | 45.9 | 55.9 |
| Poland | -1.3 | -1.0 | -0.7 | -0.5 | -0.3 |
| United Kingdom | -2.2 | -1.6 | -1.1 | -0.6 | -0.2 |
| Germany | -3.2 | -2.3 | -1.6 | -1.0 | -0.5 |
| Canada | -3.6 | -2.8 | -2.2 | -1.6 | -1.1 |
| Russian | -9.9 | -8.0 | -6.4 | -4.8 | -3.7 |
| Total | -0.1 | 31.3 | 64.3 | 97.6 | 122.7 |

## 3. Supplementary Figures

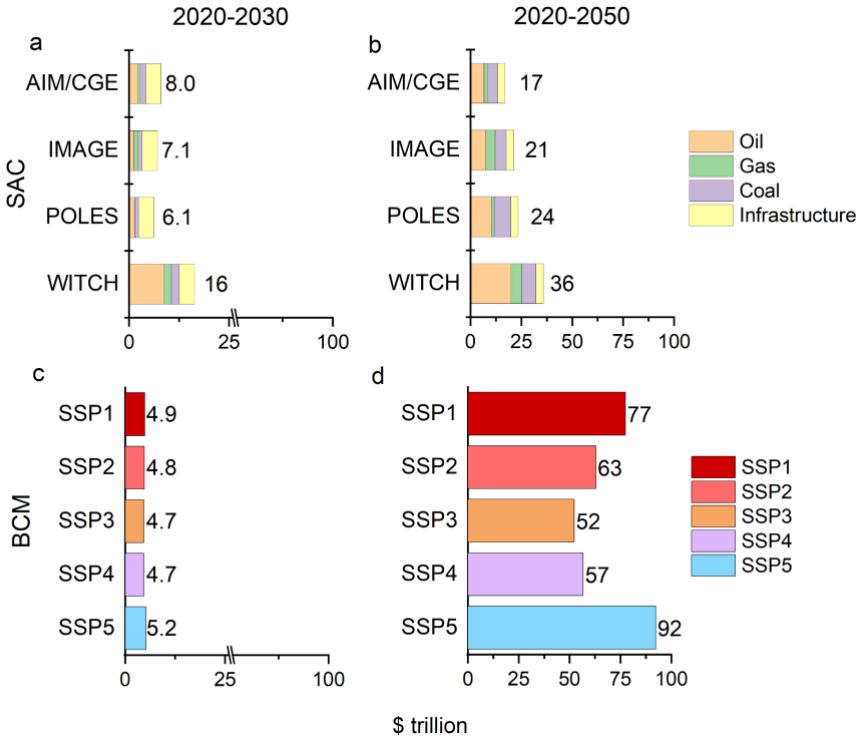


**Figure S1. Global Stranded Asset Costs inclusive of stranded infrastructure cost (SAC) and Benefits from Carbon Mitigation (BCM).**

**(a)** Global SAC across Integrated Assessment Models (IAMs) by fossil fuel for the 2020-2030 horizon. (**b)** Same as (a) for the 2020-2050 horizon. (**c)** Global GDP-based BCM across Shared Socioeconomic Pathways (SSP) for the 2020-2030 horizon. (**d)** Same as (c) for the 2020-2050 horizon. To calculate stranded infrastructure cost, we first identify 97 oil, gas and coal companies according to the Energy Intelligence Weekly[73] and S&P Global Platts Top 250 Global Energy Company Rankings[74] (Table S8). These 97 companies include 20 top fossil fuel companies that contribute to a third of global fossil fuel CO2 emissions[75,76]. We then collect the asset value from the balance sheets of these companies, obtained from the US Securities and Exchange Commission[77].

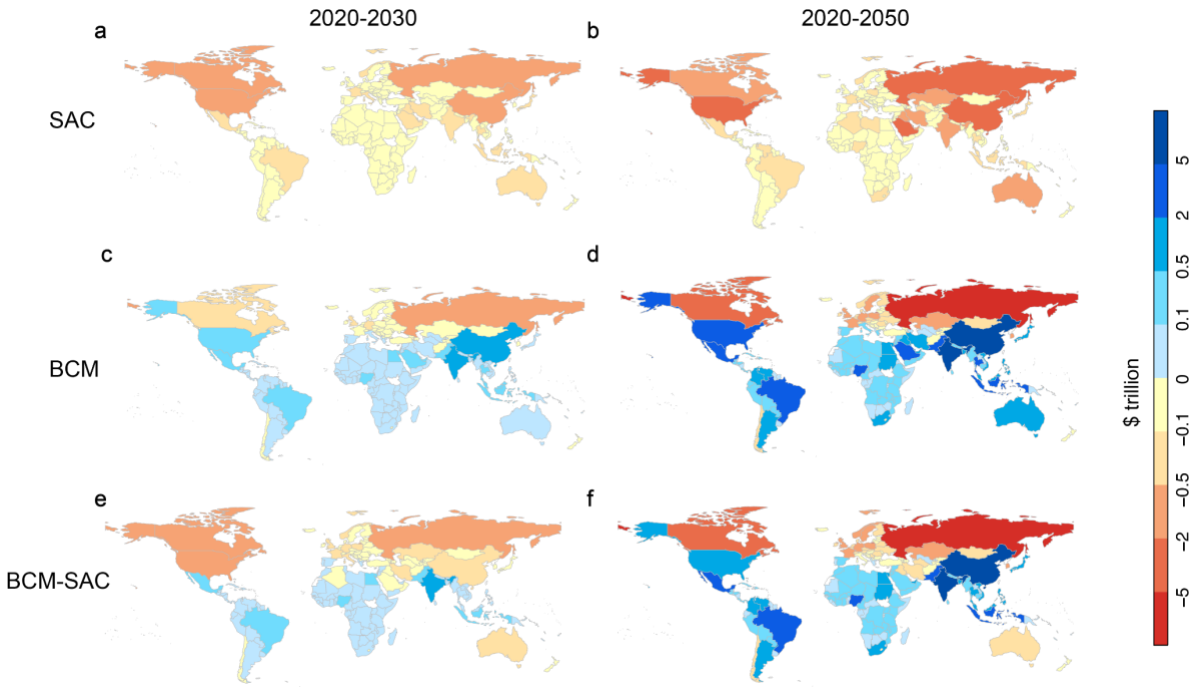


**Figure S2. Distribution of SACs inclusive of stranded infrastructure costs and BCMs across countries.**

**(a)** Country-level median SAC across IAM models for the 2020-2030 horizon. (**c)** Country-level BCM under SSP2 for the 2020-2030 horizon. (**e)** Country-level BCM (b) minus SAC (a) for the 2020-2030 horizon. (**b, d, f).** Same as panels (**a, c, e**) for the 2020-2050 horizon.

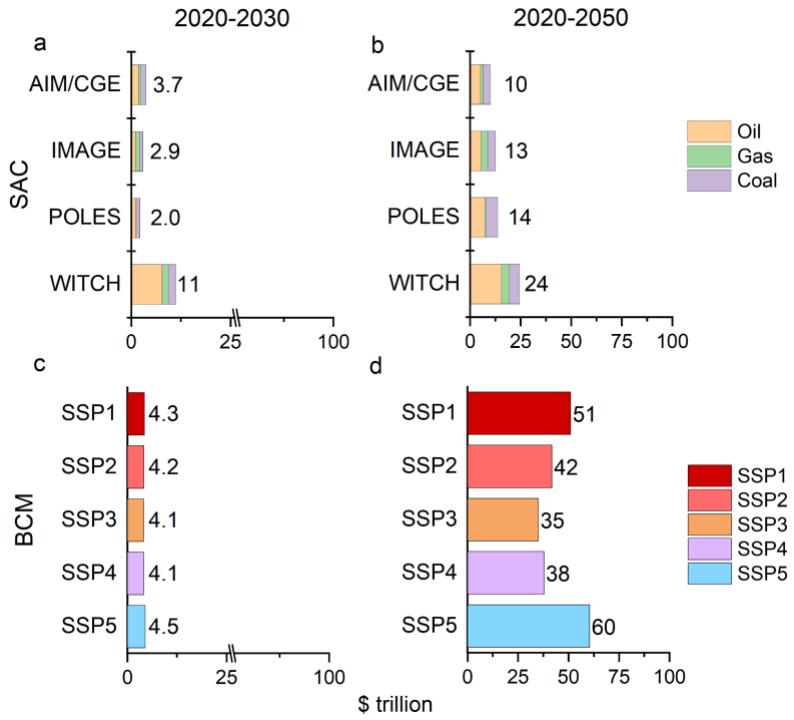


**Figure S3. Global Stranded Asset Costs (SAC) and Benefits from Carbon Mitigation (BCM) under a 5% discount rate.**

**(a)** Global SAC across Integrated Assessment Models (IAMs) by fossil fuel for the 2020-2030 horizon. (**b)** Same as (a) for the 2020-2050 horizon. (**c)** Global GDP-based BCM across Shared Socioeconomic Pathways (SSP) for the 2020-2030 horizon. (**d)** Same as (c) for the 2020-2050 horizon.

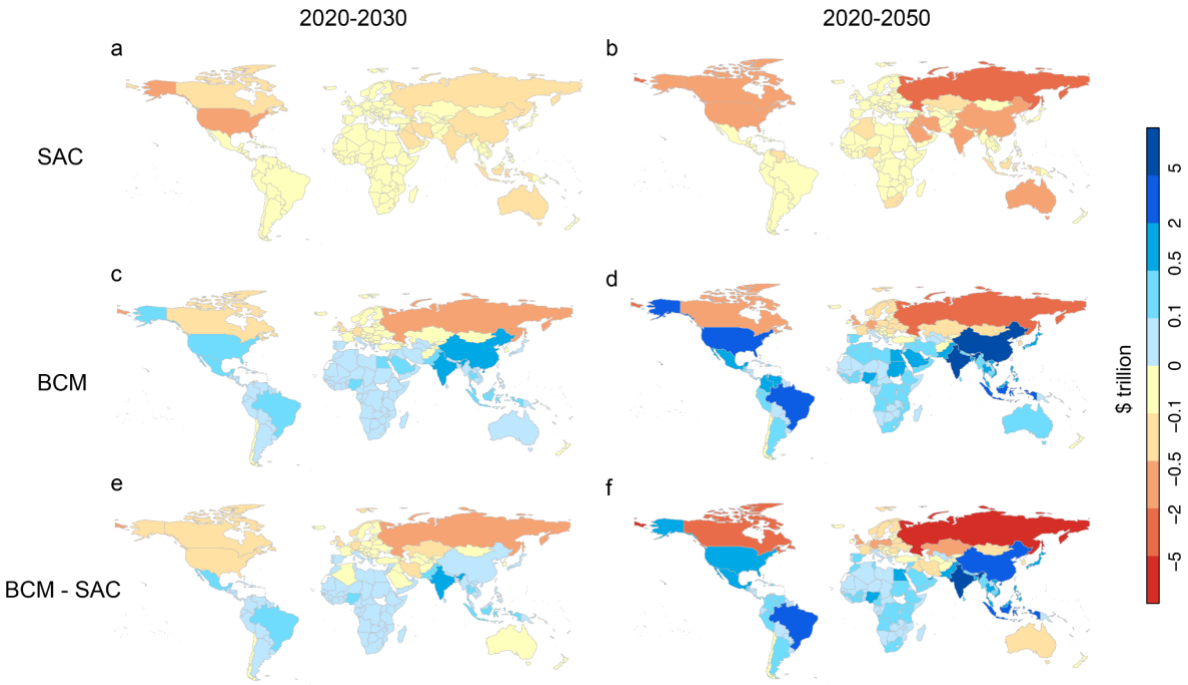


**Figure S4. Distribution of SACs and BCMs across countries under the 5% discount rate.**

**(a)** Country-level median SAC across IAM models for the 2020-2030 horizon. (**c)** Country-level BCM under SSP2 for the 2020-2030 horizon. (**e)** Country-level BCM (b) minus SAC (a) for the 2020-2030 horizon. (**b, d, f).** Same as panels (**a, c, e**) for the 2020-2050 horizon.

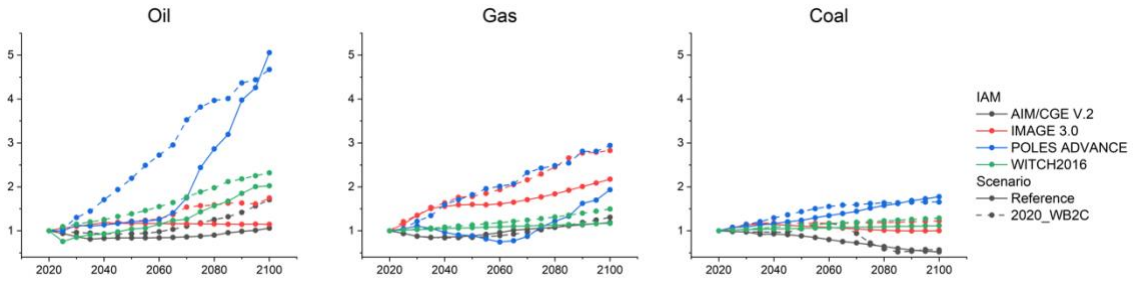


**Figure S5. Fossil fuel price trajectories across IAMs and scenarios.**

**(a) Oil prices. (b) Natural gas prices. (c) Coal prices.** Prices normalized to observed 2020 values.

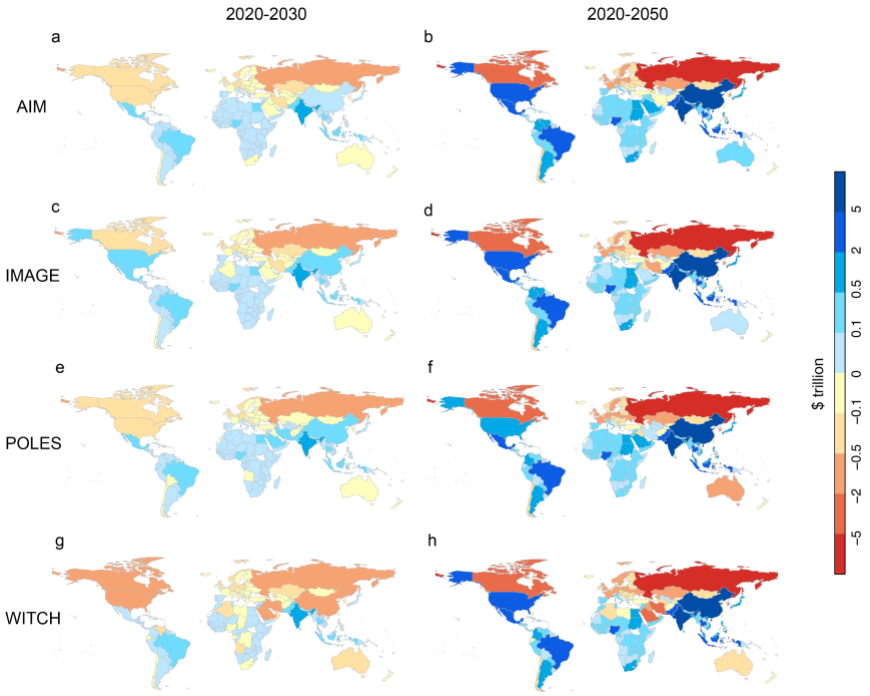


**Figure S6. Distribution of net benefits across countries under each IAM.**

**(a)** Country-level net benefits (BCM-SAC) under AIM IAM for the 2020-2030 horizon. (**b)** Country-level net benefits under AIM IAM for the 2020-2050 horizon. (**c, d)** Same as panels (**a, b**) under IMAGE IAM. (**e, f)** Same as panels (**a, b**) under POLES IAM. (**g, h)** Same as panels (**a, b**) under WITCH IAM.

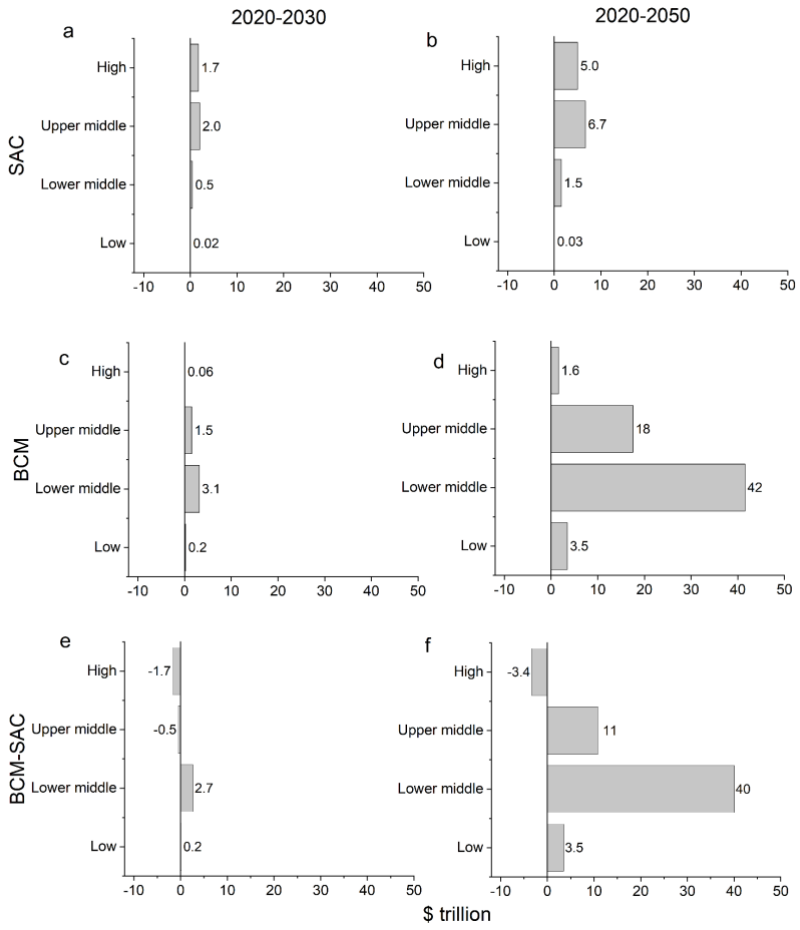


**Figure S7. SACs and BCMs by income groups from the AIM IAM**

**(a)** Income group-level total median SAC from the AIM IAM for the 2020-2030 horizon. (**c)** Income group-level total BCM under SSP2 for the 2020-2030 horizon. (**e)** Income group-level total BCM (b) minus SAC (a) for the 2020-2030 horizon. (**b, d, f).** Same as panels (**a, c, e**) for the 2020-2050 horizon.

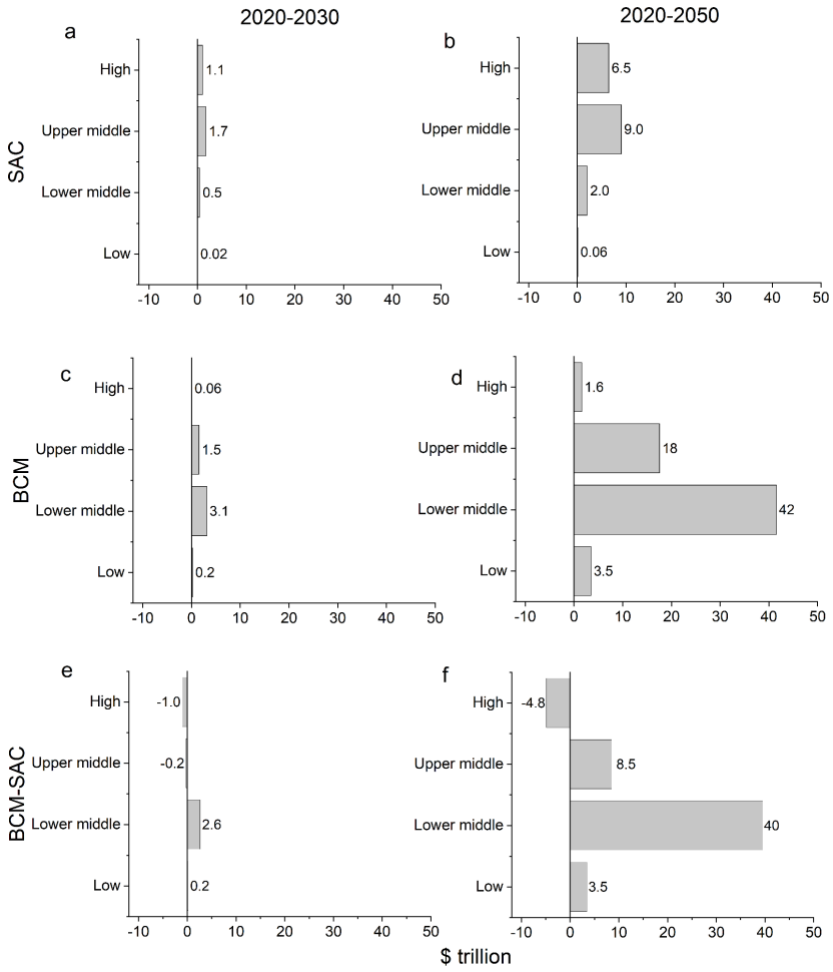


**Figure S8. SACs and BCMs by income groups from the IMAGE IAM.**

**(a)** Income group-level total median SAC from the IMAGE IAM for the 2020-2030 horizon. (**c)** Income group-level total BCM under SSP2 for the 2020-2030 horizon. (**e)** Income group-level total BCM (b) minus SAC (a) for the 2020-2030 horizon. (**b, d, f)**. Same as panels (**a, c, e**) for the 2020-2050 horizon.

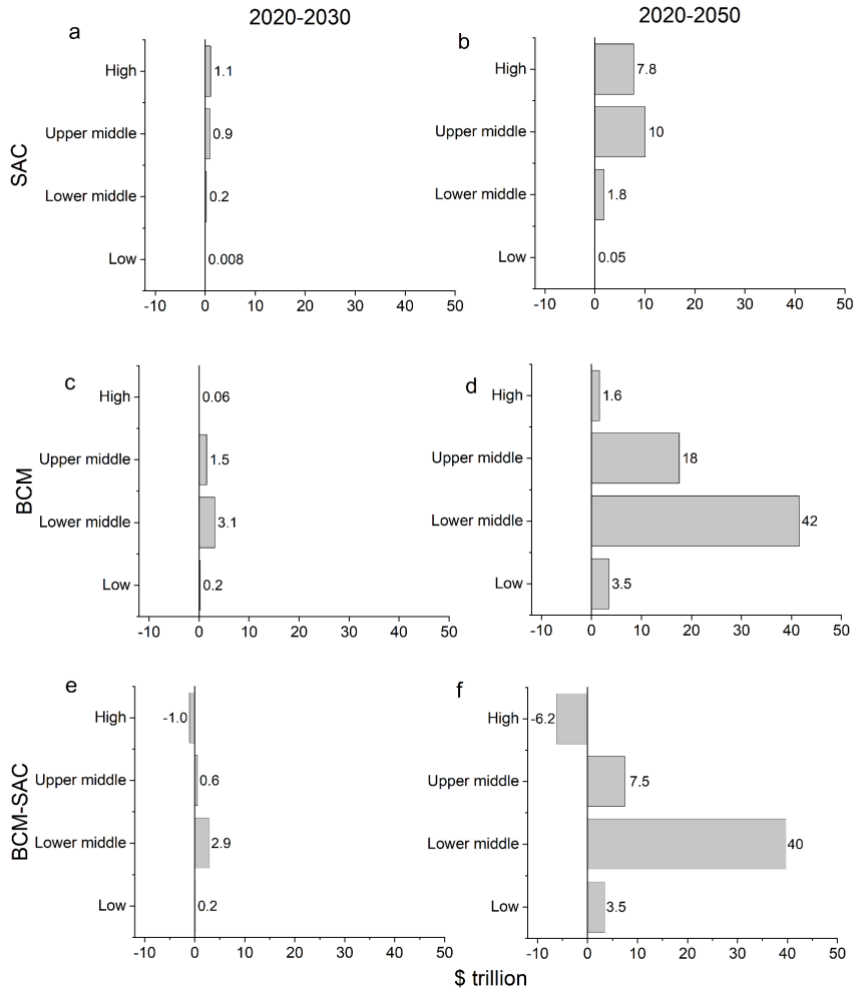


**Figure S9. SACs and BCMs by income groups from the POLES IAM**

**(a)** Income group-level total median SAC from the POLES IAM for the 2020-2030 horizon. (**c)** Income group-level total BCM under SSP2 for the 2020-2030 horizon. (**e)** Income group-level total BCM (b) minus SAC (a) for the 2020-2030 horizon. (**b, d, f).** Same as panels (**a, c, e**) for the 2020-2050 horizon.

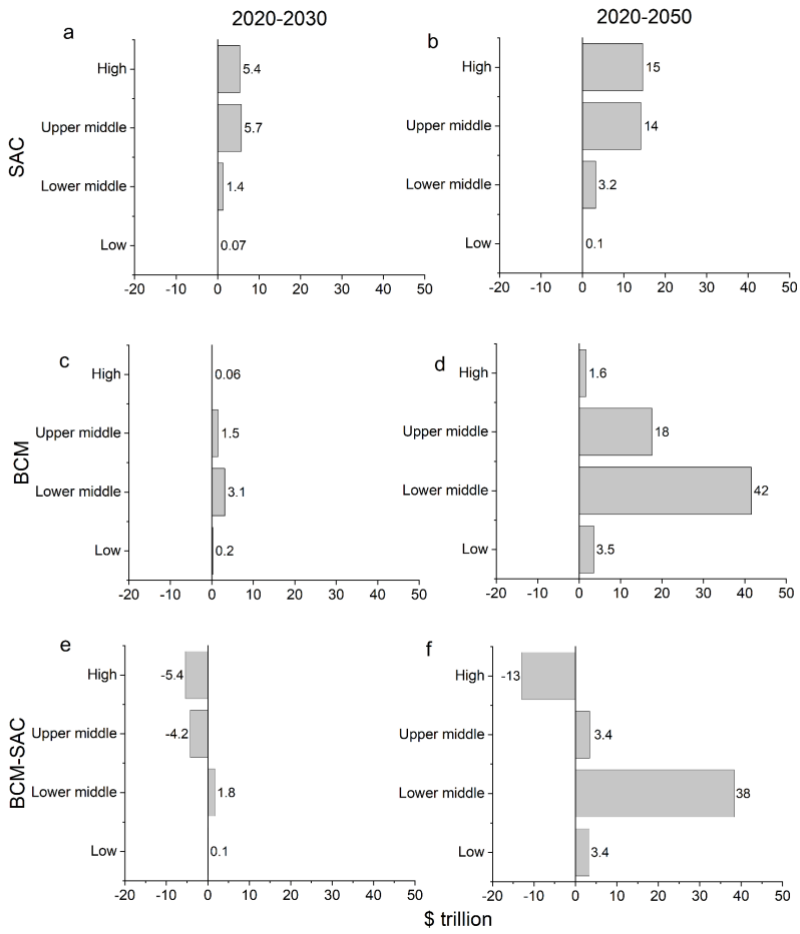


**Figure S10. SACs and BCMs by income groups from the WITCH IAM**

**(a)** Income group-level total median SAC from the WITCH IAM for the 2020-2030 horizon. (**c)** Income group-level total BCM under SSP2 for the 2020-2030 horizon. (**e)** Income group-level total BCM (b) minus SAC (a) for the 2020-2030 horizon. (**b, d, f).** Same as panels (**a, c, e**) for the 2020-2050 horizon.

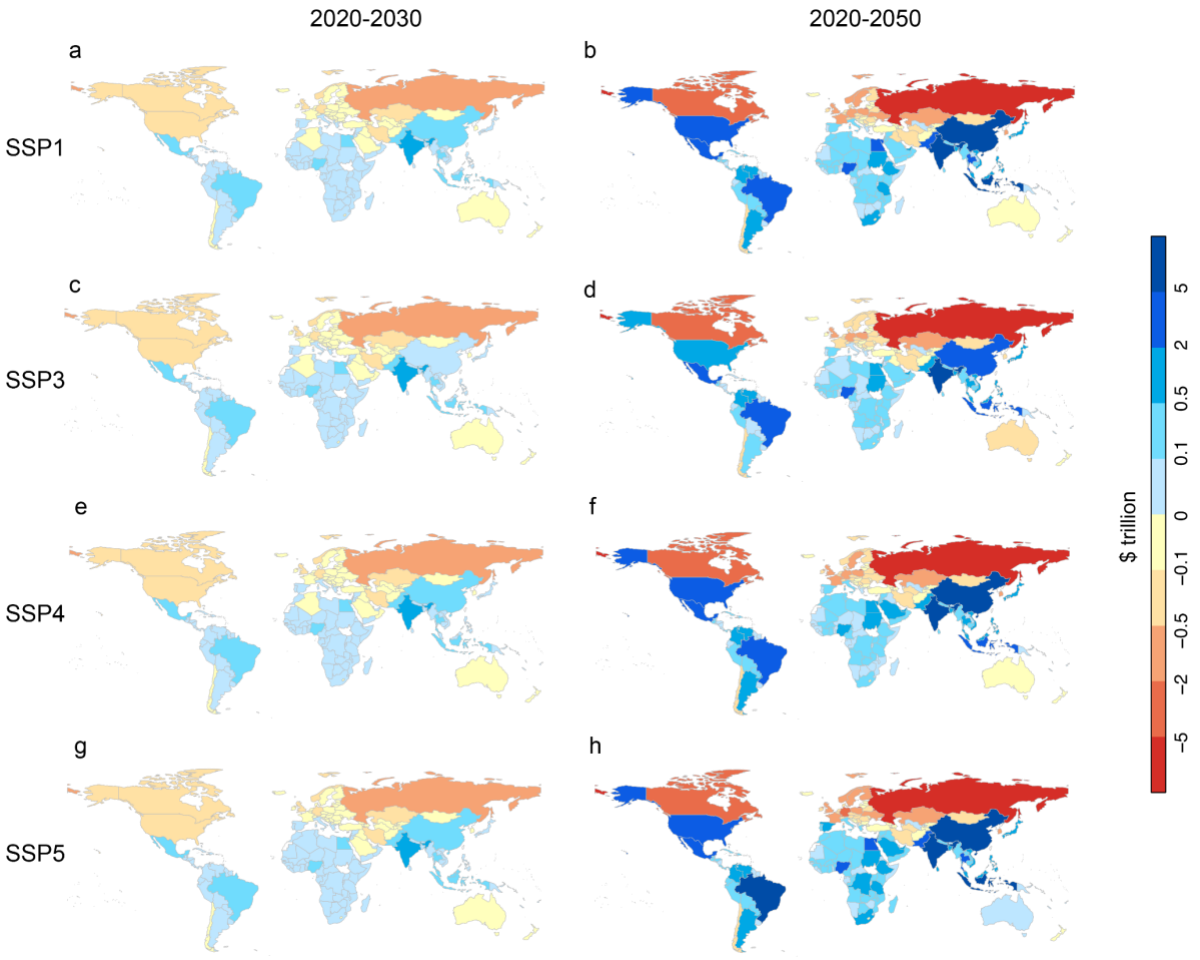


**Figure S11. Distribution of net benefits across countries under different SSP scenarios.** Under SSP1 scenario, **(a)** Country-level BCM minus SAC for the 2020-2030 horizon. **(b)** Country-level BCM minus SAC for the 2020-2050 horizon. **(c, d).** Same as panels **(a, b)** for the SSP3 scenario. **(e, f).** Same as panels **(a, b)** for the SSP4 scenario. **(g, h).** Same as panels **(a, b)** for the SSP5 scenario.

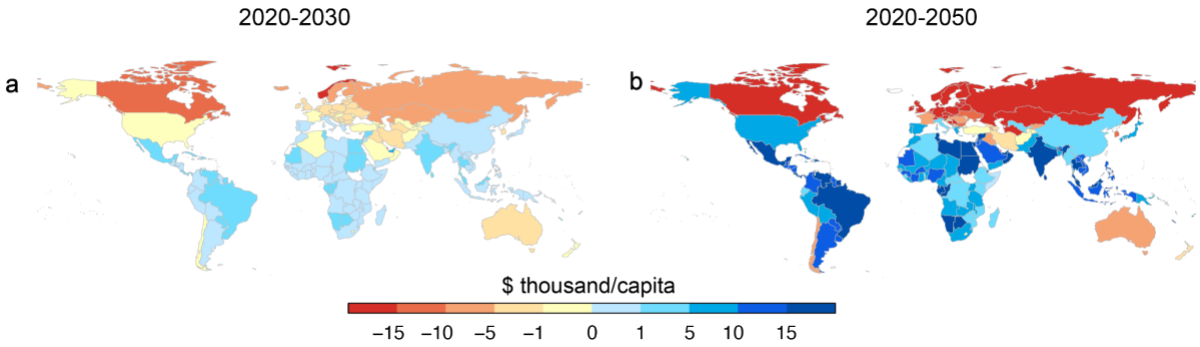


**Figure S12. Distribution of net benefits per capita across countries under different SSP scenarios.**

**(a)** Country-level BCM minus SAC per capita for the 2020-2030 horizon. **(b)** Country-level BCM minus SAC per capita for the 2020-2050 horizon.

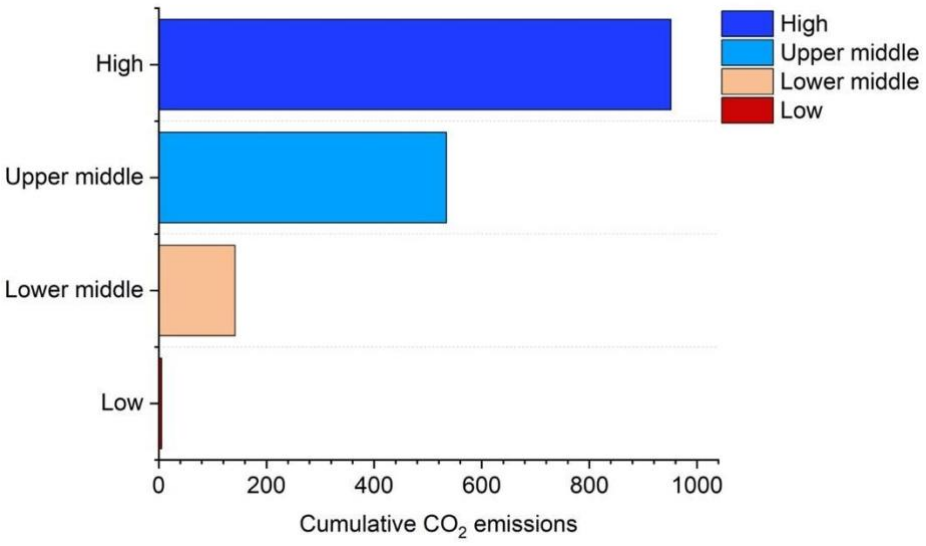


**Figure S13. Cumulative historical $CO_2$ emissions (1750-2020) by income group[78].**

# III. Economic disparity among generations under the Paris Agreement

Material from: Yang, H., Suh, S. Economic disparity among generations under the Paris Agreement. Nat Commun 12, 5663 (2021). https://doi.org/10.1038/s41467-021-25520-8

**Abstract**

The costs and benefits of climate change mitigation are known to be distributed unevenly across time and space, while their intergenerational distribution across nations has not been evaluated. Here, we analyze the lifetime costs and benefits of climate change mitigation by age cohorts across countries under the Paris Agreement. Our results show that the age cohorts born prior to 1960 generally experience a net reduction in lifetime gross domestic product per capita. Age cohorts born after 1990 will gain net benefits from climate change mitigation in most lower income countries. However, no age cohorts enjoy net benefits regardless of the birth year in many higher income countries. Furthermore, the cost-benefit disparity among old and young age cohorts is expected to widen over time. Particularly, lower income countries are expected to have much larger cost-benefit disparity between the young and the old. Our findings highlight the challenges in building consensus for equitable climate policy among nations and generations.

## *A. Introduction*

Younger generations emerged at the forefront of the global climate movement in recent years[79,80]. One of the prevailing narratives to this phenomenon is that younger and future generations are the greatest victims of climate change driven by the actions and inactions of older generations[81–83]. Supported by such narratives, some studies indicated the

presence of intergenerational gaps in the perceptions toward climate change mitigation[80,84–86]. Several studies have explored how the economic policy can be designed to reduce or eradicate the intergenerational disparity in climate change mitigation[87,88].

Though many studies have discussed the justice and inequality issues among generations under climate change[81,89–91], there were, however, no peer-reviewed literature that quantifies the costs and benefits of climate change mitigation by age cohorts at a country level.

In this study, we quantify the lifetime costs and benefits of climate change mitigation by age cohorts across countries under the Paris Agreement. In this paper, the cost of climate change mitigation refers to the gross domestic product (GDP) loss compared to the counterfactual scenario without climate change mitigation[92]. To measure the loss of GDP, Integrated Assessment Models (IAMs) are developed by many research groups to couple energy, economy, and climate (Supplementary Note). In these IAMs, the economic modules generally follow general or partial equilibrium models[93]. Here, the data for the cost of climate change mitigation is derived from several IAMs[94] in the 2014 IPCC report. According to the report, the abatement cost of climate change mitigation range 2–6% of global GDP by 2100 relative to pre-Paris Agreement policy[92].

The benefit of climate change mitigation refers to the avoided economic damage by stabilizing global temperature[7]. Burke et al.[43] developed a damage function that measures the nonlinear relationship between temperature and economic growth (BHM damage function). Using this nonlinear relationship, Burke et al. estimated that keeping the global temperature at 2010 level could save 23% of global GDP by 2100. Though the Burke

method is still under discussion[95,96], this empirical nonlinear GDP–temperature relation has been widely applied in the cost-benefit analysis of climate change mitigation[7,70,97].

The climate change mitigation scenarios under the Paris Agreement employed in our models do not consider the policies to address the intergenerational disparity. The costs and benefits of climate change mitigation are modeled for the period of 2020–2100 (Fig. S1). The benefit of climate change mitigation hereafter is quantified by the BHM damage function, and the cost of climate change mitigation is calculated by assuming a triangle distribution of GDP loss reported by the 2014 IPCC report. To quantify the cost-benefit disparity, we estimate the lifetime costs and benefits at a 3% discount rate by age cohort in 169 countries under the 2 °C target of the Paris Agreement. The lifetime cost and benefits are measured as accumulative GDP per capita (in 2018 dollars) during the lifetime of an age cohort. The lifetime of an age cohort is calculated by using the expected life expectancy for the age group[98]. The distribution of GDP per capita across age cohorts follows the income distribution from the OECD database. The Paris Agreement scenario is represented by the Representative Concentration Pathways (RCP) 2.6. The Pre-Paris Agreement scenario, which is the baseline scenario in our study, is represented by the Shared Socioeconomic Path (SSP) 4 and RCP 6.0[46] in the main text (analysis of other SSP and RCP scenarios can be found in "Data Availability").

### *B. Methods and Materials*

#### 1. Lifetime of age cohorts

The lifetime of each cohort is calculated as the life expectancy after 2020. The age-specific life expectancy is derived from United Nations, and the country-specific life

expectancy at birth is derived from World Bank. The following equations are used to derive the age- and country-specific lifetime after 2020.

$$SL = \{SY - A, if\ SL \geq 2020\ 2020, if\ SL < 2020\ (1)$$

$$EL = \{SY + E, if\ EL \leq 2100\ 2100, if\ EL > 2100\ (2)$$

SL is the start year of the lifetime for a studied age cohort. SY is the year studied, which is chosen from 2020 to 2100. *A* is the age of the age cohort. EL is the end year of the lifetime for a studied age cohort. *E* is the life expectancy of the studied age cohort. The life expectancy is collected from World Bank[99] and World Population Prospects[98].

**2. Income distribution**

The income distribution across age cohort depends on the disposable income at each age group and the mean disposable income of the total population.

$$I_{t-T,t,i} = \frac{D_{t-T,i}}{\overline{D}_i}\ (3)$$

where *t* is the future year. *T* is the birth year of the age cohort. *t-T* is the age of an age cohort in year *t.* At year *t*, $D_{t-T,i}$ is the income of an age cohort born in year *T* in country *i*. $\overline{D}_i$ is the average income in country *i*. At year *t*, $I_{t-T,t,i}$ is the ratio of the income for an age cohort born in year *T* versus the average income of the total population in country *i.* The data for the income distribution across age cohorts are collected from OECD database[100]. The income distribution of some developing countries are not included in the OECD database. Their income distribution is assumed to be the median of the income in developing countries that are included in the OECD database (Table S1). We assume the income distribution is consistent over time.

### 3. Calculation of benefits of climate change mitigation

We followed the procedure in Burke et al., 2015[43] (BHM damage function) to estimate the social benefits of climate change mitigation from 2020 to 2100, and the details are described below.

Global warming is measured by the global temperature increase between the pre-industrial level and 2100 period. The climate models in phase five of the Coupled Model Intercomparison Project (CMIP5)[101] generate the baseline temperatures from the mid-1800s to 2005 using historical radiative forcing and the future temperatures in the 21st century using radiative forcing under the RCP2.6, RCP4.5, RCP6.0 and RCP8.5 scenarios. Multiple global climate models are used to simulate each RCP scenario, and the average temperature increase in the models is used to represent the temperature increase in each of the RCP scenarios. Following the IPCC protocols, we use the years 1986–2005 as the baseline period and 2081-2100 as the RCP future period. According to the IPCC report[72], the temperature increase between the pre-industrial (1850-1900) level and the current period (2003-2012) is 0.8°C. Therefore, the projected global warming in 2100 relative to the pre-industrial level is calculated as

$$\Delta T_r = \frac{\sum_{m=1}^{N_r} \Delta T_{m,r}}{N_r} \quad (4)$$

$$\Delta T_{pre} = \Delta T_r + 0.8 \quad (5)$$

$\Delta T_{m,r}$ is the temperature increase between the 1986-2005 period and the 2081-2100 period under RCP scenario *r* using model global climate model *m*, $N_r$ is the number of models used to simulate RCP scenario *r*, $\Delta T_r$ is the average temperature increase between the 1986-2005

period and the 2081-2100 period under RCP scenario *r*, and $\Delta T_{pre}$ is the global warming relative to the pre-industrial level. We chose the RCP2.6 scenario as the mitigation scenario because the average global temperature increase in all the models for this scenario is most consistent with the target to limit the global temperature increase to 2°C.

Following the methods in Burke et al.[43] and Ricke et al.[70], we corrected the projected temperature in all RCP scenarios using the following correction equation:

$$Temp_{i,t,r} = \overline{Temp_i} + \frac{t - 2010}{2100 - 2010} \times \Delta(T_{i,r}) \quad (6)$$

where $Temp_{i,t,r}$ is the corrected temperature for country *i* in year *t* under RCP scenario *r*, $\overline{Temp_i}$ is the average temperature of the observations in country *i* from 1980-2010, and $\Delta(T_{i,r})$ is the projected temperature increase between the 1986-2005 period and 2081-2100 period in country *i* and RCP scenario *r*.

The effect of temperature on the GDP growth rate (BHM damage function) is described as

$$h(Temp_{i,t,r}) = \beta_1 Temp_{i,t,r} + \beta_2 Temp_{i,t,r}^2 \quad (7)$$

where $h(Temp_{i,t,r})$ is the effect of temperature on the GDP growth rate in country *i* at year *t* under RCP scenario *r*. The parameters $\beta_1$ and $\beta_2$ were estimated by Burke et al., 2015[16] using historical country-level temperature and economic data.

The additional effect of warming on growth in year *t* is calculated as

$$\delta_{i,t} = h(Temp_{i,t}) - h(\overline{Temp_i}) \quad (8)$$

where $\delta_{i,t}$ is the predicted additional effect of warming on GDP growth in country *i* in year *t*.

The social benefits under climate change mitigation are calculated as:

$$G_{i,t,s,r} = G_{i,t-1,s,r}\left(1 + \eta_{i,t,s} + \delta_{i,t,r}\right) (9)$$

$$B_{i,t,s,r} = G_{i,t,s,r_{mitigation}} - G_{i,t,s,r} (10)$$

$$CB_{i,T,s,r} = \sum_{t=SL}^{EL}\left[B_{i,t,s,r} \cdot I_{t-T,t,i} \times \prod_{SL}^{t}\frac{1}{1 + Dis_{i,t,s,r}}\right] (11)$$

$$Dis_{i,t,s,r} = \rho + \mu G_{i,t,s,r} (12)$$

$G_{i,t,s,r}$ is the GDP per capita in country *i* in year *t* (2020-2100) under SSP scenario *s* and RCP scenario *r*, $\eta_{i,t,s}$ is the growth rate of GDP per capita under SSP scenario *s*. $B_{i,t,s,r}$ is the annual social benefit of country *i* in year *t* under SSP scenario *s* and RCP scenario *r*. $G_{i,t,s,r_{mitigation}}$ is the GDP per capita in country *i* in year *t* under the mitigation scenario, and the mitigation scenario used in our research is RCP2.6 and SSP4. $CB_{i,T,s,r}$ is the discounted lifetime benefits of the age cohort born in year *T* from country *i* by achieving the mitigation scenario from the SSP scenario *s* and RCP scenario *r*. $Dis_{i,t,s}$ is the discount rate in country *i* in year *t*. Based on the classification of the World Bank[58], we classified the countries into four income groups: a high-income group, upper-middle-income group, lower-middle-income group and low-income group.

As shown in Equation (12), the discount rate is determined by the Ramsey endogenous rule[102], where $\rho$ is the pure time preference and $\mu$ is the elasticity of marginal utility. If $\mu$=0,

Equation (11) estimates the social benefits with a fixed discount rate. If $\mu \neq 0$, Equation (11) estimates the social benefits with a growth-adjusted discount rate.

The growth rate of GDP ($\eta_{i,t,s}$) is derived from the SSP database developed by the International Institute for Applied System Analysis[60]. We used the code and compiled datasets from Burke Lab (https://github.com/burke-lab/BDD2018) to derive the population-weighted temperature increase from 2010 to 2100 at the country level. The country-level baseline temperatures in 2010 and the original code for calculating the benefits of climate change mitigation under multiple SSP and RCP scenarios are compiled from https://country-level-scc.github.io/.

**4. Calculating the cost of climate change mitigation**

We used the loss of GDP from the 2014 IPCC report to calculate the cost of climate change mitigation.

$$C_{i,t,s,r} = G_{i,t,s,r} \cdot L_{i,t,r_{mitigation}} \quad (13)$$

$$L_{i,t,r_{mitigation}} = L_{t,r_{mitigation}} \cdot R_{k,r_{mitigation}}, i \in k \quad (14)$$

$$CC_{i,T,s,r} = \sum_{t=SL}^{EL} \left[ C_{i,t,s,r} \cdot I_{t-T,t,i} \times \prod_{SL}^{t} \frac{1}{1 + Dis_{i,t,s,r}} \right] \quad (15)$$

$C_{i,t,s,r}$ is the annual social cost of country *i* in year *t* to achieve the mitigation scenario from the SSP scenario *s* and RCP scenario *r*. $L_{t,r,mitigation}$ is the loss of global GDP in year *t* in climate change mitigation. The time series of $L_{t,r,mitigation}$ is derived by liner interpolation from the data points in 2020, 2030, 2050 and 2100. $R_{k,r,mitigation}$ is the ratio of the regional cost in region *k* relative to the global cost of climate change mitigation (Table S2). *k* represents 5 regions: OECD 1990, Asia, Middle East and Africa, Latin America and

Economics in Transition. $CC_{i,T,s,r}$ is the discounted lifetime cost of the age cohort born in year *T* from country *i*.

**5. Calculation net gain of GDP per capita during lifetime**

We calculated the net gain of GDP per capita for an age cohort from climate change mitigation from the following equations:

$$CGDP_{i,T,s,r} = \sum_{t=SL}^{EL} \left[ GDP_{i,t,s,r} \cdot I_{t-T,t,i} \times \prod_{SL}^{t} \frac{1}{1 + Dis_{i,t,s,r}} \right] \quad (16)$$

$$Net_{i,T,s,r} = CC_{i,Ts,r} - CB_{i,T,s,r} \quad (17)$$

$$RGDP_{i,T,s,r} = \frac{Net_{i,T,s,r}}{CGDP_{i,T,s,r}} \quad (18)$$

$CGDP_{i,T,s,r}$ is the cumulative GDP per capita for the age cohort born in year *T* in country *i* under the baseline scenario of SSP *s* and RCP *r*. $Net_{i,T,s,r}$ is the net gain of GDP per capita for the age cohort born in year *T* in country *i* by achieving the mitigation scenario from the SSP *s* and RCP *r*. $RGDP_{i,T,s,r}$ is the percentage change of GDP per capita for the age cohort born in year *T* in country *i* in the climate change mitigation.

**6. Calculation of breakeven year**

$$BY_{SY,i} = T_{SY}, if\ Net_{i,T_{SY},s,r} > 0\ and\ Net_{i,T_{SY}-1,s,r} < 0 \quad (19)$$

$$BY_{SY,i} = nonexistense, if\ Net_{i,T,s,r} < 0\ and\ T \in [SL, EL] \quad (20)$$

$BY_{SY,i}$ is the age cohort in country *i* that breaks even the lifetime cost and benefit of the studied age cohorts (0-100 years old) in year of SY (2020-2100). $T_{SY}$ is the age of the cohort in the year of SY. If none of the studied age cohort breaks even the lifetime cost and benefit, the age of the breakeven generation is defined as nonexistence.

### 7. Uncertainty test

The uncertainty of our calculation originates from the use of SSP and RCP scenarios, discount rates, the parameters in the equations and the model specification of Equation (6).

In this study, the RCP6.0 and SSP4 scenarios are used as the business as usual scenario, which is consistent with the global temperature increase and economic development under current policy by recent studies[101]. To analyze the uncertainty of different RCP and SSP scenarios, the social benefits under RCP4.5, RCP6.0 and RCP8.5 and all five SSP scenarios were calculated.

For the fixed discount rates, we consider 3% and 5% scenario. For the growth-adjusted discount rate, we assumed that $\rho \in \{2,1\}$ and $\mu\epsilon\{2\}$. All possible combinations of $\rho$ and $\mu$ are considered to test the sensitivity of discount rates on our results.

The uncertainty of $\beta_1$, $\beta_2$ in Equation (6) is analyzed by bootstrapping using 1000 sets of parameter values. We assume that $L_{t,r,mitigation}$ and $r_{k,r,mitigation}$ in Equation (13) follow the triangle distribution. We did 1000 times of simulation to test the uncertainty caused by parameters.

The results of the uncertainty test are provided online (https://climate-change.shinyapps.io/generation_disparity/). The influence of temperature on GDP growth includes the contemporary and the long-term effects. Rather than using pooled data, the model specification can also differentiate rich and poor countries. In Fig. S2, we show the uncertainty caused by using different function forms of temperature and GDP growth.

### *C. Results*

#### 1. Costs and benefits over generations

We first evaluate the change of lifetime GDP per capita for age cohorts born between 1920 and 2020. Our results show that climate change mitigation incurs a net reduction in lifetime GDP per capita for age cohorts born prior to 1960 across nearly all nations (Fig.1). In low-income countries, the age cohorts born before 1960 incur the largest reduction of average lifetime GDP per capita compared to the same age cohorts in countries with higher income. In low-income countries, the age cohort born between 1920 and 1960 is estimated to incur, on average, ~2.5% net reduction in lifetime GDP per capita under the Paris Agreement (Fig. 1d, h). In contrast, in high-income countries, the same age cohorts incur the least net reduction (<1%) in average lifetime GDP per capita.

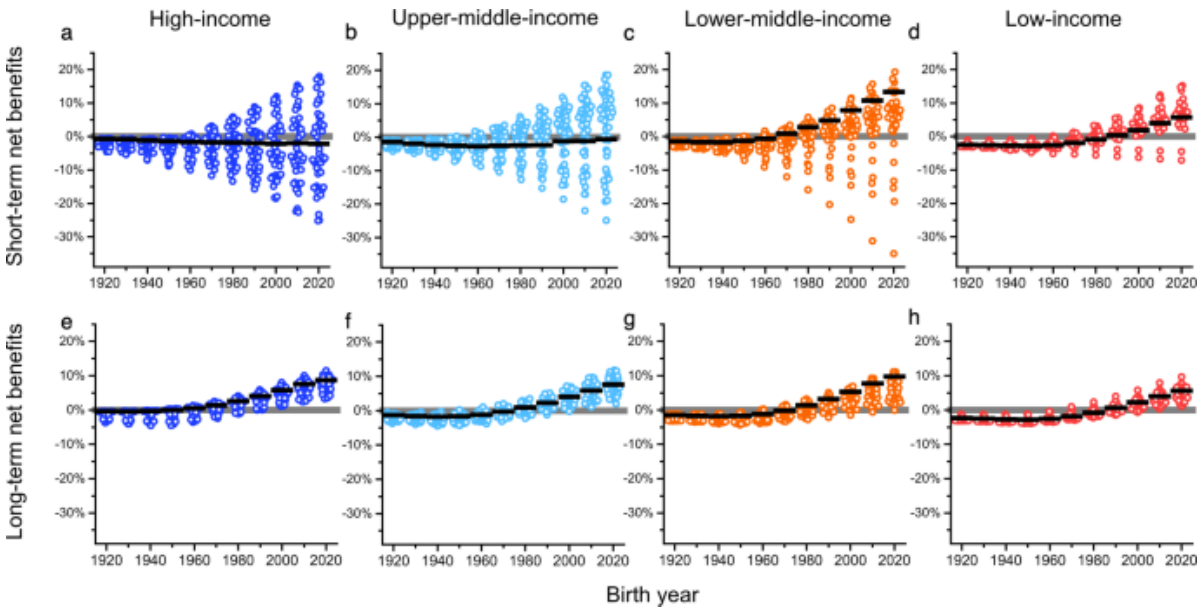


**Fig. 1: Percentage change of lifetime GDP (gross domestic product) per capita for age cohorts born during 1920–2020.**

Using the short-term BHM (Burke, Hsiang, and Miguel) damage function to calculate the lifetime benefits of climate change mitigation (short-term benefits), the percentage change of lifetime GDP per capita (short-term net benefits) for age cohorts born during 1920–2020 is shown in (**a)** high-income countries, (**b**) upper-middle-income countries, (**c**) lower-middle-income countries, and (**d**) low-income countries. Using the long-term BHM damage function to calculate the lifetime benefits of climate change mitigation (long-term benefits), the percentage change of lifetime GDP per capita (long-term net benefits) for age cohorts born during 1920–2020 is shown in (**e**) high-income countries, (**f**) upper-middle-income countries, (**g**) lower-middle-income countries and (**h**) low-income countries. The solid black lines represent the population-weighted average of the percentage change of lifetime GDP per capita for each age cohort. For age cohorts with the same birth year, the average percentage change of lifetime GDP per capita is quantified in $n = 47$ high-income countries, $n = 50$ upper-middle-income countries, $n = 43$ lower-middle-income countries, and $n = 29$ low-income countries. A circle symbol represents an age cohort in a country. The color of circles represents the income group of a country.

In most of the lower-middle-income and low-income countries, age cohorts born after 1990 will start to have a net gain of lifetime GDP per capita in the course of climate change mitigation under the Paris Agreement. By quantity, the net gain of lifetime GDP per capita among the younger age cohorts is asymmetrically larger than the net reduction among the older age cohorts. In low-income countries (Fig. 1d, h), the age cohort born in 2020 enjoys a net gain of ~6% in lifetime GDP per capita on average, while the age cohort born in 1950 incurs a net reduction of ~3%. In lower-middle-income countries (Fig. 1c, g), on average, the

largest net gain of lifetime GDP per capita is 5–8-folds larger than the net reduction in absolute value.

In high- and upper-middle-income countries, the trend of lifetime GDP per capita by age cohort is sensitive to the model specifications that measure the benefits of climate change mitigation. When using the short-term BHM damage function to measure the lifetime benefits (short-term benefits), which is commonly used in other research[7,27,39,43,70], the age cohorts in many high- and upper-middle-income countries still incur a net reduction of lifetime GDP per capita (short-term net benefits) with the progression of birth year, including the age cohorts born in 2020. The age cohorts in high and upper-middle-income countries, on average, barely gain any net benefits throughout the birth years considered (Fig. 1a, b). On average, all age cohorts in high-income countries lose 0–2% of lifetime GDP per capita, and those in upper-middle-income countries lose 0–3% of lifetime GDP per capita.

However, when using the long-term BHM damage function to measure the lifetime benefits (long-term benefits), the net gain of GDP per capita (long-term net benefits) increases in high- and upper-middle-income countries with the progression of birth years. The age cohorts born in 1960 in high-income countries (Fig.1e), and the age cohorts born in 1980 in upper-middle-income countries (Fig. 1f) start to show net gains of average lifetime GDP per capita under climate change mitigation.

The uncertainty range of the long-term BHM damage function is much wider than that of the short-term damage function (Fig. S2). Due to the large uncertainties of the long-term damage function and the lack of robust evidence for the long-term benefits, the short-term benefits of climate change mitigation are more commonly discussed in the current literature[27,27,95].

### 2. Breakeven generation

We define a breakeven generation as the age cohort that breaks even the lifetime cost and benefit from climate change mitigation under the Paris Agreement in a given year studied. An age cohort born after the breakeven generation will gain net benefits from climate change mitigation, and an age cohort born before this breakeven generation will bear net costs. In 2020, more than three-quarters of the population are born after the breakeven generation in Latin America, South Asia, and Western Asia (Fig. 2e and Fig. S3e). In Latin America and South Asia, the breakeven generations are born prior to 1970 (Fig. 2 and Fig. S3), which are the earliest across the world. However, in Eastern Europe, only the age cohorts born after 1980 enjoy a net benefit from climate change mitigation, so that more than half of the current population in that region are born before the breakeven generation (Fig. 2e and Fig. S3e).

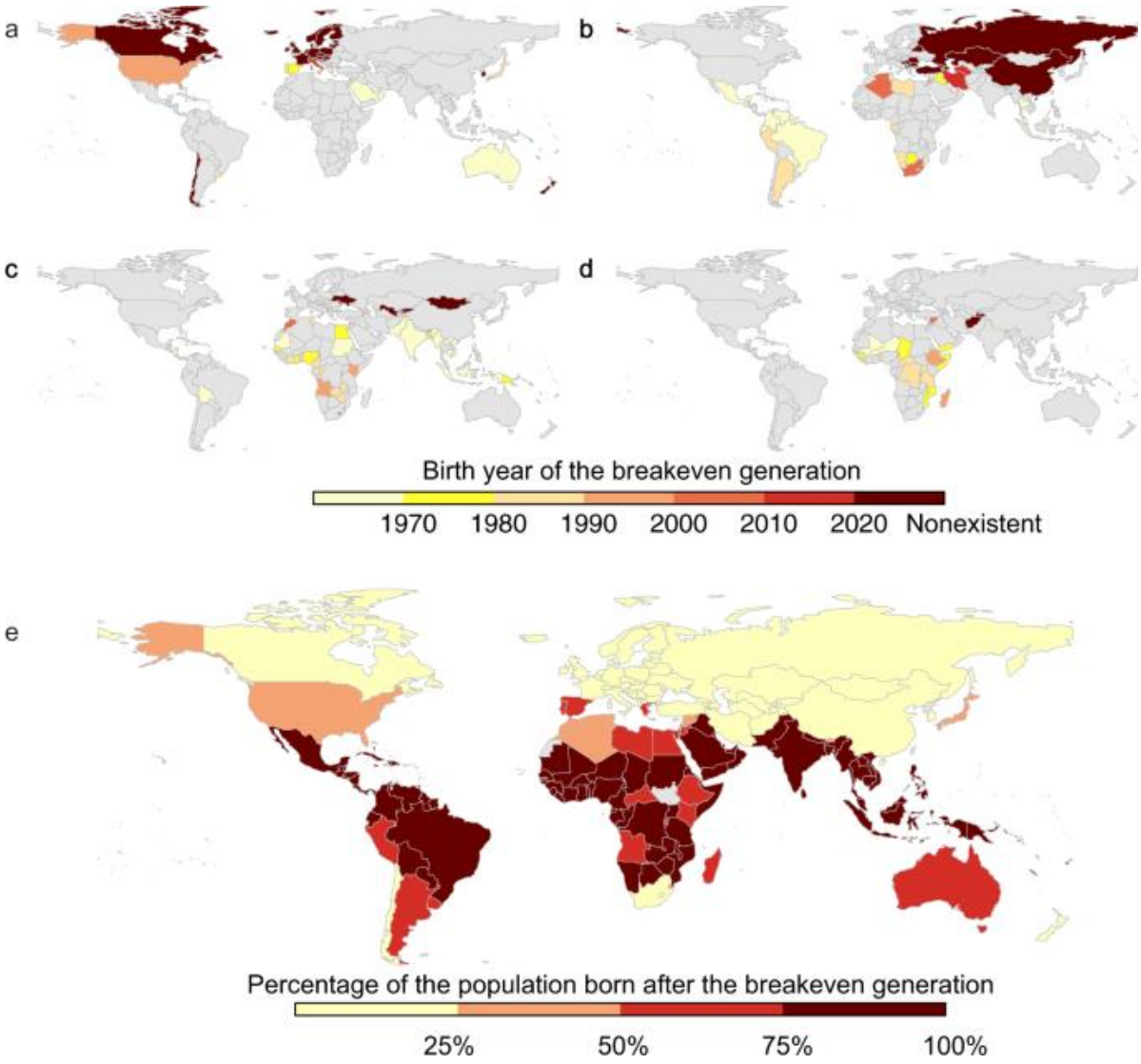


**Fig. 2: Breakeven generation and the percentage of the population born after the breakeven generation using the short-term net benefits.**

The birth year of the breakeven generation in 2020 in (**a**) high-income countries, (**b**) upper-middle-income countries, (**c**) lower-middle-income countries, and (**d**) low-income countries. (**e**) The percentage of the population born after the breakeven generation. In (**a**–**d**), different colors represent different ranges for the birth years. In (**e**), different colors represent different ranges for the percentage of the population. Here, we use the short-term benefits to measure the lifetime benefits. We use the long-term benefits in Fig. S3.

In high-income countries, the breakeven generations are born prior to 1980 in Spain, Australia, and Saudi Arabia (Fig. 2a). The birth years of the breakeven generation in Europe, Canada, and the United States are sensitive to the model specification. Using the short-term net benefits, none of the age cohorts studied (age cohorts born between 1920 and 2020) breaks even the costs and benefits of climate change mitigation in Canada and most Western European countries, and the breakeven generation in the United States is born in 1994. This is because, in colder regions, the temperature increase has neutral or positive effects on the economy in the short-term. When considering the long-term net benefits, the breakeven generation are born prior to 1970 in Canada, the United States, and Western Europe, and more than three-quarters of the current population are born after the breakeven birth year (Fig. S3).

Among the upper-middle-income countries (Fig. 2b), the breakeven generations are the youngest (born after 1990 or nonexistent) in Russia and South Africa, while they are the oldest in Latin American countries (born before 1970). In Russia, only 0–31% of the current population are born after the breakeven generation (Fig. 2e and Fig. S3e). In contrast, in Brazil and Mexico, >75% of the current population are born after the breakeven generation. The birth years of the breakeven generation in Asia are uncertain due to the model specification, ranging from 1970 to infinity (nonexistence). In China, none of the age cohorts breakeven the costs and benefits when using the short-term net benefits, but two-thirds of the current population are born after the breakeven birth year when using long-term net benefits.

In lower-middle- and low-income countries (Fig. 2c, d), the breakeven generation are generally born before 1990. As the population is younger in lower-middle and low-income countries, more than half of the current populations are born after the breakeven birth year in

the majority of these countries (Fig. 3e and Fig. S3e). The breakeven generations are the oldest in South Asia and Latin America; >75% of the population are born after the breakeven generation. In India, Pakistan, and Bolivia, the breakeven generation are all born between 1950 and 1970. In Southeastern Asia, the breakeven generations are born before 1980. The breakeven generations in Africa are born during 1980–1990, and are 10–30 years younger than Latin America and South Asia.

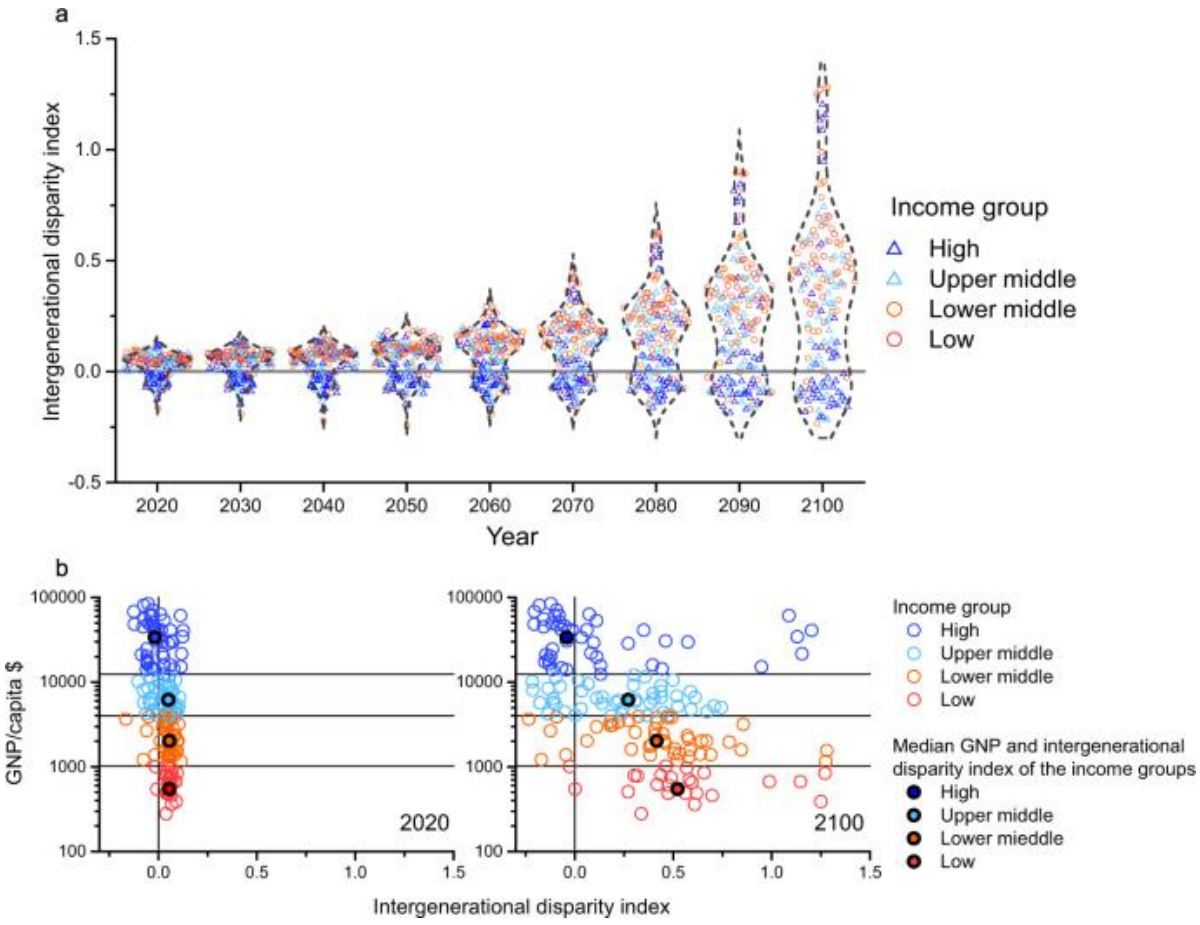


**Fig. 3: Intergenerational disparity among high-, upper-middle-, lower-middle-, and low-income countries using the short-term benefits.**

(**a**) The distribution of the intergenerational disparity index from 2020 to 2100. (**b**) Intergenerational disparity index and GNP (gross national product) per capita (using 2018 GNP per capita) in 2020 and 2100. In (**a**), a triangle symbol represents a higher-income country, and a circle symbol represents a lower-income country. In (**b**), a circle symbol represents a country, and a solid circle with the black edge represents the median GNP and the median intergenerational disparity index of an income group. In (**a**, **b**), the color of a symbol represents the income group of a country. The intergenerational disparity index is calculated as the percentage change in lifetime GDP per capita among the 25-year-old cohort minus that among the 75-year-old age cohort. Here, the intergenerational disparity index is calculated using the short-term benefits.

### 3. Future intergenerational cost-benefit disparity

The intergenerational disparity index (IDI) is calculated in this paper as the percentage change in lifetime GDP per capita among the 25-year-old age cohort minus that among the 75-years-old age cohort. For example, if the 25-year-old age cohort gains 10% of lifetime GDP per capita, and the 75-year-old age cohort loses 10% of lifetime GDP per capita, the intergenerational disparity index is 0.2 (0.1 – (−0.1)). A larger absolute value of IDI in a country indicates that the economic disparity between the young and the old under climate change mitigation is severe.

Here, we project IDIs from 2020 to 2100, and find that the intergenerational disparity is widening using the short-term net benefits. Specifically, IDIs become larger in countries with lower income over time (Fig. 3). In 2020, IDIs are <0.1 in most countries (Fig. 3b). After 2020, the intergenerational disparity grows significantly, particularly in countries with lower

income. In 2020, the median IDI is 0.05 for lower-middle-income countries and 0.06 for low-income countries. However, in 2100, the median of IDI increases to 0.42 for lower-middle-income countries and 0.52 for low-income countries. For upper-middle-income countries, IDI also increases; the median value increases from 0.05 in 2020 to 0.27 in 2100.

For high-income countries, the intergenerational disparity is the smallest compared with other income groups. From 2020 to 2100, IDI remains within −0.25 to 0.25 for most high-income countries. In 2100, the median IDI for high-income countries is only −0.04. In many high-income countries, the negative IDI indicates that the climate change mitigation under the Paris Agreement favors older age cohorts than younger age cohort in terms of lifetime GDP per capita.

On a global scale, the intergenerational disparity is widening the most in Latin America, Africa, and Western and Southern Asia (Fig. S4). From 2020 to 2100, IDIs in these countries increase from less than 0.1 to over 0.25. Furthermore, in Saudi Arabia, Sudan, Niger, and Mauritius, IDI is over 1, whereas they remain within less than 0.25 in Eastern Asia, Europe, and North America.

The use of long-term net benefits results in a similar trend (Fig. S5). IDIs are increasing over time, and they become larger in countries with lower income. In low-income countries, the median IDI increases from 0.04 (2020) to 0.34 (2100). In lower-middle-income countries, upper-middle-income countries, and low-income countries, the median IDI increases from 0.05 to 0.31, 0.28, and 0.23 during 2020–2100.

### *D. Discussion*

In this paper, we find a large cost-benefit disparity among age cohorts under the Paris Agreement. On a global level, the older age cohorts born before 1960 hardly gain in climate

change mitigation, while younger age cohorts born after 1990 are gaining large net benefits. This result indicates that younger generations may be more strongly motivated to mitigate climate change, which is well-aligned with the prevailing narrative that tries to explain the rise of the younger generation in the global climate movement.

However, country-level analysis paints a somewhat more complex picture. Our results based on the short-term damage function of climate change, for example, show that no age cohorts enjoy net benefit from climate change mitigation in most Western European countries in 2020. Therefore, the rise of the younger generation among Western European countries in climate movement cannot be explained by the economic self-interest under the short-term damage function, while using the long-term damage function, we find that younger age cohorts in Western Europe also benefit from climate change mitigation.

In addition, our results may provide an insight on the attitude toward climate change mitigation. Should the level of support to climate change mitigation be positively correlated to the net lifetime benefits from climate change mitigation, lower-income (lower-middle- and low-income) countries are likely to see more support to climate change mitigation from older generations, because more than half of the current population are born after the breakeven generation in most low-income countries. Likewise, the climate change mitigation effort is likely to face challenges in Eastern Europe, because, regardless of the model specification, less than half of the current population in Eastern Europe are likely to gain net benefits from climate change mitigation.

Furthermore, our results also show that the cost-benefit disparity between the old and the young under climate change mitigation is widening in almost all countries over time. Although all age cohorts may gain from climate change mitigation, the benefits of younger

age cohorts are much larger than that of older age cohorts. By 2100, the intergenerational disparity in most countries is over fivefold larger than that in 2020. Particularly, we find that countries with lower-income experience larger intergenerational disparity over time. The widening intergenerational disparity in the costs and benefits of climate change mitigation indicates that building consensus across generations on climate policy may not become any easier in the future. Our results provide a new insight on intergenerational equity of climate change mitigation. Closing the economic disparity among age cohorts may require different climate policies to different age cohorts. The increase in renewable asset price may alleviate the intergenerational disparity under climate change mitigation, given that different age cohorts hold varying amounts of renewable assets[87]. Our study shows that the cost-benefit distribution among age cohorts can be an important consideration for policy makers when designing tax and fiscal policies in response to climate change mitigation.

## *E. Appendix*

### 1. Data and code availability

The income distribution data used in this study are available in the OECD database (https://www.oecd.org/social/income-distribution-database). The life expectancy and age structure data are available in World Bank Open Data (https://data.worldbank.org/) and World Population Prospect (https://population.un.org/wpp/DataQuery/). The data used for replicating our analysis have been deposited in the Data for paper Economic disparity among generations under Paris Agreement[103] database under accession code https://doi.org/10.5281/zenodo.5103739. The data used to generate the interactive website have been deposited in the Data and code for the shiny app of the paper Economic disparity among generations under Paris Agreement[104] database under the accession code

https://doi.org/10.5281/zenodo.5104877. Data visualization for the analysis of other SSP and RCP scenarios can be found on our shinny app (https://climate-change.shinyapps.io/generation_disparity/). Source data are provided with this paper.

R 3.6.1 and MATLAB 2019b are used to process the data. R 3.6.1 and Origin 2019 are used for data visualization. All the scripts used in our data collection, data analysis, and data visualization are available at https://github.com/climate-change-ucsb/generation-disparity.

## 2. Supplementary Notes: Extended background on IAMs

Here we classify the current the economic modules of IAMs into three categories based on the literature[93].

### 2.1 General Equilibrium model

Computational General Equilibrium (CGE) models are an algebraic representation of the intricate functioning of a market economy based on the economic equilibrium theory. By maximizing consumer utility and producer profits, the supply and demand are in equilibrium. The general way that CGE models are used for policy analysis is to change one or more of the exogenous parameters of the economy and compute the new equilibrium. Comparing the new counterfactual equilibrium to the initial equilibrium, including activity levels, prices and utility, provides insights about the effect of a "shock" on the economy.

IAMs using the CGE principles include: AIM/CGE, GEM, REMIND, WITCH and IMACLIM.

### 1.2 Partial Equilibrium model

Partial equilibrium analysis differs from general equilibrium modelling primarily by focusing on a specific market or sector. Partial equilibrium analysis is used extensively to estimate the impacts of climate change in different sectors of the economy.

IAMs using the partial equilibrium model include: GCAM, MESSAGE, TIAM-UCL.

### 1.3 Energy system models

Energy system models can broadly be classified as optimization models or simulation models. Optimization models use information on costs and constraints of technology characteristics to identify the "best", "least-cost" or "optimal" technology. The

consumer is assumed to be rational, and energy supplies are allocated to energy demands, based on minimum lifecycle technology costs.

IAMs using the energy system models include: MESSAGE, DNE21+.

### 3. Supplementary Tables

**Table S1. The ratio of the age-specific income versus the mean income at country level.**

| Country/Age | 0-17 | 18-25 | 26-40 | 41-50 | 51-65 | 65-75 | >75 |
|---|---|---|---|---|---|---|---|
| Australia | 0.91 | 1.14 | 1.06 | 1.05 | 1.11 | 0.83 | 0.64 |
| Austria | 0.87 | 1.06 | 0.93 | 1.07 | 1.14 | 0.95 | 0.92 |
| Belgium | 0.95 | 1.07 | 1.02 | 1.07 | 1.12 | 0.85 | 0.73 |
| Canada | 0.92 | 1.01 | 0.99 | 1.06 | 1.11 | 0.94 | 0.87 |
| Chile | 0.87 | 0.92 | 1.18 | 1.05 | 1.03 | 0.96 | 0.90 |
| Costa Rica | 0.77 | 0.98 | 1.10 | 1.11 | 1.15 | 1.03 | 0.92 |
| Czech Republic | 0.97 | 1.07 | 1.09 | 1.10 | 1.08 | 0.76 | 0.68 |
| Denmark | 1.00 | 0.85 | 0.96 | 1.12 | 1.20 | 0.87 | 0.73 |
| Estonia | 1.07 | 1.02 | 1.14 | 1.10 | 1.00 | 0.74 | 0.60 |
| Finland | 1.00 | 0.85 | 0.99 | 1.14 | 1.17 | 0.90 | 0.72 |
| France | 0.91 | 0.94 | 0.94 | 1.04 | 1.16 | 1.04 | 0.94 |
| Germany | 0.93 | 0.91 | 0.96 | 1.10 | 1.16 | 0.93 | 0.85 |
| Greece | 0.92 | 0.93 | 1.04 | 1.01 | 1.10 | 1.01 | 0.88 |
| Hungary | 0.93 | 1.03 | 1.06 | 1.06 | 1.01 | 0.94 | 0.91 |
| Iceland | 0.92 | 1.07 | 0.89 | 1.05 | 1.18 | 1.04 | 0.78 |
| Ireland | 0.94 | 1.10 | 1.03 | 1.04 | 1.12 | 0.86 | 0.75 |
| Israel | 0.87 | 0.99 | 0.99 | 1.09 | 1.23 | 1.11 | 0.92 |
| Italy | 0.86 | 0.99 | 0.96 | 0.99 | 1.17 | 1.08 | 0.92 |
| Japan | 0.95 | 1.06 | 1.01 | 1.10 | 1.16 | 0.90 | 0.85 |
| Korea | 1.00 | 1.11 | 1.06 | 1.09 | 1.07 | 0.73 | 0.56 |

| | | | | | | | |
|---|---|---|---|---|---|---|---|
| Latvia | 1.07 | 1.08 | 1.19 | 1.12 | 0.95 | 0.75 | 0.59 |
| Lithuania | 0.94 | 1.13 | 1.13 | 1.10 | 1.08 | 0.75 | 0.66 |
| Luxembourg | 0.90 | 0.89 | 0.98 | 1.06 | 1.07 | 1.11 | 1.02 |
| Mexico | 0.81 | 1.11 | 1.09 | 1.06 | 1.22 | 0.98 | 0.84 |
| Netherlands | 0.97 | 0.91 | 1.00 | 1.09 | 1.12 | 0.91 | 0.77 |
| New Zealand | 0.83 | 1.01 | 0.98 | 1.12 | 1.25 | 0.95 | 0.71 |
| Norway | 0.95 | 0.86 | 0.93 | 1.08 | 1.23 | 1.01 | 0.77 |
| Poland | 1.00 | 0.98 | 1.09 | 1.04 | 0.99 | 0.86 | 0.86 |
| Portugal | 0.94 | 0.96 | 1.03 | 1.00 | 1.05 | 1.07 | 0.90 |
| Slovak Republic | 0.87 | 1.04 | 1.07 | 1.05 | 1.08 | 0.89 | 0.82 |
| Slovenia | 0.98 | 1.09 | 1.03 | 1.07 | 1.03 | 0.89 | 0.80 |
| Spain | 0.92 | 0.99 | 0.95 | 1.02 | 1.13 | 1.02 | 0.88 |
| Sweden | 0.95 | 0.99 | 0.96 | 1.10 | 1.21 | 0.97 | 0.70 |
| Switzerland | 0.89 | 1.04 | 1.00 | 1.09 | 1.16 | 0.88 | 0.76 |
| Turkey | 0.84 | 0.98 | 1.10 | 1.11 | 1.14 | 0.89 | 0.81 |
| United Kingdom | 0.91 | 1.04 | 1.04 | 1.15 | 1.08 | 0.89 | 0.77 |
| United States | 0.87 | 0.93 | 1.02 | 1.09 | 1.16 | 1.02 | 0.81 |
| Brazil | 0.75 | 0.97 | 1.04 | 1.10 | 1.24 | 1.18 | 1.18 |
| Bulgaria | 0.94 | 1.04 | 1.15 | 1.18 | 1.07 | 0.73 | 0.59 |
| China (People's Republic of) | 0.85 | 1.06 | 1.14 | 1.03 | 1.06 | 0.85 | 0.82 |
| India | 0.84 | 1.04 | 1.03 | 1.15 | 1.15 | 1.07 | 1.12 |
| Romania | 0.90 | 0.97 | 1.13 | 1.09 | 1.06 | 0.87 | 0.75 |

| | | | | | | | |
|---|---|---|---|---|---|---|---|
| Russia | 0.87 | 1.01 | 1.07 | 1.09 | 1.07 | 0.83 | 0.79 |
| South Africa | 0.76 | 0.90 | 1.07 | 1.36 | 1.47 | 0.94 | 0.99 |
| Other | 0.85 | 1.01 | 1.07 | 1.10 | 1.07 | 0.87 | 0.82 |

**Table S2. Regional relative cost of climate change mitigation versus global relative cost** [92]**.**

The relative cost is computed as the cumulative costs of mitigation over the period 2020 – 2100 divided by cumulative GDP over that period.

| Region | Median | 25% percentile | 75% percentile |
|---|---|---|---|
| OECD 1990 | 0.47 | 0.41 | 0.61 |
| Asia | 1.47 | 1.19 | 1.64 |
| Middle East and Africa | 2.29 | 1.79 | 2.79 |
| Latin America | 0.99 | 0.92 | 1.15 |
| Economies in Transition | 1.99 | 1.39 | 2.49 |

## 4. Supplementary Figures

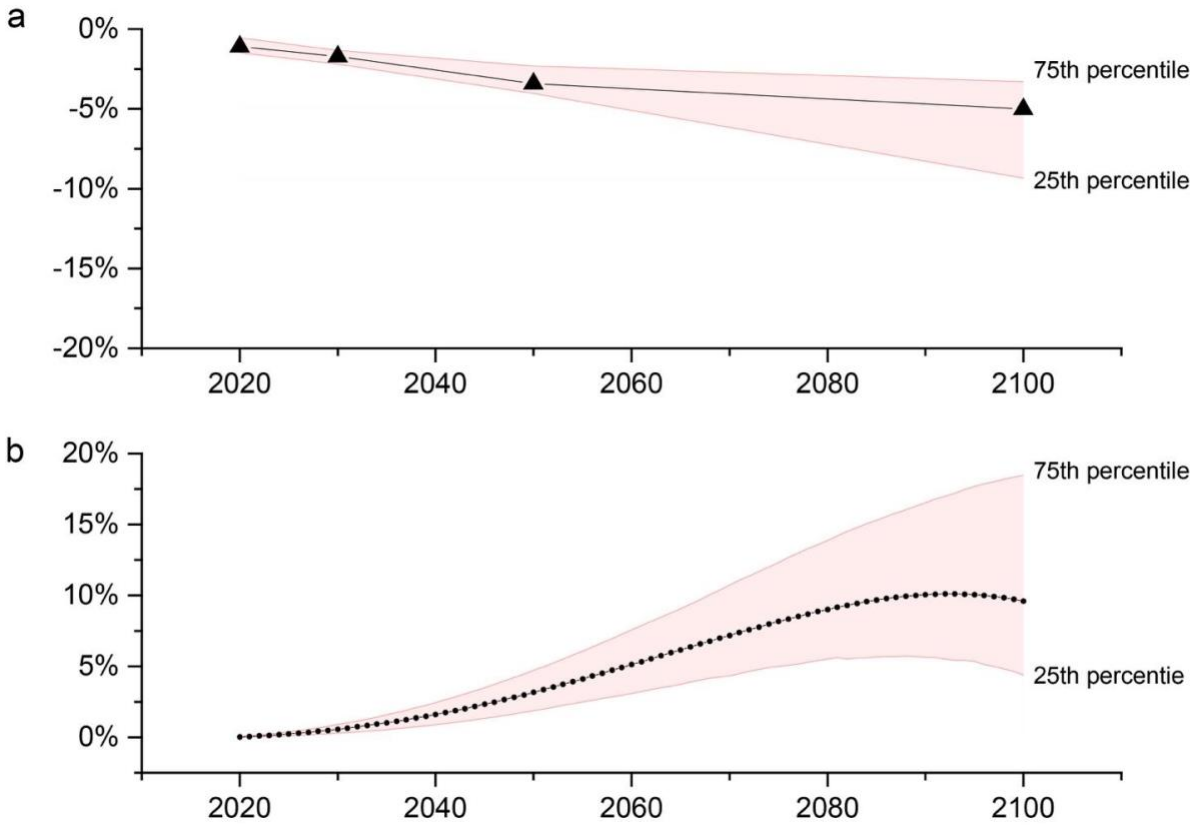


**Figure S1. Time series of the costs and benefits from 2020 – 2100.**

**a** Global cost of climate change mitigation relative to global GDP. **b** Global benefits of climate change relative to global GDP. Data are presented as median values with 25% and 75% percentile, n=17 climate models in (**a**) and n=1000 replicates in (**b**).

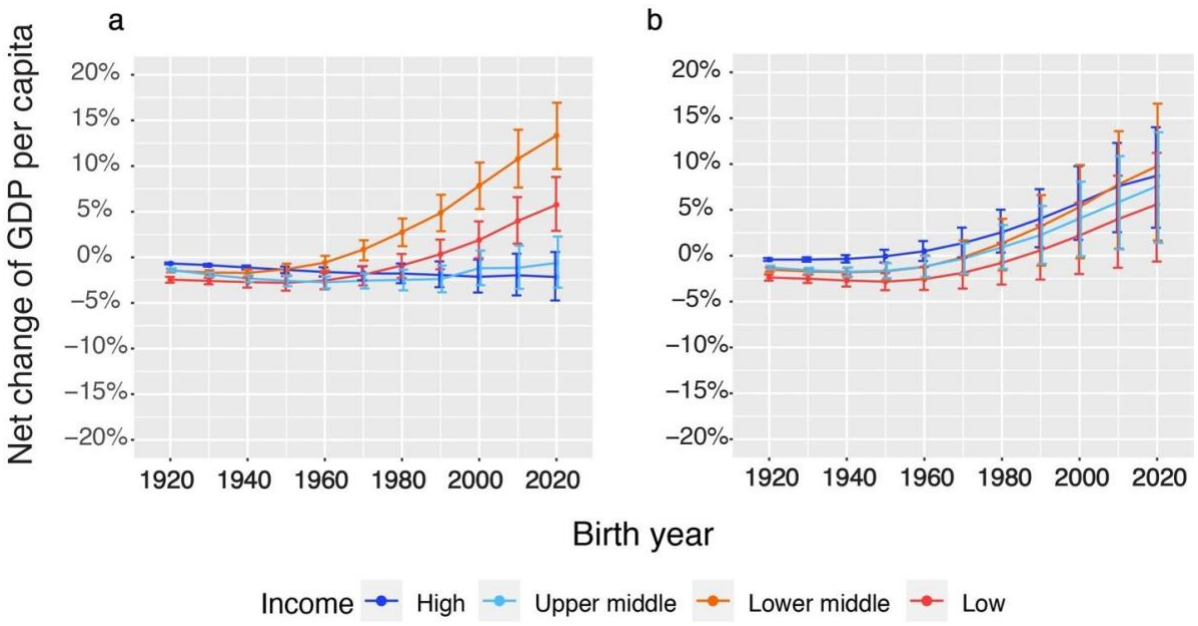


**Figure S2. The uncertainty of the population-weighted change of GDP per capita by income group when using different model specification to evaluate the temperature effects on GDP growth.**

The population-weighted average of the percentage change of GDP per capita by income group using **a** short-term BHM damage function, **b** long-term (5-year lag) BHM damage function.

The data are presented as median values, and the error bar represents the 25% and 75% percentile level, n=47 high-income countries, n=50 upper-middle-income countries, n=43 lower-middle-income countries and n=29 low-income countries.

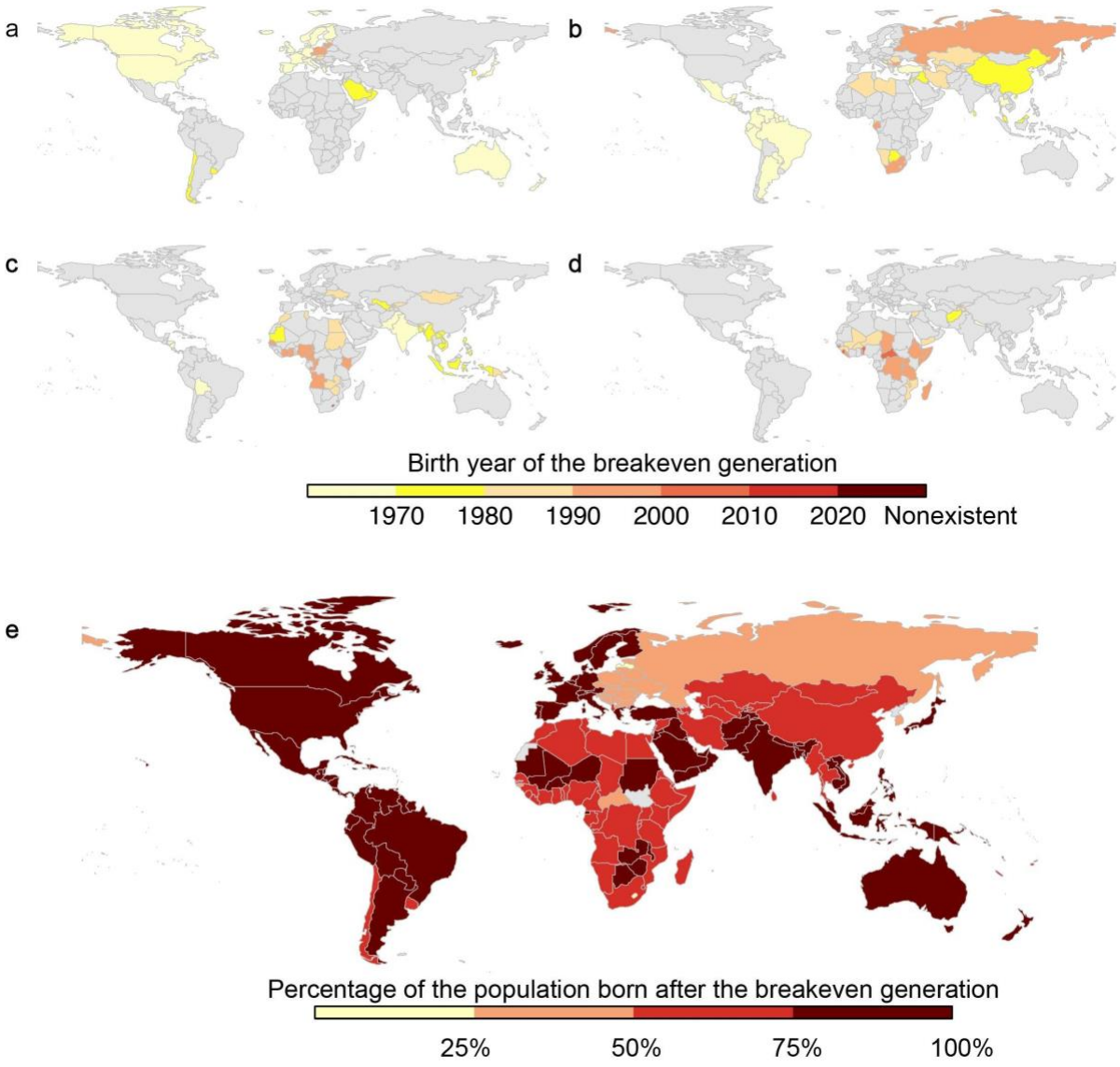


**Figure S3. Breakeven generation and the percentage of population born after the breakeven generation using the long-term net benefits.**

The birth year of the breakeven generation in 2020 in **a** high-income countries, **b** upper-middle-income countries, **c** lower-middle-income countries and **d** low-income countries. **e** The percentage of population born after the breakeven generation. In (**a**) – (**d**), different colors represent different ranges for the birth years. In (**e**), different colors represent different ranges

for the percentage of the population. Here, we use the long-term benefits of climate change mitigation to measure the benefits of climate change mitigation.

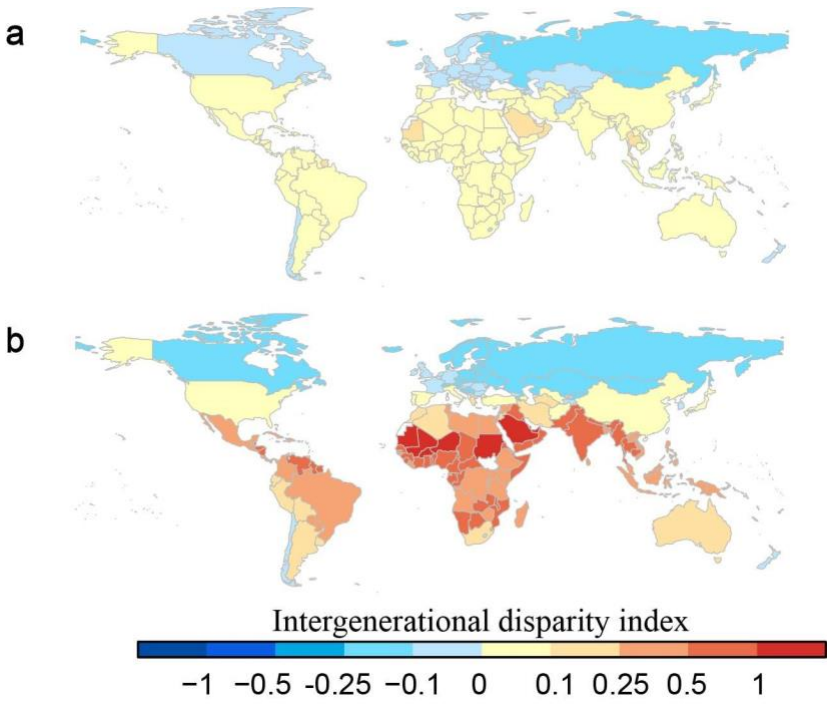


**Figure S4. The intergeneration disparity index using short-term net benefits of climate change mitigation.**

The intergeneration disparity index using short-term net benefits of climate change mitigation in **a** 2020 and **b** 2100.

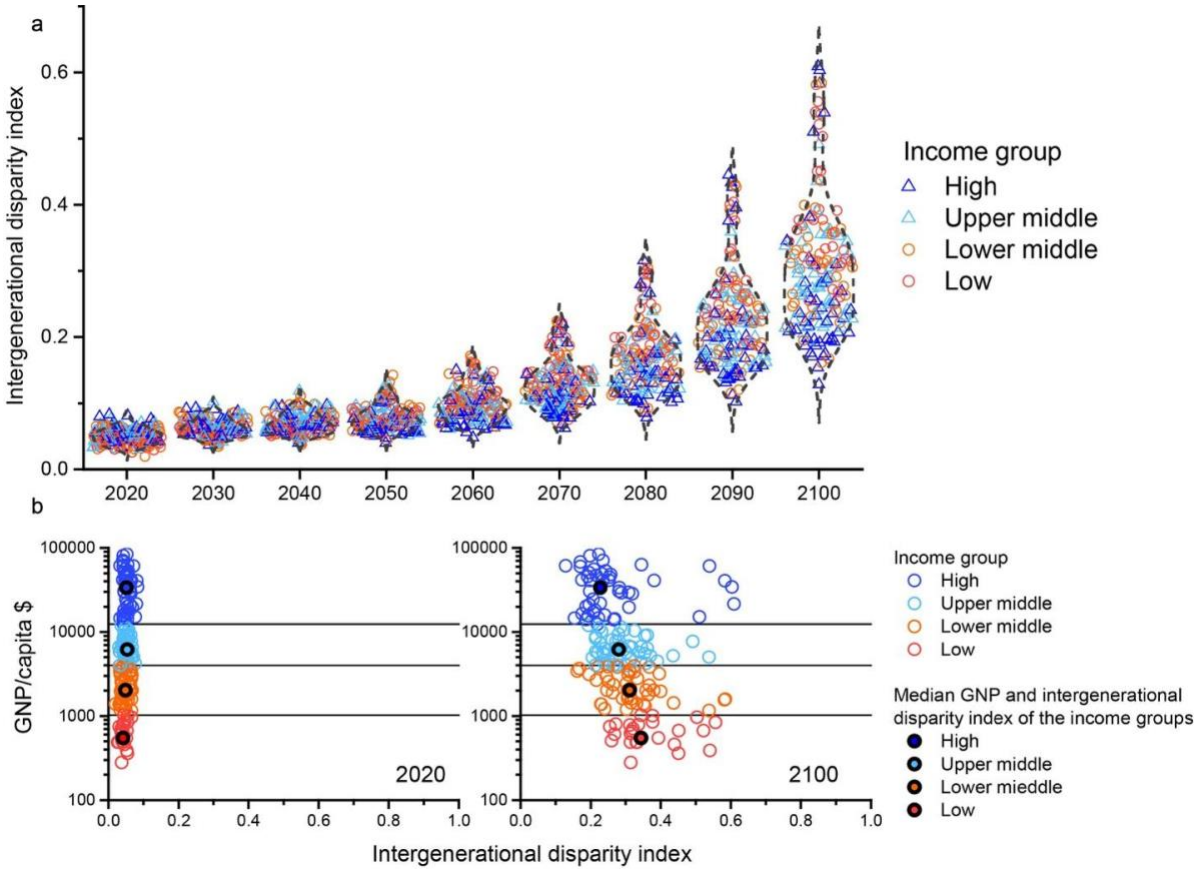


**Figure S5. Intergenerational disparity among high-, upper-middle-, lower-middle- and low-income countries using the long-term net benefits.**

**a** The distribution of the intergenerational disparity index from 2020 to 2100. **b** Intergenerational disparity index and GNP (gross national product) per capita (using 2018 GNP per capita) in 2020 and 2100. In (**a**), a triangle symbol represents a higher income country, and a circle symbol represents a lower income country. In (**b**), a circle symbol represents a country, and a solid circle with the black edge represents the median GNP and the median intergenerational disparity index of an income group. In (**a**) and (**b**), the color of a symbol represents the income group of a country. The intergenerational disparity index is calculated as the percentage change in lifetime GDP per capita among the 25-year-old age cohort minus that among the 75-year-old age cohort.

Here, the intergenerational index is calculated by assuming the long-term net benefits of climate change mitigation.

## IV. Global trans-continental power pools for low-carbon electricity system

Materials from: Yang, H., Deshmukh, R. & Suh, S. Global transcontinental power pools for low-carbon electricity. Nat Commun 14, 8350 (2023). https://doi.org/10.1038/s41467-023-43723-z


### Abstract

The transition to low-carbon electricity is crucial for meeting global climate goals. However, given the uneven spatial distribution and temporal variability of renewable resources, balancing the supply and demand of electricity will be challenging when relying on close to 100% shares of renewable energy. Here, we use an electricity planning model with hourly supply-demand projections and high-resolution renewable resource maps, to examine whether transcontinental power pools reliably meet the growing global demand for renewable electricity and reduce the system cost. If all suitable sites for renewable energy are available for development, transcontinental trade in electricity reduces the annual system cost of electricity in 2050 by 5-52% across six transcontinental power pools compared to no electricity trade. Under land constraints, if only the global top 10% of suitable renewable energy sites are available, then without international trade, renewables are unable to meet 12% of global demand in 2050. Introducing transcontinental power pools with the same land constraints, however, enables renewables to meet 100% of future electricity demand, while also reducing costs by up to 23% across power pools. Our results highlight the benefits of expanding regional transmission networks in highly decarbonized but land-constrained future electricity systems.

### *A. Introduction*

To limit the global mean temperature increase relative to the pre-industrial era within 2°C by 2100, carbon dioxide ($CO_2$) emissions from fossil fuels must approach zero by the middle of this century[105,51]. Among anthropogenic sources, the electricity sector contributes about 40% of the global energy-related $CO_2$ emissions annually[106]. In addition, electrifying other sectors including transport and industry is a predominant carbon mitigation strategy. It is, therefore, crucial to decarbonize the electricity sector, especially using abundant renewable resources[92]. In recent decades, the cost of renewable energy, especially solar and wind, has declined substantially[107–109]. The levelized cost of electricity generated by solar and wind has become competitive compared to the electricity generated by fossil fuels and nuclear[109]. The global share of wind and solar generation in total electricity supply has risen from less than 1% in 2000 to nearly 10% in 2020[108].

The global potential of renewable electricity is immense—solar, wind and hydropower electricity can supply ~135, ~840 and ~50 petawatt hours (PWh) of electricity a year, respectively, according to some estimates[110–113]. If land suitability and availability are considered, the global potential for renewable energy is reduced to 50-400 PWh per year[114], which is still ~2-17 times higher than the 23 PWh[115] of global electricity consumption in 2018. However, the temporal variability of renewable resources may limit their potential for reliably meeting electricity demand[116]. Without energy storage and over-generation (more electricity generation than demand), wind and solar may fulfill only 70% - 90% of the current electricity demand[117]. Furthermore, renewable resources are unevenly distributed across space[112,114,118], further exacerbating the problem of spatiotemporal mismatch between

supply and demand. The uneven distribution of renewable resources also creates substantial variation in the cost of renewable electricity across countries and regions[114], undermining their cost-effectiveness, especially if renewable resources are developed to meet electricity demand only within national borders. Building regional power pools and increasing electricity trade can and has been pursued to address the spatiotemporal mismatch between renewable electricity generation and demand[119]. In fact, several regional power pools have been in operation in Europe, North America and Southern Africa[120]. Existing intercontinental transmission projects include the BritNed (United Kingdom and Netherlands), NordBalt (Sweden and Lithuania), and NordNed (Norway and Netherlands)[121]. In 2020, cross-border trade of electricity accounts for 2.8% of the global supply[122].

Expanding regional power pools to continental-scale power pools can further increase electricity trade, decrease costs, and enable the integration of near-100% shares of renewable energy. Guo et al.[123] and Zhao et al.[124] examined the implications of a global power pool by modeling electricity trade between continents and found an increase in the share of renewable energy with increasing trade. However, these studies did not examine a near-100% clean energy system. Other studies, specifically from the Lappeenranta University of Technology, examined the trade of electricity between subregions across continental-scale power pools with 100% renewable electricity systems (e.g. Europe[125], Sub-saharan Africa[126], Northeast Asia[127], and MENA[128]), but these studies do not incorporate country-level spatial resolution. Further, none of these studies examined the impact of land-use constraints on renewable energy resource availability and its resulting international electricity trade and system cost implications.

Here, we model the investments and operations of 100% renewable electricity systems across 211 countries and administrative areas in 2050, to quantify the benefits in reliability and system cost through introducing transcontinental power pools, compared to the case without electricity trade. Renewable resources analyzed in this study include solar photovoltaics, concentrated solar power, onshore wind, offshore wind, and hydropower. We use their supply potentials at a 0.01°×0.01° spatial resolution across the globe. The supply potentials are then mapped with the demand balance using 2050 demand projections and an electricity-system planning model at an hourly resolution. We map the supply potential and demand at hourly intervals, first, within each country (country scenario) and, second, across transcontinental power pools (transcontinental scenario); both with only renewables.

Using the electricity system model, we co-optimize the investment and operation of electricity generation, transmission and storage using a hourly temporal resolution in 365 days of a whole year. The demand projection follows the Sustainable Development Goal (SDG scenario) by IEA[129]. We assume a penalty of $100 million per MWh for the loss of load and a 1.6% transmission loss per 1000 kilometers[130]. We assume that the loss of load in the modeled 100% renewable energy system is exogenously satisfied by fossil fuels, and that the system cost of electricity comprises the cost of renewables, fossil fuels, and climate costs set at the social cost of carbon[131].

Under the transcontinental power pool scenario, we assume that countries within a continental region engage in electricity trade and share generation resources to meet their local electricity demand. We use six continental regions based on the current structure of global electricity trade[132] and proposed regional electricity networks[125,127,133–136]. These six regions are: Sub-Saharan Africa, East Asia & Russia (East Asia, South Asia, Central Asia

and Russia), Europe & MENA (Europe, Middle East and North Africa), North America, South America, and Southeast Asia & Oceania.

To understand the implications of land constraints on renewable energy potential, costs, and benefits of transcontinental power pools, we examine two cases of land availability for renewable energy siting. First, all suitable sites for renewables are available for development. However, not all potential renewable resources can be tapped for electricity generation due to constraints on land availability not captured by available geospatial datasets, including ecological impacts, market accessibility, and local political support[118,137]. Therefore, in the second case, for each renewable energy technology (excluding rooftop PV), we assume that only the top 10% of suitable sites at the global level[118] are available for energy development. We rank and select the top 10% renewable resources based on a composite index of resource yield (annual capacity factor), land use, infrastructure, and market accessibility (see Method section).

### *B. Methods and Materials*

In the method section, we first measured the development potential of renewable resources. Then we simulated the investment and operation of renewable capacities under the country scenario and the transcontinental scenario, and estimated the costs of electricity to meet the electricity demand in 2050.

#### 1. Development potential

We used a published database to quantify the development potential for renewable energy that is not yet developed at a 0.01°×0.01° resolution[118]. Multiple factors including resource yield, market accessibility, population density, infrastructure condition, and land

cover were considered to measure the development potential of solar, wind, and hydroelectricity,

$$DPI = w_1 \cdot RY + w_2 \cdot DEG + w_3 \cdot DMR + w_4 \cdot LC + w_5 \cdot DUA + w_6 \cdot DRP + w_7 \cdot IPD \quad (1)$$

where DPI is the development potential index; *w* is the relative weight for each criterion (Table 1); RY is the resource yield, which is measured as the capacity factor; DEG is the distance to electrical grid; DMR is the distance to major roads; LC is the land cover; DUA is the distance to the urban area; DRP is the distance to railway or ports; IPD is the inverse of the population density.

The relative weights were derived using the analytical hierarchy process. The development potential is classified into 6 levels: very high (top 10%), high (top 10-25%), medium high (top 25-50%), medium low (50-bottom 25%), low (bottom 25%-10%) and very low (bottom 10%). More detailed information and data can be found in Oaklief et al.

**Table 1**. Relative weights for the criteria used in the development potential index.

| | RY | DEG | DMR | LC | DUA | DRP | IPD |
|---|---|---|---|---|---|---|---|
| CSP | 0.45 | 0.24 | 0.12 | 0.11 | 0.051 | 0.03 | |
| PV | 0.45 | 0.23 | 0.12 | 0.12 | 0.069 | 0.03 | |
| Wind | 0.42 | 0.23 | 0.11 | 0.07 | 0.023 | 0.11 | 0.04 |
| Hydropower | 0.45 | 0.11 | 0.05 | | 0.05 | 0.03 | 0.31 |

The Oaklief database does not include offshore wind and rooftop PV. For the offshore wind, we used the levelized cost to measure the development potential. We only considered the offshore areas which are within 200 kilometers of the coast. We also

excluded the protected areas[138], sea ice[139], and areas where wind speeds are less than 8 m/s. For rooftop solar, all the available urban areas are considered to have a very high potential.

**2. Potential of renewable resources**

In our main scenario, for each type of renewable energy technology, we chose a) all suitable renewable energy sites, and b) renewable energy sites with very high development potential (global top 10% suitable sites).

In a pixel *x*, we chose the renewable technology with the least levelized cost if multiple technologies are available. The capacity of renewable energy technology *t* in a pixel *x* ($C_{t,x}$) is calculated as,

$$C_{t,x} = l_t \cdot A_x \ (2)$$

where $A_x$ (km$^2$) is the area of the pixel *x*, $l_{t,x}$ (MW/km$^2$) is the land use factor for renewable energy technology *t*.

The capacity of renewable energy *t* ($C_t$) in a country equals the summation of the renewable capacity in each pixel ($C_{t,x}$) within the country.

$$C_t = \sum_x C_{t,x} \ (3)$$

$g_{t,x}$ is the maximum electricity generation in a year (8760 hours) for renewable energy *t* in the pixel *x*,

$$g_{t,x} = r_{t,x} \cdot C_{t,x} \cdot 8760 \ (4)$$

where $r_{t,x}$ is the capacity factor of renewable energy technology *t* in the pixel *x*.

$g_t$, the maximum generation of renewable energy *t* in a country, is the summation of electricity generation in pixels within a country,

$$g_t = \sum_x g_{t,x} \ (5)$$

$r_t$, the annual average capacity factor of renewable energy technology *t* in a country, is calculated as,

$$r_t = g_t/(C_t \cdot 8760) \text{ (6)}$$

The land use factors were compiled from NREL[140–142]. As the land use factor reported in NREL is measured in the alternating current power capacity per km$^2$, the land use factor for PV power plants was converted between the alternating current and direct current power capacity by a factor of 1.17[141] (Table 6). The annual hydroelectricity generation per pixel was compiled from Hoes et al.[113].

On average, 138 MW rooftop PV ($L_{rooftop}$) can be installed per square kilometer (direct area)[142]. The land use factor for rooftop PV ($l_{rooftop}$) is discounted by the ratio of rooftop area in 1 km$^2$ urban area[143] ($\mu$) and the share of suitable rooftop areas ($s$)[114] (Table S7).

$$l_{rooftop} = L_{rooftop} \cdot \mu \cdot s \text{ (7)}$$

Following the method in Wu et al.[137], the capacity factor for solar PV in a pixel ($r_{PV,x}$) is calculated as the ratio of the global titled irradiation (W/m$^2$) in a pixel and the peak solar density of 1000 W/m$^2$, adjusted for efficiency losses,

$$r_{PV,x} = \frac{GTI_x \cdot (1-\eta_0)(1-\eta_\iota)}{1000} \text{ (8)}$$

where $GTI_x$ (W/m$^2$) is the global irradiation for optimally tilted surface in pixel *x*, and was collected from the Global Solar Atlas[144]; $\eta_0$ is the outage rate; $\eta_\iota$ is the inverter and AC wiring efficiency losses. $\eta_0$ and $\eta_\iota$ were collected from Wu et al.[137].

The capacity factor of concentrated solar power with no storage in a pixel ($r_{CSP,x}$) is calculated following the empirical linear relationship between the capacity factor and direct normal irradiation[137],

$$r_{CSP,x} = 22.293ln\,(DNI_x)\ - 145.69\ (9)$$

where $DNI_x$ is the direct normal irradiation at pixel *x* and was collected from the Global Solar Atlas, which derives the average annual capacity factor using daily data from 1994 to 2017.

The capacity factor for wind power in a pixel ($r_{wind,x}$) was calculated based on the wind speed,

$$r_{wind,x} = r_{IEC\ class\ I,x}\ , wind\ speed > 8.5\ m/s\ (10.1)\quad r_{wind,x} = r_{IEC\ class\ II,x}, 7.5\ m/s <$$

$$wind\ speed\ \leq 8.5\ m/s\ (10.2)$$

$$r_{wind,x} = r_{IEC\ class\ III,x}, wind\ speed\ \leq 7.5\ m/s\ (10.3)$$

where $r_{IEC\ class\ I,x}$ is the capacity factor for IEC class I wind turbines; $r_{IEC\ class\ II,x}$ is the capacity factor for IEC class II wind turbines; $r_{IEC\ class\ III,x}$ is the IEC class III wind turbines. The average annual capacity factors and wind speeds were collected from the Global Wind Atlas[145] using 2008-2017 data.

The capacity factor for hydropower in a pixel ($r_{hydro,x}$) and the generation of hydropower were derived from Hoes et al.

$$r_{hydro,x} = 0.5\ (11)$$

**3. Electricity planning model**

We used the GridPath model[146] (https://github.com/blue-marble/gridpath), an open-source power system model, to optimize the capacity and generation of energy infrastructure (hydropower, solar, wind, storage, and transmission) in 2050, following a least-cost

principle. We optimized the capacity investment with only renewables and storage by using a hourly temporal resolution within a whole year. In the optimization model, the penalty cost for the loss of load is $100 million/MWh. The loss of load in the model will be exogenously met by fossil fuel power plants. The levelized cost of electricity includes the cost of renewable energy, the cost of fossil fuels and the social cost of carbon.

The existing capacities for solar, wind, and pumped hydro storage were collected from EIA[147]. The storage duration for the pumped hydro storage is assumed to be 10 hours. Under the transcontinental scenario, we include the existing transmission lines in Europe from Brinkerink et al[148]. We derived the capital and O&M costs (Tables S6, S8 and S9) and the cost projections (2020-2050, Tables S10 and S11) from International Renewable Energy Agency (IRENA)[107] and 2022 Annual Technology Baseline (ATB) by National Renewable Energy Laboratory (NREL)[149]. We collected the transmission loss and cost for HVDC transmission lines (Table S9) from Bogdanov et al .[130] The length of a transmission line between countries is the distance of the population centroid between countries[150].

The capacity of the renewable potential derived above is treated as the maximum capacity for new renewable capacities in each country. The planning-reserve margin is 15% of the peak load for each country. We assumed that the maximum discharge duration is 24 hours for the battery storage, and that the battery storage is only used to balance supply and demand within a day. The monetary values are all undiscounted 2050 values. Under the country scenario, no transmission lines between countries are built, and under the transcontinental scenario, HVDC transmission lines are built to link all countries within the region.

Hourly profiles for solar and wind, and load demand were derived from Tong et al.[117], which provided hourly profiles for wind and solar and load in 2018 for 42 major countries and 23 subregions. For the countries that are not included in the 42 major countries, we assumed that their generation and load profiles follow the regional profile. For hydropower, we used a monthly profile derived from IEA monthly data[151] (2015-2021). For countries without hydropower data, we assumed the monthly profile is the same as nearby countries. As there is no IEA data for African countries, we assumed the monthly capacity factor to be 0.5.

The hourly generation profile for solar and wind, and the monthly profile for the hydropower were derived as follows:

$$r_{t,h,m} = \frac{r_t}{r_t^{2018}} \cdot r_{t,h,m}^{2018} \quad (12)$$

$r_{t,h,m}$ is the capacity factor for renewable energy technology *t* at hour *h*, month *m*; $r_t^{2018}$is the annual average capacity factor in 2018 from Tong et al; $r_{t,h,m}^{2018}$ is the capacity factor for renewable energy technology *t* in 2018 at hour *h*, month *m*.

**4. Demand scenarios**

In the main scenario, we assumed that the growth rates of electricity demand during 2030-2050 follow the IEA projection under the Sustainable Development Goal (SDG scenario). In the sensitivity test, we assumed that the growth rates of electricity demand follow the IEA projection under the Net Zero 2050 scenario (NZE scenario)[152]. The electricity demand in the year 2018 was collected from the Energy Information Administration (EIA)[115]. The growth rates for the two scenarios can be found in Table S12.

**5. Country scenario**

The unmet electricity demand by renewables ($short_n$) in the country *n* under the country scenario was calculated as the difference of load demand ($load_n$) and renewable electricity production ($production\_re_n$),

$$short_n = load_n - production\_re_n \quad (13)$$

The total cost of electricity demand in the country *n* under the country scenario ($cost\_country_n$) is the aggregation of renewable electricity cost ($cost\_re_n$) and fossil fuel electricity cost ($cost\_fossil_n$) in the country *n*,

$$cost\_country_n = cost\_re_n + cost\_fossil_n \quad (14)$$

The unmet demand is assumed to be met by fossil fuels. The fossil fuel electricity cost ($cost\_fossil_n$) includes the cost of fossil fuel power plants and the carbon tax,

$$cost\_fossil_n = (\overline{lcoe\_fossil}_n + scc \cdot \bar{c}i_n) \cdot short_n \quad (15)$$

where $\overline{lcoe\_fossil}_n$ is the generation-weighted average cost of fossil fuels in country *n*; $\bar{c}i_n$ is the generation-weighted average $CO_2$ intensity of fossil fuels (ton/MWh) in the country *n*. *scc* is the social cost of carbon (i.e., carbon tax), which is \$81/tonne $CO_2$ in 2050[131] under a 3% social discount rate. The coal-gas generation mix was derived from world bank[99], and the cost is 95\$/MWh for coal and 90 \$/MWh for natural gas[53]; the $CO_2$ intensity for coal and natural gas was collected from NREL ATB.

The system cost of electricity in the country *n* under the country scenario ($lcoe\_country_n$) is the cost per load demand,

$$lcoe\_country_n = \frac{cost\_country_n}{load_n} \quad (16)$$

**6. Transcontinental scenario**

Under the transcontinental scenario, the total cost of electricity in a power pool (total_cost_continent) is the aggregation of renewable electricity cost (total_cost_re), fossil fuel cost (total_cost_fossil), and the transmission cost (total_cost_trans),

$$total\_cost\_continent = total\_cost\_re + total\_cost\_fossil + total\_cost\_trans \quad (17)$$

The system cost in the country *n* ($lcoe\_continent_n$) is equal to the demand-weighted average system cost in a power pool,

$$lcoe\_continent_n = \frac{total\_cost\_continent}{total\_load} \quad (18)$$

where total_load is the total load demand in a power pool.

The change of system cost ($\Delta cost$) compared to the country scenario is,

$$\Delta cost = lcoe\_continent_n - lcoe\_country_n \quad (19)$$

### *C. Results*

**1. Mismatch between renewable resources and electricity demand**

Globally, with all suitable land for renewable resources, the renewable potential reaches ~3500 PWh. If each country sources renewable resources within their national border to meet their national demand, renewable resources can supply 42 PWh of global electricity demand, but are 0.8 PWh or 2% short of the global annual demand in 2050 (Fig 1a).

We find that renewables alone reliably meet 100% of electricity demand in three quarters of the countries. However, they fall short in meeting hourly demand in several countries. Notably, in South Korea, the renewable potential (0.6 PWh) is lower than the

demand (1.1 PWh) by 0.5 PWh, leading to over 30% of unmet demand. In Switzerland, although the renewable potential (0.14 PWh) exceeds the annual demand (0.08 PWh), 0.01 PWh or 16% of the demand is not met by renewables alone. This is because the battery storage only balance the diurnal variability of renewable energy, and cannot balance the seasonal variation.

If only the top 10% suitable land is used, the global renewable potential is reduced by 80% to 665 PWh. Globally, 4.1 PWh of demand shortage is solely caused by a lack of aggregate renewable resources within the country boundary (Fig. S1). After considering the temporal mismatch between renewable energy generation and demand, the renewable potential is 5.2 PWh or 12% short of annual electricity demand, if sourced within each national border (Fig 1b). Because of the temporal variation in renewable energy generation, some countries cannot meet their demand by only renewables even if their annual renewable potential exceeds demand. For example, India is unable to meet ~11% of its demand with renewables alone because the renewable potential is only 1% higher than the demand. On the other hand, abundant resources are unutilized in countries with rich endowments of renewables. In China, for example, about one-third of the renewable potential is not utilized, if consumed only within the national border. In the United States, Brazil and Saudi Arabia, the potential of renewable resources is higher than the annual demand by an order of magnitude.

Under the constrained land availability scenario, in 2050, because of the uneven spatial distribution and the temporal variability of renewable resources, renewable electricity generation alone is unable to reliably meet over 20% of electricity demand in nearly one-third of the countries (Fig 1d), mainly in Southeast Asia and East Asia. In many South

European countries, over 10% of demand is unmet by renewables. Across North America, South America, Western Asia, Africa, and China, Mongolia and Russia, however, less than 3% of demand was unmet by renewables. Adding existing inter-country transmission lines reduces the gap in demand and renewable energy supply because of electricity trade (Table S1), e.g., unmet demand in southern European countries decreases from 10-20% to 5-10% (Fig. S2).

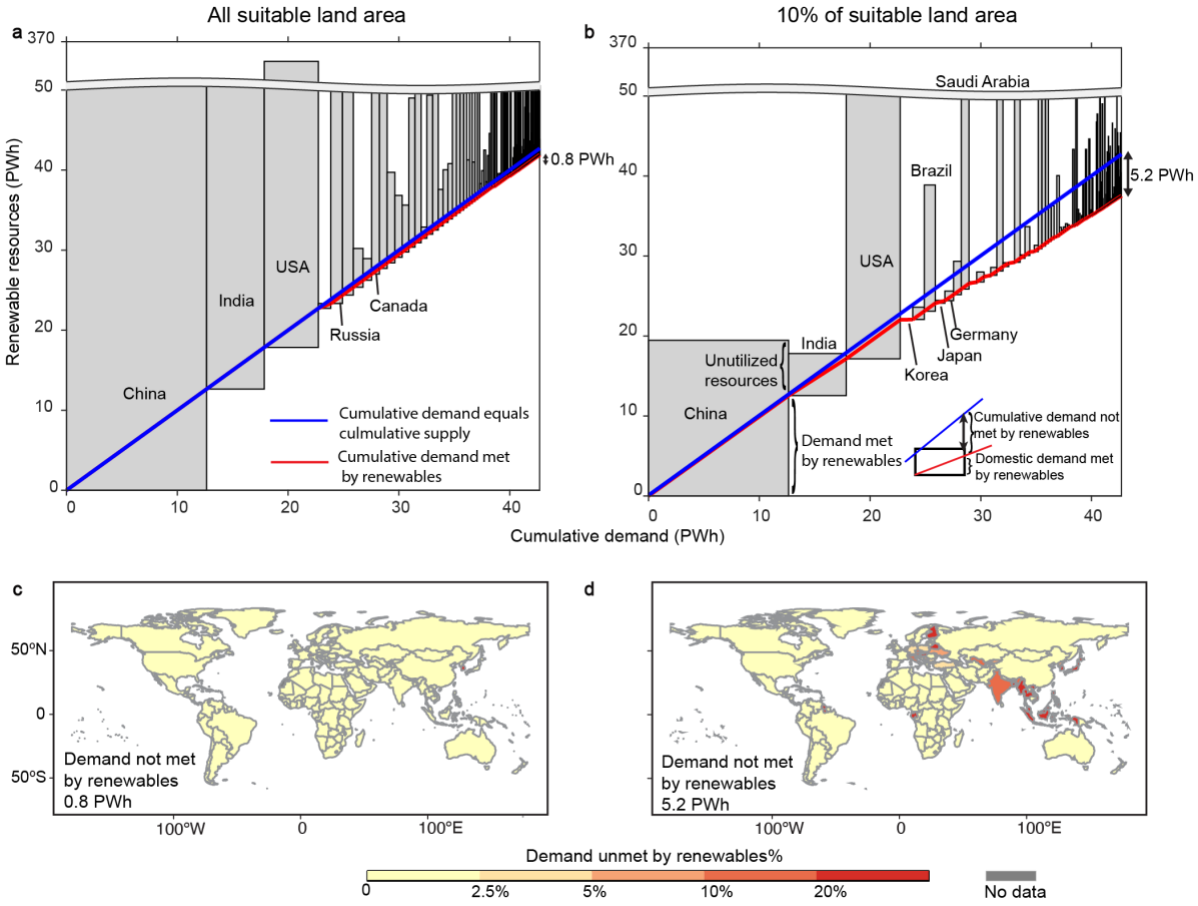


**Figure 1. Supply and demand of renewable electricity in 2050.**

Renewable generation and electricity demand in 2050 by country under the country scenario, assuming **(a)** all suitable sites for renewables and **(b)** top 10% suitable sites at the global level. Unmet demand with only supply of renewable resources under the country scenario, assuming **(c)** all suitable sites for renewables and **(d)** top 10% suitable sites at the

global level. In (**a)** and **(b),** each rectangle represents the demand for electricity (horizontal dimension) and the available renewable resources potential (vertical dimension). The blue diagonal line represents demand equals renewable electricity generation by country (y=x line). The red line represents the cumulative demand met by renewable electricity generation by country. Within a country's rectangle, when the slope of the red line is smaller than the slope of the blue line, country-level electricity demand remains unmet using only renewable energy supply.

**2. Large variation in system cost of electricity**

Due to the heterogeneity in renewable resource quality and abundance, we find that the system costs of electricity vary greatly across countries under the country scenario (Fig.2a,b). These costs vary both across and within the 6 regions that we define for forming the transcontinental power pools (Fig 2c). By utilizing all suitable sites, the country-level system costs of electricity are highest among countries in Europe, and East and Southeast Asia, exceeding $60/MWh. The lowest system cost occurs in South America, North America, Sub-Saharan Africa and Oceania, estimated to be around $30/MWh.

In Europe & MENA, East Asia & Russia, and Southeast Asia & Oceania, countries with large unutilized renewable potential have lower system costs (Fig 2d). Within Europe & MENA, Middle Eastern and North African countries have over 20 PWh of excess renewable resources, and their system costs are much lower than those in Europe (Fig 2a). Within the East Asia & Russia region, Russia, Pakistan and Afghanistan have over 10 PWh of excess renewable resources, with system costs (~$35/MWh) much lower than the average system cost in the region ($57/MWh). In Southeast Asia & Oceania, countries in Oceania

have excess renewable resources and lower system costs, while Southeast Asian countries have higher costs or less renewable resources.

Limiting the available renewable resources to the global top 10% suitable sites substantially increases the system costs of electricity in countries with fewer renewable resources compared to their electricity demand (Fig 2e). Within Southeast Asia & Oceania, 70% of the countries (mostly in Southeast Asia) suffer from a shortage of renewable resources, resulting in system costs of over $70/MWh. Only in countries such as Australia and Cambodia that have large renewable resources relative to their demand, system costs remain low (~$50/MWh). In East Asia & Russia, Pakistan, Afghanistan and Russia are the only three countries with over 0.5 PWh of excess renewable resources relative to demand and low system costs (~$40/MWh), whereas over half of the countries in the region have system costs over $60/MWh. In Europe & MENA and Sub-Saharan Africa regions, over half of the countries have system costs over $60/MWh and $50/MWh, respectively, because of limited renewable resources compared to demand.

In contrast, some regions and countries do not see a substantial increase in system costs under constraints on suitable sites. Because the top 10% suitable sites across South America and North America include abundant high-quality renewable resources to meet the electricity demand, system costs remain low. Similarly, countries that have high-quality renewable resources, such as wind resources in the United Kingdom, can access the same resources as the scenario without land constraints and as such, do not experience much system cost increases. Lastly, the average system cost in Europe & MENA see a decrease under a land constraint scenario. When 10% of the suitable sites are available, 0.4 PWh (6%) of the demand is exogenously met by fossil fuels, which is ~120 $/MWh. When all

suitable sites are used, over 99% of electricity demand is met by renewables alone by building over capacities of solar and wind. Even if adding the fossil fuel cost, the average system cost with 10% suitable sites is lower than the average system cost with all suitable sites (Fig 3).

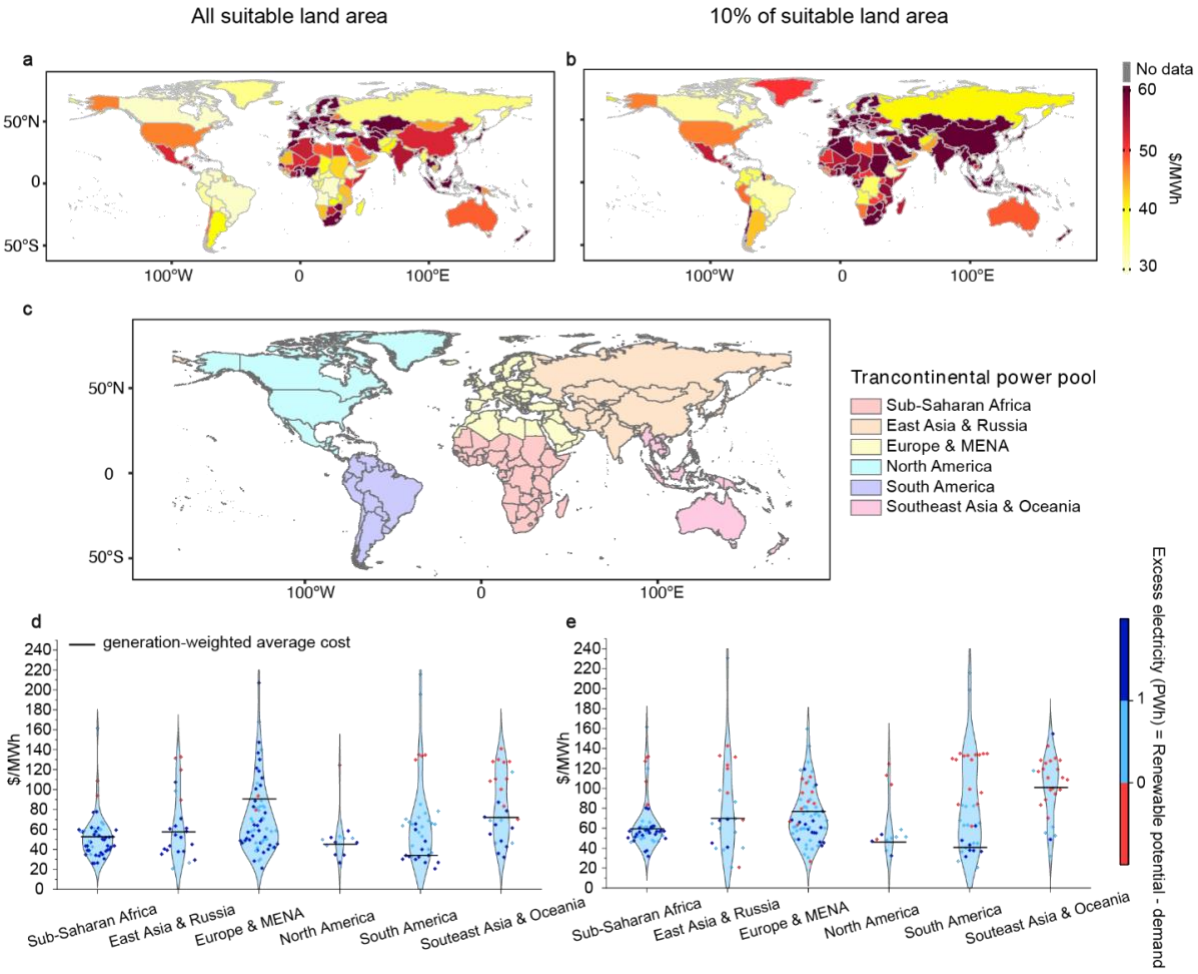


**Figure 2. The system cost of electricity (cost per unit of electricity demand) under the country scenario.**

The system cost of electricity under the country scenario assuming (**a)** all suitable sites for renewables, and **(b)** only the global top 10% suitable sites for renewables are available for development. **(c)** Classification of the transcontinental power pools. Distribution of system costs across countries within the six regions assuming (**d)** all suitable sites for renewables,

and **(e)** only the global top 10% suitable sites for renewables are available for development. In (**d)** and **(e)**, the color of scatters represents renewable energy potential excess or deficit (renewable energy potential minus electricity demand) in 2050.

### 3. Transcontinental power pools avoid shortages and reduce costs

Under the transcontinental scenario, countries with an excess of renewable resources export their renewable electricity to countries with insufficient renewable resources. By utilizing all suitable sites for renewable resources, regional renewable resources are larger than their electricity demand by 27-1000 times (Fig 3a). In Sub-Saharan Africa, the renewable resources potential (926 PWh) is nearly 1000 times the 2050 electricity demand (0.9 PWh). In East Asia & Russia where the regional demand is the largest across all regions at 23 PWh, the renewable resources potential is 628 PWh or 27 times the electricity demand. By integrating the regional renewable resources through transcontinental power pools, globally, the unmet demand by renewables decreases from 0.8 PWh (2%) to 0.0 PWh.

Compared to the country scenario, transcontinental power pools decrease system costs of electricity by 12-52% across all regions except for North America (Fig 3c). Cost reductions in North America are small (5%) because of abundant renewable resources in each of the member countries. The largest reductions in system cost resulting from transcontinental power pools occur in Europe & MENA, with an average reduction of 52% or $47/MWh across all countries (Fig 3c). These cost reductions are largely driven by the international trade of electricity requiring fewer capacities of renewables and battery storage. In Europe & MENA, the decrease in cost for PV is the largest at $24 /MWh, followed by the onshore wind ($10/MWh) and storage ($8/MWh). Assuming existing inter-

country transmission lines in the Europe & MENA region in the country scenario reduces the system cost reduction benefits of a transcontinental power pool to 46% (Table S2).

Cost reductions are also substantial in other power pools compared to the country scenario – over 10% in Sub-Saharan Africa, East Asia & Russia, South America, and Southeast Asia & Oceania. The cost reduction in these power pools is mainly driven by fewer installed PV and battery storage capacities in the transcontinental scenario.

By restricting renewable energy development to only the top 10% of suitable sites, regional renewable resources are still greater than the regional electricity demand in 2050 (Fig 3b). Specifically, in Southeast Asia & Oceania and East Asia & Russia, renewable resources are more than tenfold and threefold of the demand in power pools, respectively. Globally, if renewable resources are shared within the six continental regions defined in this study, the unmet demand decreases from 5.2 PWh (12%) in the country scenario to 0.0 PWh, which is similar to the unmet demand if all suitable renewable energy sites were developed.

When utilizing only the top 10% suitable renewable energy sites, benefits of building transcontinental power pools in reducing unmet demand are more pronounced at the regional power pool level (Fig 3d). Compared to the country scenario, transcontinental power pools reduce unmet demand in East Asia & Russia from 2.7 PWh (12% of regional demand) to 0; in Southeast Asia & Oceania from 2.0 PWh (65%) to 0; and in Europe & MENA from 0.4 PWh (6%) to 0.

Restricting renewable energy development to the top 10% suitable sites results in high system costs in the country scenario. In this case, transcontinental power pools can enable a substantial reduction in system costs, especially in Europe & MENA, South

America, and Sub-Saharan Africa because of the development of higher quality renewable energy sites, better balancing of the variability of renewable energy and electricity demand through international trade, and a reduced need for fossil fuel generation to meet electricity demand unmet by renewables. In Europe & MENA, compared to the country scenario assuming no prior interconnections, the transcontinental power pool reduces system cost by 23% because of fewer installed capacities of renewable energy and battery storage, and lower demand for fossil fuel generation. If existing interconnections are considered, this benefit is reduced to 21% but is still large (Table S2). The transcontinental power pool scenario also reduces system costs substantially in South America (23%) and Sub-Saharan Africa (14%) compared to the country scenario. The benefits of a transcontinental power pool are modest in North America (6%) because the countries are mostly large in size, providing sufficient high-quality renewable resources within the country boundaries. System cost increases from transcontinental power pools in East Asia & Russia and Southeast Asia & Oceania are modest—3% and 0.7%, respectively—because decreases in fossil fuel costs and renewable energy are offset by large increases in transmission interconnection costs.

For robustness checks, we also modeled a scenario with only the top 25% suitable sites available for development (Fig. S3 and Fig. S4) as well as a scenario with 76 PWh of electricity demand in 2050 (~75% greater than the reference scenarios). For all land availability scenarios (10%, 25%, and all), we find that transcontinental power pools meet 100%of global demand with renewables and reduce overall system costs. With the higher 2050 electricity demand, renewables also meet nearly 100% of demand and reduce system costs in all power pools, except that in East Asia & Russia and Southeast Asia & Oceania,

the increase in renewable and transmission investment outweighs the decrease in fossil fuel costs when 10% of suitable land is used.

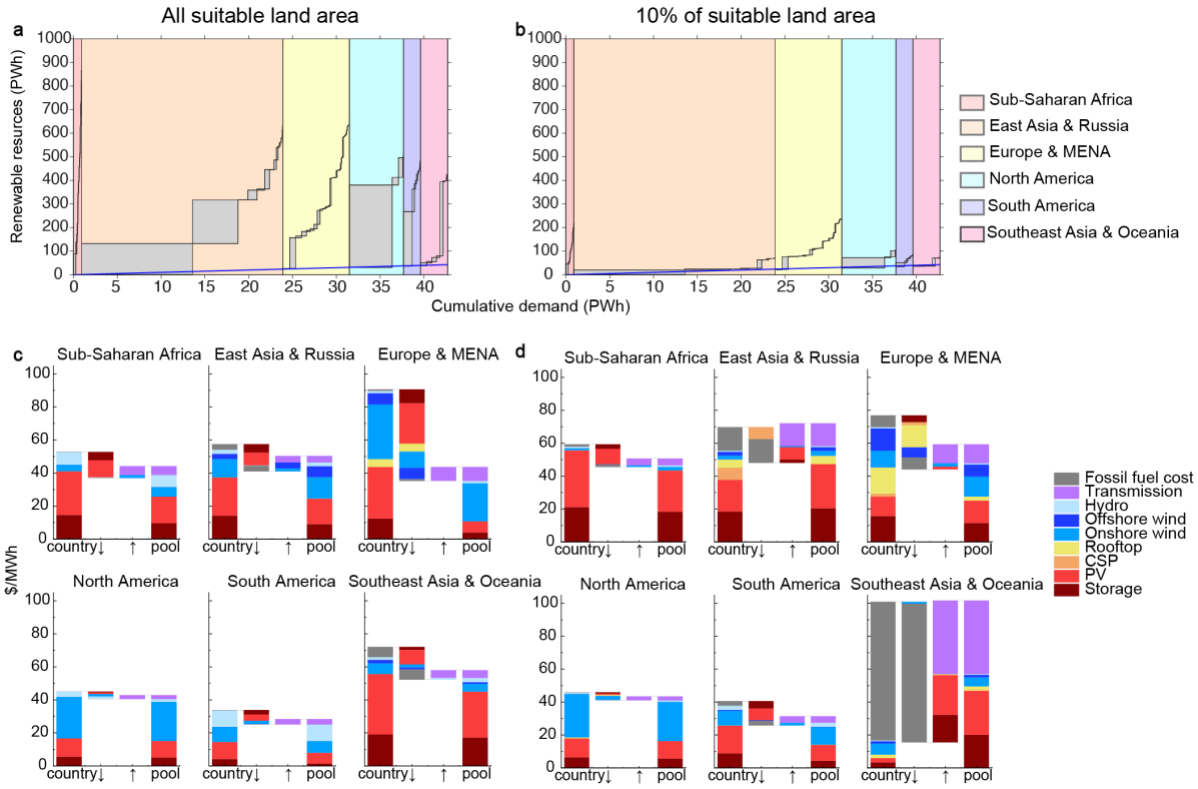


**Figure 3. Supply and demand balance of renewable electricity under the transcontinental and country scenarios and the corresponding cost reductions.**

**(a)** Renewable resources with all suitable sites and the 2050 electricity demand by country within continental regions. (**b)** Renewable resources with top 10% suitable sites and the 2050 electricity demand by country within continental regions. Changes in system cost of electricity ($/MWh) under the transcontinental power pool scenario compared to the country scenario assuming (**c)** all suitable sites for renewables and (**d)** only the global top 10% suitable sites are available for development. In (**a)** and (**b)**, each rectangle represents electricity demand and renewable resource availability. The blue line represents when cumulative demand equals available renewable resources (y = x line). Within each region,

the left-bottom corner of the first rectangle starts at the blue diagonal line because renewable resources are shared only within the continental region.

Transcontinental power pools enable electricity trade where countries endowed with inexpensive and abundant renewable resources export electricity to countries with poor endowments of renewable resources (Fig. 4a, b). Using all suitable sites for renewables, the annual trade of electricity reaches ~16% of global demand (Fig 4a). In Europe & MENA, the annual trade of electricity accounts for nearly 40% of electricity demand. Syria and Oman are the two largest net exporters, followed by Spain and France, all net exporting over 0.2 PWh in a year (Fig 4a, c). Germany is the largest net importers, net importing nearly 0.5 PWh. In other power pools, the share of traded electricity is over 20% of demand for Sub-Saharan Africa and Southeast Asia & Oceania, and ~10% for East Asia &Russia, North America and South America. Globally, the largest net importer and net exporter both occur in East Asia & Russia: China is the largest net exporter (0.9 PWh), while South Korea is the largest net importer (0.7 PWh).

By utilizing the top 10% suitable sites, the continental trade of electricity plays a more dominant role, reaching ~30% of the global demand (Fig 4b). In Southeast Asia & Oceania, the annual trade of electricity reaches three-quarters (2 PWh) of the regional demand, and nearly all of the net imported electricity is sourced from Australia (Fig 4b, d), and destined to Indonesia (0.5 PWh), Vietnam (0.5 PWh) Thailand (0.4 PWh) and Malaysia (0.4 PWh). The annual trade of electricity is the largest in East Asia & Russia, reaching 5 PWh, which contributes to a quarter of the regional demand. Specifically, South Korea (1 PWh), India (1 PWh) and Japan (0.6 PWh) are the largest net importers of renewable

electricity, while Paksitan (1.5 PWh), Iran (1.3 PWh), Afghanistan (0.8 PWh) and Kazakhstan (0.3 PWh) are the largest net exporters. In Europe & MENA, imported electricity accounts for over 40% (3 PWh) of the regional demand. The largest net exporters are Syria, United Kingdom, Morocco and Libya, aggregately net exporting ~1.5 PWh of electricity for regional trade; large net importers are distributed in Western (e.g., Germany) and Southern Europe (e.g., Italy), benefiting from the inexpensive electricity from the Northern Europe and MENA. In North America, Canada is the largest net exporters (0.3 PWh), while the USA is the largest net importer (0.2 PWh).

To estimate the country-level net benefits or costs of transcontinental power pools compared to the country scenario, we assume that the generation, storage and transmission costs in a power pool are shared by all countries, proportional to each country's electricity demand. By exporting and importing electricity with neighboring countries, in several net exporters, the transcontinental power pools reduce system costs by reducing generation curtailment, compared to the country scenario (Fig 4e,f). In both scenarios of land constraints— all suitable sites and only the top 10% suitable sites available for renewable energy development—about a quarter of the approximately 80 net exporters enjoy over $10/MWh reduction in system cost. These benefits in cost reduction are largest in Europe where net exporters experience over $20/MWh decline in system cost.

However, system costs increase in about half of the net exporters because they install more renewable energy capacities and share the cost of electricity generation and transmission (Fig. S5) with the net importers within their transcontinental power pool. For example, when utilizing the top 10% suitable sites, the system costs increase by over

$20/MWh in Pakistan and Australia because they export large amounts of electricity but share the cost with other members of their power pool (Fig 4b).

When either all or the top 10% suitable renewable energy sites are available for development, about three-quarters of the net importing countries reduce $5/MWh of the system cost by sharing renewable resources within transcontinental power pools (Fig 4g, h). Again, net importing countries in Europe experience some of the largest reductions in system costs of electricity (>$20/MWh).

Several importers also see an increase in system costs in transcontinental power pools compared to the country scenario (Fig 2a and b) when net importers share the system costs with the net exporters in the power pool. Yet, the total system cost of the power pool decreases (Fig 3c,d) because international trade reduces generation curtailment in the net exporters. For example, the system cost in Canada, a net importer when all suitable sites are used, increases, but the curtailment in the United States, a net exporter, is reduced by 1.3 PWh depending on land constraints.

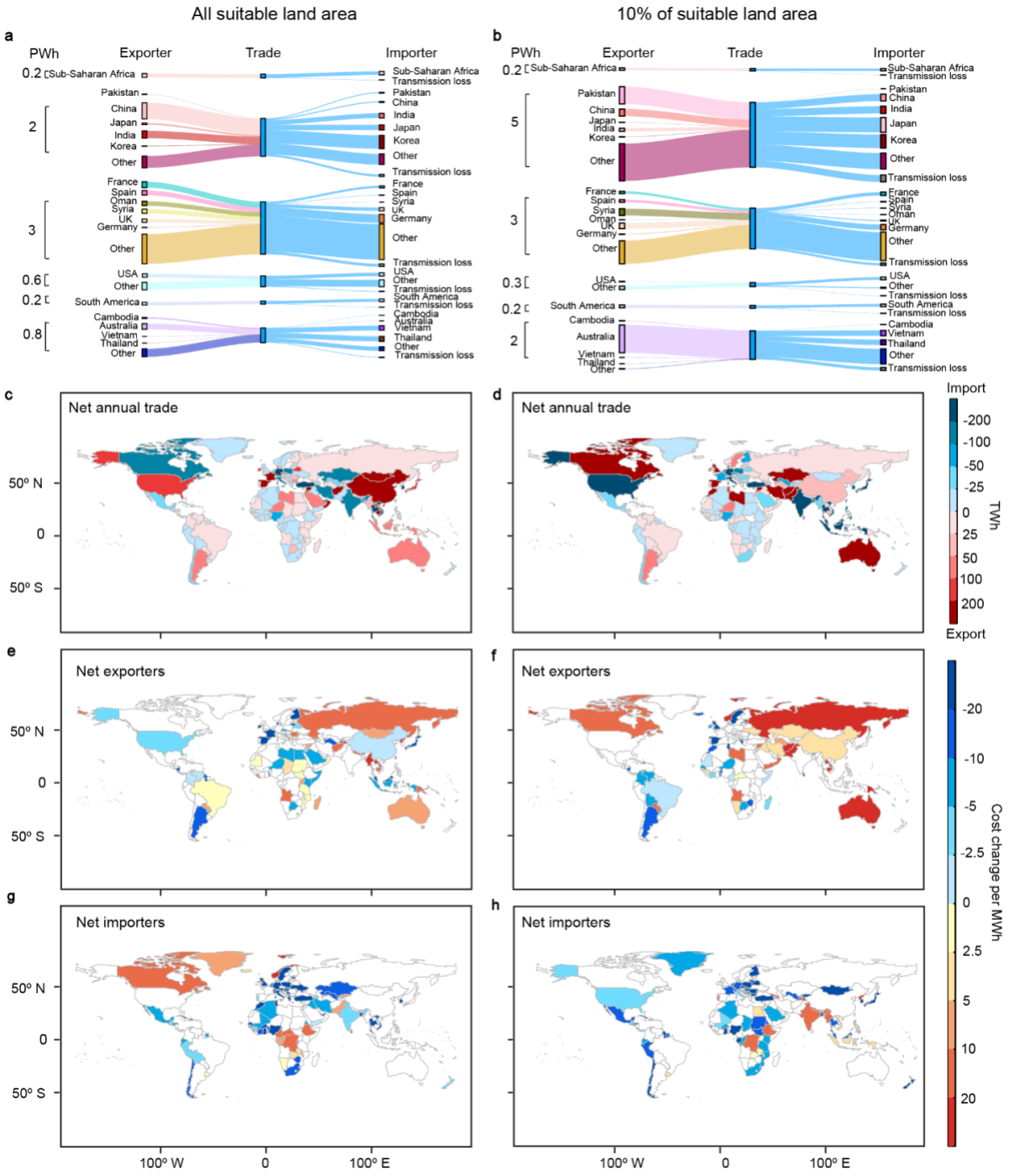


**Figure 4. Electricity trade and change in electricity costs under the transcontinental scenario compared to the country scenario.**

Annual imports and exports of renewable electricity assuming (**a)** all suitable sites for renewables, and (**b)** global top 10% suitable sites are available for development. Annual net

export of electricity assuming (**c)** all suitable sites, and (**d)** global top 10% suitable sites are available for development. Change of system cost in net exporters assuming (**e)** all suitable sites for renewables, and (**f)** global top 10% suitable sites are available for development. Change of system cost in net importers assuming (**g)** all suitable sites for renewables, and (**h)** top 10% suitable sites are available for development.

### *D. Discussion*

To achieve net zero greenhouse gas emissions by 2050, it is critical to decarbonize the electricity sector by replacing fossil fuels with renewables. Power pools can reduce costs and help accelerate the phase-out of fossil fuels. Existing examples of multi-country power pools include the Southern African Power Pool, Eastern Africa Power Pool, and Nord Pool[153]. Grid integration projects such as Medgrid[154] and North Seas Energy Cooperaton[155] have been launched to integrate renewable resources in North Europe, North Africa and the Middle East.

Constraints on land use because of conservation, food production, and other uses can restrict the amount of land required for developing renewable energy. As shown in this study, renewable energy resources can be insufficient to meet all electricity demand within some countries in the absence of international trade, especially with greater constraints on land. Poor endowments of renewable resources, e.g. in Japan and South Korea, can result in high electricity costs and hinder the low-carbon transition in the electricity sector. Transcontinental power pools can not only enable most countries to meet their electricity demand through international trade but also substantially reduce electricity costs by developing the most suitable and least expensive renewable energy sites.

The cross-boundary trade of renewable electricity indicates a new landscape in the global energy market. Historically, fossil fuel resources have also been unequally distributed across countries, and the international trade of fossil fuels has enabled huge profits for exporters of fossil fuels. Building transcontinental power pools is likely to benefit both importers and exporters of renewable energy. By importing electricity, nearly all net importers reduce domestic investments in expensive renewables and storage (Fig. S6). By reducing curtailment (Fig. S7), about half of the exporters decrease their domestic investment. In this study, we assume that all countries within each transcontinental power pool share the costs in a regional wholesale electricity market. Other cost allocation models such as allocating the lowest-cost renewable resources to consumers within exporting countries and then selling higher-cost resources to importing countries within power pools can change the distribution of system costs across importers and exporters. How to design pricing mechanisms for the transcontinental power pool market remains an open question. The new mechanism needs to equitably allocate the profits from the trade of the electricity market, especially when transmission lines span across several countries.

Geopolitics would be a barrier to building a transcontinental power pool[121]. Creating transcontinental power pools will require a large-scale integration of regional transmission infrastructure, and thus has many challenges including grid ownership, stakeholder roles, financial responsibilities, and revenue allocation between participating countries[156]. Collaboration between countries will be critical in addressing these challenges. Common policy frameworks and agreements need to be reached between national governments[157]. Regional electricity markets and pricing mechanisms need to be established to coordinate between system operators across territories to facilitate power pool operations[20]. The

electricity markets of the transcontinental power pools are required to provide a win-win trading mechanism for both exporters and importers.

In the capacity expansion model, we managed to use a time-step of 1 hour in a whole year to capture the variation of weather in all 365 days (Table S3). Following the state-of-the-art, by picking 24 representative days (one peak demand day and one average demand day in a month) and adding 15% planning reserves margins, the transcontinental power pools incurred ~1% load curtailment in the hourly operation model (Table S4). Using all 365 days in the capacity expansion model provides more robust quantification results in system costs (Table S5) and reliability of the electricity system.

Our research focused on addressing the low-carbon electricity with existing technologies that are commercially mature. Long-term storage technologies (i.e. hydrogen) which could balance the seasonal variability of renewables, are not included in our technologies. Green hydrogen has become a promising long-term storage alternative, but whether green hydrogen can be put into large-scale commercial use is under debate[158,159]. Country-level data on underground storage capacity for hydrogen is also lacking. Using synthetic methane as the long-term storage is technically mature by using existing infrastructure for natural gas[160,161], but the round-trip efficiency is ~30%[162]. Without the power pools, incorporating long-term storage into our system could reduce the load curtailment by balancing the seasonal variability of renewables, but the transcontinental power pools are still able to reduce the system cost after the inclusion of the long-term storage[163]. Furthermore, under a land-constrained scenario, long-term storage is unable to address the demand shortage caused by the local shortage of renewable energy resources without the international trade of electricity. If renewable energy resources are sourced only

within the country boundary, 4.1 PWh of demand shortage still exists due to a shortage of aggregate renewable energy resources when only the top 10% suitable sites are utilized (Fig. S1). Our research proves that, without long-term storage, 100% renewable electricity is reliable and economically feasible by expanding transmission lines within continents.

Due to data limitations, our study used uniform cost projections for renewable and storage technologies for all countries and regions. However, costs can vary across countries and regions for various reasons including differences in the cost of capital, access to technologies, and availability of skilled labor. Future analysis could incorporate these cost variations.

Land-use factors for renewables have significant uncertainties given the competing uses of land for agriculture, conservation, and other needs. For example, some sources report land use factors that are double our assumptions adopted from NREL[140,141]. Furthermore, we assumed that only the technology with the least levelized cost can be installed at a particular site. Co-locating renewable energy technologies like wind and solar PV can increase the area of suitable sites and the overall renewable potential.

Last, the cost of transmission in our study was conservatively estimated and may well be an overestimation. We assumed that the cost for HVDC (high-voltage direct current) transmission lines would remain at the 2020 level across the timeframe, but that the transmission cost would decrease due to technology learning. Given these potential overestimations for the costs of transmission lines, the actual economics of transcontinental power pools may be more favorable than how it is portrayed in our study.

## *E. Appendix*

### 1. Data and code availability

The data used for replicating our analysis are available in the Global Transcontinental Power Pool database under accession code https://doi.org/10.5281/zenodo.

The electricity planning model, GridPath 0.10.1, is available at https://github.com/blue-marble/gridpath. Matlab 2019a and Python 3.8 were used to process the data. Matlab 2019a, Origin 2023 and R 3.6.1 are used for data visualization. All the scripts used in our data collection, data analysis, and data visualization are available at https://github.com/cetlab-ucsb/Transcontinental-power-pool.

## 2. Supplementary Tables

**Table S1**. Unmet demand (PWh) in Europe & MENA under the country scenario, with and without existing transmission lines.

| Sites | No transmission lines | Existing transmission lines |
|---|---|---|
| 10% | 0.4 (5%) | 0.3 (4%) |
| All | 0.05 (0.7%) | 0.03 (0.4%) |

**Table S2**. System cost ($/MWh) in Europe & MENA under the country scenario with and without existing transmission lines, and the system cost under the 'transcontinental' scenario.

| Sites | No transmission lines | Existing transmission lines | Power pool |
|---|---|---|---|
| 10% | 77 | 75 | 59 |
| All | 91 | 81 | 44 |

**Table S3**. The unmet demand using the capacity expansion model with an 8760-hour operation model. The 2050 global demand is 43 PWh under the SDG (sustainable development goal) scenario.

| Scenario | Top 10% sites + SDG | Top 100% sites + SDG |
|---|---|---|
| Country | 12% | 1.9% |
| Transcontinental | 0 | 0 |

**Table S4**. The unmet demand using the capacity expansion model with 24 representative days, and the validation using an 8760-hour operation model. The 2050 global demand is 43 PWh under the SDG scenario.

| Scenario | Model | Top 10% sites + SDG | Top 100% sites + SDG |
|---|---|---|---|
| Country | Reduced[(1)] | 12% | 1.9% |
| | 8760[(2)] | 12% | 2.2% |
| Transcontinental | Reduced | 0 | 0 |
| | 8760 | 0.7% | 0.9% |

[(1)] Optimized the capacity investment by using 24 representative days (576 hours) within a year,

[(2)] Simulated the operation with fixed capacities across 8760 hours.

**Table S5**. Change of the system cost in transcontinental power pools compared with the case without power pool by using different temporal resolutions in the capacity expansion model.

| Pool | 100% land availability | | 10% land availability | |
|---|---|---|---|---|
| | 24 days | 3-hour | 24 days | 3-hour |
| Sub-Saharan Africa | -14% | -16% | -11% | -14% |
| East Asia & Russia | -13% | -12% | -5.6% | 3.3% |
| Europe & Middle East | -44% | -52% | -32% | -23% |
| North America | -2.9% | -4.7% | -3.4% | -5.5% |
| South America | -13% | -16% | -19% | -23% |
| Southeast Asia & Oceania | -15% | -19% | -4.4% | 0.7% |

**Table S6**. Cost parameters for renewable energy technology in 2020.

| | PV power plant | Rooftop PV | CSP-no storage | Onshore wind | Offshore wind | Hydro-power |
|---|---|---|---|---|---|---|
| Land use factor ($MW/km^2$) | 37[141] (31×1.17) | 12[141] | 15[141] | 3[140] | 3[140] | |
| Capital cost ($/kW)[107] | 883 | 1817[(1)149] | 3907[(2)149] | 1355 | 3185 | 1870 |
| O&M cost[149] ($/kW) | 23 | 29 | 66 | 43 | 109 | 30 |
| Variable cost[149] ($/MWh) | 0 | 0 | 3.5 | | | |

(1) The capital cost for utility-scale and rooftop PV is $1333/kW and $2734/kW from NREL. The global average capital cost for rooftop PV is calculated as 883·2734/1333=1817.

(2) The capital cost for CSP-no storage=Turbine cost + 1.2 · field cost.

**Table S7**. Assumptions for the rooftop PV.

| Parameter | Value |
|---|---|
| Ratio of urban area[143] | 0.25 |
| Share of suitable rooftop[149] | 0.33 |

**Table S8**. Cost parameters for the storage technology[149] in 2020.

| | Battery storage | Pumped hydro |
|---|---|---|
| Capital cost ($/kW) | 249 | 1999 |
| Energy cost ($/kWh) | 369 | NA |
| O&M cost ($/kW) | 6 | 18 |
| O&M cost ($/kWh) | 9 | NA |
| Variable cost ($/MWh) | 0 | 0.5125 |
| Roundtrip efficiency | 85% | 80% |

**Table 9**. Cost parameters for the HDVC[130].

| | HVDC |
|---|---|
| Capital cost ($/(km·kW)) | 1.044 |
| O&M cost (($/(km·kW)) | 0.003 |
| Lifetime (years) | 50 |
| Transmission loss (%/1000 km) | 1.6 |
| Converter capital cost ($/kW) | 180 |
| Converter O&M ($/kW) | 1.8 |
| Converter pair loss (%) | 1.4 |

**Table S10**. Cost projection for capital cost from 2030-2050[149].

| Technology | 2020 | 2030 | 2040 | 2050 |
|---|---|---|---|---|
| Battery storage capacity | 1.00 | 1.06 | 0.93 | 0.80 |
| Battery storage energy | 1.00 | 0.43 | 0.37 | 0.32 |
| PV | 1.00 | 0.56 | 0.51 | 0.46 |
| Rooftop | 1.00 | 0.37 | 0.33 | 0.29 |
| CSP | 1.00 | 0.68 | 0.59 | 0.57 |
| Wind | 1.00 | 0.65 | 0.58 | 0.52 |
| Offshore | 1.00 | 0.73 | 0.66 | 0.62 |
| Pumped hydro | 1.00 | 1.00 | 1.00 | 1.00 |
| Hydropower | 1.00 | 1.00 | 1.00 | 1.00 |
| HVDC | 1.00 | 1.00 | 1.00 | 1.00 |

**Supplementary Table 11**. Cost projection for O&M cost from 2030-2050[149].

| Technology | 2020 | 2030 | 2040 | 2050 |
|---|---|---|---|---|
| Battery storage power | 1.00 | 1.06 | 0.93 | 0.80 |
| Battery storage energy | 1.00 | 0.43 | 0.37 | 0.32 |
| PV | 1.00 | 0.67 | 0.63 | 0.59 |
| Rooftop | 1.00 | 0.45 | 0.42 | 0.38 |
| CSP | 1.00 | 0.86 | 0.85 | 0.85 |
| Wind | 1.00 | 0.91 | 0.84 | 0.77 |
| Offshore | 1.00 | 0.77 | 0.69 | 0.63 |
| Pumped hydro | 1.00 | 1.00 | 1.00 | 1.00 |
| Hydro | 1.00 | 1.00 | 0.96 | 0.96 |
| HVDC | 1.00 | 1.00 | 1.00 | 1.00 |

**Table S12**. Growth rates of electricity demand under SDG (Sustainable development goal)[129] and NZE[152] (Net zero emission) scenarios.

| | SDG | NZE |
|---|---|---|
| North America | 0.7% | 2.3% |
| United States | 0.6% | 2.3% |
| Central & South America | 2.0% | 4.7% |
| Brazil | 1.7% | 4.7% |
| Europe | 1.2% | 2.3% |
| European Union | 1.1% | 2.3% |
| Africa | 4.1% | 4.7% |
| South Africa | 0.8% | 4.7% |
| Middle East | 2.4% | 4.7% |
| Eurasia | 0.5% | 4.7% |
| Russia | 0.4% | 4.7% |
| Asia Pacific | 2.4% | 4.7% |
| China | 2.1% | 4.7% |
| India | 4.5% | 4.7% |
| Japan | -0.2% | 2.3% |
| Southeast Asia | 3.2% | 4.7% |

## 3. Supplementary Figures

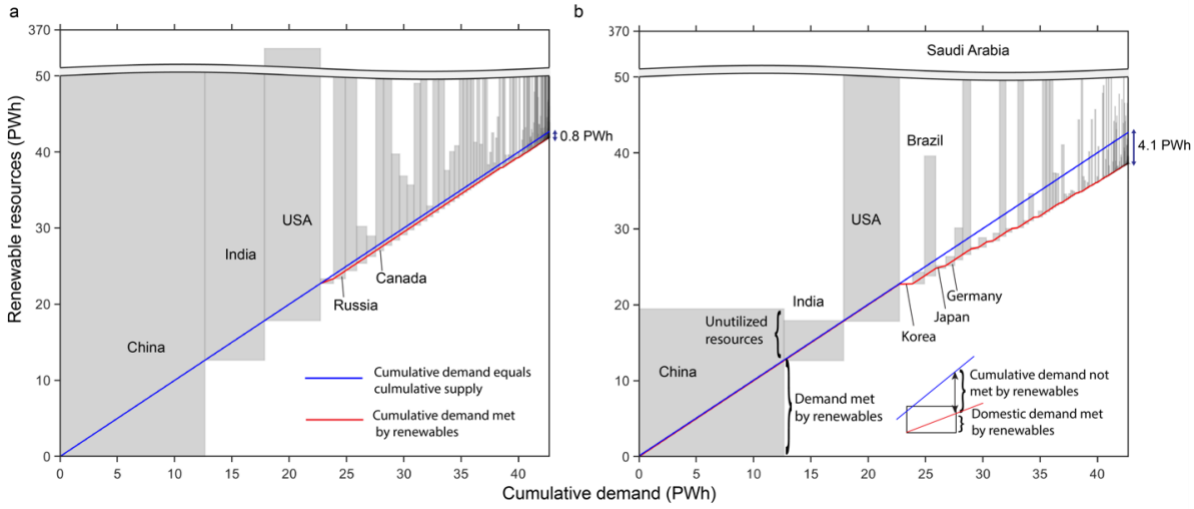


**Figure S1. Supply and demand of renewable electricity in 2050 without considering the temporal variation of renewable energy.**

Renewable potential and electricity demand in 2050 by country under the country scenario using **a** all suitable sites for renewables and **b** top 10% of suitable sites at the global level. In **a** and **b,** each rectangle represents the demand for electricity (horizontal dimension) and the available renewable resources potential (vertical dimension). The blue diagonal line represents demand equals renewable electricity potential by country ($y = x$ line). The red line represents the cumulative demand met by renewable potential by country, without considering the temporal variation of renewables. Within a country's rectangle, when the slope of the red line is smaller than the slope of the blue line, country-level electricity demand is infeasible to be met only by renewable potential.

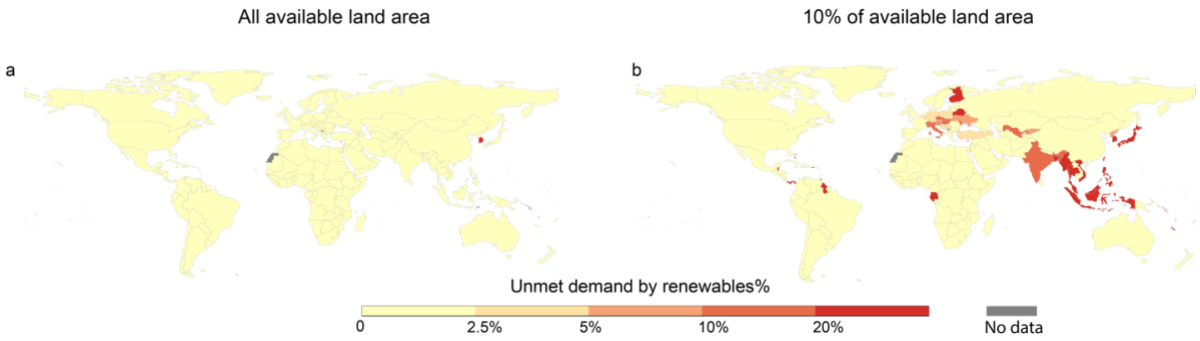


**Figure S2. Unmet demand with only the supply of renewable resources under the country scenario after adding existing transmission lines in Europe.**

**a** all available sites for renewables and **b** top 10% suitable sites at the global level.

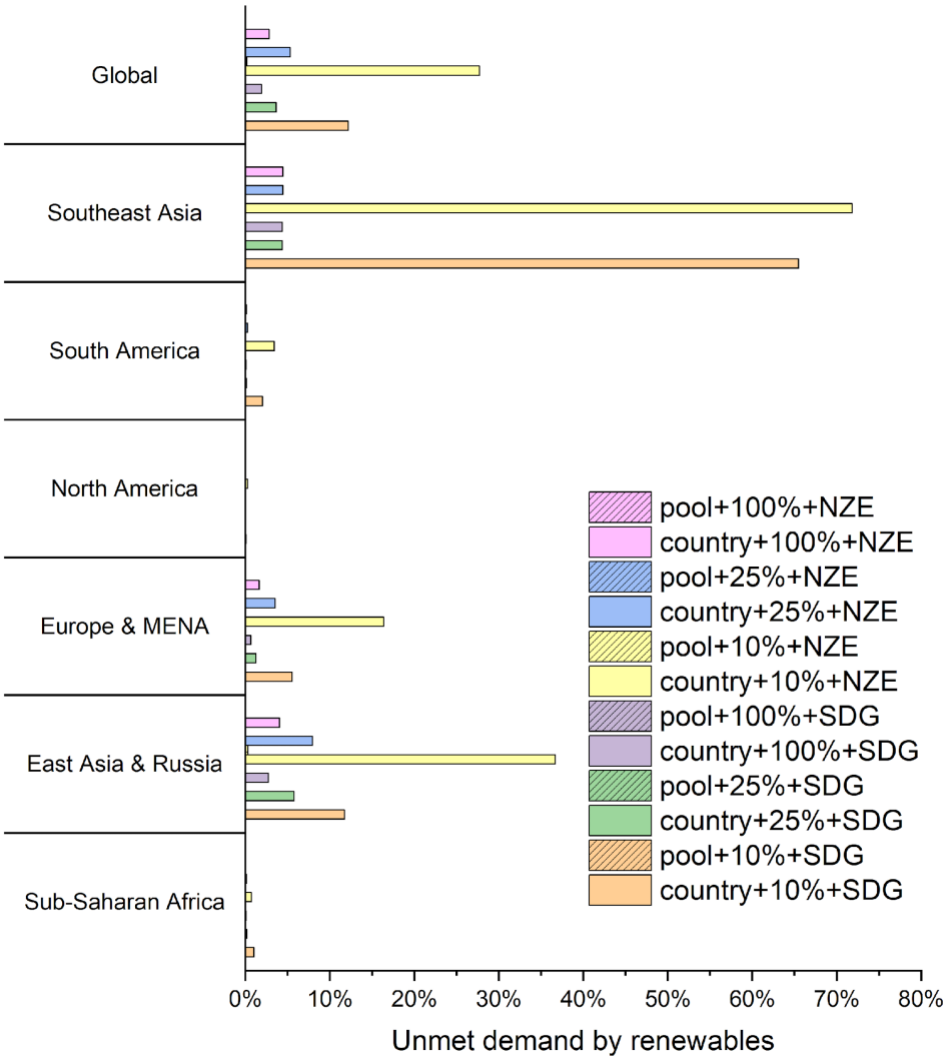


**Figure S3. Unmet demand by renewable electricity generation under different scenarios.**

'country' and 'pool' refer to the country and transcontinental scenario. '10%', '25%' and 100% refer to the top 10% sites, top 25% sites and all suitable sites for renewables. SDG and NZE refer to the demand scenarios under the UN Sustainable Development Goals and the IEA Net Zero Emissions by 2050, respectively.

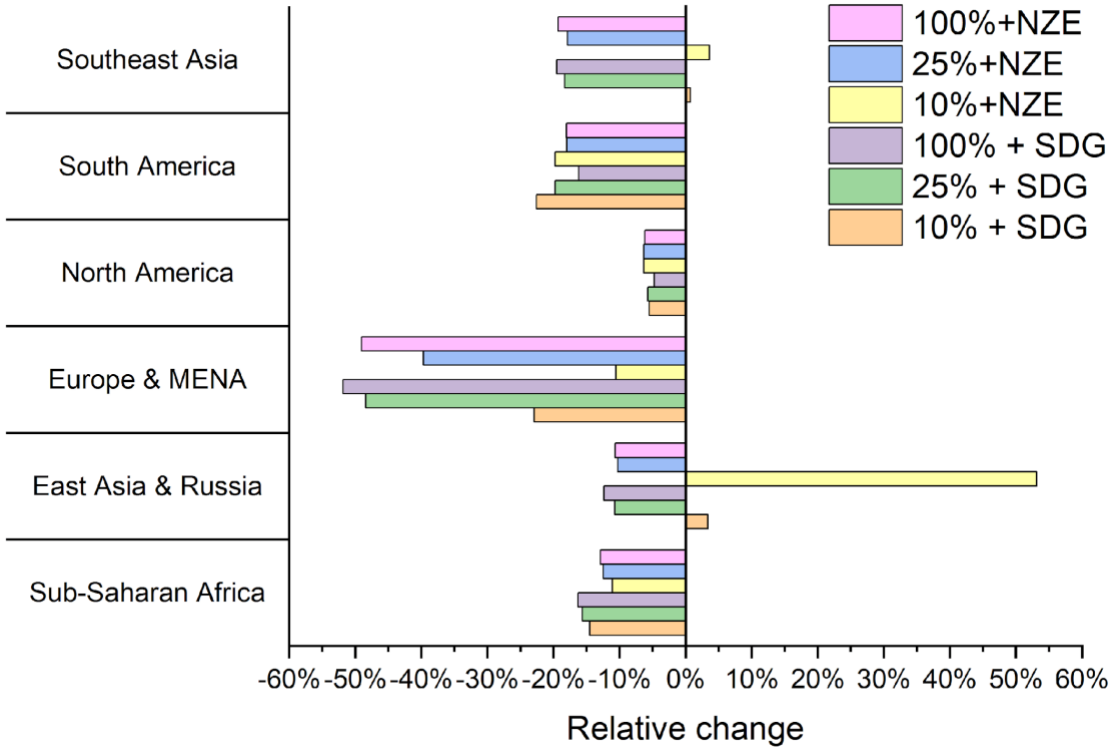


**Figure S4. Cost change ($/MWh) by transcontinental power pools under different scenarios compared to the country scenario.**

'10%', '25%' and 100% refer to the top 10% sites, the top 25% sites and all suitable sites for renewables. SDG and NZE refer to the demand scenarios.

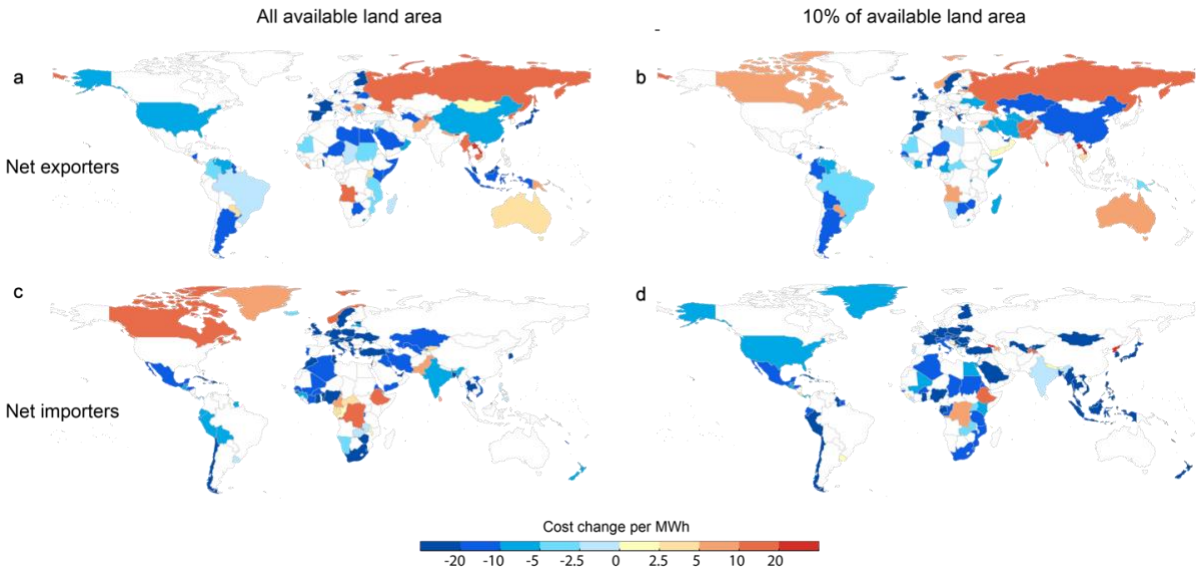


**Figure S5. Change in system costs without the cost of transmission under the transcontinental scenario compared to the country scenario.**

Change of system costs in net exporters assuming **a** all suitable sites for renewables, and **b** global top 10% suitable sites. Change of system costs in net importers assuming **c** all available sites for renewables, and **d** top 10% suitable sites.

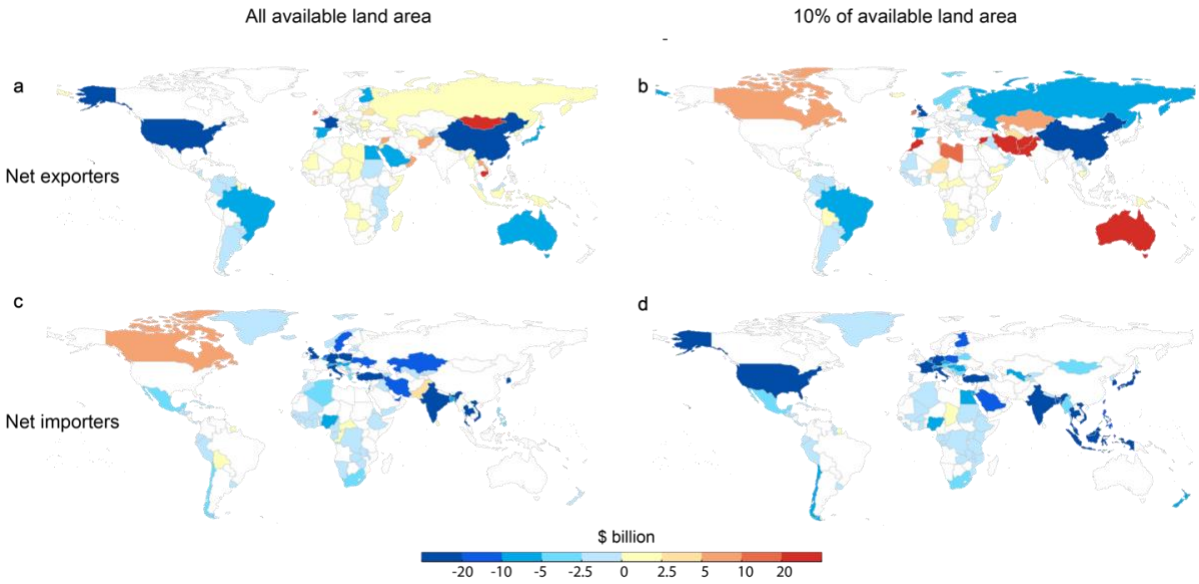


**Figure S6. Change in investment costs within the boundary under the transcontinental scenario compared to the country scenario.**

Change of investment cost in net exporters assuming **a** all suitable sites for renewables, and **b** global top 10% suitable sites. Change of investment cost in net importers assuming **c** all suitable sites for renewables, and **d** top 10% suitable sites.

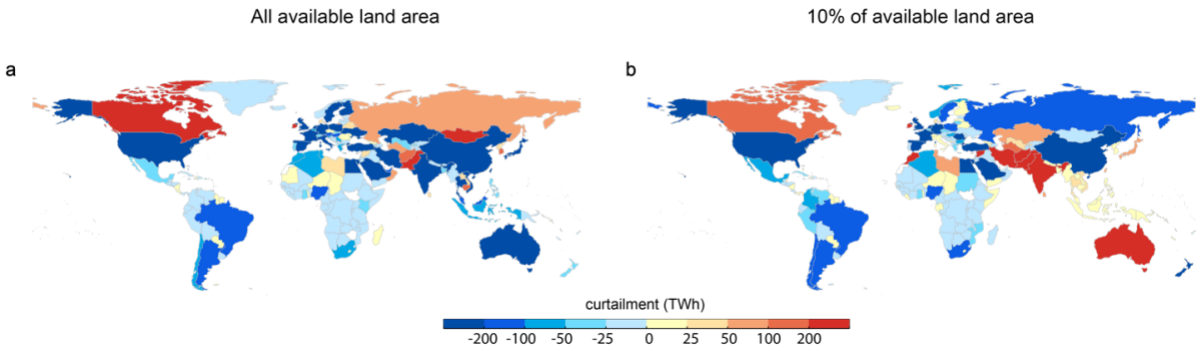


**Figure S7. Change of curtailment (TWh) by transcontinental power pools under different demand scenarios compared to the country scenario.**

Change of curtailment in net exporters assuming **a** all suitable sites for renewables, and **b** global top 10% suitable sites. Change of system costs in net importers assuming **c** all available sites for renewables, and **d** top 10% suitable sites.

# V. Regional disparities in health and employment outcomes of China's transition to a low-carbon electricity system

Materials from: Yang, H. et al. Regional disparities in health and employment outcomes of China's transition to a low-carbon electricity system. Environ. Res.: Energy 1, 025001 (2024). https://doi.org/10.1088/2753-3751/ad3bb8

**Abstract**

Understanding the costs and the spatial distribution of health and employment outcomes of low-carbon electricity pathways is critical to enable an equitable transition. We integrate an electricity system planning model (GridPath), a health impact model (InMAP), and a multiregional input-output model to quantify China's provincial-level impacts of electricity system decarbonization on costs, health outcomes, employment, and labor compensation. We find that even without specific $CO_2$ constraints, declining renewable energy and storage costs enable a 26% decline in $CO_2$ emissions in 2040 compared to 2020 under the Reference scenario. Compared to the Reference scenario, pursuing 2ºC and 1.5ºC compatible carbon emission targets (85% and 99% decrease in 2040 $CO_2$ emissions relative to 2020 levels, respectively) reduces air pollution-related premature deaths from electricity generation over 2020-2040 by 51% and 63%, but substantially increases annual average costs per unit of electricity demand in 2040 (21% and 39%, respectively). While the 2ºC pathway leads to a 3% increase in electricity sector-related net labor compensation, the 1.5ºC pathway results in a 19% increase in labor compensation driven by greater renewable energy deployment. Although disparities in health impacts across provinces narrow as fossil fuels phase out, disparities in labor compensation widen with wealthier East Coast provinces gaining the

most in labor compensation because of materials and equipment manufacturing, and offshore wind deployment.

### *A. Introduction*

China's electricity sector emitted 4.8 gigatonnes (Gt) of carbon dioxide ($CO_2$) in 2020, contributing over 40% of China's annual energy-related $CO_2$ emissions and 13% of global fossil $CO_2$ emissions[164]. Air pollution from China's predominantly fossil fuel-based power plants also caused 100,000~170,000 premature deaths in 2018[165,166]. Decarbonizing China's electricity system is thus critical not only to limit global average temperature increase to 1.5ºC or 2ºC by the end of this century, but also to mitigate health damages caused by air pollution released by power plants. For example, Tong et al. show mitigating $CO_2$ emissions in the electricity sector in line with the 1.5ºC climate target avoids about 1.1 million premature deaths caused by air pollution in China over 2010-2050[166].

At the same time, because China's electricity sector is a major employer, a transition to low-carbon electricity will have a large impact on employment, and labor compensation in the power generation sector[167]. Employment in the electricity sector includes two components—direct jobs hired by the electricity sector and indirect jobs created in the upstream sectors of the electricity sector. The labor compensation measures wages from both the direct and indirect jobs. In 2017, nearly 3 million people were directly employed in the electricity generation sector, and another 3 million were employed in coal mining and gas extraction, two sectors that provide inputs to fossil-fueled electricity production[168]. Phasing out fossil fuels will eliminate some jobs, while investments in new wind, solar, storage, and other infrastructure will create new ones. Previous studies have shown gains in employment from a low-carbon transition in China. To achieve 80% renewable generation,

Abhyankar et al. estimated a 1.9 million increase in job-years cumulative over 2020-2035[169]. Zhang et al. estimate a net increase of 1.4 million jobs per year by 2030 and 5.8 million jobs per year by 2050 in the electricity sector for decarbonization pathways compatible with China's carbon neutrality goal by 2060[170]. Similarly, Pai et al. projected a 10% increase in energy sector jobs in 2050, compared to 2020, under a climate target below 2ºC[171], and Zhou et al. predicted an increase of 1.5 million jobs in 2050 compared to 2020 under a 1.5ºC climate target[172].

Health and employment are the two main effects that communities experience in an energy transition and that are not captured by changes in system costs. Often, the distribution of these effects is not equitable across regions and communities. A low-carbon transition will no doubt lead to overall health benefits driven by reduced air pollution from fossil fuel power plants, but the distribution of these benefits will depend on where and when these power plants reduce their generation or completely retire. The distribution of employment effects is less clear as provinces will experience job losses in fossil fuel mining and power generation while gaining employment through clean energy investments, the scale of which will depend on the renewable energy potential and associated manufacturing industries across provinces. Previous studies have highlighted the inequitable distribution of benefits and losses across regions and communities in low-carbon energy transitions[173,174].

However, few studies have examined the trade-off between the health and employment effects of low-carbon energy transitions across China's regions and provinces[175]. Moreover, while previous studies, highlighted above, have separately quantified the health and employment effects of decarbonization at the national level, they have not examined the distribution of these effects across China's regions and provinces,

which is critical to plan a low-carbon transition that is also equitable. Furthermore, spillover effects, where renewable energy installations in one province create jobs in other provinces through interregional trade, have not been considered when measuring employment effects[170,172]. As China decarbonizes its electricity sector, differences in economic and labor market conditions, fossil fuel and renewable energy resources, and population distribution across regions will likely cause disparate health and employment effects across China's communities. For example, the East Coast region covers a tenth of China's total area, but had 40% of China's population and contributed to 52% of its national gross domestic product (GDP) in 2021. In contrast, the West region occupies over 70% of the total area, but in 2021, was home to only 27% of China's population and contributed 21% of the national GDP[168]. Whereas several of the lower-income provinces in the West region are rich in wind and solar resources, the higher-income provinces in the East Coast region rely heavily on fossil fuel power plants, exposing their communities to local air pollution and its associated health impacts[176,177].

In this study, we deploy a multi-model framework to develop a current-policy (Reference scenario) and low-carbon transition pathways for China's power system from 2020 to 2040 and compare the cumulative system costs, carbon emissions, and health and labor impacts of those pathways. First, we develop an electricity system planning model[146] (GridPath-China) to identify cost-optimal generation, storage, and transmission investments under various technical, economic, and carbon emission constraints. Second, using the temporally and spatially-explicit power plant generation outputs from the GridPath-China model, we use a reduced-form air pollution transport model (InMap—An Intervention Model for Air Pollution) for China[178] to estimate the distribution of ambient concentration of

air pollutants, specifically fine particulate matter ($PM_{2.5}$), and the resulting premature mortality within the population. Third, we incorporate the electricity infrastructure investments and operations projections from the GridPath-China model into a multiregional input-output model to quantify the change in direct and indirect employment and labor compensation induced by the decarbonization of China's electricity system.

We compare three main scenarios: a current-policy (Reference) scenario with no cap on carbon emissions and two low-carbon scenarios with carbon emission caps that are consistent with pathways that limit global temperature rise to 2ºC and 1.5ºC by 2100[179]. In all scenarios, the generation capacity of coal after 2020 is limited to less than 1100 GW based on the policy to avoid the over-capacity of coal power generation[180]. To disentangle the effects of decarbonization on supply-side investments, pollution, and employment, we assume the same electricity demand across the three main scenarios even though the low-carbon scenarios will likely see a higher demand because of greater electrification of end uses. Investment and operation decisions in all scenarios are made to minimize total system costs over 2020-2040. Using these results, we assess the changes in the distribution of health and labor effects across China's four main economic regions[181]—East Coast, Central, West, and Northeast—and provinces resulting from the pursuit of low-carbon targets. To examine the robustness of our results, we also perform sensitivity tests on electricity demand growth and technology cost projections.

### *B. Method and Materials*

#### 1. Scenarios

The 'Reference' scenario is a least-cost investment system operations pathway. The Reference scenario has no constraint on $CO_2$ emissions from China's power system and the electricity demand trend assumes current policies. In the low-carbon scenarios, $CO_2$ emissions are compatible with the 2°C and 1.5°C climate targets, and electricity demand is the same as the Reference scenario. The 2°C scenario is defined as the scenario where the $CO_2$ emissions in China's power system and the electricity demand follow the trajectory to limit the global average temperature increase by 2°C. The 1.5°C scenario is defined as the scenario where the $CO_2$ emissions in China's power system and the electricity demand follow the trajectory to limit the global average temperature increase by 1.5°C.

The annual carbon emission budgets for the three scenarios were compiled from the median projections of 8 Integrated Assessment Models (IAMs) in the CD-LINKS (Linking Climate and Development Policies – Leveraging International Networks and Knowledge Sharing) Database (Table S1-S3)[51,182]. These IAMs include AIM/CGE 2.1, COPPE-COFFEE 1.0, DNE21+ V.14, GEM-E3 V1, IMAGE 3.0.1, MESSAGEix-GLOBIOM 1.0, REMIND-MAgPIE 1.7-3.0, and WITCH-GLOBIOM 4.4. In the CD-LINKS database, the NPi, NPi2020_1000 and NPi2020_400 scenarios correspond to the Reference scenario, 2°C scenario, and 1.5°C scenario in our study. The NPi scenario includes currently implemented climate policies and assumes the policies continue after the duration of the policy. The NPi2020_1000 assumes a carbon budget of 1000 Gt $CO_2$ for the period 2011-2100, corresponding to staying below 2°C at >66% probability through the 21st century. The

NPi2020_400 assumes a carbon budget of 400 Gt $CO_2$ for the period 2011-2100, corresponding to staying below 1.5°C at >66% probability through the 21st century.

In our main scenarios, we assumed that electricity demand is the same across the Reference, 2°C, and 1.5°C scenarios. All scenarios used the median values for electricity demand under the NPi scenario (Reference scenario) across the IAMs. The electricity demand projections from CD-LINKS for all years were multiplied by a constant factor so that the calibrated 2020 electricity demand from IAMs equals the actual 2020 demand (7.6 PWh).

To assess the impact of different demand trajectories under the 2°C, and 1.5°C scenarios, we performed sensitivity analyses by designing a demand growth scenario (Table S4). In the demand growth scenario, the electricity demand under the 2°C and 1.5°C scenarios is the median of the selected IAMs in the NPi2020_1000 and NPi2020_400, respectively.

**2. Electricity Model**

We used the GridPath model, an open-source power system model, to optimize the total investment and operation costs of electricity infrastructure (coal, natural gas, nuclear, hydropower, solar, wind, storage and transmission) in China from 2020 to 2040[146,183,184]. We chose 2040 as our end-year because it is near enough to limit uncertainty in technology cost trajectories and far enough to develop meaningful pathways for policy-making. In our GridPath-China model, the 31 provinces in China are classified into 32 load zones, where Inner Mongolia is split into an Eastern Inner Mongolia load zone and a Western Inner Mongolia load zone. We modeled three investment periods — 2020 (2020 - 2025), 2030

(2025 - 2035) and 2040 (2035-2045). Within each investment period, we modeled one day per month with 24 hours to represent each of the 12 months. This representative day has the average hourly load for the month. To ensure reliability during peak load hours, we assumed a planning-reserve margin of 15% of the peak load. Total coal capacity after 2020 is constrained to less than 1100 GW in all scenarios based on National Development and Reform Commission's policy to avoid the over-capacity of coal generation[180]. Carbon capture and storage is not allowed in our model. The minimum generation level assumed is 100% of rated capacity for nuclear power plants, 40% for coal power plants and gas turbines, and 45% for combined cycle gas turbines. The hourly ramp rate of the rated capacity is 30% for coal power plants and 60% for gas power plants. An 8% discount factor is used to calculate the net present value of system costs, similar to assumptions in other studies[185].

We collected the latitudes and longitudes for existing coal power plants and their heat rates from Global Energy Monitor[186], which are critical for the air quality model. Existing generation capacities for all technologies, projected generation capacities for hydropower and nuclear, monthly average capacity factors of hydropower, and provincial-level fuel costs were compiled from the SWITCH-China model[187]. We collected the existing and planned hydropower and pumped hydro capacities larger than 1 GW from Global Energy Monitor[188]. We collected data for existing transmission lines from State Grid[189] and Southern Grid[190]. The derating factors of coal and nuclear capacities are collected from the 2020 Electric Power Yearbook[191]. Hourly load, and projected generation capacity factors for solar, onshore, and offshore wind were collected from Abhyankar et al[169]. China-specific costs (2020) of renewable energy are from the International Renewable Energy Agency[107],

and costs of battery storage technologies and fossil-fuel technologies were collected from Zhuo et al[192] (Table S5, S6). We then applied normalized cost projection curves from 2020 to 2040, derived from the NREL 2021 Annual Technology Baseline (ATB) database[193] (Table S7), to the China-specific technology costs. The projected cost for transmission lines was collected from Grid Project Construction Cost Analysis in the 12th Five-year Period[194].

Scenarios shown in the main text assumed the 'moderate' cost projection scenario from NREL's ATB. In addition, we performed sensitivity analyses assuming two different cost projections (Table S8). The low and high-cost scenarios assume the 'advanced' and 'conservative' cost projection trends from the NREL ATB database.

## 3. Employment and labor compensation

### 3.1 Direct employment and labor compensation

For each investment period, the direct jobs refer to the employment created by the operation and maintenance (O&M) of the power plants.,

The number of direct jobs for energy technology $m$ ( $DJ_r^m$) was calculated as the product of the total installed capacity for energy technology $m$ in region r ($C_r^m$) and the employment factor per unit installed capacity ($F_m$).

$$DJ_r^m = C_r^m \cdot F_m \quad (1)$$

The direct labor compensation was calculated as the product of direct jobs ( $DJ_r^m$) and wages ( $w_r^m$) for energy technology $m$ and region $r$.

$$DL_r^m = DJ_r^m \cdot w_r^m \quad (2)$$

### 3.2 Indirect employment and labor compensation

The multiregional input-output (MRIO) model was used to calculate changes in indirect employment and associated labor compensation due to decarbonization of the electricity sector.

The basic formula for the MRIO model shows relationship between the total monetary output **X** and the final demand Y**,**

$$X = (I - A)^{-1}Y \quad (3)$$

where $(I - A)^{-1}$ is the Leontief Inverse Matrix, which captures both direct and indirect inputs to satisfy one unit of final demand in monetary value; **I** is the identity matrix; **A** is the matrix showing the coefficient for intermediate input.

The number of jobs directly hired by region *r*, industry *i* ($job_{r,i}$) divided by the monetary output in region *r*, industry *i* ($x_{r,i}$) derived the job intensity (job/$) in region *r*, industry *i* ($ej_{r,i}$),

$$ej_{r,i} = \frac{job_{r,i}}{x_{r,i}} \quad (4)$$

The matrix for indirect jobs ($IJ$) measures the indirect job driven by the final demand,

$$IJ = diag(ej)(I - A)^{-1}Y \quad (5)$$

where *ej* is the vector of job intensity ($ej_{r,i}$).

The wage per job in region *r*, industry *i* ($wage_{r,i}$) divided by the output in region *r* industry *i* was the wage intensity in region *r*, industry *i* ($ew_{r,i}$),

$$ew_{r,i} = \frac{wage_{r,i} \cdot job_{r,i}}{x_{r,i}} \quad (6)$$

The matrix for indirect labor compensation ($IL$) measures the indirect labor compensation driven by the final demand,

$$IL = diag(ew)(I - A)^{-1}Y \quad (7)$$

where *ew* is the vector of wage intensity ($ew_{r,i}$).

We used the synthetic industry approach[195] to represent the energy technologies (wind, solar, hydropower, coal, natural gas, nuclear, storage and grid) that are not identified as an industry in the input-output table. In the synthetic industry approach, we created a proxy vector of demand for the energy technology *m* ($Y^m$), which is a package of goods and services from region *s*, industry *j* ($y_{s,j}^m$).:

For each investment period, $IJ^m$ and $IL^m$ are vectors showing the number of jobs and labor compensation created by the final demand of the energy technology *m*,

$$IJ^m = diag(ej)(I - A^*)^{-1}Y^m \quad (8)$$

$$IL^m = diag(ew)(I - A^*)^{-1}Y^m \quad (9)$$

where $A^*$ is the intermediate input matrix, where the elements are zeros in the columns and rows representing the electricity sector.

The synthetic industries for energy technology are split into two categories: total investment and operation. The total investment quantifies the indirect jobs created by the investment in new capacity, and the operation quantifies the indirect jobs created by the operation of the existing and new capacity.

In region *r*, the total indirect jobs created by the energy technology *m* ($IJ_r^m$) was calculated as the summation of jobs created in region *r*, industry *i*, which are driven by investments or operations of technology *m* in region *s*, industry *j* ( $IJ_{r,i,s,j}^m$).

$$IJ_r^m = \sum_i \sum_s \sum_j IJ_{r,i,s,j}^m \quad (10)$$

Similarly, in region *r*, the indirect labor compensation created by the energy technology *m* ($IL_r^m$) was calculated as the summation of labor compensation in region *r*, industry *i* created by the investments or operations of energy technology *m* in region *s*, industry *j* ( $IL_{r,i,s,j}^m$).

$$IL_r^m = \sum_i \sum_s \sum_j IL_{r,i,s,j}^m \quad (11)$$

We used the 2017 multiregional input-output table (MRIO)[196]. The final demand in the synthetic industry (i.e., investment and operation costs) was derived from the GridPath model. Data for the demand vector of the goods and services making up the synthetic industries were derived from Garrett-Peltier et al.[195], NREL[197] and Chen et al.[198]. Employment and wage data were collected from China Labor Statistical Yearbook[199] and the National Bureau of Statistics[168].

### 3.3 Total employment and labor compensation

For each energy technology, the total job-years in region *r* ($TJ_r$) was calculated as,

$$TJ_r = \sum_t \left( DJ_{r,t} \cdot p_t + IJ_{r,t}^{operation} \cdot p_t + IJ_{r,t}^{investment} \right) \quad (12)$$

where $DJ_{r,t}$ represents the direct jobs in region *r* over the investment period *t*, $IJ_{r,t}^{operation}$ represents the indirect jobs created by the operation of capacities in region *r* over time period *t*, $IJ_{r,t}^{investment}$ represents the indirect jobs created by the investment of new

capacities in region *r* during period *t*, and $p_t$ is the years represented by the investment period *t* in the electricity system planning model. $DJ_{r,t}$ and $IJ_{r,t}^{operation}$ are created in each year over the period *t*, and hence are multiplied by $p_t$ to estimate total jobs. $IJ_{r,t}^{investment}$ are jobs created through total investments in new capacity during an investment period and thus are not multiplied by $p_t$.

For each energy technology, the total labor compensation in region *r* ($L_r$) was calculated as,

$$L_r = \sum_t \left( DL_{r,t} \cdot p_t + IL_{r,t}^{operation} \cdot p_t + IL_{r,t}^{investment} \right) \quad (13)$$

where $DL_{r,t}$ represents the direct labor compensation in region *r* over the investment period *t*, $IL_{r,t}^{operation}$ represents the indirect labor compensation created by the operation of capacities in region *r* over the investment period *t*, $IL_{r,t}^{investment}$ represents the indirect labor compensation created by the investment of new capacities in region *r* during period *t*.

The data for the employment factor was compiled from prior studies[171,200]. The average wages of the fossil fuel, nuclear, hydropower, solar, wind, and storage sectors were collected from US Bureau of Labor Statistics[201]. The average wage in China's electricity sector is scaled based on the average wage of the electricity sector in China and the US (Table S9-S10)[168].

Employment intensities under the Reference scenario in 2040 for each technology are shown in Table S11. A comparison of the total employment in our research and other studies is shown in Tables S12-S13, while we assume that the productivity (job/dollar derived from the MRIO and job/MW from O&M) remains constant over 2020-2040.

**4. Air quality and health benefits**

We used InMAP (Intervention Model for Air Pollution), a reduced-form air pollution model, to simulate the $PM_{2.5}$ under the different scenarios[202]. InMAP China has been shown to capture the effect of emissions changes on predicted $PM_{2.5}$ concentrations when compared with a weather forecasting model with a state-of-the-science chemical transport model (i.e., WRF-CMAQ)[178]. We compiled $SO_2$, $NO_x$, and $PM_{2.5}$ emissions (Table S14) for the electricity sector using the activity (generation) data generated by GridPath, the location of power plants, and emission factors derived from published emission standards (i.e., ultra-low emission standard)[203]. Emission factors are a product of regulated emission intensity ($ug/m^3$) and the emitted volume ($m^3$/kg fuel). Emissions for other sectors and meteorological data were derived from InMAP China[178]. To quantify the impact of electricity generation in China, we first run InMap with emissions from power plants, and then run InMap without the emissions from the power plants. The Cox Proportional Hazards model[204] was used to estimate premature deaths due to $PM_{2.5}$ pollution, and avoided premature deaths are estimated as the difference in premature deaths associated with the simulation with power plant emissions and the one without the power plant emissions.

In each grid cell used by InMap, we first calculated the hazard ratio (*HR*) when the concentration of $PM_{2.5}$ ($\mu g/m^3$) is *C*,

$$HR = e^{\beta C} \quad (13)$$

where $\beta$ is the parameter in the exposure-response function.

The attributable fraction (*AF*) measures the premature deaths attributed to $PM_{2.5}$,

$$AF = \frac{HR - 1}{HR} \quad (14)$$

The mortality attributed to $PM_{2.5}$ (M) was calculated as,

$$M = AF \cdot A \cdot P \ (15)$$

where *A* is the age-standardized all-cause mortality rate of the population in China; *P* is the population.

In each year y, the value of statistical life ($V_y$) was calculated as,

$$V_y = V_{base} + (I_y - I_{base}) \cdot MV \ (16)$$

$V_{base}$ is the baseline value of statistical life in 2020 value ($1.0 million); $I_y$ is the disposable income per capita in year y; $I_{base}$ is the baseline value of the disposable income per capita ($0.006 million); *MV* is the marginal value of statistical life per capita disposable income (99.8).

The value of premature mortality (VM) was the product of the value of statistical life (V) and the number of premature deaths (M).

$$VM = V \cdot M(17)$$

The value of the parameter $\beta$ is based on a long-term cohort study in China, which is age-standardized[205]. The all-cause mortality rate was compiled from Institute for Health Metrics and Evaluation (IHME)[206]. Population density was compiled from the Center for International Earth Science Information Network[207], and was assumed to follow the population growth trajectory in CD-LINKS. The value of statistical life varies between different studies, which is related to the economic and social status of the surveyed samples. People in countries with higher incomes tend to have a higher value of statistical life. For example, the value of statistical life is higher in the US than China. The US Environmental Protection Agency uses $7.4 million[208], while the US Department of Transportation uses $12.5 million[209]. The value of a statistical life in the base year and the marginal value of a

statistical life per disposable income per capita were collected from Tang et al., which used local data from China[210]. The trend of disposable income was derived from CD-LINKS. We compare our estimates to those from other studies in Table S15.

**5. Cost of carbon emissions**

We used the social cost of carbon ($CS_t$) to calculate the total cost of carbon ($TC_t$) associated with the greenhouse gas emissions ($GHG_t$) in year *t* as

$$TC_t = GHG_t \cdot CS_t \quad (18)$$

We used the trajectory of the social cost of carbon under a 3% discount rate, published by the White House[131]. We include only $CO_2$ emissions in the greenhouse gas emission estimates. The net present value for the total cost of carbon is discounted at a 3% social discount rate.

### *C. Results*

**1. New capacity investments and energy generation**

Under the Reference and both low-carbon scenarios, renewable energy (hydro, wind, and solar) capacity and generation increase their share. Under the Reference scenario, although the total fossil fuel installed capacity in 2040 (~1,700 GW) increases compared to that in 2020 (~1,400 GW), the share of fossil fuels in the total installed capacity decreases from 57% to 32% (Fig 1A). More importantly, energy generation from fossil fuels decreases by 20% in 2040 compared to 2020, comprising only 35% of total generation (Fig 1B). Driven by a rapid decline in renewable energy costs, specifically for wind and solar photovoltaic technologies (Table S1-S4), renewable energy capacity in the Reference

scenario grows four-fold to 3,500 GW, contributing over 50% of the energy generation in 2040.

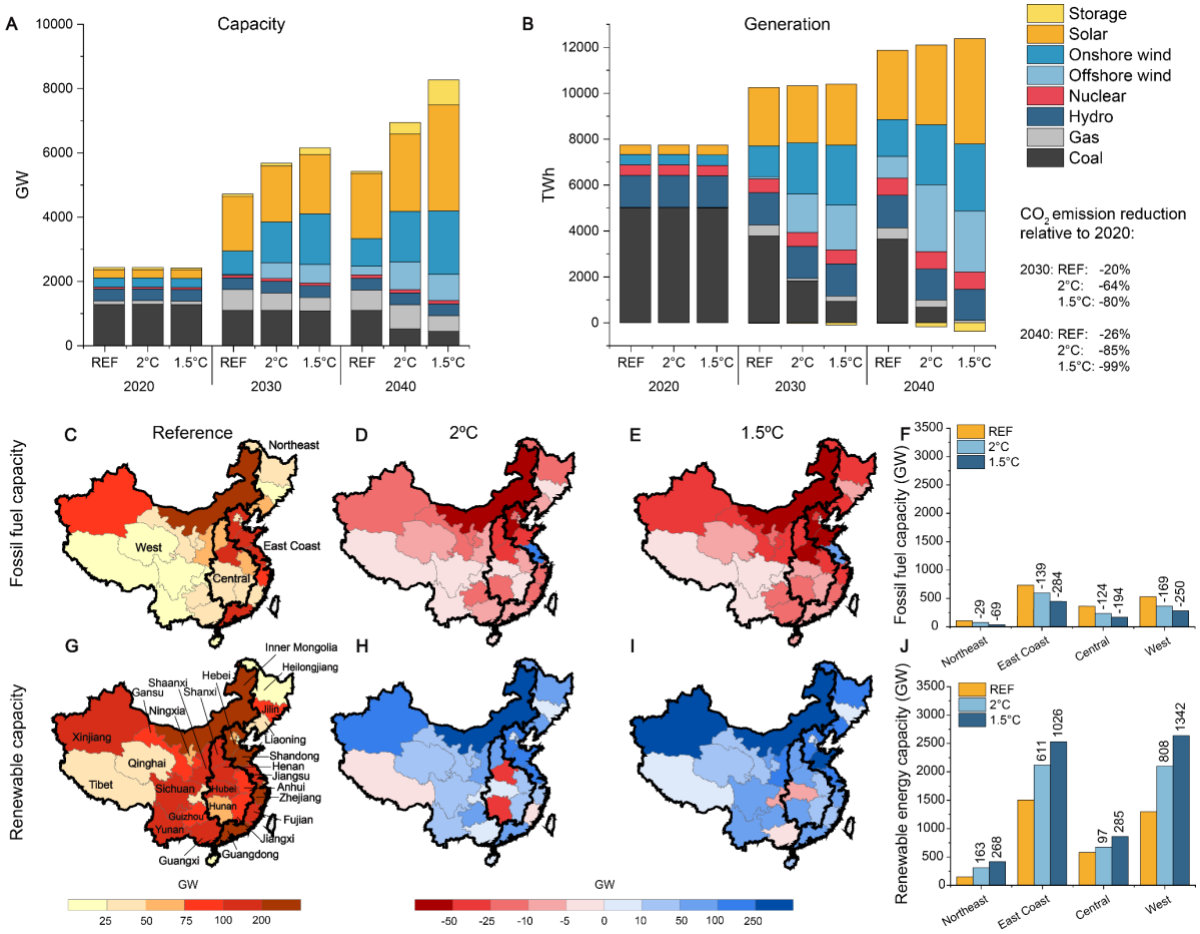


**Figure 1. Capacity and generation**

(A) Capacity mix and (B) generation mix of technologies from 2020 to 2040 under the Reference scenario (REF), 2ºC and 1.5ºC scenarios. In 2040, capacities of fossil fuels (coal and natural gas) under the Reference scenario (C) and change in capacities of fossil fuels (D) under the 2ºC scenario and (E) under the 1.5ºC scenario compared to the Reference scenario. In 2040, (F) capacities of fossil fuels under the Reference, 2ºC and 1.5ºC scenarios by region. In 2040, (G) capacities of renewable energy (hydropower, solar and wind) under the

Reference scenario, and change in capacities of renewable energy (H) under the 2ºC scenario and (I) under the 1.5ºC scenario compared to the Reference scenario. In 2040, (J) capacities of renewables under the Reference, 2ºC and 1.5ºC scenarios by region. The Reference scenario assumes no carbon emission cap, and the 2ºC and 1.5ºC scenarios are compatible with the 2ºC and 1.5ºC targets proposed by the Paris Agreement.

Under the 2ºC scenario, our results show that in 2040, fossil fuel capacity is reduced by 40% to 1,300 GW and its electricity generation decreases by over three quarters to only 8% of the total. The decrease in fossil fuel generation is compensated for by greater renewable energy capacity (~5,200 GW) and generation (87% of the total).

Under the more tightly carbon-constrained 1.5ºC scenario, the total installed capacity increases by 50% in 2040 compared to the Reference scenario. This increase is driven by lower capacity factors of renewable energy compared to fossil fuel power plants, which require more capacity to generate the same amount of electricity. The share of fossil fuel capacity plummets by two-thirds compared to the Reference scenario, whereas renewable energy capacity, predominantly wind and solar, doubles to ~6,400 GW. Balancing the variability in electricity generation from this large increase in wind and solar capacities also requires a significant scale-up of battery storage capacity, an eight-fold or ~730 GW (4,900 GWh of energy capacity) increase compared to the Reference scenario. The total transmission capacity also increases mainly to access geographically diverse renewable resources (Fig S1-S3).

At the regional level, fossil fuel capacity declines follow historical patterns of fossil fuel power plant distribution in 2020, whereas increases in renewable energy capacities are

driven by resource availability. Under the Reference scenario, fossil fuel capacities are predominantly concentrated in the East Coast and West regions in 2040 (Fig 1C,F), similar to the pattern in 2020 (Fig S4, S5). As expected, these regions experience largest reductions in fossil fuel capacities (Fig 1D-F) under the low-carbon scenarios.

Renewable energy installations, under the Reference scenario, are mainly concentrated in the West Region (1,300 GW, 37% of total renewable energy capacity) because of an abundance in solar and wind resources, as well as in the East Coast region (1,500 GW, 43% of total renewable energy capacity) driven by offshore wind resources (Fig 1H-J). Under the 2ºC scenario, the increase (1,700 GW) in renewable energy capacity is also concentrated in the East Coast and West regions. Under the more stringent 1.5ºC scenario, renewable energy capacity doubles compared to the Reference scenario—1,300 GW in the West region, 1,000 GW in the East Coast region, and 270 GW in the Northeast region.

A lack of a carbon target in the Reference scenario results in a relatively modest 26% reduction in annual $CO_2$ emissions in 2040 compared to 2020. However, under the low-carbon scenarios, annual $CO_2$ emissions in 2040 decrease by 85% (2ºC scenario) and 99% (1.5ºC scenario) relative to 2020 because of the imposition of carbon caps across the planning period.

The regional pattern of renewable energy deployment is similar across electricity demand and technology cost sensitivity scenarios (Fig S6-S8). High costs of renewable energy and storage decrease renewable energy capacity and increase fossil fuel capacity under the Reference scenario, but achieve a similar mix in the 2ºC and 1.5ºC scenarios across all cost scenarios because of the need to meet low-carbon targets. Without any constraint on coal

generation capacity (Fig S6G), the share of coal capacity remains at about 50% of the total installed capacity over 2020-2040 under the Reference scenario.

### 2. National-level outcomes of China's energy transition pathways

We estimate cumulative system costs, which include investment, fuel, and operations costs, and carbon emissions from 2020 to 2040 to assess the economic and climate impacts from each scenario. To compare employment and health outcomes across scenarios, we estimate job-years and labor compensation, and premature deaths due to air pollution caused by electricity generation, respectively, across the study period. We present both total cumulative system costs (net present value discounted at a private discount rate of 8%(24)) and annual average costs per unit of electricity generation. We also compare the net present value of total wages, monetized value of avoided premature mortality, and climate damages using a social cost of carbon, all discounted at a social discount rate of 3%.

Cumulative total system costs, including both investment and operations costs, increase slightly across 2020-2040 under the 2ºC scenario and significantly under the 1.5ºC scenario, when compared to the Reference scenario. Under the Reference scenario, the total discounted system cost over 2020-2040 is $6.1 trillion, whereas average costs per unit of electricity demand decrease from $58 per MWh in 2020 to $52 per MWh in 2040 (Fig 2A,B). Under the 2ºC and 1.5º C scenarios, total discounted system costs over 2020-2040 increase by 8% and 16%, respectively, and annual average costs per unit of electricity demand in 2040 increase by 21% and 39%, respectively, compared to the Reference scenario. This increase in system cost will ultimately lead to higher rates for consumers. Our study is limited to estimating only direct electricity system costs and does not include other

costs to the overall economy imposed by higher electricity prices, which could subdue electricity demand and GDP growth.

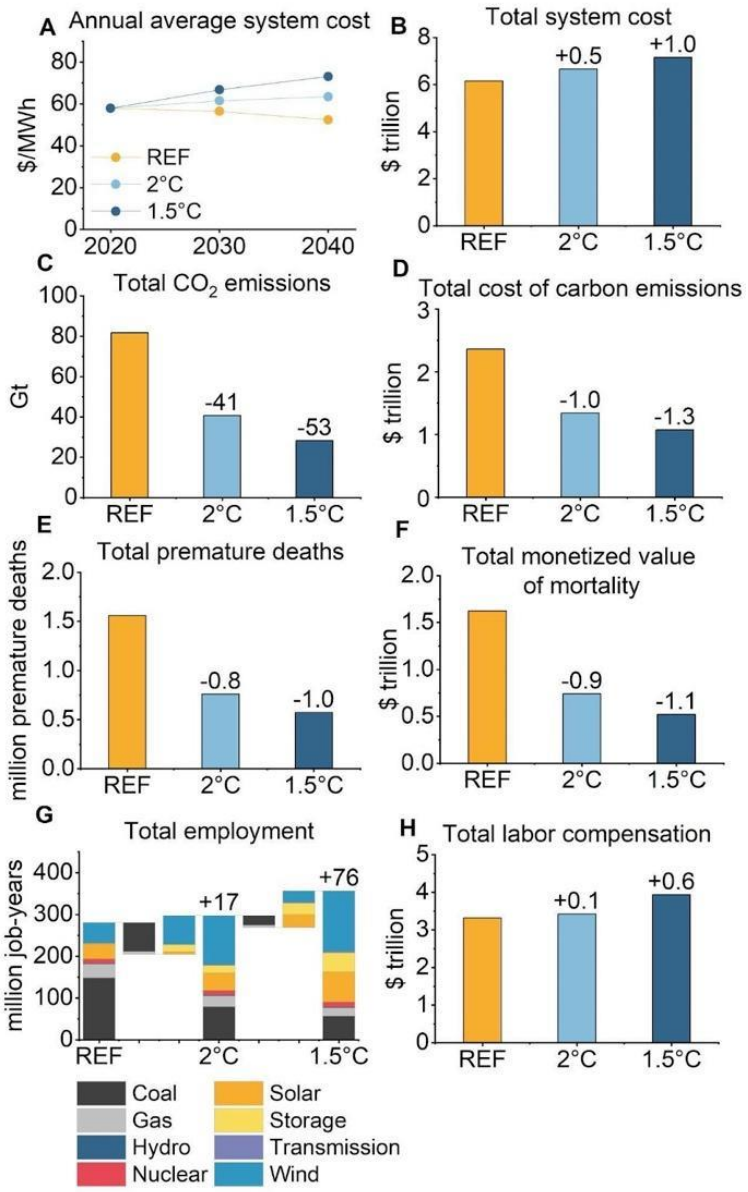


**Figure 2. Total impacts from 2020 to 2040 of China's electricity sector under the Reference scenario pathway (REF) and low-carbon scenario pathways compatible with 2ºC and 1.5ºC.**

(A) Annual average system costs per unit of electricity demand ($/MWh), (B) net present value of cumulative system cost ($ trillion), (C) cumulative $CO_2$ emissions (Gt), (D) total cost of carbon emissions ($ trillion). (E) cumulative premature deaths caused by $PM_{2.5}$ pollution from the electricity sector, (F) cumulative monetized value of premature deaths caused by the electricity sector ($ trillion), (G) cumulative employment (job-years) created by each technology/sector including differences in employment between scenarios, (H) cumulative labor compensation ($ trillion). Cost and value estimates are in 2020 USD. The net present value of system costs is calculated assuming a private discount rate of 8%. Net present value of labor compensation, monetized value of premature deaths, and cost of carbon emissions calculated assuming a social discount rate of 3%.

Employment and labor compensation patterns across scenarios are similar to those of the total system costs. Under the 2ºC scenario, 17 million more cumulative electricity sector-related job-years (both direct and indirect jobs) are created from 2020 to 2040 compared to the 280 million job-years created under the Reference scenario (Fig 2G). The loss of employment due to lower fossil fuel investments and generation is 76 million job-years, whereas the expansion of renewables, storage systems, and electricity grids adds 93 million job-years. Similarly, labor compensation also increases by 3% or $0.1 trillion compared to a total of $3.3 trillion under the Reference scenario (Fig 2H). Under the 1.5ºC scenario, job gains from greater investment in renewables compensate for job losses from phasing out fossil fuel generation, leading to a net cumulative employment increase (76 million job-years, or 27%) compared to the Reference scenario. Phasing out fossil fuels leads to a reduction of 104 million job-years compared to the Reference scenario, while new jobs

created by renewables, storage systems and electricity grids reach 179 million job-years. This net increase in employment raises total labor compensation by 19% or $0.6 trillion. In sensitivity tests, scenarios with higher costs for generation and storage technologies incur higher employment and labor compensation compared to the base low-carbon scenarios (Fig S9-S10). These estimates do not include jobs that are likely to be created for energy efficiency and end-use electrification retrofits, or job losses that may be incurred in fossil fuel transportation and other sectors (e.g., heating) due to greater electrification of end uses.

Air pollution and carbon emissions from fossil fuel generation cause substantial health and climate damages but these damages decrease with increasing levels of decarbonization. From 2020 to 2040, air pollution under the Reference scenario causes 1.6 million premature deaths and result in $1.6 trillion in health damages, while $CO_2$ emissions reach 82 Gt and result in climate damages of $2.4 trillion (Fig 2C-F). Meeting the carbon emissions cap compatible with the 2ºC target avoids 0.8 million (51%) of the premature deaths associated with power plant emissions and 41 Gt (41%) of cumulative $CO_2$ emissions under the Reference scenario, across 2020-2040 (Fig 2 C,E). This reduction in premature deaths and carbon emissions under the 2ºC scenario corresponds to a decrease of $0.9 trillion in health damages and $1.0 trillion in climate damages (Fig 2F). Compared to the Reference scenario, the 1.5ºC scenario avoids 1.0 million air pollution-related premature deaths (63%) and $1.1 trillion in monetized health damages, while also avoiding 53 Gt of $CO_2$ emissions or $1.3 trillion in climate costs (Fig 2C-F).

### 3. Labor compensation gains and losses across regions and provinces

Among the four economic regions, the East Coast region experiences the largest total employment and labor compensation under the Reference scenario. The region accounts for approximately half the total cumulative employment and total labor compensation over 2020-2040 (Fig 3A,B, Fig S11). More importantly, per capita employment and labor compensation in the East Coast region are about 20-50% greater than the other regions (Fig S12, S13).

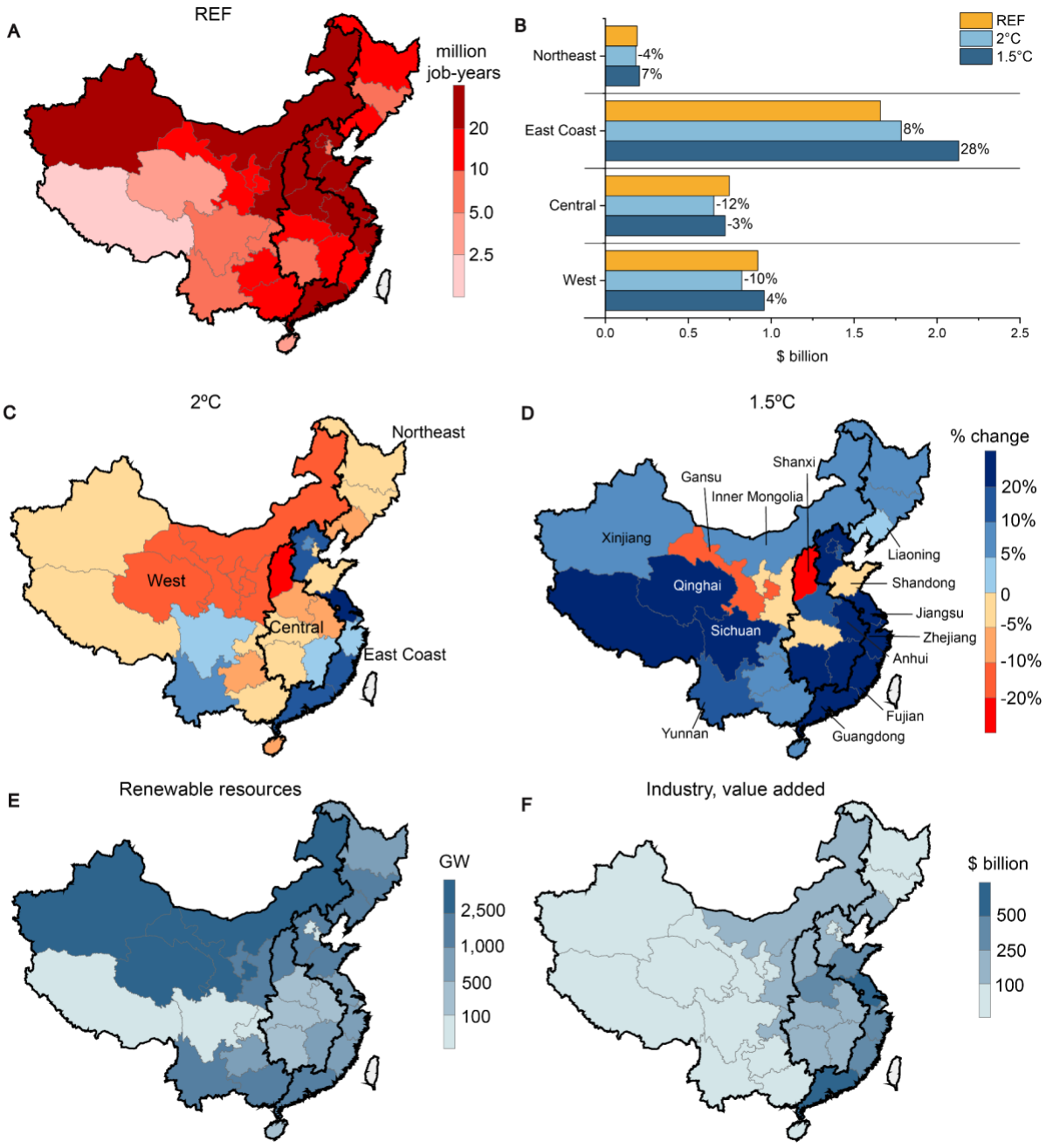


**Figure 3. Labor compensation across provinces and regions.**

(A) Cumulative electricity sector-related labor compensation across 2020-2040 under the Reference scenario (REF). (B) Cumulative labor compensation ($ billion) under the Reference, 2 ºC and 1.5 ºC scenarios in the four economic regions (numbers indicate the relative change from the Reference scenario). Change in cumulative labor compensation (%)

under the (C) 2 ºC scenario and (D) 1.5 ºC scenario, relative to the Reference scenario. (E) Renewable energy resources (GW) by province. (F) industrial value added in 2022($ billion) in China[168].

Under the 2ºC scenario, labor compensation in the Northeast, West, and Central China regions decreases because labor compensation losses from phasing out of fossil fuels are not fully compensated by increases in labor compensation driven by the build-up in renewable energy capacity (Fig 3B). The GDP per capita in most provinces (19 out of 21) across these three regions is at or below the national average.

However, under a more stringent carbon target in the 1.5ºC scenario, these three regions experience a modest rise in net employment and labor compensation, compared to the Reference scenario Employment and labor compensation driven by new renewable capacity are assumed to be proportional to the investments in renewable energy. A more stringent carbon target requires greater investments in renewable energy, which results in greater employment and labor compensation gains compared to losses due to fossil fuel infrastructure phaseouts. This effect is most pronounced in the West region, which has abundant renewable resources (Fig 3E), where the number of jobs and labor compensation decreases by 0.5% and 10% under the 2ºC scenario, respectively, but increases by 9% and 4% in the 1.5ºC scenario compared to the Reference scenario. This increase is mainly driven by renewable energy installations in Inner Mongolia, which contribute about 20% of the growth in jobs and 40% of the growth in labor compensation in the region.

For the East Coast region, net employment and labor compensation increase in both low-carbon scenarios, thus increasing the gap in employment between regions (Fig 3B, job

and wage per capita shown in Fig S12,S13). Two reasons account for this increase. First, the East Coast region has mature manufacturing industries, and thus more indirect jobs are created in the manufacturing sector (Fig 3F). Second, by harnessing the high-quality offshore wind resources in the region, the East Coast region installs ~2100 GW of renewable energy capacity in the 2ºC scenario and ~2400 GW in the 1.5ºC scenario by 2040, which accounts for ~40% of the total installed renewable energy capacity in each scenario. Under the 2ºC scenario, the East Coast region experiences an increase of 18% in employment and 8% in labor compensation. This rise is greater under the 1.5ºC scenario, with job increases of 34% and labor compensation increases of 28% (Fig 3B).

Although the 1.5ºC low carbon scenario improves labor market outcomes in the majority of China's provinces compared to the Reference scenario, several provinces are still expected to experience employment losses due to their reliance on fossil fuel generation and mining, and a lack of high-quality renewable resources (Fig 3C,D). Shanxi province in the Central region, the largest supplier of coal (~30%) in China[211], loses nearly 10 million job-years (-36%) and $98 billion of labor compensation (-35%) under the 1.5ºC scenario. Shaanxi province, the third largest coal supplier in China (~15%), also loses jobs and labor compensation under both low-carbon scenarios. Similarly, Shandong province in the East Coast region relies heavily on fossil fuels and the growth in renewable energy capacity under the low-carbon scenarios fails to negate the compensation losses in the fossil fuel industries. Other provinces, including Ningxia, Gansu, and Hubei, also lose jobs under both low-carbon scenarios. We found that the renewable resources in Ningxia and Gansu, though abundant, are mainly used to meet demand within the province. Inner Mongolia and Xinjiang are the major net exporters of electricity in the Northwest. As electricity demand

and exports are both low in Gansu and Ningxia (Fig S14), the low-carbon transition does not lead to a loss in employment and labor compensation. These results show that the labor market implications of decarbonizing the electricity sector can vary greatly across regions.

### 4. Health benefits from electricity sector decarbonization across regions and provinces

To assess the health effects of decarbonization pathways, we estimate exposure to air pollution, specifically $PM_{2.5}$, from coal and gas-fired power plants and its impacts on premature mortality at a spatial resolution of 36 km. We present results aggregated at the province level in the main text (Fig 4).

As China's electricity sector decarbonizes from 2020 to 2040 in the Reference scenario, annual health impacts due to air pollution caused by the electricity sector decrease across regions but historical inter-regional inequities persist. Annual premature mortality in 2040 drops by 50-60% compared to 2020 across all regions, with the East Coast and Central regions being the largest beneficiaries (Fig S15). Because of their continued reliance on fossil fuel generation under the Reference scenario and their higher population density, the East Coast and Central regions experience the largest cumulative premature deaths due to air pollution from electricity generation across our planning horizon—0.7 million (45% of the total premature deaths) and 0.5 million (31% of the total premature deaths), respectively (Fig 4A,B). Cumulative premature deaths per capita are also highest in these regions (Fig S16).

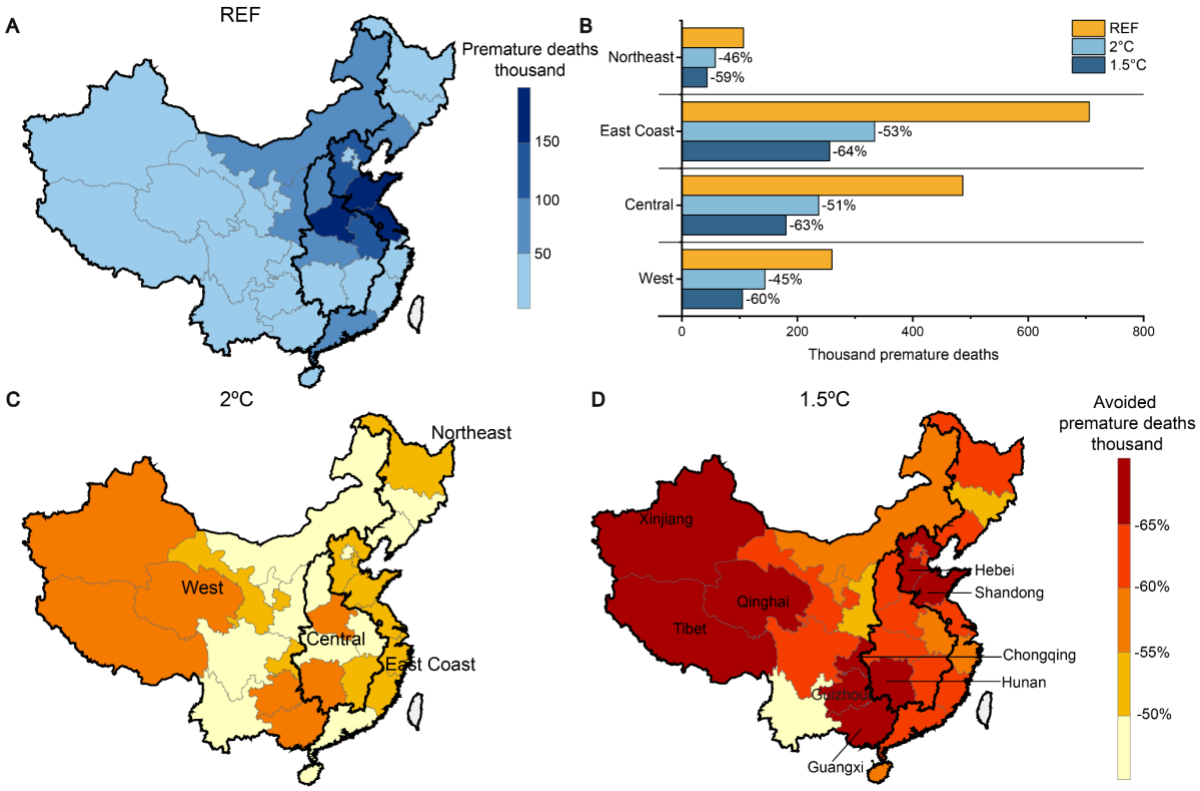


**Figure 4. Health benefits across provinces and regions.**

(A) Cumulative premature deaths caused by air pollution from the electricity sector across 2020-2040 under the Reference scenario (REF). (B) Cumulative premature deaths during 2020-2040 under the Reference, 2ºC, and 1.5ºC scenarios in the four economic regions (numbers indicate the change from the Reference scenario). Avoided premature deaths under (C) the 2ºC scenario and (D) the 1.5ºC scenario, relative to the Reference scenario.

Under the low carbon scenarios, regions with the largest health burden under the Reference scenario also account for the largest shares of health benefits attained by the reduction in air pollution from electricity generation (Fig 4B). Under the 2ºC and 1.5ºC scenarios, the East Coast and Central regions together experience the largest share (~75%) of the total reduction in cumulative premature deaths across 2020-2040 (Fig 4B). Under the

2ºC scenario, 0.37 million cumulative premature deaths (47% of total reduction) are reduced in the East Coast region, followed by 0.25 million (32% of total reduction) in the Central region. Premature deaths are further reduced under the 1.5ºC scenario, with 0.45 million (46% of total reduction) in the East Coast region and 0.31 million (31% of total reduction), relative to the Reference scenario. At the province level, Shandong and Jiangsu in the East Coast region and Henan in the Central region experience the largest cumulative premature mortalities caused by air pollution from fossil fuel generation over 2020-2040 in the Reference scenario, but also experience large gains in avoided premature mortalities in the low-carbon scenarios (Fig 4 C,D, Fig S17). The relative reduction in premature deaths in the low-carbon scenarios is also large in West and Northeast regions, but the absolute reduction is much lower, because these regions have historically been less impacted by air pollution from electricity generation.

**5. Potential trade-offs between employment effects and health benefits**

Compared to the Reference scenario, all provinces gain health benefits due to the phase-down of fossil fuel power plants under the low-carbon scenarios. However, we found that provinces, especially those with low GDP per capita, are more likely to experience a trade-off between health benefits and labor compensation losses because these provinces lose jobs related to the coal industry (Fig 5A). On average, high-income provinces experience benefits in both health and labor compensation under the low-carbon scenarios, while upper- and lower-middle-income groups lose labor compensation under the 2ºC scenario and gain labor compensation under the 1.5ºC scenario. Average labor compensation

in the low-income provinces decreases under the 1.5ºC scenario, mainly driven by the coal-producing Shanxi province.

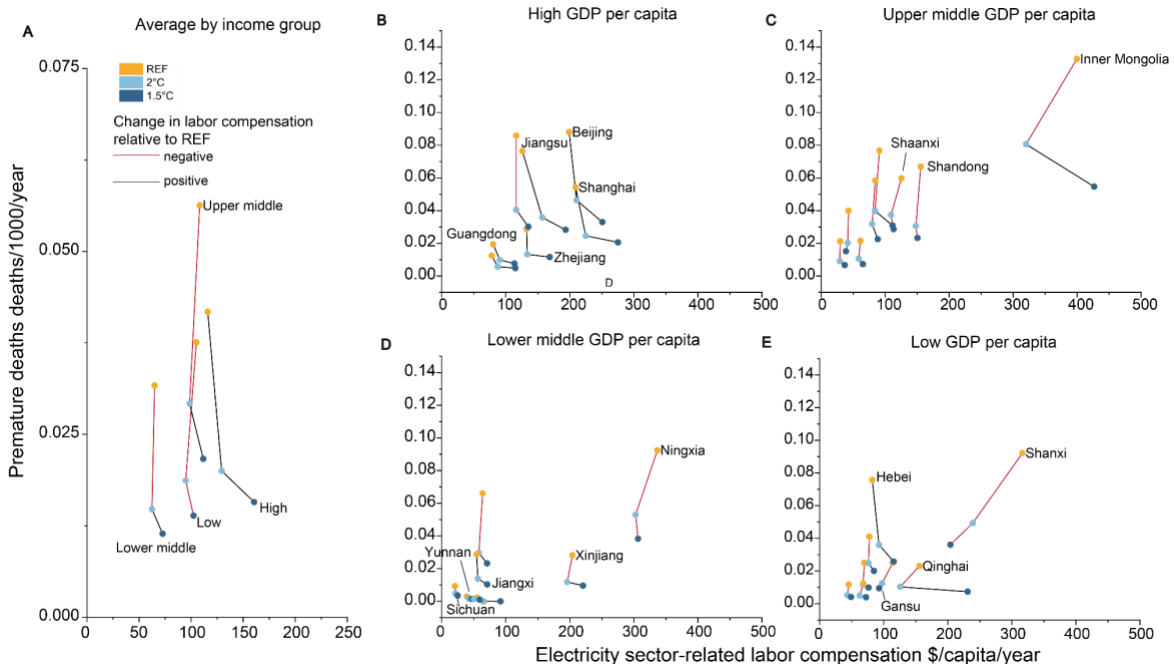


**Figure 5. Trade-off between health and labor compensation.**

(A) Average premature deaths (deaths per 1,000 per year) and electric sector-related labor compensation ($/capita/year) under the Reference, 2ºC and 1.5ºC scenarios by income group. Premature deaths and labor compensation under the Reference, 2ºC and 1.5ºC scenarios in (B) high-income, (C) upper-middle-income, (D) lower-middle-income and (E) low-income provinces. The income level is classified based on the four quantiles of the provincial GDP per capita in year 2020. The red lines represent a decrease in labor compensation compared to the Reference scenario.

At the provincial level, while all provinces experience health benefits, the employment and labor compensation outcomes have mixed results. Nearly all high-income

provinces experience gains in both health benefits and labor compensation. Beijing, Shanghai, Jiangsu, Guangdong, Fujian and Zhejiang, experience an increase in labor compensation and a decrease in premature deaths under both the 2ºC and 1.5ºC scenarios relative to the Reference scenario (Fig 5B). In contrast, only a few provinces in the lower-middle-income and low-income groups—Jiangxi, Hebei, Yunnan and Sichuan—experience an increase in labor compensation and a decrease in premature deaths under both the 2ºC and 1.5ºC scenarios. Nine out of the 16 lower-middle and low-income provinces experience labor compensation loss while avoiding premature deaths in health outcomes in the 2ºC scenario compared to the Reference scenario. Six provinces experience a decrease in labor compensation while avoiding premature deaths under both 2ºC and 1.5ºC scenarios–Shanxi, Ningxia, Gansu, Shaanxi, Hubei, and Shandong. Five out of these six provinces are major coal producers and the first three are from the low-income and lower-middle-income groups. These three provinces account for almost one-third of China's coal production and 10% of coal generation capacity. Phasing out coal power plant capacity and energy generation reduces premature deaths, but also results in unemployment and reduced labor compensation in these provinces. Decreases in labor compensation, especially in provinces with lower GDP per capita highlight the need to create new employment opportunities in coal-producing provinces, which will be critical for equitable development as coal infrastructure retires and coal-dependent jobs are lost.

To understand the temporal trends in employment impacts, we examined how the regional disparities in employment and avoided premature deaths evolve with a finer 5-year investment period (Fig S18). Compared to the reference scenario, in the low-carbon scenarios, while health benefits accrue across all regions in each investment period, the East

region begins experiencing larger gains in employment right from 2025 compared to the other regions. Furthermore, the 2ºC scenario creates fewer jobs in the three regions–West, Central, and Northeast–from 2035 onwards compared to reference. However, in the 1.5ºC scenario, health benefits and employment gains occur in all investment periods across all provinces, except for a dip in employment in 2035 in the West and Central regions.

### *D. Discussion*

China has pledged to reach peak $CO_2$ emissions by 2030 and achieve carbon neutrality by 2060. In its Nationally Determined Contribution (NDC), China also committed to installing at least 1,200 GW of wind and solar capacity by 2030, more than doubling its 2020 capacity[212]. Our results show that even without imposing a carbon emissions target, under the cost-optimal Reference scenario, total wind and solar capacity in 2030 is more than double the NDC commitment and annual carbon emissions in 2030 decrease by 20% compared to 2020. More importantly, achieving a carbon emissions goal compatible with the 2ºC warming target (85% lower in 2040 compared to 2020) has slightly higher total system costs than the Reference scenario. Further, the 2ºC pathway results in an increase in the number of job-years and labor compensation, and large benefits in terms of avoided health and climate damages. Achieving an even more ambitious low-carbon pathway compatible with a 1.5ºC target (99% lower in 2040 compared to 2020) costs significantly more, but also results in larger increases in labor compensation, health benefits, and avoided climate damages.

Our results for wind and solar installed capacities are similar to studies that assumed recent cost projections for these technologies[187], but they are greater than others that imposed limitations on the growth of manufacturing capacities[192]. Compared to the

employment effects in our study, the estimate from Zhang et al[170] is 40% lower than ours due to the omission of the indirect employment impacts from a life-cycle perspective (Table S10), and the estimate from Zhou et al[172] is 60% lower than ours due to the omission of the private sector employment (Table S11). Similarly, our estimates of premature deaths in 2020 under the Reference scenario are lower than those of other studies because of higher shares of clean energy in 2020 and our assumption that the emission standards have perfect compliance (Table S17)[166].

**1. Low-carbon pathways bring significant health benefits beyond already implemented low sulfur regulations**

Although China has made large strides in limiting the sulfur emissions from its coal power plants through the enforcement of ultra-low sulfur standards[203], further phasing out fossil fuel generation in line with 2ºC and 1.5ºC targets can lead to significant health benefits—0.8 million and 1.0 million avoided deaths, respectively, over 2020-2040. Under both the low-carbon scenarios, about 80% of the reduction in cumulative premature deaths occurs in provinces of the East Coast and Central regions, which have historically disproportionately borne the pollution burden from fossil fuel generation.

Our study only considers the direct air pollutant emission from power plants and has not calculated the air pollutant emissions from a life-cycle perspective from the transportation and industrial sectors. This omission may underestimate the health benefits because the life-cycle particulate matter emissions from wind and PV are substantially lower than coal and natural gas generation[213]. Further, we only quantified the impacts of $PM_{2.5}$ on premature mortality. Accounting for additional health end-points (e.g., impacts on chronic

respiratory disease) and other air pollutants released by power plants (e.g., $NO_x$ and ambient ozone) would increase the health benefits attributable to the decarbonization of the electricity sector. Overall, we find that health benefits are likely to be higher in low-carbon scenarios, especially in the 1.5ºC scenario, which assumes greater electrification of end-uses.

**2. Net gains and losses in employment driven by fossil fuel phaseout, renewable resource endowments, and manufacturing**

Decarbonization of China's electricity system is expected to exert distinct impacts on employment across provinces. Although total employment and labor compensation at the national level increases under the 2ºC compatible carbon emissions target, most provinces in the West, Central and Northeast regions, which account for 80% of the jobs in the coal mining sector, experience a net loss in employment and labor compensation compared to the Reference scenario. In other words, the growth in renewable capacities in these regions is not enough to balance the loss in employment and labor compensation in the fossil fuel sector (Fig S19). In contrast to the provinces in the West, Central, and Northeast regions, most of which have a low GDP per capita, East Coast provinces (e.g., Jiangsu, Guangdong, and Zhejiang) with high GDP per capita experience a net gain in employment and labor compensation. This gain is driven by the development of offshore wind in the region, spillover effects of employment through renewable energy development in other regions, and a relatively low loss of employment in the fossil fuel sector because of the region's small share of coal mining jobs (7% excluding Shandong).

Under the more stringent 1.5ºC compatible carbon emissions target, most provinces gain employment due to the expansion of renewable energy capacity. However, in Shanxi, Shandong, Hubei, Gansu, Ningxia and Shaanxi provinces, jobs and labor compensation decrease due to a phase-out of their large existing capacity of fossil fuel generation and mining or a relatively poor quality of renewable resources.

Creating employment opportunities in low-income provinces is important for a low-carbon energy transition to be equitable and inclusive. Our results show an increasing gap in employment impacts between the high-income East Coast region and other regions with more stringent decarbonization targets. Net gains in employment and labor compensation are greater in the East Coast region than all other regions, partly because the East Coast region absorbs ~20-30% of the jobs created by energy infrastructure development in other regions driven by spillover effects (Fig S20). The West region, even with its greater development of solar and wind resources, creates only half of the resulting cumulative job increases locally because of its reliance on material and manufactured goods imports from the East Coast region (Fig S20). In addition to its highly developed manufacturing industry, the East Coast region's development of large-scale offshore wind capacities, higher investment costs of which create more indirect jobs than onshore wind, exacerbates regional disparities in employment.

In the provinces that experience job losses and reduced labor compensation under the low-carbon scenarios, installing carbon capture and storage (CCS) could extend some level of coal generation while meeting emissions targets and thus avoid large employment losses (Fig. S20). We observe an increase in employment and labor compensation in most provinces to achieve low-carbon targets. Shanxi and Hubei provinces still experience a reduction in employment and labor compensation because CCS cannot reduce all carbon emissions to zero

and some coal capacity is retired to meet carbon targets, but the relative decrease in employment is much more modest compared to the scenario without CCS. As coal and gas capacities with CCS continue to operate, provinces, especially in the West region, see fewer investments in renewable energy and thus a smaller increase in employment and labor compensation compared to the scenario without CCS. We do not estimate health benefits of CCS scenarios because of significant uncertainties in emissions of criteria pollutants from power plants with CCS but expect that overall health benefits of the low-carbon scenarios will be reduced because of greater coal capacity and energy generation with CCS systems.

**3. Policy and program interventions needed to ensure an equitable low-carbon transition**

Our results show that the low-carbon transition in China's electricity sector will likely yield uneven employment outcomes across low- and high-income provinces. In the absence of policy interventions, some low-income provinces, especially those that have historically relied on fossil fuel extraction such as Shaanxi, are likely to experience significant employment losses but relatively modest health benefits, deepening regional disparities in economic development. While new employment opportunities will mostly arise in regions with high-quality wind and solar energy resources, materials and manufacturing industries that support the low-carbon transition could be encouraged in lower-income regions and provinces which have especially relied heavily on coal mining. Toward this goal, in its 14th Five-Year Plan, China pledges to reduce the regional disparity by incentivizing the transfer of job opportunities from the wealthier East Coast region to the West, Central and Northeast regions[214]. China has already announced a few regional development plans—China Western

Development Plan, Northeast Area Revitalization Plan and Rise of Central China Plan—that encourage the transfer of manufacturing industries from the East Coast region to the Central, West and Northeast regions, and further develop renewable energy resources in the West region. Such programs have contributed to narrowing the gap in employment opportunities; however, their actual effects deserve further research. Targeted social assistance, financial transfers, and revenue sharing for renewable development in low-income regions could facilitate a just transition. For example, first, the central government could strengthen the social safety net to ease the burden of the transition for affected coal workers. Currently, these programs are run at the provincial level. Nationalizing these programs would provide more stability for workers in the most vulnerable regions and sectors. Second, carbon tax and dividend payments could be used to collect necessary revenue to pay for assistance programs during the transition. Third, local and provincial governments in fossil fuel-dependent regions could create opportunities to address environmental damages from coal mining and ecosystem restorations, which in turn could provide stimulus to local economic revitalization. More studies, especially at the sub-provincial level and across multiple dimensions in addition to GDP disparities, will be needed to better understand and plan for the impacts of the low-carbon energy transition in China.

## *E. Appendix*

### 1. Data and code availability

GridPath model code is available at https://github.com/blue-marble/gridpath. The code for the paper is available at https://github.com/cetlab-ucsb/China-low-carbon. The data are available at https://zenodo.org/records/10873443.

## 2. Supplementary notes and tables

**Note S1. Carbon budget and electricity demand under the Reference, 2ºC and 1.5ºC scenarios.**

The parameters are derived from the corresponding scenarios in the CDLINKS database.

**Table S1**. Scenarios used in this study and the corresponding scenarios in CDLINKS.

| Scenario | Scenario in CDLINKS | Description |
|---|---|---|
| Reference | NPi | National Policies implemented scenario includes currently implemented climate, energy and land policies and extrapolates the implied effort beyond the direction of the policies |
| 2°C | NPi2020_1000 | NPi scenario until 2020 with a transition to a globally cost-effective implementation of a carbon budget for the period 2011-2100 of 1000 $GtCO_2$ afterwards, corresponding to staying below 2°C at >66% through the 21st century |
| 1.5°C | NPi2020_400 | NPi scenario until 2020 with a transition to a globally cost-effective implementation of a carbon budget for the period 2011-2100 of 400 $GtCO_2$ afterwards, corresponding to a chance of >66% for staying below 1.5°C in 2100 |

**Table S2**. Budget of $CO_2$ (Mt/year) under different scenarios.

| Scenario | Model | 2030 | 2040 |
|---|---|---|---|
| 2°C | AIM/CGE 2.1 | 568 | 28 |
| | COPPE-COFFEE 1.0 | 2142 | 645 |
| | DNE21+ V.14 | 2246 | 949 |
| | GEM-E3 V1 | 3342 | 922 |
| | IMAGE 3.0.1 | 3406 | 2068 |
| | MESSAGEix-GLOBIOM 1.0 | 1449 | 619 |
| | REMIND-MAgPIE 1.7-3.0 | 2173 | 531 |
| | WITCH-GLOBIOM 4.4 | 393 | -290 |
| | Median | 2157 | 632 |
| 1.5°C | AIM/CGE 2.1 | 440 | 3 |
| | COPPE-COFFEE 1.0 | 682 | 0 |
| | DNE21+ V.14 | 657 | 68 |
| | GEM-E3 V1 | 1448 | 158 |
| | IMAGE 3.0.1 | 2347 | 179 |
| | MESSAGEix-GLOBIOM 1.0 | 784 | 37 |
| | REMIND-MAgPIE 1.7-3.0 | 2051 | 242 |

| | | | |
|---|---|---|---|
| | WITCH-GLOBIOM 4.4 | -59 | -314 |
| | Median | 733 | 52 |

**Table S3**. Raw data for electricity demand (EJ/year) from CD-LINKs.

| Scenario | Model | 2020 | 2030 | 2040 |
|---|---|---|---|---|
| REF | AIM/CGE 2.1 | 21 | 26 | 29 |
| | COPPE-COFFEE 1.0 | 18 | 27 | 30 |
| | DNE21+ V.14 | 23 | 33 | 40 |
| | GEM-E3 V1 | 23 | 30 | 33 |
| | IMAGE 3.0.1 | 27 | 36 | 43 |
| | MESSAGEix-GLOBIOM 1.0 | 24 | 29 | 31 |
| | REMIND-MAgPIE 1.7-3.0 | 26 | 39 | 51 |
| | WITCH-GLOBIOM 4.4 | 28 | 43 | 55 |
| | Median | 24 | 31 | 36 |

**Note S2. Electricity demand**

We use the median electricity demand in each period across 8 IAMs under the NPi scenario to derive the electricity demand. In 2020, the electricity demand is 7.6 PWh[168].

**Table S4**. Electricity (PWh) demand across 2020-2040 in this study.

| | Fixed demand | | | Demand growth | | |
|---|---|---|---|---|---|---|
| | Reference | 2ºC | 1.5ºC | Reference | 2ºC | 1.5ºC |
| 2020 | 7.6 | 7.6 | 7.6 | 7.6 | 7.6 | 7.6 |
| 2030 | 10.1 | 10.1 | 10.1 | 10.1 | 9.3 | 9.7 |
| 2040 | 11.7 | 11.7 | 11.7 | 11.7 | 10.7 | 11.8 |

**Note S3. Cost projection**

China-specific cost for energy technologies in 2020 is derived from published literature[192] and International Renewable Energy Agency[107]. An exchange rate of 6.5 is used to convert RMB to 2020 US dollars. The NREL 2021 Annual Technology Baseline (ATB) is used to derive the normalized cost projection curve for the cost of energy technologies. We assume that China's energy cost follows the same projection as the ATB database[193].

**Table S5**. Capital cost, and operation and Maintenance (O&M cost) for electricity generation technologies in the year 2020[107,192,193]. The cost data for solar are quoted as dollar per-watt of direct current.

| Technology | sub-technology | Capital cost $/kW | O&M cost $/kWh/yr |
|---|---|---|---|
| Solar | Solar-utility | 651 (DC) | 10 |
| | Solar-commercial | 691 (DC) | 10 |
| | Solar-residential | 746 (DC) | 14 |
| Wind | Onshore wind | 1264 | 22 |
| | Offshore wind | 2968 | 67 |
| Hydropower | Hydropower | 2240 | 40 |
| Coal | Coal | 622 | 10 |
| | Coal-IGCC | 1120 | 19 |
| Natural gas | Natural gas-OCGT | 324 | 12 |
| | Natural gas-CCGT | 367 | 15 |
| Nuclear | Nuclear | 2462 | 86 |

**Table S6**. Capital cost, and operation and maintenance (O&M cost) for energy storage technologies in the year 2020[192].

| | Capacity cost $/kW | Energy cost $/kWh | O&M cost $/kW/yr |
|---|---|---|---|
| Battery | 492 | 246 | 25 |
| Pumped hydro | 918 | NA | 23 |

**Table S7**. Normalized cost projections derived from ATB database[193]. The cost projection is assumed to be 1 in the year 2020.

| Cost projection | Low | | | Moderate | | | High | | |
|---|---|---|---|---|---|---|---|---|---|
| Period | 2020 | 2030 | 2040 | 2020 | 2030 | 2040 | 2020 | 2030 | 2040 |
| Battery_capacity | 1.00 | 0.41 | 0.33 | 1.00 | 0.53 | 0.45 | 1.00 | 0.70 | 0.70 |
| Battery_energy | 1.00 | 0.42 | 0.34 | 1.00 | 0.77 | 0.74 | 1.00 | 0.81 | 0.81 |
| Central_PV | 1.00 | 0.46 | 0.41 | 1.00 | 0.56 | 0.51 | 1.00 | 0.86 | 0.71 |
| Commercial_PV | 1.00 | 0.40 | 0.35 | 1.00 | 0.52 | 0.46 | 1.00 | 0.83 | 0.68 |
| Residential_PV | 1.00 | 0.29 | 0.24 | 1.00 | 0.37 | 0.33 | 1.00 | 0.83 | 0.60 |
| Gas_CT | 1.00 | 0.91 | 0.86 | 1.00 | 0.91 | 0.86 | 1.00 | 0.91 | 0.86 |
| Gas_CCGT | 1.00 | 0.95 | 0.91 | 1.00 | 0.95 | 0.91 | 1.00 | 0.95 | 0.91 |
| Wind | 1.00 | 0.51 | 0.45 | 1.00 | 0.68 | 0.61 | 1.00 | 0.72 | 0.68 |

| | | | | | | | | | |
|---|---|---|---|---|---|---|---|---|---|
| Offshore_Wind | 1.00 | 0.62 | 0.51 | 1.00 | 0.67 | 0.58 | 1.00 | 0.79 | 0.73 |
| Coal | 1.00 | 0.89 | 0.80 | 1.00 | 0.93 | 0.85 | 1.00 | 0.96 | 0.89 |
| Coal_IGCC | 1.00 | 0.92 | 0.88 | 1.00 | 0.92 | 0.88 | 1.00 | 0.92 | 0.88 |
| Nuclear | 1.00 | 0.93 | 0.87 | 1.00 | 0.93 | 0.87 | 1.00 | 0.93 | 0.87 |

**Table S8**. Cost scenarios in this study and the corresponding cost projections in 2021 ATB[193].

| Sensitivity test | Scenario in 2021 ATB |
|---|---|
| High cost | Conservative |
| Moderate cost | Moderate |
| Low cost | Advanced |

**Note S4. Calculation of labor compensation**

The weekly average wages for US power plants are collected from the Quarterly Census of Employment and Wages of US Bureau of Labor Statistics (BLS, https://www.bls.gov/cew/). There is no specific industry for the storage system, and we use the power distribution industry as a proxy.

The wage for long-term jobs is derived from the average wage in the US and China. China's National Bureau of Statistics only records the average wage of the electricity sector in China. We assume that the average wage in China corresponds to the fossil fuel power

generation industry in the US. The average wage for the electricity sectors in China is assumed to follow the same sector-specific wage ratios in the US.

**Table S9**. The weekly average wage for US and China power plants.

| | Power plant | Weekly average ($/week) | Industry in BLS |
|---|---|---|---|
| US | Coal | 2321 | Power generation, fossil fuel |
| | Gas | 2321 | Power generation, fossil fuel |
| | Hydro | 2202 | Power generation, hydroelectric |
| | Nuclear | 2920 | Power generation, nuclear electric |
| | Solar | 1921 | Power generation, solar electric |
| | Storage | 2073 | Electric power distribution systems |
| | Wind | 2012 | Power generation, wind electric |
| China | Coal and gas | 333 | |

**Table S10**. The wage for long-term jobs in the operation and maintenance of power plants in 2020 ($/job-year).

| | Coal | Gas | Hydro | Nuclear | Solar | Storage | Wind |
|---|---|---|---|---|---|---|---|
| Beijing | 28732 | 28732 | 27259 | 36147 | 23781 | 25662 | 24907 |
| Tianjin | 25660 | 25660 | 24345 | 32282 | 21238 | 22918 | 22244 |
| Hebei | 16909 | 16909 | 16042 | 21273 | 13995 | 15102 | 14658 |
| Shanxi | 14158 | 14158 | 13432 | 17812 | 11718 | 12645 | 12273 |
| Inner Mongolia | 17520 | 17520 | 16621 | 22041 | 14500 | 15648 | 15187 |
| Liaoning | 13213 | 13213 | 12536 | 16623 | 10936 | 11801 | 11454 |
| Jilin | 14305 | 14305 | 13572 | 17997 | 11840 | 12777 | 12401 |
| Heilongjiang | 13384 | 13384 | 12698 | 16838 | 11078 | 11954 | 11602 |
| Shanghai | 35849 | 35849 | 34011 | 45100 | 29670 | 32018 | 31076 |
| Jiangsu | 23510 | 23510 | 22304 | 29577 | 19458 | 20998 | 20380 |
| Zhejiang | 23997 | 23997 | 22766 | 30190 | 19861 | 21433 | 20802 |
| Anhui | 18924 | 18924 | 17954 | 23808 | 15663 | 16902 | 16405 |
| Fujian | 18971 | 18971 | 17998 | 23867 | 15701 | 16944 | 16445 |

| | | | | | | | |
|---|---|---|---|---|---|---|---|
| Jiangxi | 13988 | 13988 | 13271 | 17598 | 11577 | 12494 | 12126 |
| Shandong | 17652 | 17652 | 16747 | 22208 | 14610 | 15766 | 15302 |
| Henan | 14578 | 14578 | 13830 | 18340 | 12065 | 13020 | 12637 |
| Hubei | 18919 | 18919 | 17949 | 23802 | 15659 | 16898 | 16401 |
| Hunan | 15751 | 15751 | 14943 | 19816 | 13036 | 14068 | 13654 |
| Guangdong | 23154 | 23154 | 21967 | 29130 | 19164 | 20680 | 20071 |
| Guangxi | 16318 | 16318 | 15482 | 20530 | 13506 | 14575 | 14146 |
| Hainan | 16797 | 16797 | 15935 | 21131 | 13902 | 15002 | 14560 |
| Chongqing | 15146 | 15146 | 14369 | 19055 | 12536 | 13528 | 13130 |
| Sichuan | 17700 | 17700 | 16792 | 22267 | 14649 | 15808 | 15343 |
| Guizhou | 18251 | 18251 | 17315 | 22961 | 15106 | 16301 | 15821 |
| Yunnan | 17234 | 17234 | 16350 | 21682 | 14264 | 15392 | 14939 |
| Tibet | 16325 | 16325 | 15488 | 20538 | 13512 | 14581 | 14152 |
| Shaanxi | 17494 | 17494 | 16597 | 22009 | 14479 | 15625 | 15165 |
| Gansu | 13911 | 13911 | 13198 | 17501 | 11513 | 12424 | 12059 |
| Qinghai | 17557 | 17557 | 16657 | 22088 | 14531 | 15681 | 15220 |
| Ningxia | 19082 | 19082 | 18104 | 24006 | 15793 | 17043 | 16541 |

| | | | | | | | |
|---|---|---|---|---|---|---|---|
| Xinjiang | 17030 | 17030 | 16157 | 21426 | 14095 | 15211 | 14763 |

**Note S5. Calculation of jobs**

The indirect employment is the jobs directly hired by the electricity sector, the manufacture sector, construction sector and the mining sector. Other studies use the employment factor (job/MW or job/MWh) to estimate the direct employment.

In this study, we used the MRIO method to estimate the indirect employment, and used the employment factor to estimate the direct employment from the maintenance of power plants. The indirect employment in MRIO is the jobs created along the supply chain of these inputs, including the job in the service sectors, financial sectors, etc.

**Table S11**. Jobs per unit capacity. Jobs by investment and operation are using the national average in 2040 under the Reference scenario.

| | Coal | Gas | Solar | Wind | Battery | Transmission |
|---|---|---|---|---|---|---|
| Jobs in O&M (per MW) | 1.32 | 0.77 | Central: 0.50<br>Commercial: 0.75<br>Residential: 1.0 | Onshore: 0.38<br>Offshore: 0.17 | 0.75 | |
| Jobs by investment (per million $) | 6.1 | 5.6 | 5.1 | 5.1 | 5.6 | 6.2 |
| Jobs by operation (per GWh) | 0.90 | 1.5 | | | | |

**Table S12**. Comparison of employment (million jobs) related to the electricity sector in 2020.

| Studies | Direct employment | Indirect employment |
|---|---|---|
| This study | 3.4 | 4.5 |
| Pai et al.[171] | 5.9 | NA |
| Ram et al.[200] | 5.0 | NA |
| Zhang et al.[170] | 4.6 | NA |

**Table S13**. Comparison of employment (million jobs) related to the electricity sector in 2020. Zhou et al.[172] used the labor data in China Population and Employment Statistics Yearbook, which only accounts for 170 million jobs in public sectors. This study accounts for the jobs in the agriculture, private and public sectors[168], which covers 730 million jobs.

| Studies | Employment in power plants | Employment in upstream sectors |
|---|---|---|
| This study | 2.2 | 5.7[172] |
| Zhou et al. | 1.25 | 1.77 |

**Note S6. Health burden**

We calculate air pollutant emissions and compare the annual $PM_{2.5}$-related premature deaths caused by the power system with other studies.

**Table S14**. Annual emissions of $PM_{2.5}$, $SO_2$ and $NO_x$ (tonne).

| | | 2020 | 2030 | 2040 |
|---|---|---|---|---|
| $PM_{2.5}$ | REF | 41,201 | 20,409 | 16,380 |
| | 2ºC | 39,200 | 7,819 | 3,003 |
| | 1.5ºC | 39,314 | 3,890 | 568 |
| $SO_2$ | REF | 858,096 | 515,043 | 395,547 |
| | 2ºC | 839,207 | 210,908 | 42,660 |
| | 1.5ºC | 838,684 | 78,900 | 1,340 |
| $NO_x$ | REF | 1,083,638 | 828,799 | 664,262 |
| | 2ºC | 1,072,713 | 319,229 | 122,650 |
| | 1.5ºC | 1,074,115 | 157,695 | 23,261 |

**Table S15**. Comparison of the $PM_{2.5}$-related premature deaths caused by the power system with other studies.

| **Studies** | **Year** | **Premature death (thousand)** |
|---|---|---|
| Hu et al[215] | 2013 | 134 |
| Gao et al[216] | 2013 | 268 |
| Wu et al[165] | 2015 | 94 |
| Tong et al[166] | 2018 | 170 |
| This study | 2020 | 94 |

## 3. Supplementary Figures

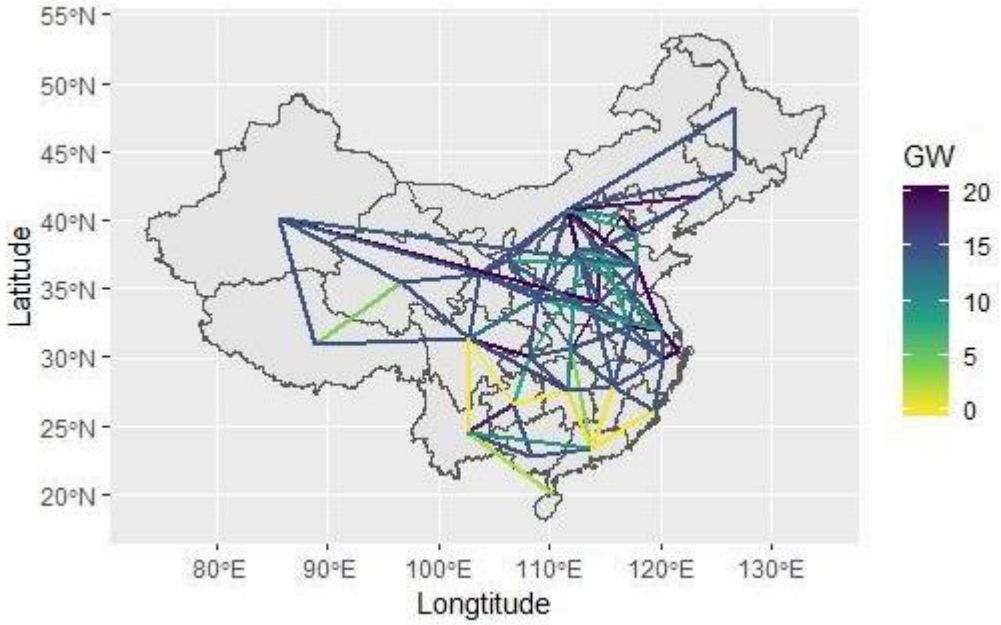


**Figure S1**. Transmission capacities in the year 2040 under the Reference scenario.

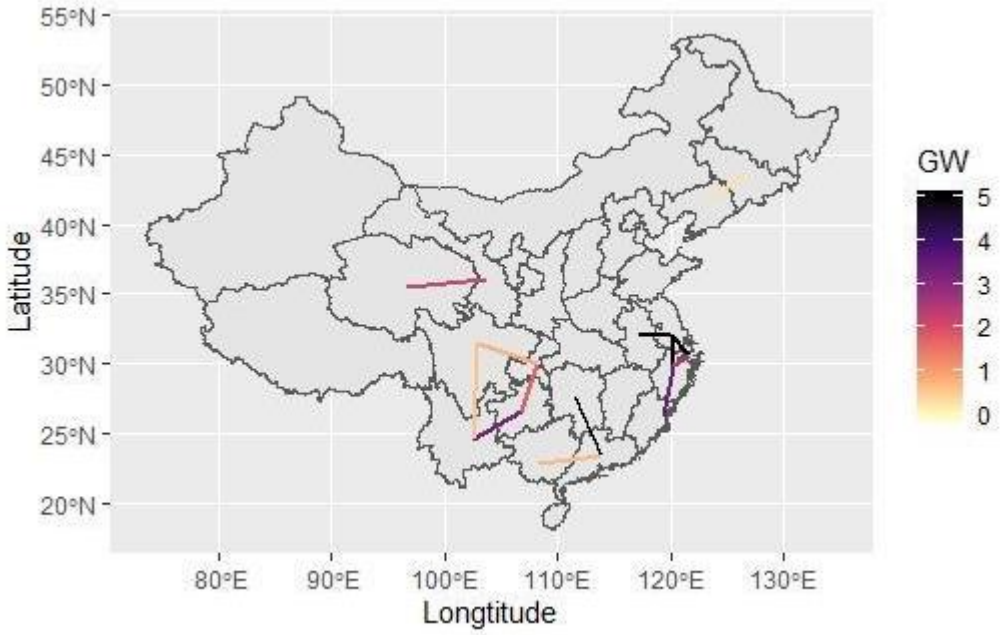


**Figure S2**. Cumulative new transmission capacities under the 2ºC scenario compared to the Reference scenario.

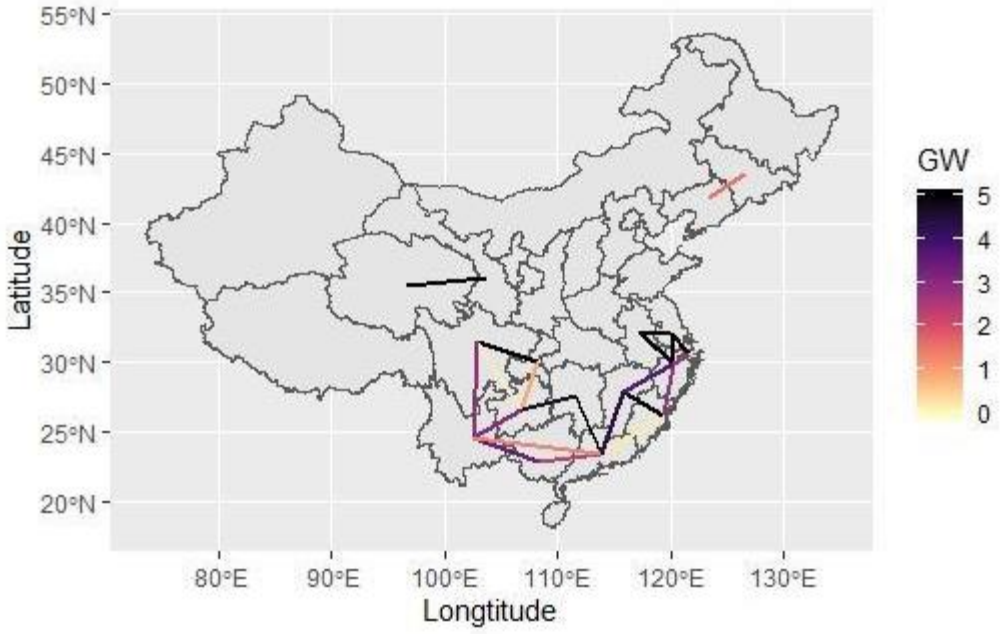


**Figure S3**. Cumulative new transmission capacities under the 1.5ºC scenario compared to the Reference scenario.

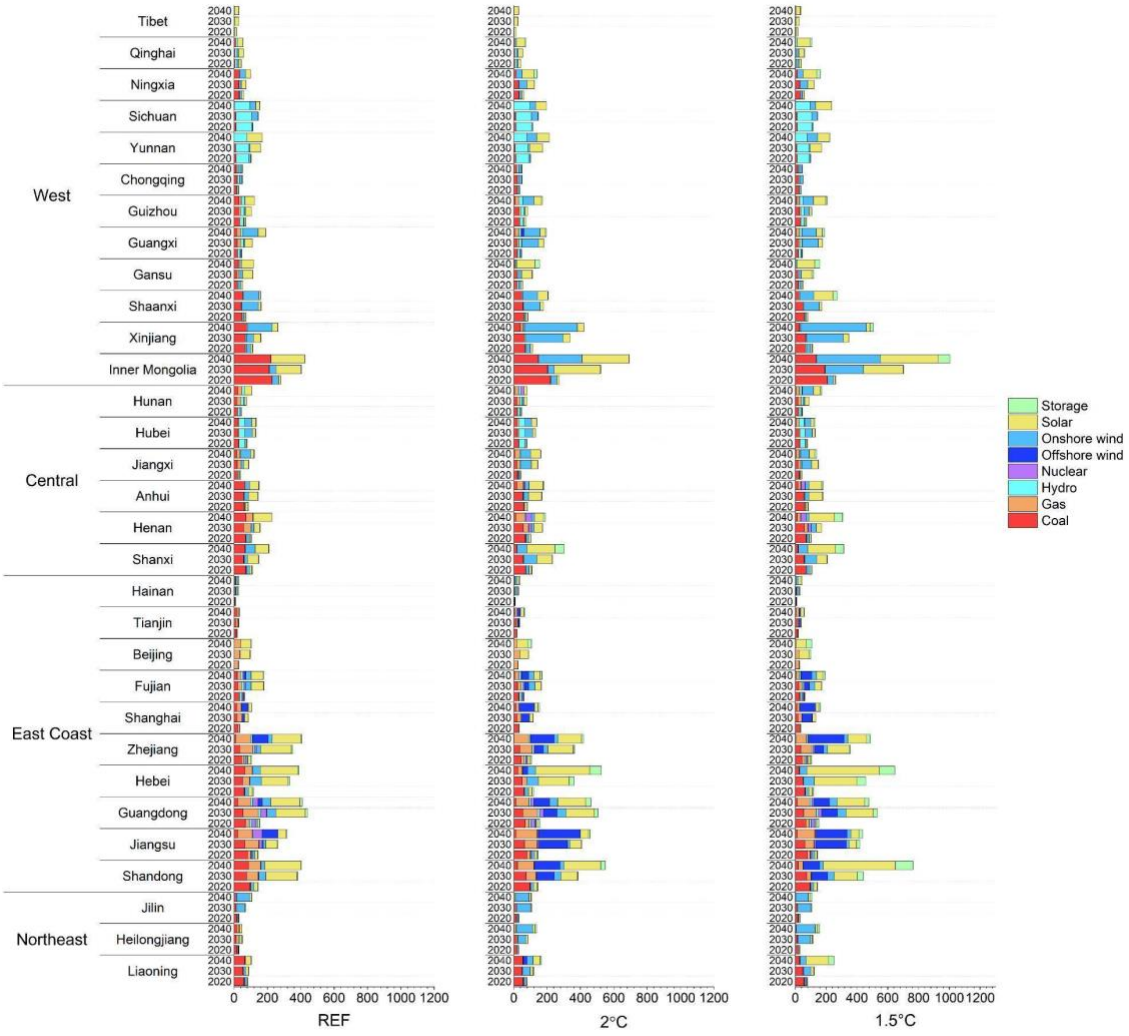


**Figure S4**. Capacity mix (GW) for technologies at the provincial level in the investment period of 2020, 2030 and 2040.

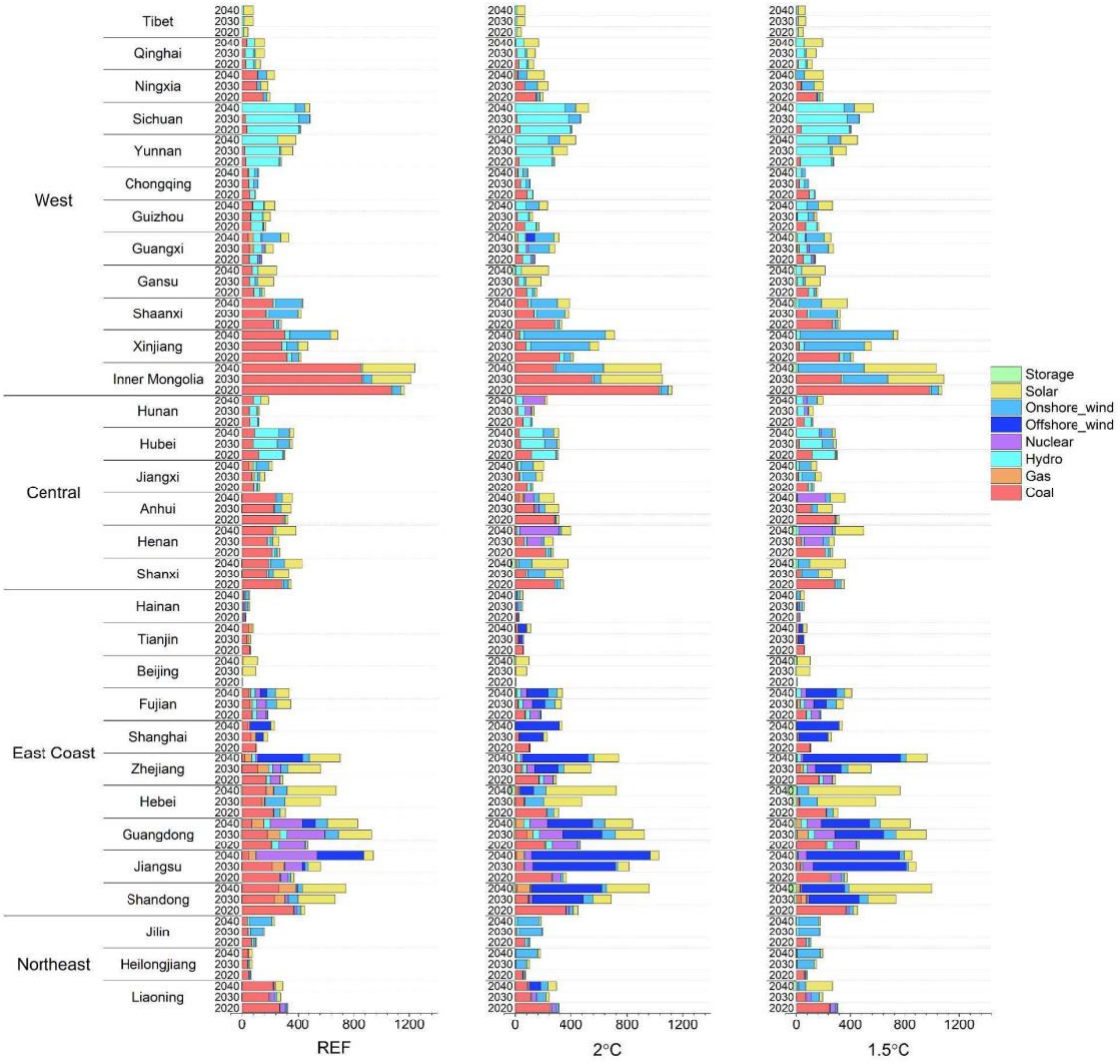


**Figure S5**. Generation mix (TWh) for technologies at the provincial level in 2020, 2030 and 2040. For each province, the three bars show the 2020, 2030, and 2040 generation mix from the bottom to the top.

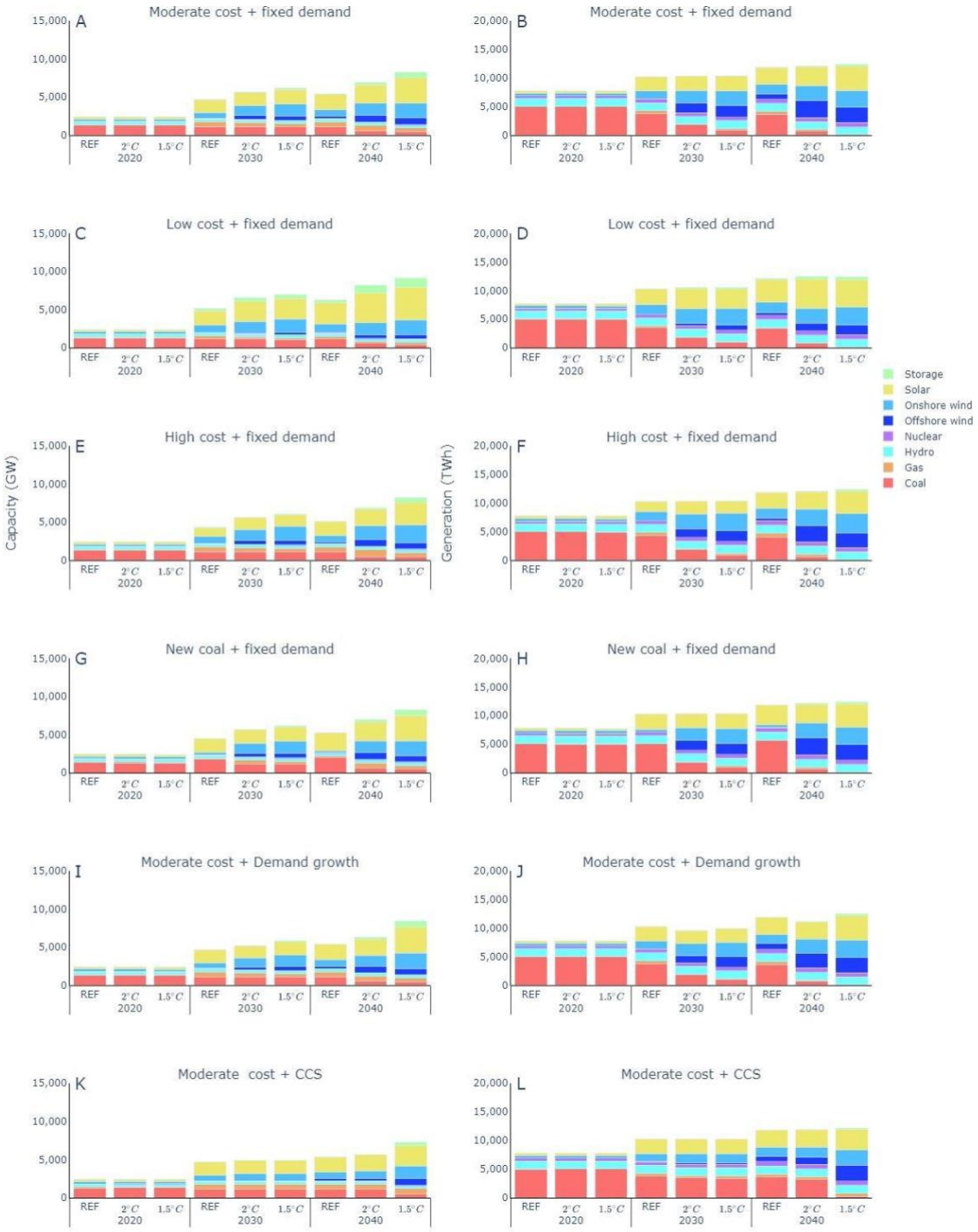


**Figure S6**. Capacity and generation mix under different cost scenarios. (A), (B) Main scenario in the main text, where there is a cap (1100 GW) on coal capacities and uses medium cost projection. (C), (D) Low cost. (E), (F) High cost. (G), (H) No cap on coal

capacity. (I), (J) Demand growth. (K), (L) Main scenario but with CCS. In the demand growth scenario, the electricity demand is consistent with the values in the Reference, 2ºC, and 1.5ºC scenarios in Table S4.

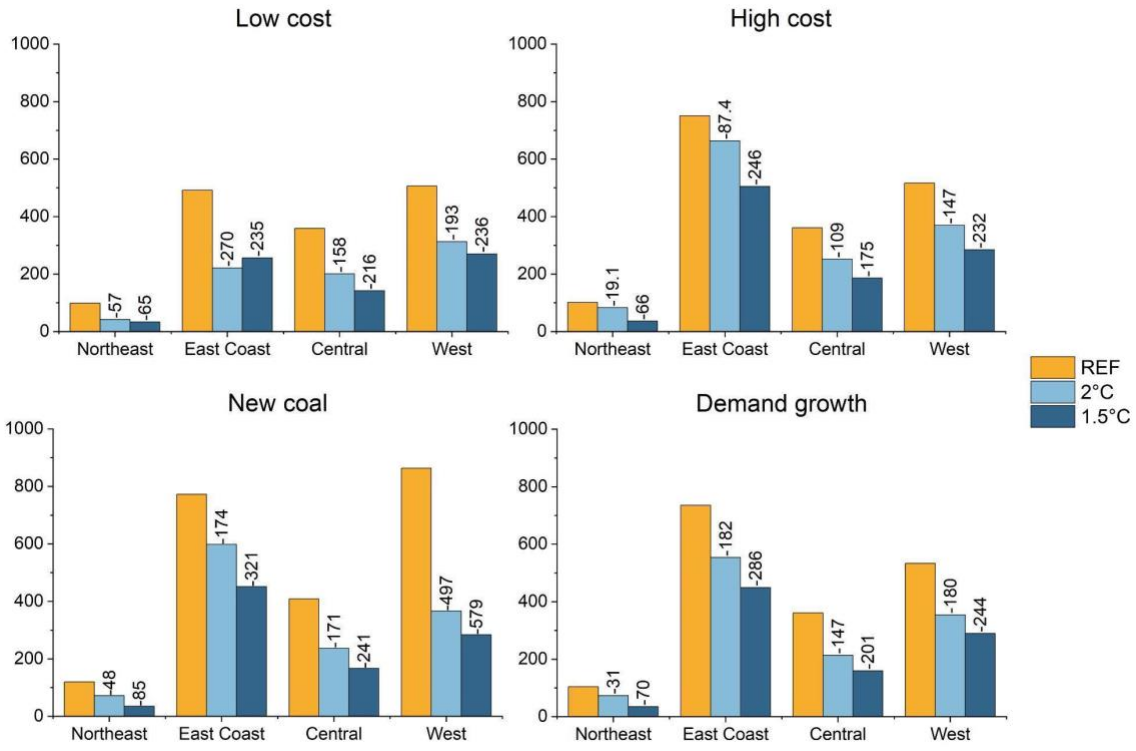


**Figure S7**. Fossil fuel capacities (GW) under different cost and demand scenarios in 2040. The explanation for the 'New coal' and 'Demand growth' scenarios can be found in the figure caption of Fig S6.

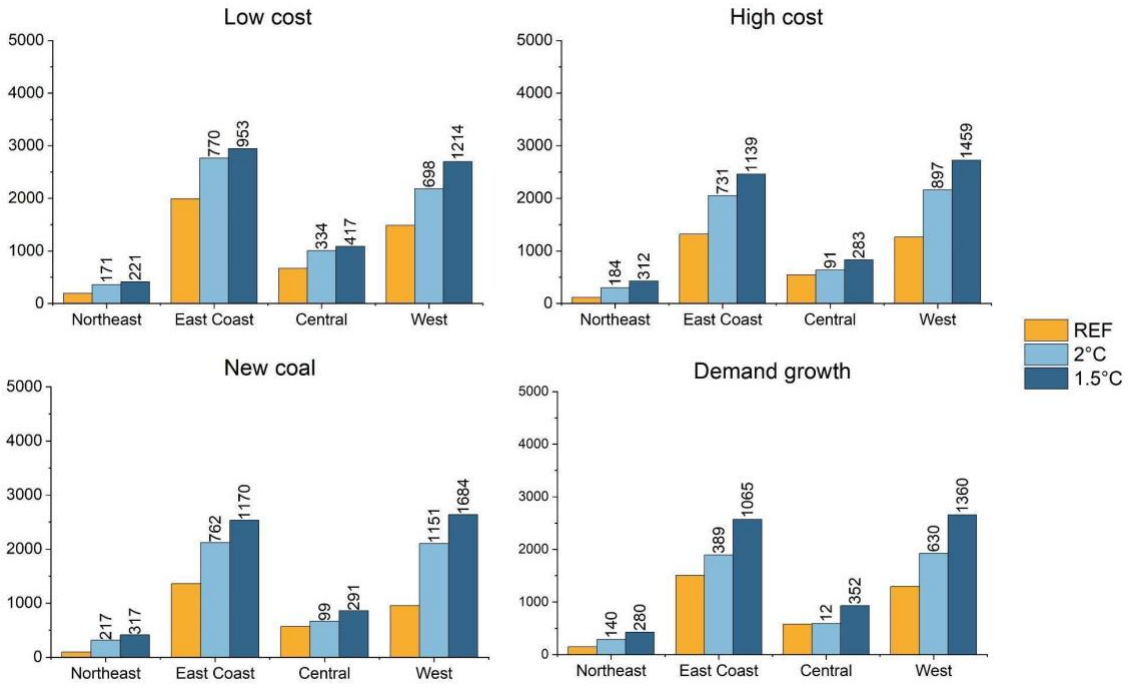


**Figure S8**. Renewable capacities (GW) under different cost and demand scenarios in 2040.

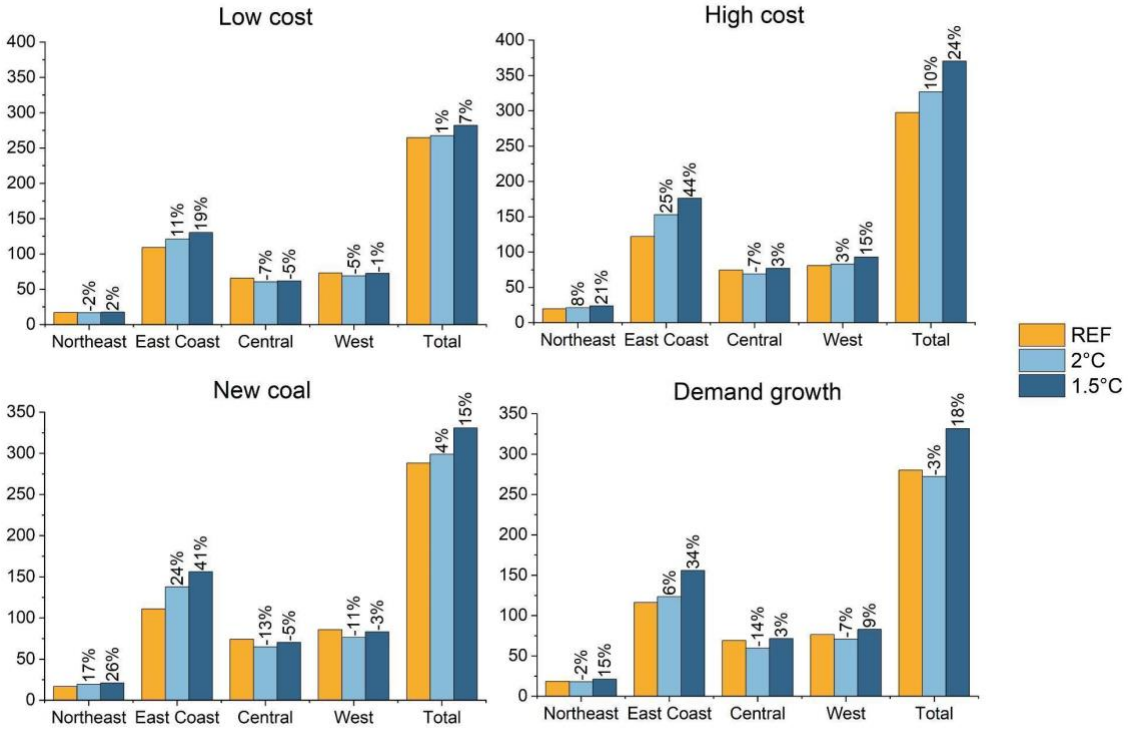


**Figure S9**. Electricity sector-related employment (million job-years) under different demand and cost scenarios.

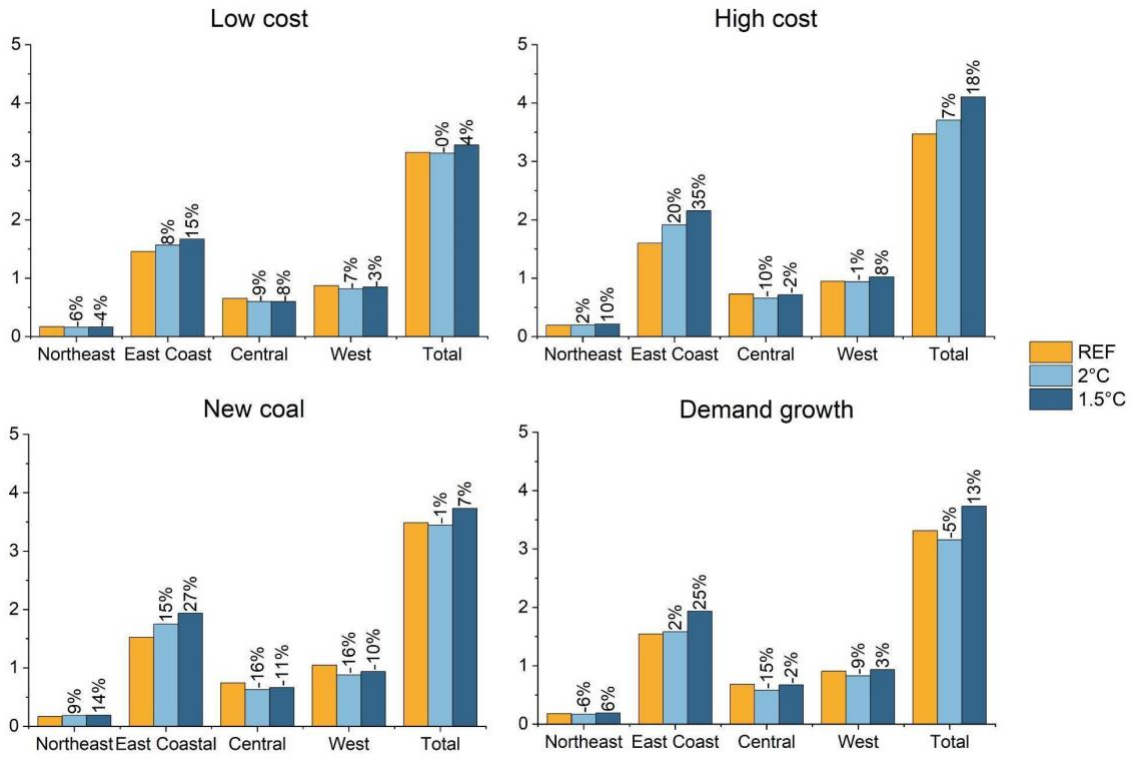


**Figure S10**. Electricity sector-related labor compensation ($ billion) under different demand and cost scenarios.

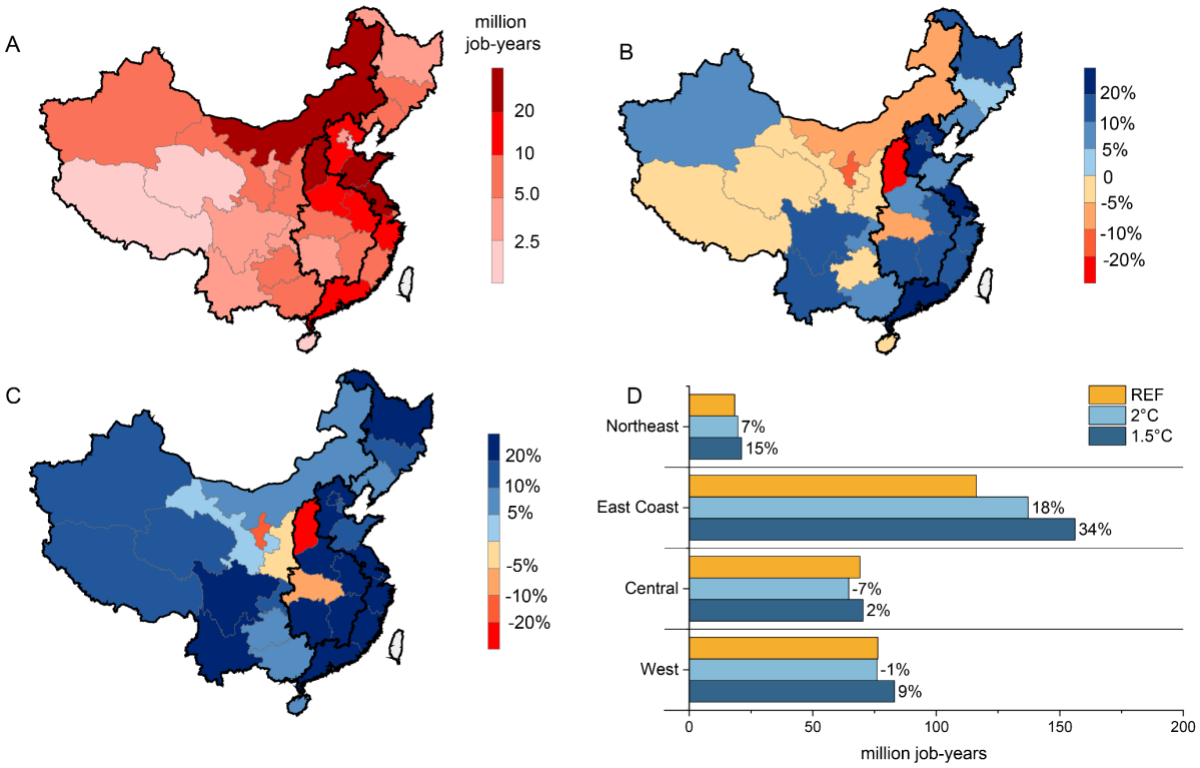


**Figure S11**. (A) Cumulative jobs (job-years) created by the electricity sector under the Reference scenario. Compared to the Reference scenario, (B) relative change in cumulative jobs under the 2 ºC scenario, and (C) 1.5 ºC scenario. (D) Cumulative jobs created by the electricity sector in the four economic regions under different scenarios.

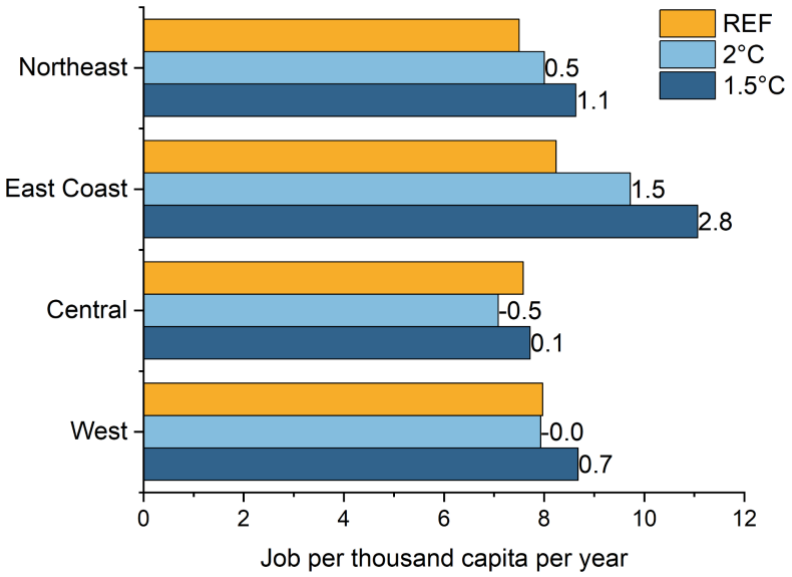


**Figure S12**. The electricity sector-related jobs per thousand capita per year within the four economic regions under the Reference and low-carbon scenarios.

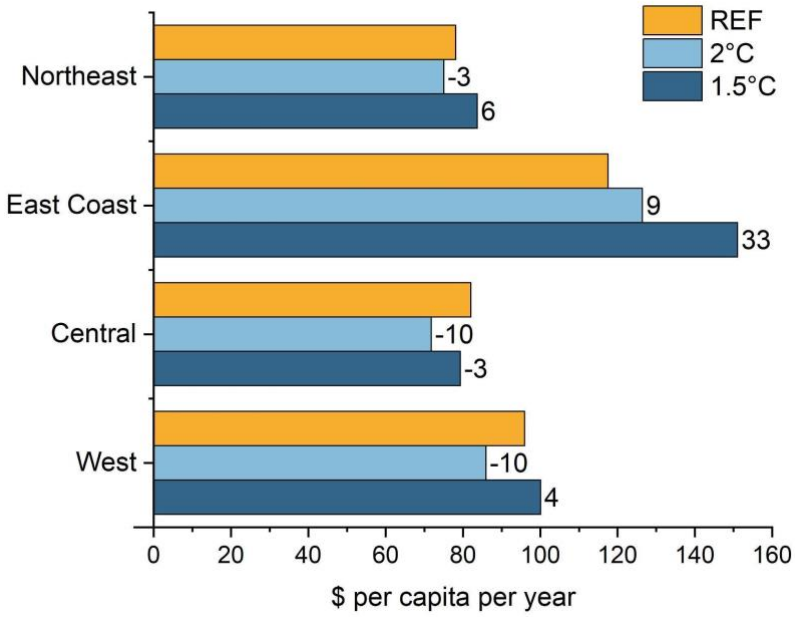


**Figure S13**. The electricity sector-related labor compensation per capita per year within the four economic regions under the Reference and low-carbon scenarios.

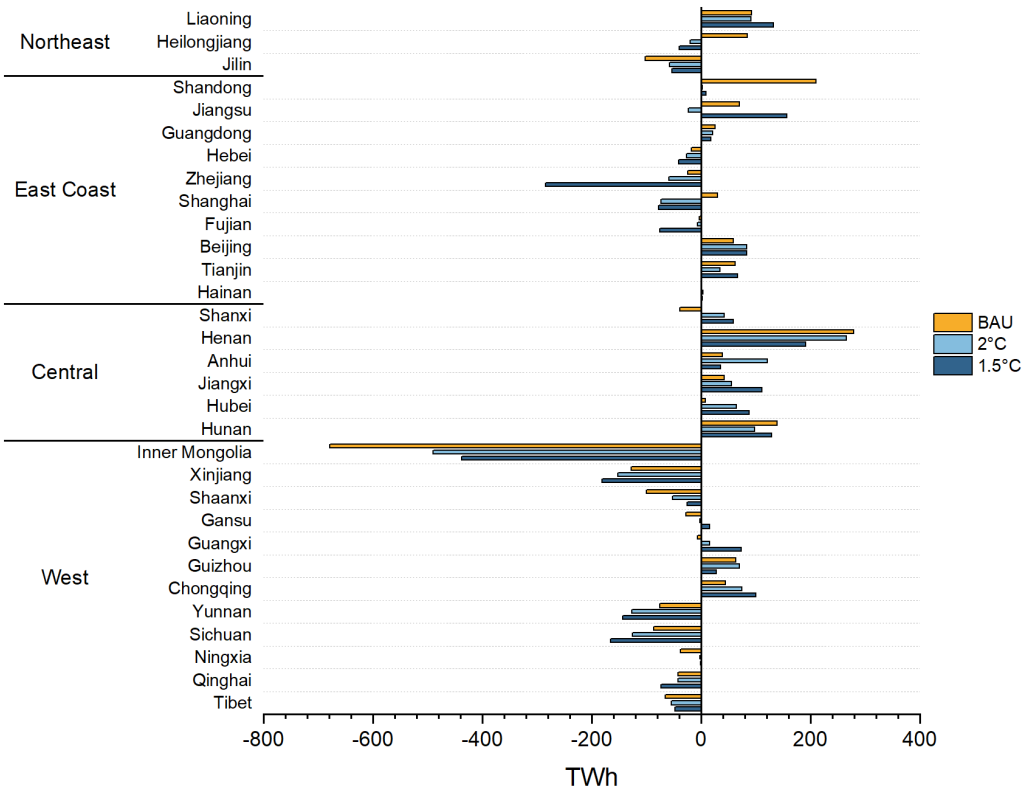


**Figure S14**. Annual net import of electricity (TWh) by province in 2040.

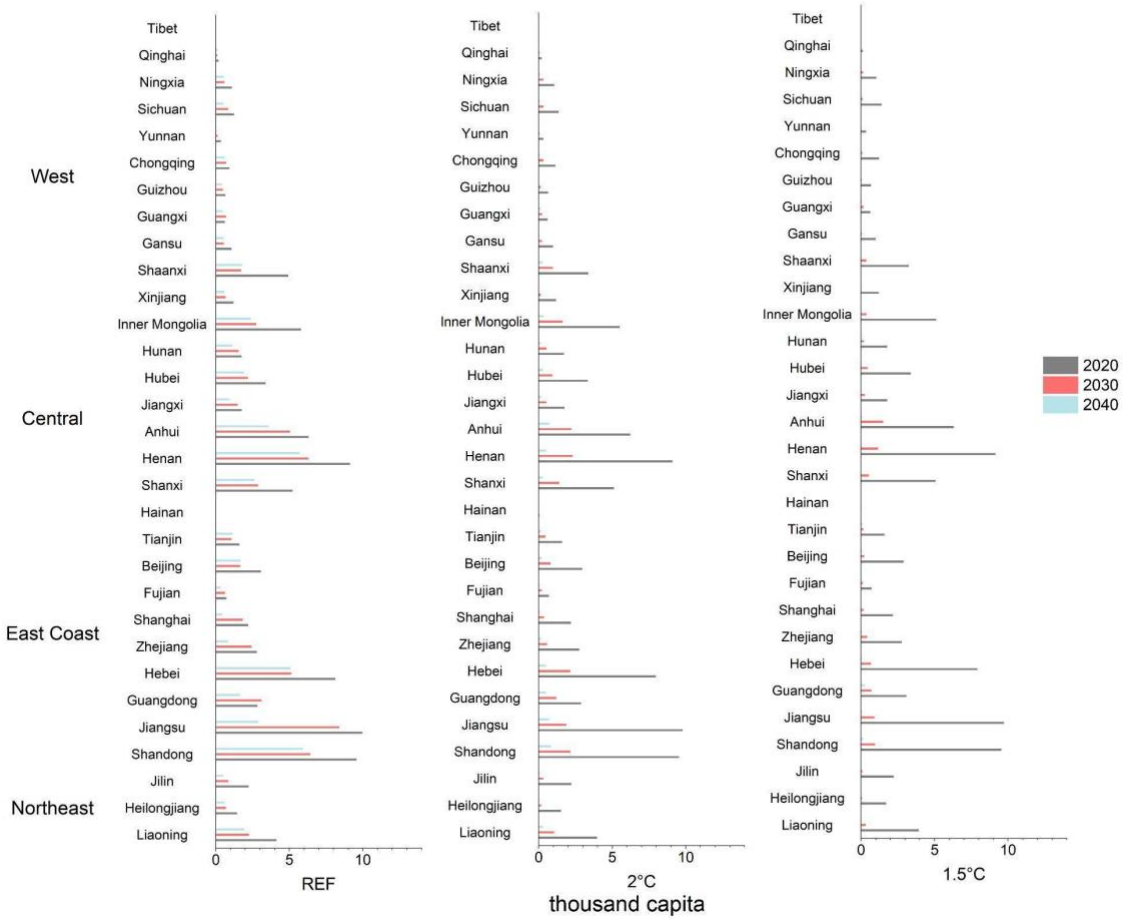


**Figure S15**. Electricity sector-related premature deaths (thousands) by province during each period over 2020 -2040.

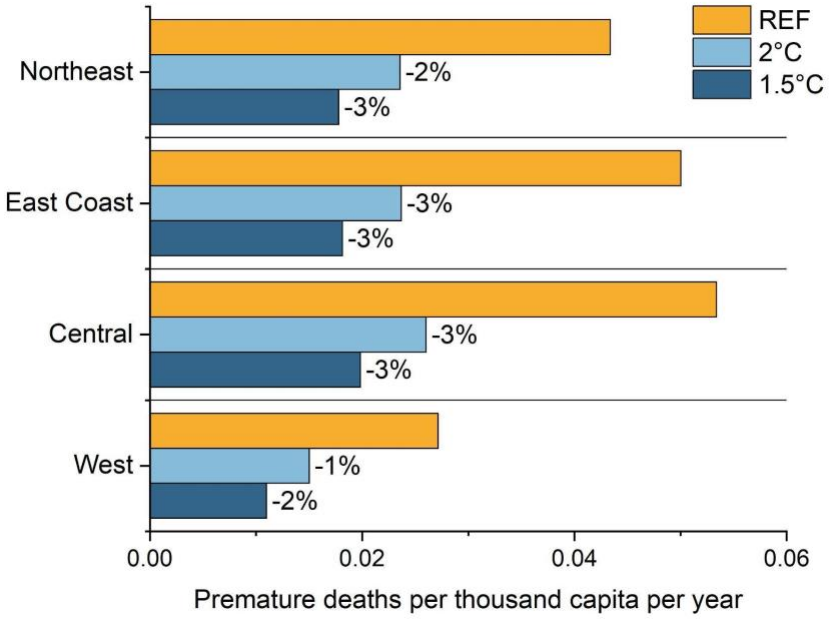


**Figure S16**. The electricity sector-related premature deaths per thousand capita per year within the four economic regions under Reference and low-carbon scenarios.

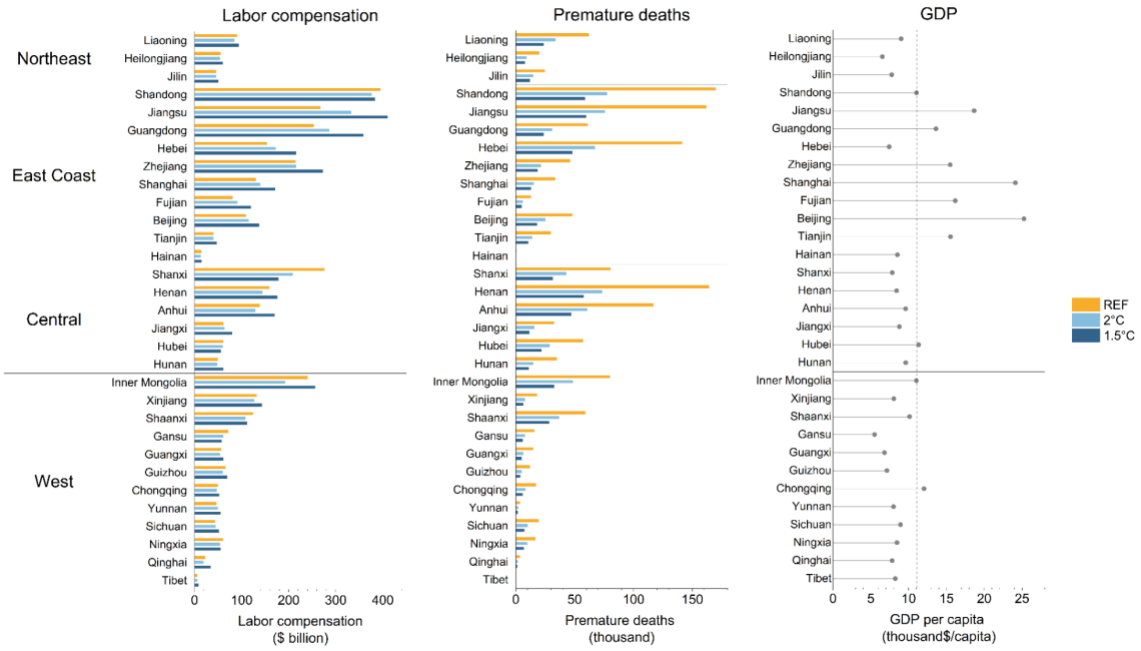

**Figure S17**. Cumulative electricity sector-related labor compensation ($ billion) and cumulative premature deaths related to the electricity sector across 2020-2040 under the Reference, 2ºC and 1.5ºC scenarios and gross domestic product (GDP) per capita in 2020 by province and economic region. The vertical line shows the national average GDP per capita in 2020.

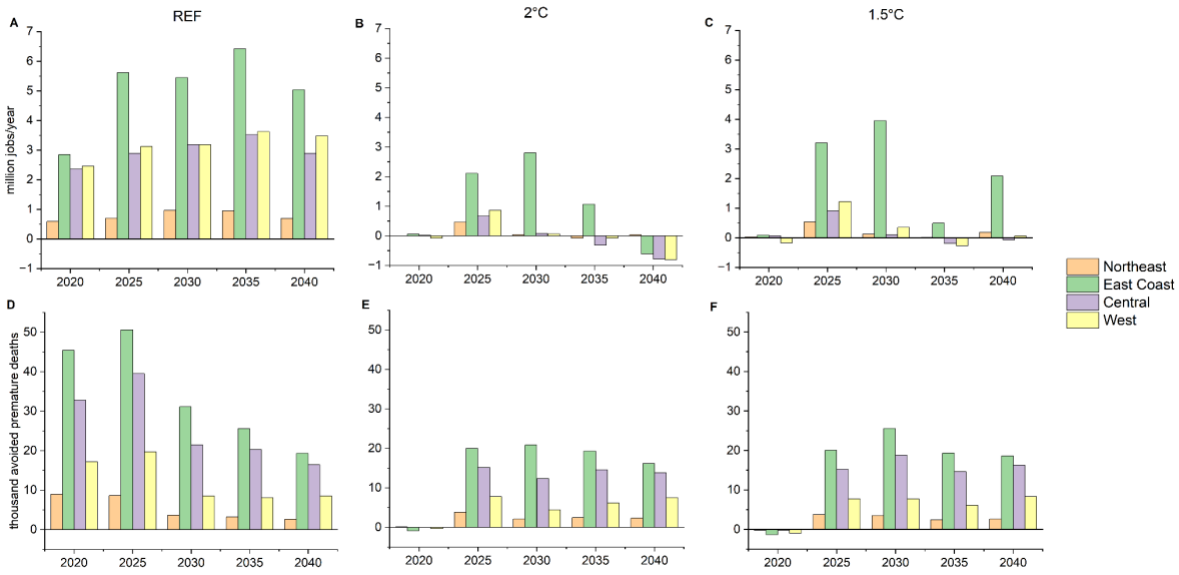


**Figure S18**. Employment under (A) Reference scenario. Relative to the Reference scenario, change of employment under (B) 2ºC and (C) 1.5 ºC scenarios. Avoided premature deaths under (D) Reference scenario. Relative to the Reference scenario, change in avoided premature deaths under (E) 2ºC and (F) 1.5 ºC scenarios. The time period is 5 years.

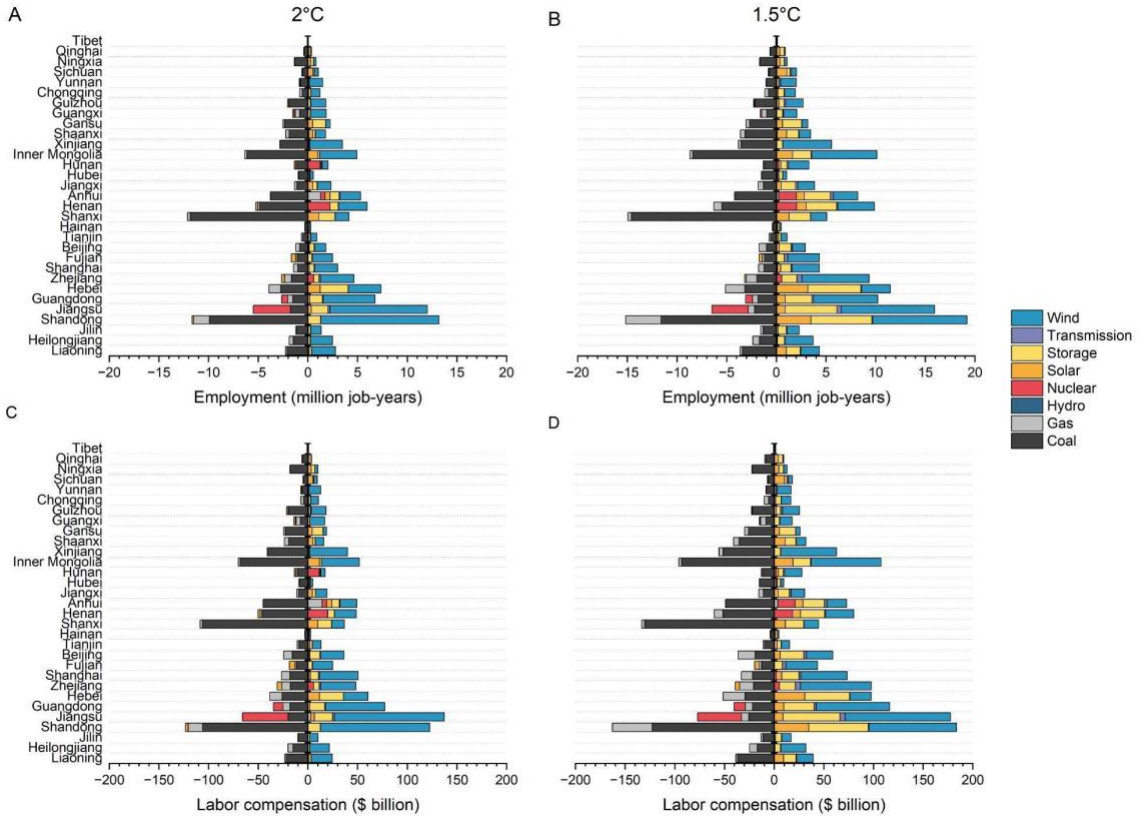


**Figure S19**. Relative to the Reference scenario, change of electricity sector-related employment under the (A) 2ºC scenario and (B) 1.5ºC scenario, and change of labor compensation under the (C) 2ºC scenario and (D) 1.5ºC scenario.

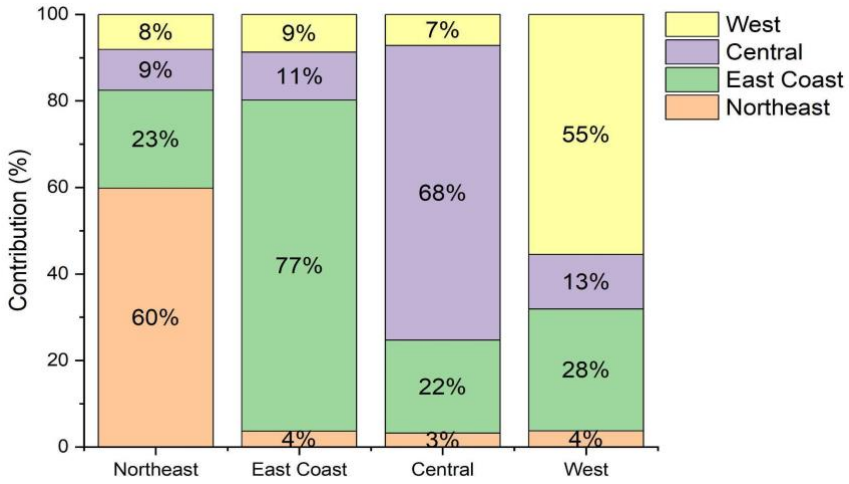

**Figure S20**. The spillover effects of the investment for jobs. Each column shows the distribution of the jobs created by the investment in a region under the Reference scenario.

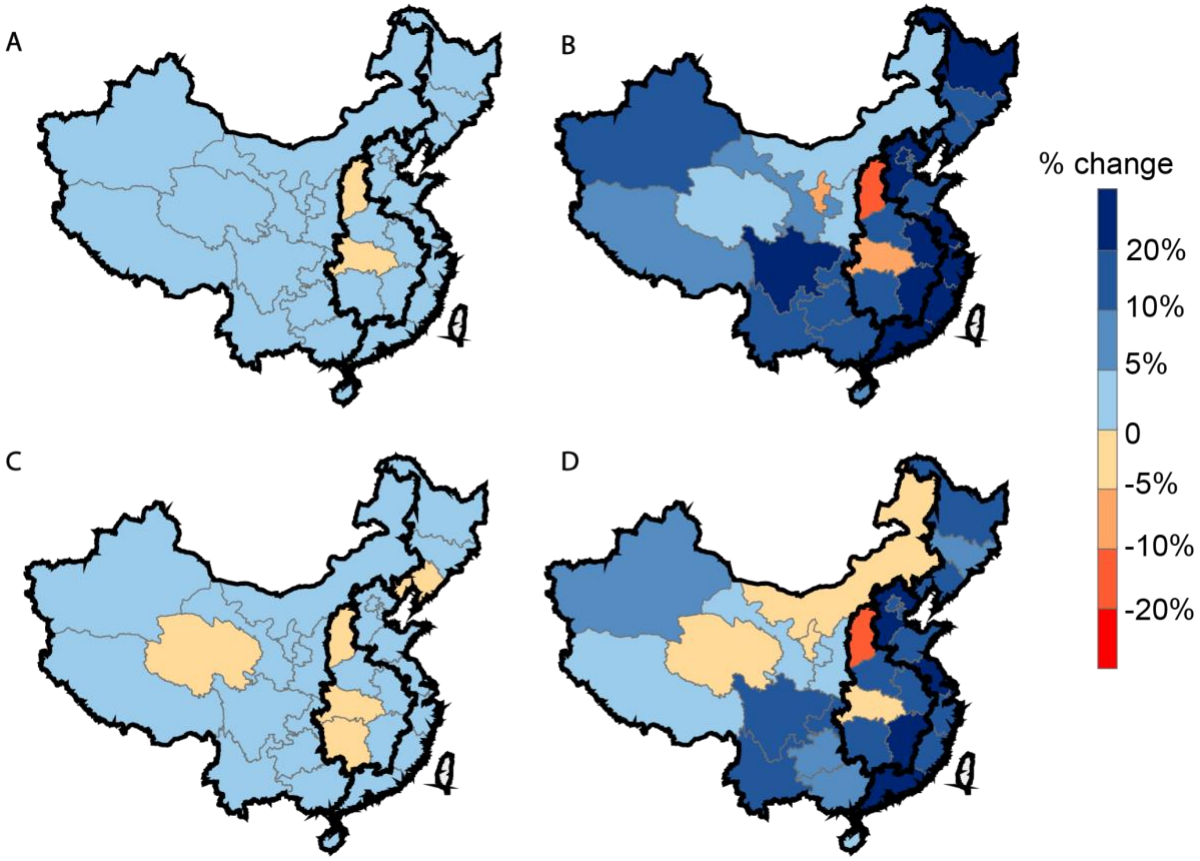


**Figure S21**. With carbon capture and storage technology. Compared to the Reference scenario, (A) relative change in cumulative jobs under the 2 ºC scenario, and (B) 1.5 ºC scenario. Compared to the Reference scenario, (C) relative change in cumulative labor compensation under the 2 ºC scenario, and (D) 1.5 ºC scenario.

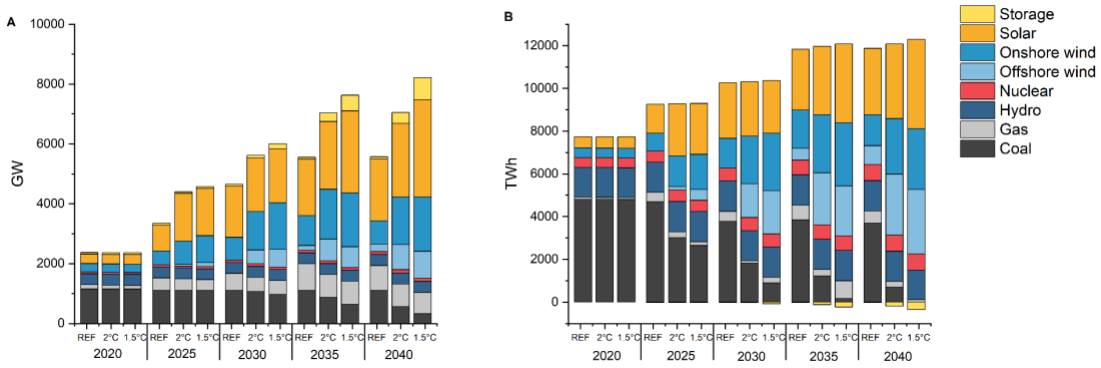


**Figure S22**. (A) Capacity mix and (B) generation mix of technologies from 2020 to 2040 under the Reference scenario (REF), 2ºC and 1.5ºC scenarios with a 5-year time period.

# VI. Role of hydrogen in China's zero-carbon electricity system


## Abstract

Hydrogen emerges as a solution to reduce the cost of a zero-carbon electricity system, offering long-term storage of electricity. However, disparity exists on the potential role of hydrogen in decarbonizing the electricity system and energy as a whole. Here, we used an electricity planning model, GridPath, to quantify the cost implications of hydrogen penetrations in China's zero-carbon electricity system, and how hydrogen interplays with firm low-carbon technologies and hard-to-abate sectors. Hydrogen enables a reduction in the levelized cost by 17% in a zero-carbon electricity system relative to that without hydrogen. Cost reductions hinge on underground hydrogen storage capacities and transmission expansion. Expanding nuclear capacities synergize with hydrogen in reducing the cost of a zero-carbon electricity system. Conversely, carbon capture and removal technologies crowd out hydrogen. Apart from the role of long-term storage, hydrogen from the zero-carbon electricity system is cost-competitive compared to the hydrogen produced by fossil fuels given an increasing energy price.


### *A. Introduction*

China's electricity sector contributed roughly 10% of global greenhouse gas emissions in 2020[164]. As the Chinese government pledges to reach carbon neutrality by 2060[212], it is crucial to achieve a zero-carbon electricity system in a cost-effective manner.

Despite the rapid decline in the cost of solar and wind energy[217], achieving a zero-carbon electricity system with only solar and wind increases the costs by two- or threefold relative to the cost-optimal system[218]. This spike in cost is caused by the diurnal and seasonal

variation of solar and wind[219,220,117]. Hydrogen, which stores electricity for tens of days, has emerged as a promising long-term energy storage technology that can potentially reduce the cost of a zero-carbon electricity system with high penetrations of renewables[221,222]. Given abundant underground storage sites, previous research has shown that hydrogen could reduce the cost of zero-carbon electricity systems in the United States[223] and Europe[163,224] by approximately 15% compared to that without hydrogen.

In addition to serving as long-term storage in the electricity system, hydrogen is also a promising alternative fuel or material in hard-to-abate sectors including iron and steel, ammonia, methanol, transportation, and heating[22]. Currently, hydrogen is mainly produced by fossil fuels (grey hydrogen). A zero-carbon electricity system provides carbon-free hydrogen (green hydrogen) to meet the demand in these hard-to-abate sectors, and help achieve a zero-carbon energy system.

However, while hydrogen is critical in achieving China's zero-carbon electricity and energy system, previous research has rarely systematically examined its role in cost reduction. While many studies revealed the importance of hydrogen in the decarbonization of China's electricity system and hard-to-abate sectors[225–228], several key questions remain unanswered. First, how much cost can be reduced by hydrogen, and what are the limiting geographical and technological factors for hydrogen development? Second, how does hydrogen interplay with other low-carbon firm capacities like nuclear and CCS coupled with DAC. To achieve a zero-emission electricity system without hydrogen, previous research found that nuclear power capacity roughly quadruples and hydropower capacity doubles, relative to 2020 levels[192,229]. Coal, natural gas, or bioenergy power plants aggregately provide 10-20% of electricity demand, with their carbon emissions captured by CCS[192,229–231]. Lastly, how do costs of

hydrogen from the zero-carbon electricity system compare with hydrogen produced by fossil fuels?

Here, we examine the role of hydrogen in China's zero-carbon electricity systems, the interaction between hydrogen and other low-carbon firm capacities, and its cost implications for hard-to-abate sectors. This study builds upon the GridPath modeling platform by adding the capability to model hydrogen electrolyzers, fuel cells, and combustion turbines, carbon capture capacity with both existing and new coal and gas power plants, direct air capture capacity, and storage and pipeline capacities for both hydrogen and carbon dioxide. See the Methods section and Supplementary Information (SI) for more details.

We selected 3 representative days per month with an hourly resolution to capture diurnal, multi-day, and seasonal variability but limiting the burden on computational resources required for co-optimizing both investment and operational costs. Following the cost-optimal principle, in the baseline scenario, we simulated the investment and operation of a zero-carbon emission electricity system in 2050 (ZE scenario, Table 1). In an alternative scenario, hydrogen technologies are not available (ZE w/o $H_2$ scenario). To compare with other low-carbon capacities, we examined scenarios where nuclear capacities were expanded (ZE + Nuclear) and CCS and direct air capture (DAC) were installed (ZE + CCS + DAC). To examine the role of hydrogen in the whole energy system, we build a scenario where the zero-carbon electricity system meets external hydrogen demand in hard-to-abate sectors (ZE + Hydrogen demand), and a scenario where the external hydrogen demand is met by the zero-carbon electricity system, SMR and gasification coupled with CCS and DAC (ZE + Hydrogen demand + Blue).

In the ZE scenario, we limited hydropower capacity (including pumped hydro) to 430 GW based on existing and planned capacities[188], and nuclear capacities to 120 GW according to the projection from China's official goal[232]. Following China's policy on coal power plants[180], the maximum coal capacity is limited to 1100 GW. Our analysis includes the following technologies (Table 2): direct carbon capture (DAC), power-to-gas (P2G) and gas-to-power (G2P) technologies, steam methane reforming (SMR), coal gasification, underground storage for hydrogen (i.e., salt caverns) and carbon dioxide (i.e., depleted gas and oil reservoirs, and saline aquifers), and the transportation pipelines for hydrogen and carbon dioxide. The underground storage capacities for hydrogen[233] and carbon[234] are limited to only those provinces with suitable sites. Due to a lack of data on China's potential for underground storage, we assume unlimited underground hydrogen and carbon storage capacity (Table S1).

**Table 1**. Main scenario description in our study

| Scenario | Emission | Low-carbon technologies | Hydrogen demand |
|---|---|---|---|
| ZE | Zero | $H_2$, nuclear | No |
| ZE w/o $H_2$ | | Nuclear | |
| ZE + Nuclear | | 500 GW nuclear | |
| ZE + CCS +DAC | | $H_2$, nuclear, coal, natural gas | |

| | | | |
|---|---|---|---|
| ZE + Hydrogen demand | | $H_2$, nuclear | Hard-to-abate sectors |
| ZE + Hydrogen demand + Blue | | $H_2$, nuclear, SMR, gasification | Hard-to-abate sectors |

**Table 2**. Technologies assessed in this study to decarbonize China's future electricity system

| Classification | Technology |
|---|---|
| Conventional energy | Coal, gas, nuclear, and hydropower |
| Renewable energy | Solar PV, onshore wind, offshore wind |
| Conventional storage | Battery storage, pumped hydro storage |
| Power-to-gas (G2P) | Electrolyzer |
| Gas-to-power (P2G) | Hydrogen combustion turbine, fuel cell |
| Hydrogen storage | Underground storage (i.e. salt cavern), tank storage |
| Energy and $CO_2$ transport | Electricity grid, hydrogen pipeline, and $CO_2$ pipeline |
| Carbon removal technologies | Carbon capture and storage (CCS), direct air capture (DAC), and underground $CO_2$ storage |
| Fossil-based hydrogen production (gray hydrogen) | Steam methane reforming (SMR), and gasification |

### *B. Method and Materials*

#### 1. Electricity model

We used the GridPath model, an open-source power system model, to optimize the total investment and operation costs of electricity infrastructure in China in 2050.[235,236] In our GridPath-China model, the 31 provinces in China are classified into 32 load zones, where

Inner Mongolia is split into an Eastern Inner Mongolia load zone and a Western Inner Mongolia load zone. Each month in the model has three representative days with hourly resolution. The representative days are selected based on maximum, median and minimum electricity demand in each month. The representative days with minimum electricity demand represent weekend days, while the maximum and median days represent weekdays. To ensure reliability during peak load hours, we assumed a planning reserve margin of 15% of the peak load. Total coal capacity is constrained to less than 1100 GW in all scenarios based on the National Development and Reform Commission's policy to avoid over-capacity of coal generation.[180] The minimum generation level assumed is 100% of rated capacity for nuclear power plants, 40% for coal power plants and gas turbines, and 45% for combined cycle gas turbines. The hourly ramp rate of the rated capacity is 30% for coal power plants and 60% for gas power plants.[187] The energy loss of transmission lines and hydrogen pipelines is shown in Table S6

Existing generation capacities for all technologies, projected generation capacities for hydropower and nuclear, monthly average capacity factors of hydropower, and provincial-level fuel costs were compiled from He et al (2016)[185]. We collected the existing and planned hydropower and pumped hydro capacities larger than 1 GW from Global Energy Monitor.[188] We collected data for existing transmission lines from State Grid[189] and Southern Grid[190]. Hourly demand and projected generation capacity factors for solar and onshore, and offshore wind were collected from Abhyankar et al.[169] The distribution of salt caverns and carbon storage sites were collected from Zhu et al[233] and Fan et al[234].

In this study, we improved the GridPath model by adding a hydrogen module, including P2G, G2P and hydrogen storage technologies. We also added hydrogen pipelines

into the model, which allows the transportation of hydrogen across load zones. Another improvement is that we added a CCS/DAC module, which optimizes the investment and operation of carbon capture. Our CCS/DAC considers the storage of carbon emissions, and the transport of carbon emissions through pipelines.

**2. Cost assumptions**

China-specific renewable energy capital costs were collected from the International Renewable Energy Agency[107], and China-specific capita costs of battery and pumped hydro storage technologies, and fossil-fuel technologies were collected from Zhuo et al (Table S3)[192]. The O&M costs for renewables, storage and fossil fuels were collected from Zhuo et al[192]. We then applied normalized cost projection curves from 2020 to 2050, derived from the moderate cost projection from the NREL 2023 Annual Technology Baseline (ATB) database[237] to the China-specific technology costs.

The costs for the electrolyzers, salt cavern, hydrogen storage tank, CCS underground storage (depleted oil and gas reservoirs and saline aquifers), hydrogen and CCS pipeline, and DAC were from the Danish Energy Agency (Table S4-S6)[238]. The costs for CCS were collected from the Global CCS Institute (Table S5)[239]. The projected cost for transmission lines was collected from Grid Project Construction Cost Analysis in the 12th Five-year Period (Table S6)[194]. The fuel costs of coal, natural gas, and uranium were curated by Gang et al.[185,187] and Luo et al[184] (Table S7).

**3. Scenario**

The base scenario, "ZE", in this analysis is China's 2050 electricity system with zero carbon emissions. In this scenario, no fossil fuel generation is allowed. The hydropower and

pumped hydro capacities include existing and planned capacities. The 'ZE w/o $H_2$' scenario refers to an electricity system with zero carbon emissions, but without any hydrogen generation or infrastructures.

We include various scenarios to assess the uncertainty associated with input costs and technologies. These include zero-emission scenarios with low (ZE + Low cost) and high-cost ('ZE + High cost') hydrogen technologies. The 'ZE + High cost + Low efficiency' assesses a zero-emission scenario with high-cost and low-efficiency hydrogen technologies.

We then assess the impact of constraints on the various types of electricity and hydrogen infrastructure on costs and emissions compared to the base zero-emission (ZE) scenario. These zero-emission scenarios include those without new electricity transmission lines ('ZE w/o new electricity grid'), without new H2 pipelines ('ZE w/o $H_2$ pipeline'), without both new electricity transmission lines and H2 pipelines ('ZE w/o new electricity grid and $H_2$ pipeline'), without underground storage for hydrogen ('ZE w/o underground storage'), and without new hydrogen combustion turbines ('ZE w/o $H_2$ turbine').

The reference ('REF') scenario has no constraint on $CO_2$ emissions from China's power system. In '90R' and '80R' scenarios, $CO_2$ emissions from the electricity system are reduced by 90% and 80% respectively relative to 2020.

To understand the effect of other low-carbon technologies on hydrogen infrastructure investments and system costs, we include scenarios with both CCS combined with DAC and nuclear. We simulate a zero-emission scenario with CCS and DAC technologies ('ZE + CCS + DAC') By assuming that the cost of CCS and DAC stay the same as 2020 and a CCS capture rate of 85%. To assess the effects of technology and cost improvements, we also include a

low-cost, high-efficiency CCS and DAC scenario ('ZE + CCS + DAC'), where the costs of CCS and DAC decline by 50% and the CCS capture rate improves to 95%.

In the zero-emission scenario with expanded nuclear power plant deployment ('ZE + Nuclear'), we allow nuclear capacity to expand from 120 GW in the base scenario to 500 GW. We assume a minimum generation level for nuclear power plants of 50% instead of 100% under the base ZE scenario. To assess the effect of higher costs of nuclear energy ('ZE + Nuclear (high cost)' scenario), we assume the relatively conservative nuclear cost projection from NREL while keeping the same input assumptions as the 'ZE + Nuclear' scenario. We also include a zero-emission scenario with no constraints on nuclear capacity expansion ('ZE + Unlimited nuclear' scenario). Lastly, we simulate a zero-emission scenario with both CCS combined with DAC and high nuclear scenario ('ZE + CCS + DAC + Nuclear') where the new nuclear buildout follows the assumptions under the 'ZE + Nuclear' scenario, and CCS and DAC infrastructure follows the assumption under the 'ZE + CCS +DAC' scenario.

Finally, we include a zero-emission scenario where China's 2050 electricity system serves additional hydrogen demand from hard-to-abate sectors including industry (e.g., direct reduced iron, methanol, ammonia, and industry heat), transportation (heavy duty vehicle), and building ('ZE + Hydrogen demand'). To compare with fossil-based hydrogen, we built a zero-emission scenario where the additional hydrogen demand from hard-to-abate sectors can also be sourced from SMR and gasification coupled with CCS + DAC ('ZE + Hydrogen demand + Blue'). In this 'ZE + Hydrogen demand + Blue' scenario, to be more conservative, we assume the CCS capture rate is 95%, and the cost of CCS and DAC decline by 50%.

### 3. Electricity and hydrogen demand

The 2050 electricity demand was collected from Abhyankar et al.[169] In our main scenarios ('ZE'), when hydrogen is only used as long-term storage in the electricity system, external hydrogen demand from hard-to-abate sectors is zero.

In the 'ZE + Hydrogen demand' scenario, the national hydrogen demand (excluding the hydrogen demand in the electricity system) in a net-zero energy system is equal to the demand estimated by the China Hydrogen Association (124 million tonne), which is reported by the International Energy Agency.[240] The lower heating value of hydrogen (120 MJ/kg) is used to convert hydrogen between mass and energy values. The hourly curve of hydrogen demand follows the normalized hourly curve of electricity demand. A sensitivity test with a flat demand curve for hydrogen demand is shown in Fig S8.

For the zero-carbon electricity system, the levelized cost of hydrogen (LCOH) for the hydrogen demand in hard-to-abate sectors (HD) is calculated as:

$$LCOH = \frac{Totol\ cost^{ZE\ +\ Hydrogen\ demand} - Totol\ cost^{ZE}}{HD}$$

where $Totol\ cost^{ZE\ +\ Hydrogen\ demand}$ is the total cost to meet both electricity and hydrogen demand under the ZE + Hydrogen demand scenario, and $Totol\ cost^{ZE}$ is the total cost to meet only electricity demand under the ZE scenario.

## *C. Results*

### 1. Effects of hydrogen on deployment and costs

Hydrogen decreases the levelized cost of a zero-emission electricity system (ZE) by 17% (ranging from 11-20% due to uncertainties in electrolyzers, fuel cells, and storage costs

and efficiencies, Fig S1) relative to the system without hydrogen (ZE w/o $H_2$ scenario) (Fig 1f).

A zero-emission electricity system with hydrogen (ZE scenario) decreases the need for wind and solar capacity (4% and 30 %) and yet their generation increases by 6-35% relative to a system without hydrogen (ZE w/o H2 scenario) because long-duration hydrogen storage reduces energy curtailment (Fig 1e). The availability of hydrogen storage also reduces the need for battery storage capacity. Under the ZE scenario, the battery capacity halves relative to the ZE w/o H2 scenario (Fig 1c). Hydrogen displaces battery capacity not only because it balances energy supply and demand across seasons but also between weekdays and weekends. It shifts energy generation from weekends with low electricity demand to weekdays with high electricity demand, providing additional flexibility during weekdays and thus displacing short-duration battery storage (Fig S2). Lastly, hydrogen also avoids substantial electricity grid capacity (40%) in the zero-emission system even though some hydrogen pipeline capacity needs to be built because of heterogeneity in underground storage availability across provinces (Fig 1b).

Without a carbon emissions target, the reference scenario (REF) results in an emissions reduction of 15% in 2050 compared to 2020. Only 48% of energy comes from variable wind and solar resources (Fig 1e) and no hydrogen storage is cost-optimally built (Fig 1d). As the carbon emissions cap is tightened (80R, 90R, and ZE), wind and solar capacity are increasingly installed (Fig 1a) and contribute 80%, 84%, and 88%, respectively, to total energy generation. Commensurately, the deployment of hydrogen storage capacity for long-duration storage services increases exponentially with the 80R, 90R, and ZE scenarios deploying 76 TWh, 152 TWh, and 620 TWh of hydrogen storage capacity, respectively, by

2050 (Fig 1d). That storage capacity in the ZE scenario is equivalent to 18 days of daily average electricity demand. Similarly, hydrogen electrolyzer capacity increases from 600 GW to 950 GW as the carbon cap increases from 80% to 100% (Fig 1e). In all three low-carbon scenarios (i.e., 80R,90R and ZE), hydrogen decreases system costs. While cost decreases with hydrogen in the 80R and 90R scenarios relative to those without hydrogen are relatively modest (3% and 4%, respectively),

Though hydrogen enables a lower levelized cost under the ZE scenario, reaching a zero-carbon system remains expensive. Compared to the least cost REF scenario, the levelized cost of electricity increases by 72% under the ZE w/o H2 scenario. With hydrogen, the increase in levelized cost relative to the REF scenario is lower but still substantial at 44% (38-53% accounting for uncertainties in hydrogen infrastructure costs).

Due to the complexity of time, we used 36 representative days in our capacity expansion model, which may miss some extreme days with wind or solar drought. To prevent demand loss, we assumed a 15% planning reserves margin. To examine the reliability of the zero-carbon electricity system, we ran an operation model with fixed capacities in 8760 hours (Table S2). We found that in a zero-carbon electricity system with hydrogen, the demand can be met at every hour.

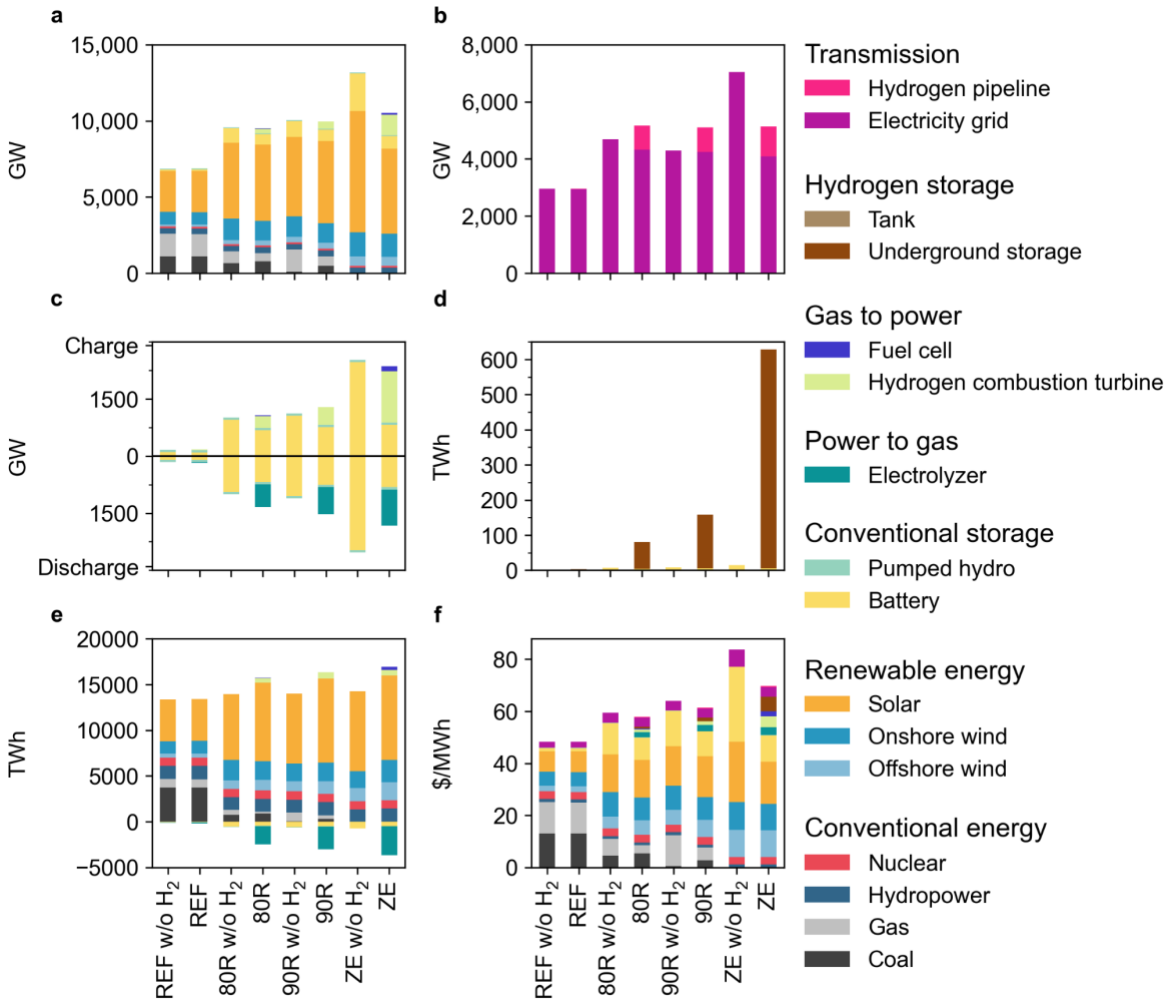


**Figure 1**. **a**. Generation capacity, **b**. transmission capacity, **c**. power capacity of charging and discharging storage, **d**. energy capacity of storage, **e**. generation, and **f**. levelized cost of electricity under low-carbon scenarios in 2050. In **e**, the negative value for the electrolyzer represents the electricity input for hydrogen. Different colors refer to different technologies. REF refers to the scenario without a carbon emission target. 80R, 90R, and ZE refer to the scenarios where carbon emissions are reduced by 80%, 90%, and 100% relative to 2020 levels.

**2. Transmission and underground storage are key for the deployment of hydrogen**

The levelized cost of the zero-carbon electricity system depends on both technological and geographical factors. To understand the effect of investments in key hydrogen and electricity infrastructure components in China's zero-emission electricity system, we exclude each component from available investment options and examined their impact on system costs, hydrogen and battery storage requirements, and hydrogen and electricity trade. We found that the expansion of the electricity grid and hydrogen pipelines, and the availability of abundant underground hydrogen storage are key to lowering the levelized cost of electricity (Fig 2).

Not expanding the existing energy transport network increases the levelized cost by 34% compared to the ZE scenario that allows unlimited expansion of both transmission lines and hydrogen pipelines (Fig 2a). The cost increase is mainly driven by the expansion of offshore wind capacities in East Coast China to compensate for the scarce onshore renewable energy resources in those provinces (Fig S3, S4). Additionally, the tank storage of hydrogen in provinces without underground storage sites increases the cost. In provinces with limited high-quality renewable resources, P2G technologies need to have higher hydrogen-to-power efficiencies to meet local demand; therefore, more capacities of high-efficiency but expensive fuel cells are installed (Fig S3, S5). The hydrogen storage capacity increases by 200 TWh (35%) relative to the ZE scenario because the existing limited transmission network cannot balance the variability of renewable energy (Fig 2b).

Solely expanding electricity grids without hydrogen pipelines bumps the levelized cost by only 0.8%, which is similar to the levelized cost when both electricity and hydrogen

networks are expanded (Fig 2a). Under the ZE scenario, hydrogen is produced in inland provinces with high-quality wind and solar resources, and sent to East Coast provinces for storage via hydrogen pipelines (Fig S6). Without hydrogen pipelines, hydrogen is produced and stored in the East Coast provinces by importing electricity from inland provinces. In this scenario, the reliance on electricity trade increases. The capacity of the electricity grid increases to 4,800 GW compared to the 4,100 GW in the ZE scenario, and the annual trade of electricity reaches ~7,800 TWh, increasing from 5,800 TWh under the ZE scenario (Fig 2c).

Expanding only hydrogen pipelines increases the levelized cost by 7% (Fig 2a) compared to the ZE scenario. Without transmission lines, more expensive but more efficient fuel cells are built to make the best use of limited high-quality renewables. The energy storage capacity slightly increases to 700 TWh, but the annual trade of hydrogen between provinces doubles to 5,300 TWh compared to that in the ZE scenario (Fig 2c).

Among the hydrogen technologies, inexpensive underground storage (i.e., salt caverns) is the most crucial to lowering the levelized cost (Fig 2a). Without underground storage, no hydrogen technologies are selected because the energy capacity cost of the alternative – tank storage – is greater than the underground storage by 15 times. As for the G2P (gas-to-power) technologies, without hydrogen combustion turbines, electricity generation from hydrogen is limited to using only fuel cells, which results in an 11% increase in the levelized cost relative to the ZE scenario. The use of only fuel cells also shrinks the capacity for underground hydrogen storage by a quarter to 430 TWh due to its higher gas-to-power efficiency (Fig 2b).

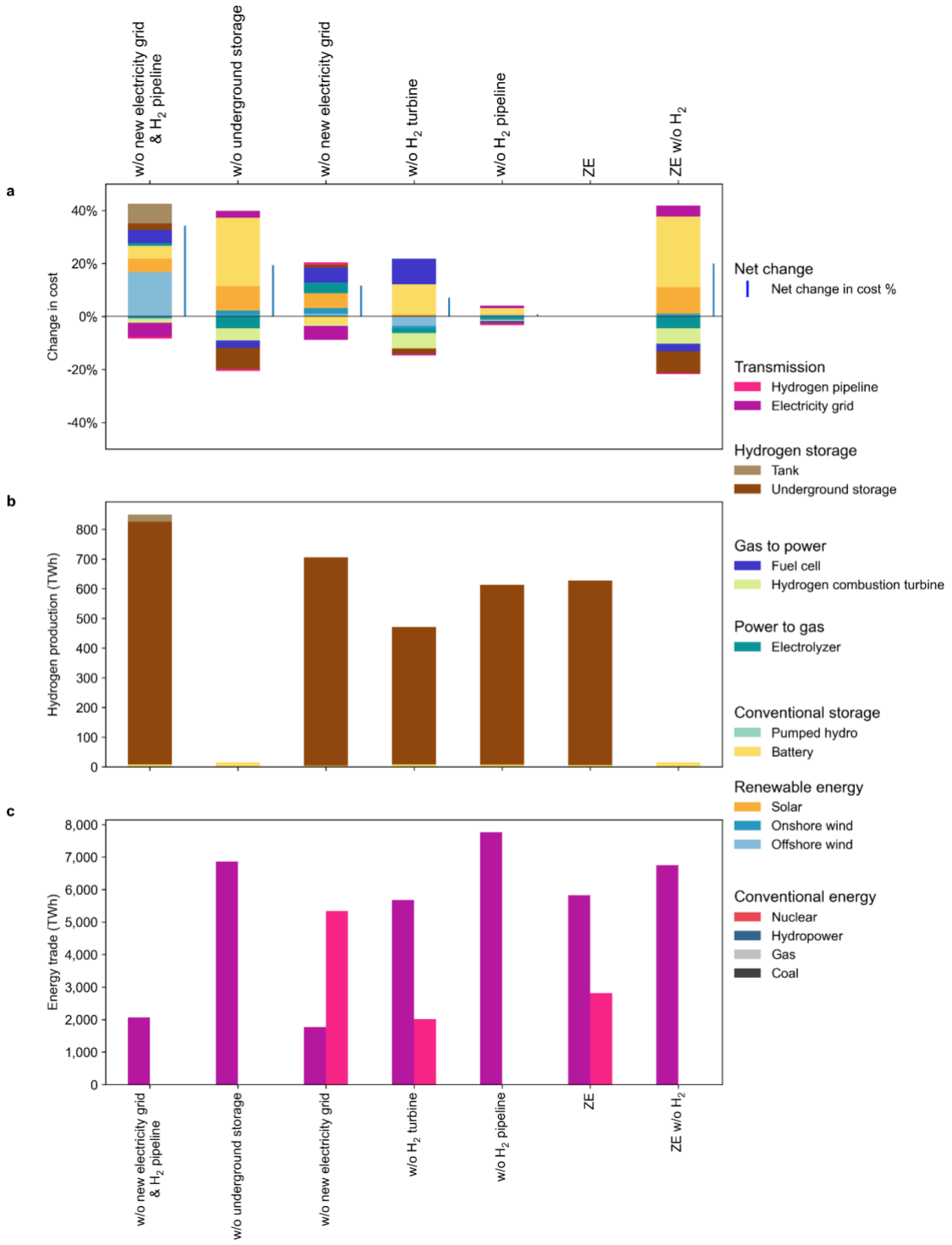


**Figure 2**. Sensitivity to new investments in electricity and hydrogen infrastructure, **a**. change in cost per unit electricity demand relative to the zero-emission scenario (ZE), **b**. energy

capacity of battery and hydrogen storage, and **c**. annual trade of electricity and hydrogen. Vertical blue lines in **a** represent the net percentage change in levelized cost.

### 3. Interaction of hydrogen with other low-carbon firm capacities

Green hydrogen infrastructure (P2G, storage and G2P) can provide low-carbon firm capacity to an electricity system but other technologies including flexible nuclear power plants, and CCS and DAC coupled with coal and gas power plants could also provide similar services. We assessed the impact of these low-carbon firm capacities on hydrogen infrastructure and other investments and system costs. Under the ZE + Nuclear scenario, we increase the available nuclear capacity from 120 GW to 500 GW, and assume that the nuclear fleet is more flexible by allowing it to operate at 50% of its rated capacity instead of 100% under the ZE scenario. For coal and gas power plants coupled with CCS and DAC technologies (ZE + CCS + DAC scenario), we assume an 85% capture rate for CCS and constant costs for CCS and DAC from 2020-2050 (Table S5).

Overall, adding nuclear, CCS, and DAC technologies reduces the cost of the zero-carbon electricity system. A larger flexible nuclear fleet (ZE + Nuclear scenario) decreases the levelized cost of electricity by 11% compared to the ZE scenario. Allowing investments in CCS and DAC capacities (ZE + CCS + DAC scenario) decreases the levelized cost of electricity by 4% relative to the ZE scenario (Fig 3f). If the capture efficiency of CCS improves from 85% to 95% and capital costs of both CCS and DAC technologies decline by over 50%, the levelized cost decreases by 13% compared to the ZE scenario (Fig S7). Expanding nuclear and installing CCS and DAC at the same time reduces system costs by

15% relative to the ZE scenario, and reduces the capacity requirement of underground hydrogen storage by 70% to 160 TWh (Fig S7).

Installing CCS and DAC capacities increases the electricity generation of coal and natural gas to 5% of the total electricity demand (Fig 3e), generated from a fleet of 1,100 GW compared to none in the ZE scenario (Fig 1a). The cost increase from fossil fuel power plants, CCS and DAC is balanced by lower investment in renewable energy and storage. Relative to the ZE scenario, the solar, wind and battery storage capacities drop by 4-11% (Fig 3a), and the energy capacity of hydrogen storage shrinks by 70% (Fig 3d).

Carbon capture and removal technologies clash with hydrogen. Due to high operating costs of capturing $CO_2$, fossil power plants are operated not as baseload supply but as marginal capacity operated during peak load hours. As a result, the need for energy storage during peak hours reduces. Thus, the capacity of electrolyzers decreases by 21% from 950 GW to 740 GW (Fig 3c), and the capacity of hydrogen pipelines decreases by 20% from 1,100 GW to 840 GW (Fig 3b).

Expanding nuclear power plants reduces the over-capacity of renewable energy. The share of nuclear power in total electricity generation increases from 7% under the ZE scenario to 23% under the ZE + Nuclear scenario. Solar, wind, and battery capacities decrease by 19-39% relative to the ZE scenario. Due to low operating costs, nuclear power plants offer baseload generation, but do not balance the seasonal variation of renewable energy. Bulk hydrogen storage capacities are still required to balance the variation in renewable energy generation across seasons. Relative to the ZE scenario, the energy capacity of hydrogen storage decreases by only 7%.

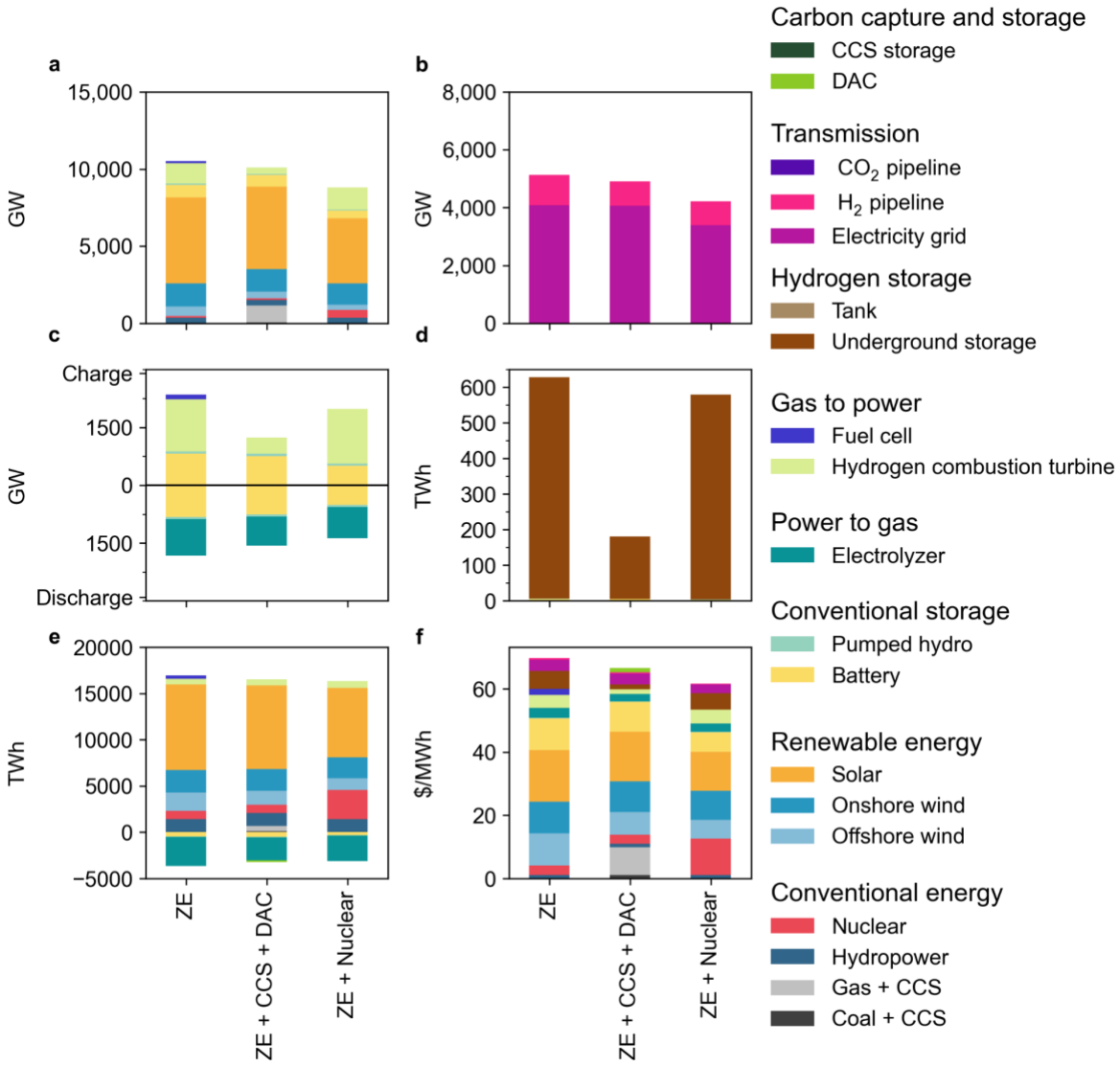


**Figure 3**. **a**. Generation capacity, **b**. transmission capacity, **c**. power capacity of charging and discharging storage, **d**. energy capacity of storage, **e**. generation, and **f**. levelized cost of electricity under ZE, ZE + CCS +DAC, and ZE + Nuclear scenarios. Different colors refer to different technologies.

### 4. Cost-competitiveness of green hydrogen for hard-to-abate sectors

Green hydrogen demand in China's hard-to-abate sectors including heavy industry, transportation, and heating is expected to rise to 124 TWh by 2050 in scenarios compatible

with 1.5ºC end-of-century warming (see Method). When China's zero-emission electricity system meets this additional hydrogen demand (ZE + Hydrogen scenario), hydrogen use for long-term storage in the electricity sector decreases (Fig 4a,b). When hydrogen solely serves as long-term storage, electricity generation from G2P technologies balances energy supply and demand across seasons (Fig 4a). Hydrogen is produced and stored between March and August, and discharged in other months, generating 990 TWh of electricity from G2P technologies. In contrast, when hydrogen provides both long-term storage and external hydrogen demand, electricity generated by G2P technologies decreases to 290 TWh (Fig 4b). This is because to meet the additional hydrogen demand from hard-to-abate sectors, more wind and solar capacity is deployed. This additional renewable energy capacity contributes more towards meeting demand in peak hours, and thus reduces the need for hydrogen storage compared to the ZE scenario. At the same time, more electrolyzers are built to meet hydrogen demand from the hard-to-abate sectors, but capacity of G2P technologies decreases because of the expansion in renewable energy capacities. Despite the increase in renewable energy capacities, generation curtailment decreases because hydrogen is produced and stored during times of overgeneration of electricity.

Relative to the ZE scenario, the levelized cost of energy (both electricity and hydrogen production for non-electricity sectors) is 5% lower in the ZE + Hydrogen demand scenario (Fig 4c). Allowing blue hydrogen production through SMR and coal gasification coupled with CCS and DAC (ZE + Hydrogen demand + Blue) yields a similar levelized cost of energy (only a reduction of 0.4 $/MWh) as the green hydrogen scenario (ZE + Hydrogen demand).

For China, the cost of producing green hydrogen in 2050 can be similar to and even lower than the cost of coal and gas-based hydrogen. In this study, we assume that the total

cost of green hydrogen production is the difference in cost between the ZE and the ZE + Hydrogen demand scenarios. This method yields a levelized cost of hydrogen of 58 (56-72) $/MWh or 1.93 (1.88-2.40) $/kg. This range of costs of green hydrogen production overlaps significantly with the range of costs expected from both coal and gas-based hydrogen (grey hydrogen) assuming fossil fuel costs remain at levels seen during 2018-2023 (Figs. 4d and 4e). If China's natural gas price rises above ~11 $/MWh or coal prices exceed ~2.5 $/mmBtu in 2050, green hydrogen from the zero-emission electricity system is likely to be cheaper than natural gas and coal-based hydrogen (Fig 4d and 4e), a plausible future given the rising real energy prices of fossil fuels.

The hourly demand curve of hydrogen is lacking due to data availability. In the main text, we assumed that the demand curve of hydrogen follows the pattern of electricity demand. In Fig S8, we assessed the robustness of our results assuming that, in each province, hourly hydrogen demand follows a uniform distribution. The results show that the pattern of the hourly demand curve of hydrogen does not affect the cost of energy.

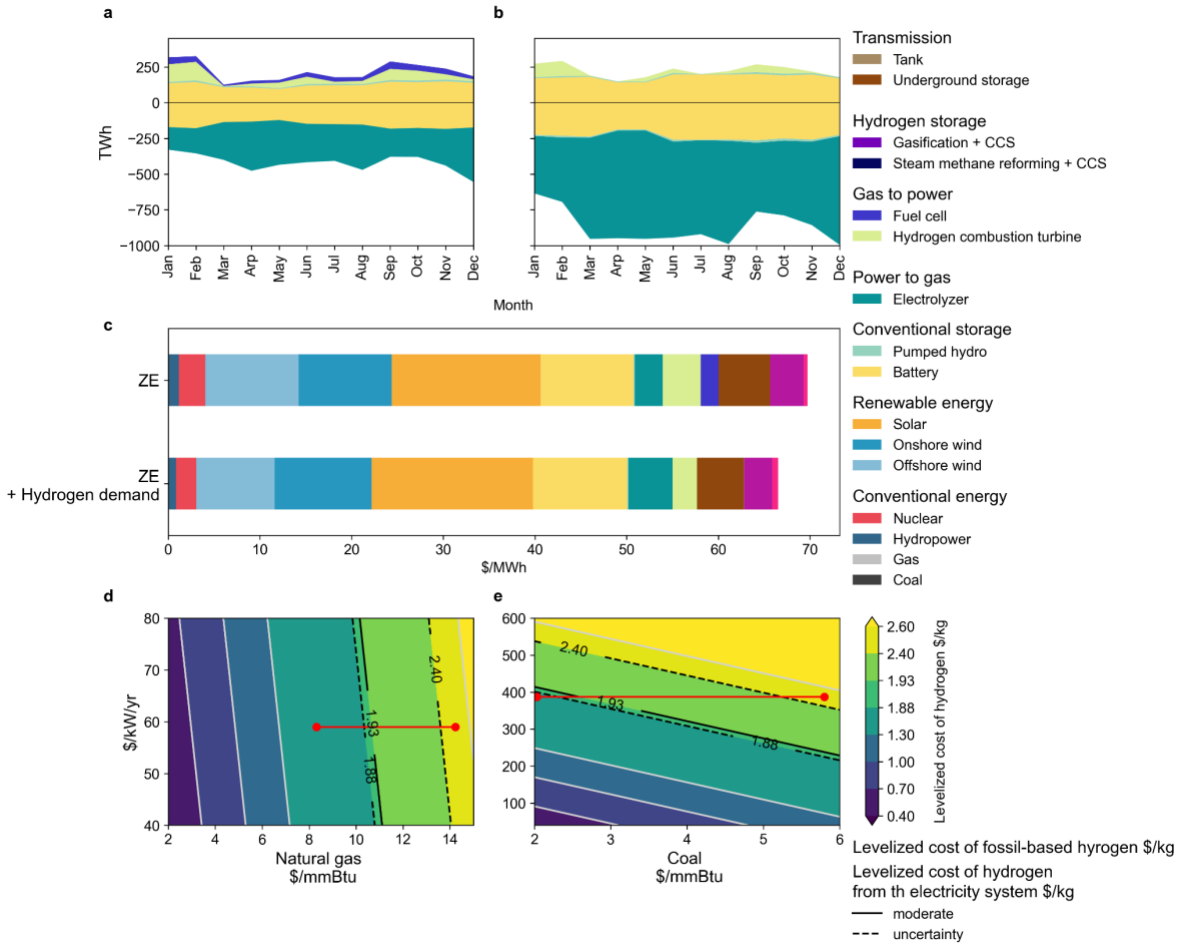


**Figure 4**. Generation curve of hydrogen by month under **a**. ZE and **b**. ZE + Hydrogen demand scenarios. **c**. Levelized cost of electricity under the ZE and ZE + Hydrogen demand and ZE + Hydrogen + Blue scenarios. Contour maps showing the levelized cost under different fixed costs and fuel costs for the **d**. natural gas-based grey hydrogen (SMR) and **e**. coal-based grey hydrogen (gasification). The capacity factor of SMR and gasification is assumed to be 100%. The solid black lines represent the combination of fixed cost and fuel cost where the levelized cost of grey hydrogen equals the levelized cost of green hydrogen. The dashed black lines represent the combination where the levelized cost of the grey hydrogen equals the lower higher bound of the levelized cost for green hydrogen. The red lines represent the levelized cost of grey hydrogen given fuel costs over the past five years[53].

### *D. Discussion*

As the world's largest greenhouse gas emitter, China has pledged a zero-carbon electricity system by 2060 to mitigate climate change. However, without technological innovations, achieving a zero-carbon electricity system can be expensive. Here, we find that including hydrogen as long-term storage can reduce the levelized cost of electricity by 17% in a zero-carbon electricity system where fossil fuels are entirely phased out. We also find that a zero-carbon electricity system can supply hydrogen demand in hard-to-abate sectors at a reasonable cost. If the price of natural gas increases to over 13 $/mmBtu and the price of coal increases to over 2.5 $/mmBtu, hydrogen produced by zero-carbon electricity is likely to be cheaper than fossil-based hydrogen. Relative to the cost-optimal scenario with no carbon cap, however, the levelized cost of electricity in the ZE still increases by 44% assuming a moderate rate of cost decline in electrolyzers, fuel cells, and hydrogen storage (Table S3-S7), and potentially imposes a large financial burden for investors and consumers.

Several factors overshadow the prospects of hydrogen use in China. First, the availability of underground storage is the limiting factor for using hydrogen as long-term storage. Without underground storage, using tanks to store hydrogen will be a more expensive option. Salt caverns are the best sites to store hydrogen,[241,242] and our research estimates that the underground hydrogen capacity should reach ~600 TWh. While Europe has found a total of 84.8 PWh hydrogen storage sites,[243] the potential for salt cavern capacity is unknown in China. The latest research shows that the operating salt cavern in China can store only 0.3 TWh hydrogen, which is 3 orders of magnitude lower than the required capacity.[233]

Adding other low-carbon firm capacities like nuclear power plants to the ZE electricity system further reduces the cost. Carbon capture (CCS) and removal (DAC)

technologies squeeze out hydrogen technologies, as they both serve as moderators for the variability of renewable energy. If CCS and DAC technologies are available, the levelized cost of electricity decreases by 4% relative to the zero-carbon electricity system with hydrogen, and the hydrogen storage capacity decreases. This antagonistic effect indicates that the prospect of hydrogen as long-term storage depends on whether the Chinese government decides to fully phase out fossil fuel power plants by 2060.

While these pathways with nuclear, CCS, and DAC technologies may be economically feasible, they pose socio-political challenges. Introducing new nuclear power plants raises risk concerns in the public[244]. Coal power plants cause ~100,000 annual premature deaths due to air pollution[245]. Reliance on natural gas casts doubt on energy security, given that 40% of China's natural gas was imported in 2020, while supplying 3% of electricity generation[246]. Other pathways that include hydropower and bioenergy expansion, which were not examined in this study, also face sociopolitical risks. Expanding hydropower capacities results in the change of ecosystem[247] and the resettlement of communities[248,249]. Moreover, to meet China's carbon-neutral target, bioenergy reduces food supply by 8% without food import[250].

Expanding the electricity transmission network is crucial for hydrogen use. Solely expanding electricity transmission lines can achieve similar cost reduction as expanding both pipelines and the electricity transmission lines. By retrofitting China's existing natural gas pipelines to hydrogen, the cost can be further reduced.

More importantly, hydrogen from the electricity sector is cost-effective to replace the traditional fossil-based hydrogen pathways, facilitating decarbonization in the hard-to-abate sectors. Given China's reliance on expensive imported natural gas, scaling up hydrogen using natural gas is not economically or politically feasible.

## *E. Appendix*

### 1. Code availability

GridPath model code is available at https://github.com/cetlab-ucsb/gridpath/tree/H2_CCS.

## 2. Supplementary Tables

**Table S1. Sites for underground hydrogen and carbon storage**

| **Technology** | **Province** | **Reference** |
|---|---|---|
| Underground hydrogen | Anhui, Hebei, Henan, Shandong, Hubei, Hunan, Sichuan, Jiangsu, Jiangxi, Guangdong, Yunnan, Chongqing, Gansu, Inner Mongolia | Zhu et al[233] |
| Underground $CO_2$ | Onshore: Anhui, Chongqing, Jiangsu, Jilin, Hebei, Heilongjiang, Hubei, Henan, Inner Mongolia, Liaoning, Qinghai, Sichuan, Tianjin, Xinjiang<br><br>Offshore: Fujian, Guangxi, Guangdong, Hainan, Jiangsu, Liaoning, Shandong | Fan et al[234] |

**Table S2. Examine the demand curtailment of the capacity expansion model**

| Scenario | Temporal resolution | Demand curtailment |
|---|---|---|
| 'ZE' | 36 days[1] | 0% |
| | 8760[2] | 0% |

[1] Optimized the capacity investment by using 36 days in a whole year,

[2] Simulated the operation with fixed capacities across 8760 hours.

**Table S3.** Cost assumptions for conventional electricity generation and storage technologies. We assumed that the exchange rate between RMB and the US dollar is 6.5:1. O&M costs are all from NREL ATB databases[237].

| $/kW or $/kWh | | 2020 | | 2050 | | Ref |
|---|---|---|---|---|---|---|
| | | Capital | O&M | Capital | O&M | |
| Coal | Coal | 622 | 10 | 495 | 8 | Zhuo[192] |
| | IGCC | 1090 | 19 | 1030 | 18 | |
| Natural gas | CT | 367 | 15 | 286 | 13 | |
| | CCGT | 409 | 20 | 318 | 15 | |
| Nuclear | | 2462 | 86 | 1739 | 86 | |
| Hydropower | | 2240 | 40 | No new hydropower | | |
| PV | Utility | 628 | 10 | 308 | 6 | IRENA[107] |
| | Residential | 746 | 10 | 292 | 4 | |

| | | | | | | |
|---|---|---|---|---|---|---|
| Wind | Onshore | 1157 | 22 | 784 | 17 | |
| | Offshore | 2857 | 67 | 1947 | 44 | |
| Battery | Power ($/kW) | 492 | 25 | 412 | 20 | Zhuo[192] |
| | Energy ($/kWh) | 246 | | 111 | | |
| Pumped hydro (10-hour) | | 918 | 23 | No new pumped hydro | | |

**Table S4.** Cost and parameter assumptions for hydrogen technologies. The exchange rate between the Euro and the US dollar is 1.1:1.

| $/kW or $/kWh | | Capital | | | | O&M | Efficiency | Ref |
|---|---|---|---|---|---|---|---|---|
| | | 2020 | 2050 | | | | | |
| | | | Low | Medium | High | | | |
| Electrolyzer | | 1245 | 283 | 311 | 385 | 4% | 70%<br>Low:55% | Danish Energy Agency[238] |
| Hydrogen combustion turbine | | 315 | 305 | | | Gas CT | 40% | McPherson[251] |
| Fuel cell | | 1562 | 600 | 962 | 1087 | 5% | 60%<br>Low: 40% | Danish Energy Agency[238] |
| | Tank | 69 | 25 | 25 | 42 | 2% | 90% | |

| | | | | | | | | |
|---|---|---|---|---|---|---|---|---|
| Hydrogen storage ($/kWh) | Underground | 3.6 | 1.2 | 1.6 | 2.2 | 0 | 99% | |

**Table S5.** Cost and parameter assumptions for CCS and DAC technologies.

| $ million per tonne per hour | | 2020 | | 2050 | | Electricity (MWh/ tonne) | Ref |
|---|---|---|---|---|---|---|---|
| | | Capital | O&M | Capital | O&M | | |
| CCS | Coal | 3.1 | 0.02 | 1.4 | 0.008 | 0.15 | Global CCS Institute[239] |
| | Natural gas | 3 | 0.03 | 1.4 | 0.01 | 0.16 | |
| | SMR/ gasification | 0.8 | 0.0003 | 0.4 | 0.0003 | 0.61 | |
| CCS storage | Onshore | 2.8 | 0.0 | 2.3 | 0.0 | | Danish Energy Agency[238] |
| | Offshore | 4.7 | 0.0 | 3.8 | 0.0 | | |
| DAC | | 7 | 0.4 | 2 | 0.4 | 1.5 | |

**Table S6.** Cost and parameter assumptions for CCS and DAC technologies. The 2020 exchange rate between the Euro and the US dollar is 1.1:1.

| | $/MW/km<br>$/tonne/km | Loss/1000 km | Ref |
|---|---|---|---|
| Transmission line | 340 | 5.3% | Electric Power Planning Design General Institute[194] |
| Hydrogen pipeline | 226 | 1.3% | Danish Energy Agency[238] |
| $CO_2$ pipeline | 1.7 | 0 | |

**Table S7.** Fuel cost. The data for the fuel cost is from He et al.[187] ang Luo et al[184].

| Fuel | Region | $/mmBtu |
|---|---|---|
| Coal | Anhui | 4.61 |
| Coal | Beijing | 4.93 |
| Coal | Chongqing | 3.82 |
| Coal | Inner Mongolia | 2.80 |
| Coal | Fujian | 5.77 |
| Coal | Gansu | 3.60 |
| Coal | Guangdong | 6.17 |
| Coal | Guangxi | 6.17 |
| Coal | Guizhou | 6.17 |
| Coal | Hainan | 6.17 |
| Coal | Hebei | 4.93 |
| Coal | Heilongjiang | 4.23 |
| Coal | Henan | 4.87 |
| Coal | Hubei | 4.41 |

| | | |
|---|---|---|
| Coal | Hunan | 4.72 |
| Coal | Jiangsu | 5.77 |
| Coal | Jiangxi | 4.72 |
| Coal | Jilin | 3.15 |
| Coal | Liaoning | 3.38 |
| Coal | Ningxia | 3.19 |
| Coal | Qinghai | 3.09 |
| Coal | Shaanxi | 3.15 |
| Coal | Shandong | 4.93 |
| Coal | Shanghai | 5.77 |
| Coal | Shanxi | 4.22 |
| Coal | Sichuan | 3.82 |
| Coal | Tianjin | 4.93 |
| Coal | Xinjiang | 2.60 |
| Coal | Yunnan | 6.17 |

| | | |
|---|---|---|
| Coal | Zhejiang | 5.77 |
| Gas | National | 13.68 |
| Uraniam | National | 0.82 |

## 3. Supplementary Figures

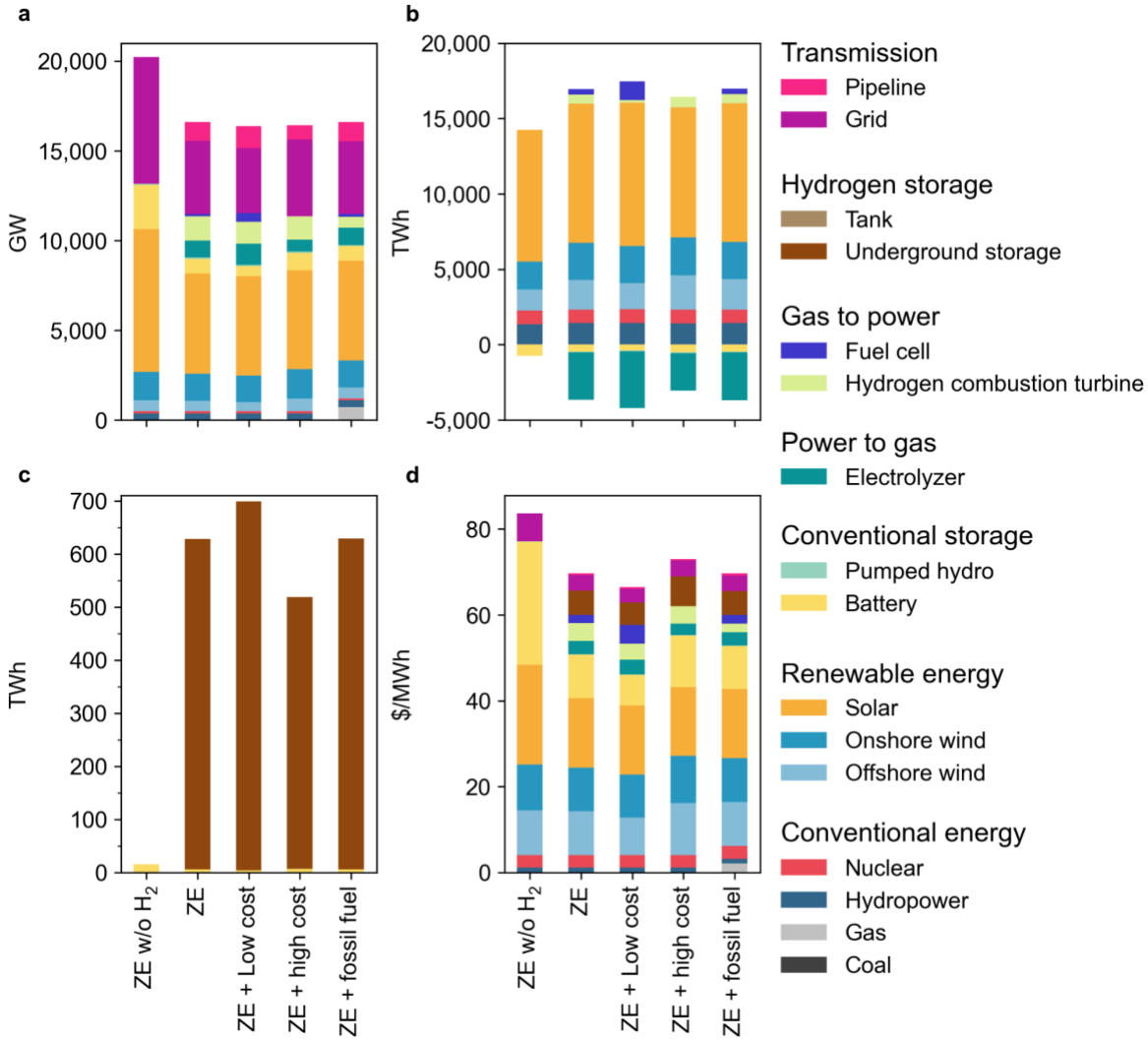


**Figure S1. a**. Generation capacity, **b**. transmission capacity, **c**. power capacity of storage, **d**. energy capacity of storage, **e**. generation, and **f**. levelized cost of electricity under low-carbon scenarios in 2050. Different colors refer to different technologies. ZE + Low cost refers to the ZE scenario with low-cost hydrogen technologies. ZE + High cost refers to the ZE scenario with high-cost hydrogen technologies. ZE + High cost + Low efficiency refers to the ZE scenario with high-cost and low-efficiency hydrogen technologies

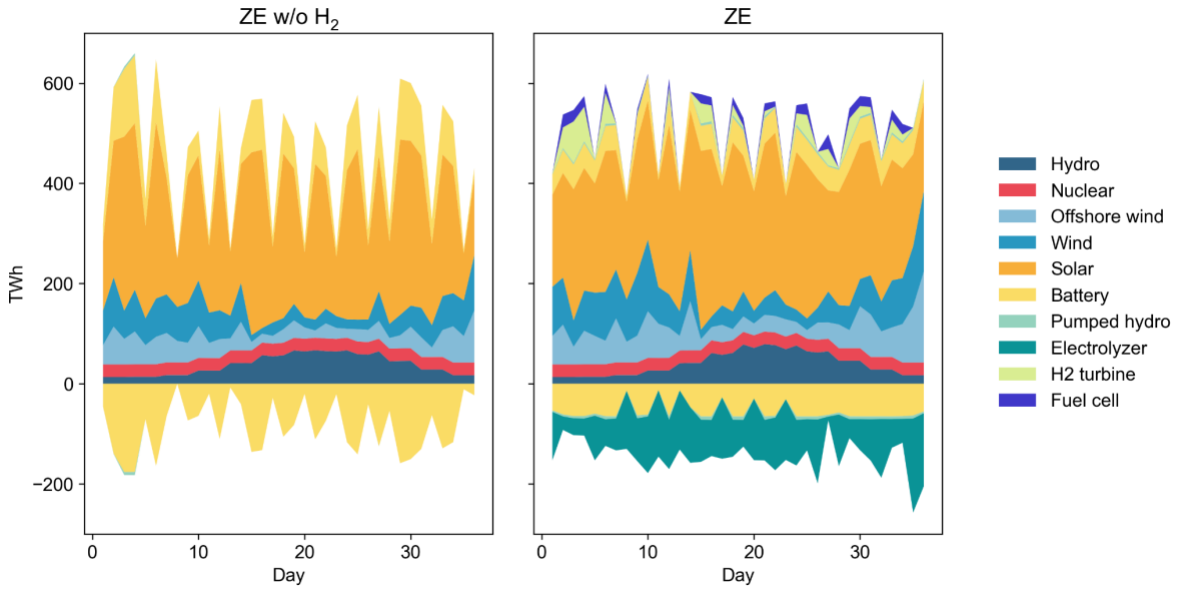


**Figure S2. Daily generation of electricity in the 36 representative days under ZE w/o $H_2$ and ZE scenarios.**

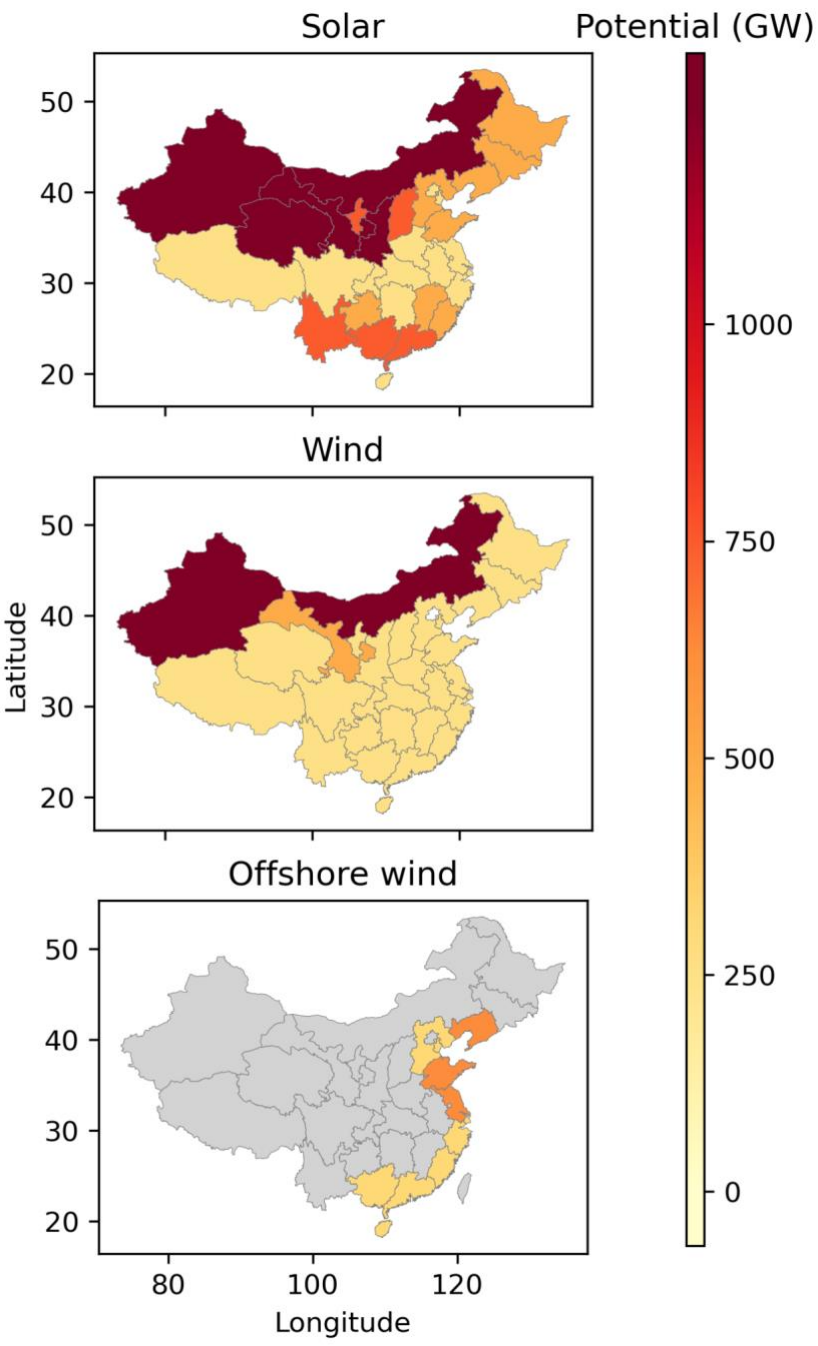


**Figure S3. The potential of solar, onshore wind and offshore capacities.**

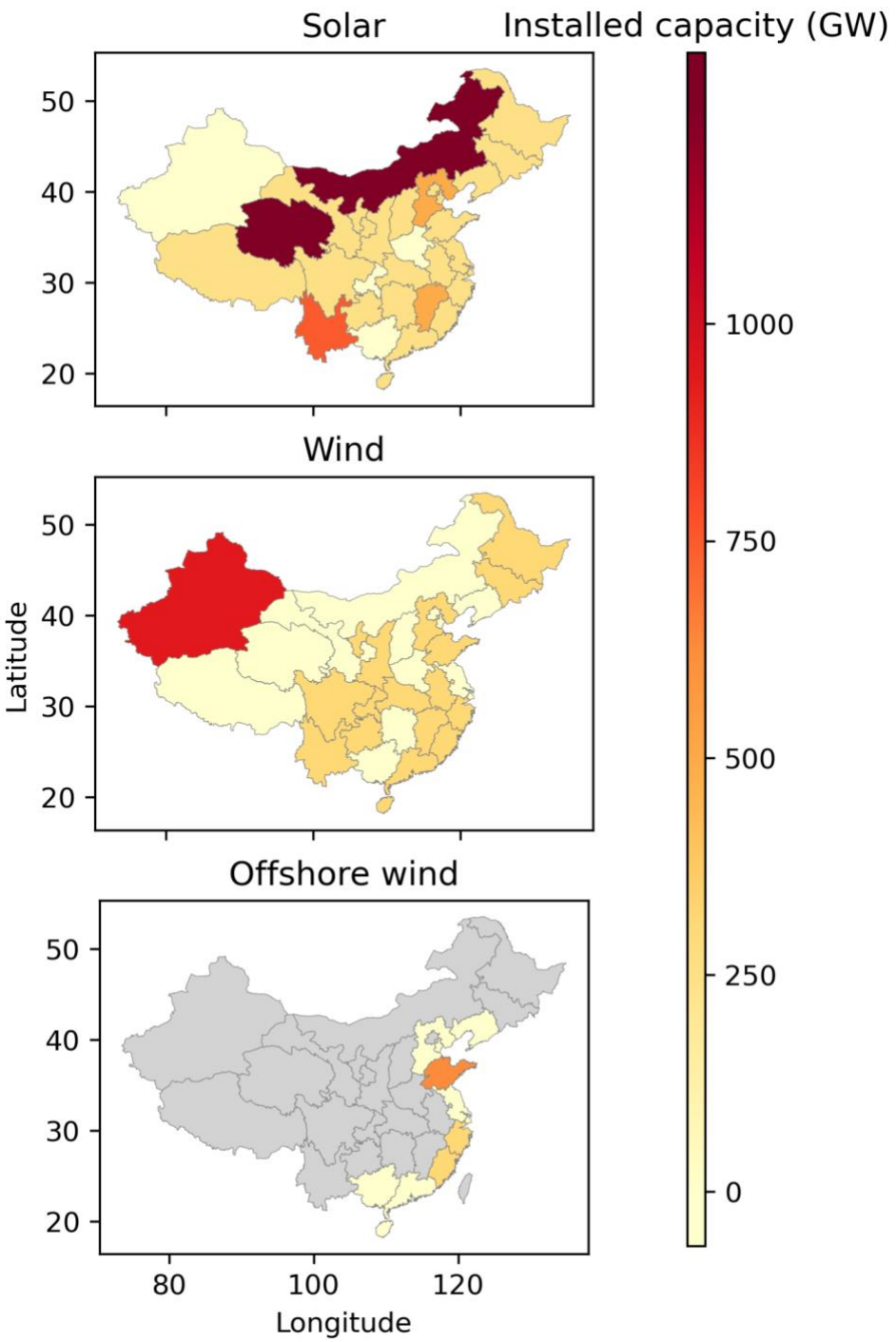


**Figure S4. The installed capacities of solar, onshore wind and offshore capacities under the ZE scenario.**

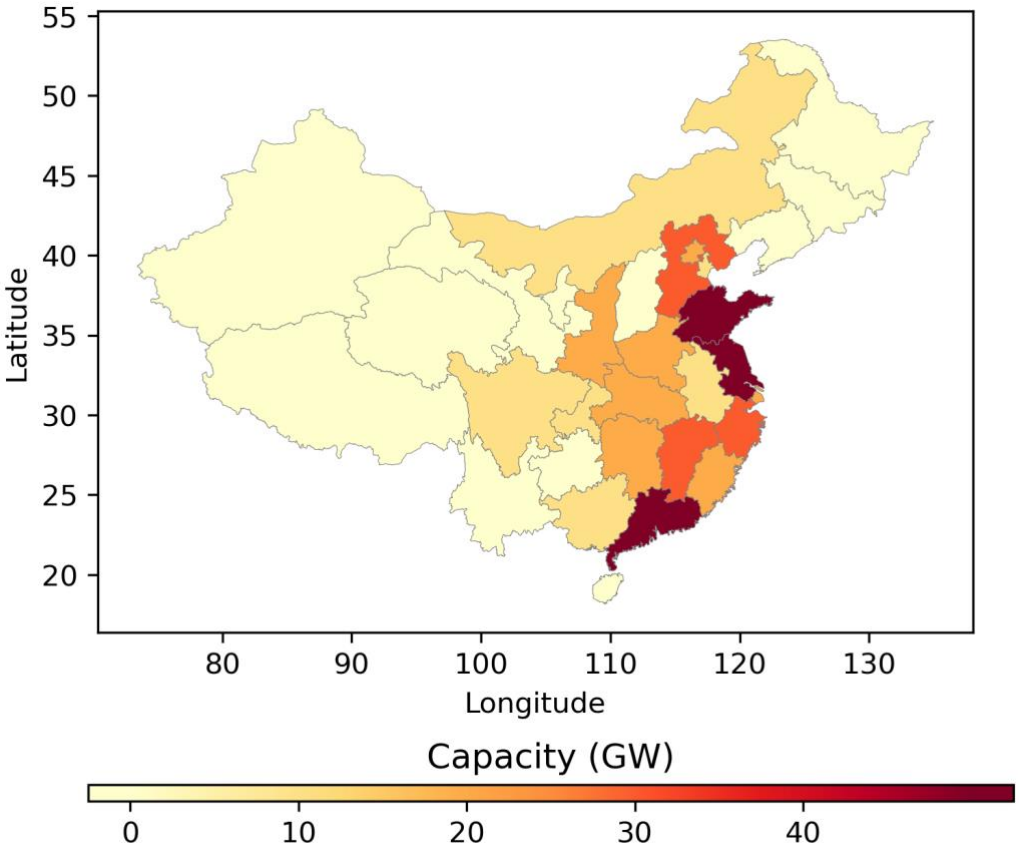


**Figure S5. Fuel cell capacities under the ZE scenario but without new transmission and hydrogen pipelines.**

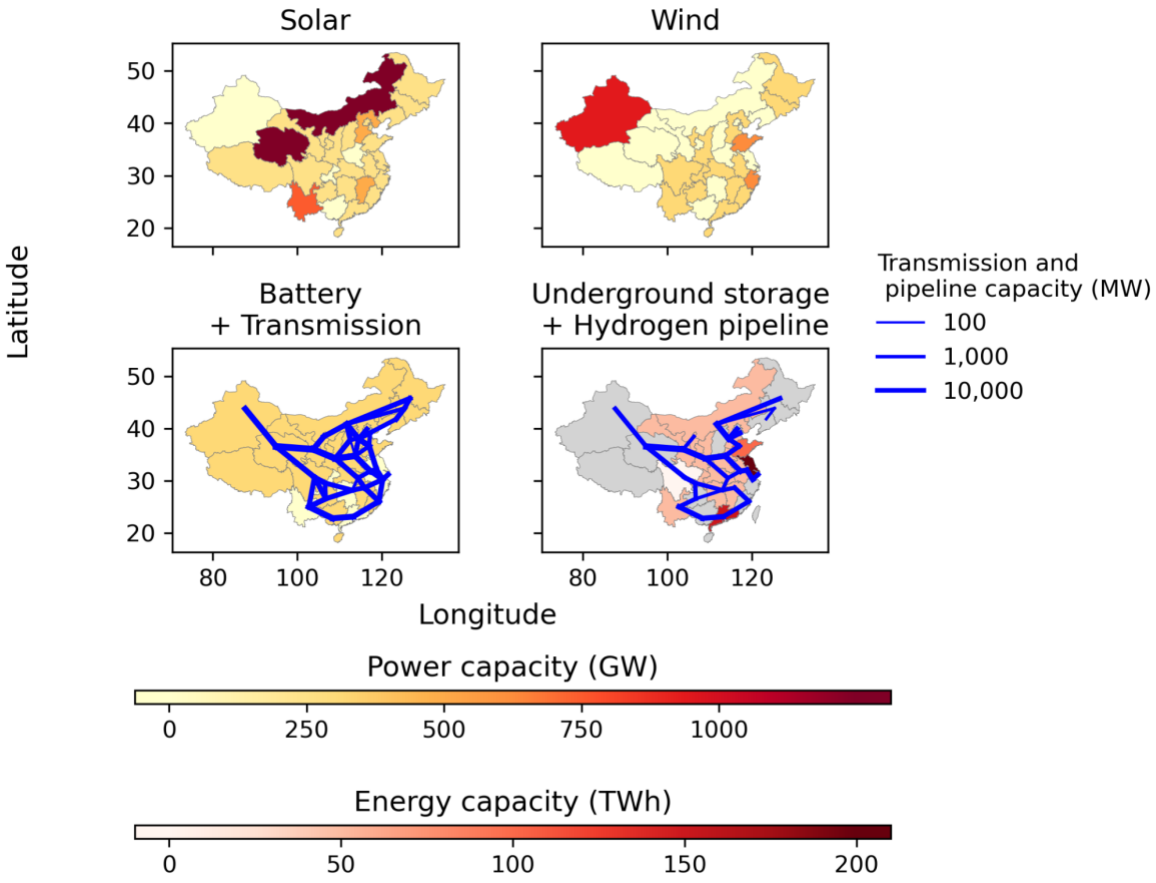


**Figure S6. Capacities of solar, wind, battery, underground storage, transmission lines and hydrogen pipelines. The color grey means that no underground storage is available in the area.**

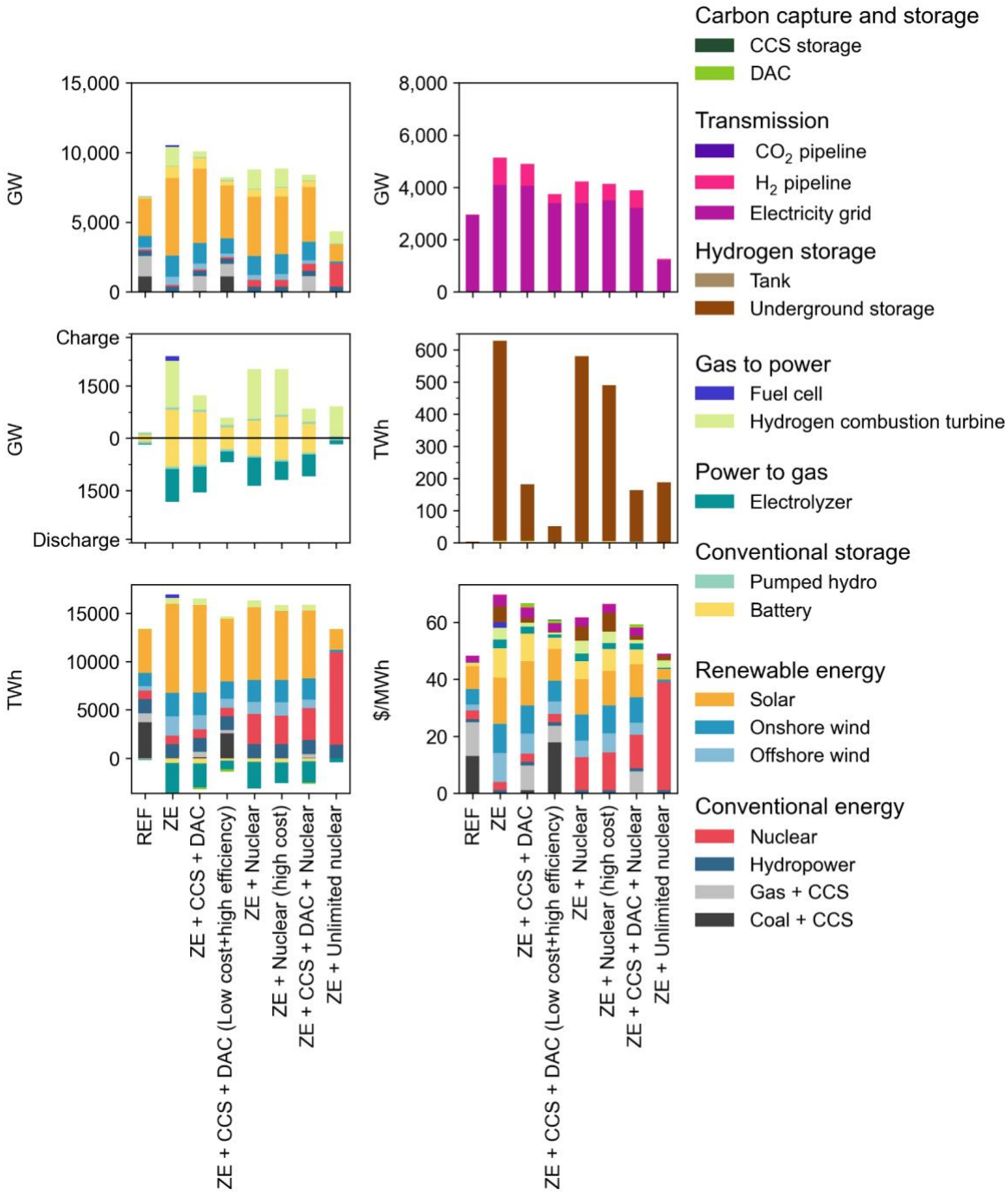


**Figure S7. a**. Generation capacity, **b**. transmission capacity, **c**. power capacity of charging and discharging storage, **d**. energy capacity of storage, **e**. generation, and **f**. levelized cost of electricity under different zero-carbon scenarios. Different colors refer to different technologies. REF refers to the scenario without a carbon emission target. The scenario 'CCS

+ DAC + Low cost' refers to a scenario where the CCS and DAC follow the cost projection in 2050, and the CCS capture rate reaches 95%. 'Unlimited nuclear' refers to a scenario where no capacity cap is imposed on nuclear power plants.

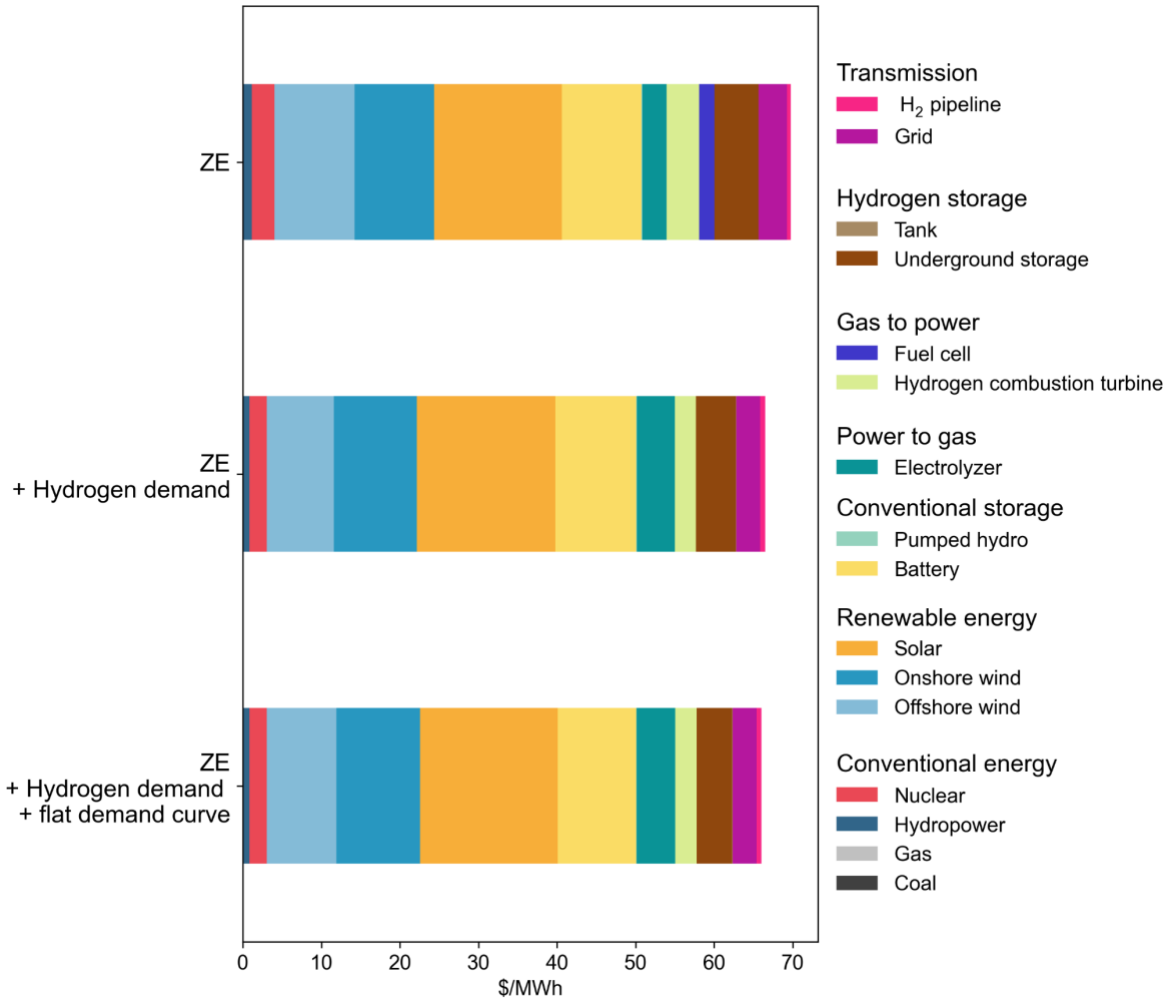


**Figure S8. Levelized cost of energy demand under different scenarios.**

The flat demand curve scenario refers to the scenario where in each province, the hourly hydrogen demand is the same across every hour.

# VII. Conclusion

This dissertation evaluates the opportunities and challenges in the lower-carbon transition of the energy system. It seeks to answer what socioeconomic challenges are hindering more ambitious climate actions among countries and individuals. While socioeconomic factors are typically viewed as barriers, this dissertation examines the potential of socioeconomic factors to accelerate the low-carbon transition of the energy system.

In Chapter II, I quantify the stranded asset costs of the low-carbon transition, and compare with the benefits to stabilize the temperature within 2ºC. The unequal spatial distribution of the stranded assets in higher and lower income countries may partly explain the disparate stances among countries, given varying endowments of fossil fuel reserves. Higher income countries experience a loss of $3.7 trillion stranded fossil fuel assets; but only receive $1.7 trillion benefits from joining a global 2°C target. In contrast, lower income countries bear a stranded asset cost of $0.5 trillion, and receive $3.3 trillion of benefits. This unequal cost-benefit landscape between higher and lower income countries implies the free-rider problem in climate change mitigation.

In Chapter III, I develop a cost-benefit framework to analyze how the costs and benefits are distributed across different age cohorts in the low-carbon transition. Globally, the year 1960 is the breakeven year for the age cohorts to gain net benefits from the low-carbon transition. However, country-level analysis paints a somewhat more complex picture. In many African and Latin American countries, over half of the current population gains net benefits, whereas no age cohorts benefit in most Western European countries. Should the public be well aware of the net lifetime benefits from the low-carbon transition, older

generations in Africa and Latin America are likely to see more support for the low-carbon transition, while the young generations in Europe may change their attitudes.

Chapter IV examines whether building transcontinental power pools achieves a reliable and economically feasible zero-carbon electricity system within constraints on land availability. Only using 10% of the suitable sites for renewable energy, the international trade of electricity reliability meets electricity demand with 100% renewable energy. Relative to the case without international trade, if countries participate in the transcontinental power pool, the aggregate system cost of the countries is reduced by 5-23%. While global transcontinental power pools address the shortage of land at an affordable cost, geopolitical concerns would be the major barriers to implementing the power pools.

Chapter V zooms into the socioeconomic barriers at the regional level. Using a multi-model framework, this chapter examines the provincial and regional distribution of health and employment outcomes by the low-carbon transition of China's electricity sector. At the national level, the low-carbon transition increases the number of jobs and labor compensation, and incurs large benefits in terms of avoided health and climate damages. However, the decarbonization of China's electricity system is expected to exert distinct impacts on employment across provinces. The economically developed East Coast region experiences a higher increase in employment, while less economically developed regions experience a much smaller increase in employment. While economic feasibility is important to accelerate China's low-carbon transition of the electricity sector, addressing the regional disparity in employment outcomes is also critical.

Chapter VI explores the economic implications of hydrogen in a zero-carbon electricity system, which is a politically feasible pathway compared to pathways with

nuclear expansion and carbon removal technologies. My research demonstrates that hydrogen reduces the cost of a zero-carbon electricity system by 16%, compared with a scenario without hydrogen. The cost reduction relies on the availability of underground hydrogen storage capacities and the expansion of the transmission capacities. Carbon removal technologies achieve larger cost reduction in the zero-carbon electricity system, and crowd out hydrogen. Apart from the role of long-term storage, hydrogen from the zero-carbon electricity system can be used to meet hydrogen demand in hard-to-abate sectors, while incurring a slight decrease in the unit cost of energy demand.

## VIII. References


1. IPCC. *Climate Change 2022: Impacts, Adaptation, and Vulnerability. Contribution of Working Group II to the Sixth Assessment Report of the Intergovernmental Panel on Climate Change*. (Cambridge University Press., Cambridge, UK and New York, NY, USA).
2. The Paris Agreement | UNFCCC. https://unfccc.int/process-and-meetings/the-paris-agreement.
3. Ritchie, H. Sector by sector: where do global greenhouse gas emissions come from? *Our World in Data* (2020).
4. Rogelj, J. *et al.* Energy system transformations for limiting end-of-century warming to below 1.5 °C. *Nature Clim Change* **5**, 519–527 (2015).
5. IPCC. Summary for Policymakers. in (Cambridge University Press, Cambridge, UK and New York, NY, USA).
6. Davis, S. J. *et al.* Net-zero emissions energy systems. *Science* **360**, eaas9793 (2018).
7. Glanemann, N., Willner, S. N. & Levermann, A. Paris Climate Agreement passes the cost-benefit test. *Nature Communications* **11**, 110 (2020).
8. van der Wijst, K.-I. *et al.* New damage curves and multimodel analysis suggest lower optimal temperature. *Nat. Clim. Chang.* **13**, 434–441 (2023).
9. Kotz, M., Levermann, A. & Wenz, L. The economic commitment of climate change. *Nature* **628**, 551–557 (2024).
10. Luderer, G. *et al.* Economic mitigation challenges: how further delay closes the door for achieving climate targets. *Environ. Res. Lett.* **8**, 034033 (2013).
11. Lamboll, R. D. *et al.* Assessing the size and uncertainty of remaining carbon budgets.

*Nat. Clim. Chang.* **13**, 1360–1367 (2023).

12. Climate Action Tracker. *Glasgow's 2030 Credibility Gap: Net Zero's Lip Service to Climate Action*. https://climateactiontracker.org/documents/997/CAT_2021-11-09_Briefing_Global-Update_Glasgow2030CredibilityGap.pdf (2021).
13. Environment, U. N. Emissions Gap Report 2023. *UNEP - UN Environment Programme* http://www.unep.org/resources/emissions-gap-report-2023 (2023).
14. Peng, W. *et al.* Climate policy models need to get real about people — here's how. *Nature* **594**, 174–176 (2021).
15. Aklin, M. & Mildenberger, M. Prisoners of the Wrong Dilemma: Why Distributive Conflict, Not Collective Action, Characterizes the Politics of Climate Change. *Global Environmental Politics* **20**, 4–27 (2020).
16. Colgan, J. D., Green, J. F. & Hale, T. N. Asset Revaluation and the Existential Politics of Climate Change. *International Organization* **75**, 586–610 (2021).
17. Meckling, J. & Karplus, V. J. Political strategies for climate and environmental solutions. *Nat Sustain* **6**, 742–751 (2023).
18. Mosnier, A. *et al.* A decentralized approach to model national and global food and land use systems. *Environ. Res. Lett.* **18**, 045001 (2023).
19. Wu, G. C. *et al.* Minimizing habitat conflicts in meeting net-zero energy targets in the western United States. *Proceedings of the National Academy of Sciences* **120**, e2204098120 (2023).
20. Chatzivasileiadis, S., Ernst, D. & Andersson, G. The Global Grid. *Renewable Energy* **57**, 372–383 (2013).
21. Brinkerink, M., Gallachóir, B. Ó. & Deane, P. A comprehensive review on the benefits

and challenges of global power grids and intercontinental interconnectors. *Renewable and Sustainable Energy Reviews* **107**, 274–287 (2019).

22. Yang, X., Nielsen, C. P., Song, S. & McElroy, M. B. Breaking the hard-to-abate bottleneck in China's path to carbon neutrality with clean hydrogen. *Nat Energy* **7**, 955–965 (2022).
23. Żuk, P. & Żuk, P. National energy security or acceleration of transition? Energy policy after the war in Ukraine. *Joule* **6**, 709–712 (2022).
24. Blondeel, M. *et al.* Global energy scenarios: A geopolitical reality check. *Global Environmental Change* **84**, 102781 (2024).
25. European Comission. Implementing the repower eu action plan: investment needs, hydrogen accelerator and achieving the bio-methane targets.
26. 45V: Credit for production of clean hydrogen. (12/262023).
27. Burke, M., Davis, W. M. & Diffenbaugh, N. S. Large potential reduction in economic damages under UN mitigation targets. *Nature* **557**, 549–553 (2018).
28. Warren, R., Hope, C., Gernaat, D. E. H. J., Van Vuuren, D. P. & Jenkins, K. Global and regional aggregate damages associated with global warming of 1.5 to 4 °C above pre-industrial levels. *Climatic Change* **168**, 24 (2021).
29. Köberle, A. C. *et al.* The cost of mitigation revisited. *Nat. Clim. Chang.* **11**, 1035–1045 (2021).
30. Caldecott, B., Harnett, E., Cojoianu, T., Kok, I. & Pfeiffer, A. Stranded assets: a climate risk challenge. *Washington DC: Inter-American Development Bank* (2016).
31. Ansari, D. & Holz, F. Between stranded assets and green transformation: Fossil-fuel-producing developing countries towards 2055. *World Development* **130**, 104947 (2020).

32. Mercure, J.-F. *et al.* Macroeconomic impact of stranded fossil fuel assets. *Nature Climate Change* **8**, 588–593 (2018).
33. Bauer, N. *et al.* Global fossil energy markets and climate change mitigation – an analysis with REMIND. *Climatic Change* **136**, 69–82 (2013).
34. Hundreds of fossil fuel lobbyists flooding COP26 climate talks. *Global Witness* https:///en/press-releases/hundreds-fossil-fuel-lobbyists-flooding-cop26-climate-talks/.
35. Outcomes of the Glasgow Climate Change Conference - Advance Unedited Versions (AUVs) | UNFCCC. https://unfccc.int/process-and-meetings/conferences/glasgow-climate-change-conference-october-november-2021/outcomes-of-the-glasgow-climate-change-conference.
36. McGlade, C. & Ekins, P. The geographical distribution of fossil fuels unused when limiting global warming to 2 °C. *Nature* **517**, 187–190 (2015).
37. Welsby, D., Price, J., Pye, S. & Ekins, P. Unextractable fossil fuels in a 1.5 °C world. *Nature* **597**, 230–234 (2021).
38. Edwards, M. R. *et al.* Quantifying the regional stranded asset risks from new coal plants under 1.5°C. *Environ. Res. Lett.* (2022) doi:10.1088/1748-9326/ac4ec2.
39. Diffenbaugh, N. S. & Burke, M. Global warming has increased global economic inequality. *Proc Natl Acad Sci USA* **116**, 9808 (2019).
40. Gazzotti, P. *et al.* Persistent inequality in economically optimal climate policies. *Nat Commun* **12**, 3421 (2021).
41. Tietenberg, T. & Lewis, L. *Environmental and Natural Resource Economics*. (Routledge, 2018).
42. van der Ploeg, F. & Rezai, A. Stranded Assets in the Transition to a Carbon-Free

Economy. *Annual Review of Resource Economics* **12**, 281–298 (2020).

43. Burke, M., Hsiang, S. M. & Miguel, E. Global non-linear effect of temperature on economic production. *Nature* **527**, 235–239 (2015).
44. Riahi, K. *et al.* The Shared Socioeconomic Pathways and their energy, land use, and greenhouse gas emissions implications: An overview. *Global Environmental Change* **42**, 153–168 (2017).
45. Rogelj, J. *et al.* Paris Agreement climate proposals need a boost to keep warming well below 2 °C. *Nature* **534**, 631–639 (2016).
46. Hausfather, Z. & Peters, G. P. Emissions – the 'business as usual' story is misleading. *Nature* **577**, 618–620 (2020).
47. Hotelling, H. The economics of exhaustible resources. *Journal of political Economy* **39**, 137–175 (1931).
48. Devarajan, S. & Fisher, A. C. Hotelling's" economics of exhaustible resources": Fifty years later. *Journal of Economic Literature* **19**, 65–73 (1981).
49. Leaton, J., Ranger, N., Ward, B., Sussams, L. & Brown, M. Unburnable Carbon 2013: Wasted capital and stranded assets. *Carbon Tracker and Grantham Research Institute on Climate Change and the Environment, London School of Economics, London. http://www. carbontracker. org/wastedcapital* (2013).
50. Vrontisi, Z. *et al.* Enhancing global climate policy ambition towards a 1.5 °C stabilization: a short-term multi-model assessment. *Environ. Res. Lett.* **13**, 044039 (2018).
51. Luderer, G. *et al.* Residual fossil CO 2 emissions in 1.5–2 °C pathways. *Nature Clim Change* **8**, 626–633 (2018).

52. Byers, E. *et al.* AR6 Scenarios Database hosted by IIASA. International Institute for Applied Systems Analysis https://doi.org/10.5281/zenodo.7197970 (2022).
53. Commodity Markets. *World Bank* https://www.worldbank.org/en/research/commodity-markets.
54. Total Energy Annual Data. *U.S. Energy Information Administration (EIA)* https://www.eia.gov/totalenergy/data/annual/index.php.
55. BGR BGR Energy Study. Data and Developments Concerning German and Global Energy Supplies - Summary. https://www.whymap.org/EN/Themen/Energie/Produkte/energy_study_2018_summary_en.html (2018).
56. Rystad Energy. Rystad Ucube Database. (2020).
57. Mercure, J.-F. *et al.* Reframing the climate policy game. *PREPRINT (Version 1) available at Research Square* (2021) doi:https://doi.org/10.21203/rs.3.rs-150151/v1.
58. Country Classification – World Bank Data Help Desk. *World Bank* https://datahelpdesk.worldbank.org/knowledgebase/topics/19280-country-classification.
59. IPCC. *Climate Change 2022: Mitigation of Climate Change*. (2022).
60. SSP Database. *International Institute for Applied Systems Analysis* https://tntcat.iiasa.ac.at/SspDb.
61. Climate Action Tracker. Global update: Governments still showing little sign of acting on climate crisis | Climate Action Tracker. https://climateactiontracker.org/press/global-update-governments-showing-little-sign-of-acting-on-climate-crisis/ (2019).
62. Semieniuk, G. *et al.* Stranded fossil-fuel assets translate to major losses for investors in advanced economies. *Nat. Clim. Chang.* **12**, 532–538 (2022).

63. Saygin, D., Rigter, J., Caldecott, B., Wagner, N. & Gielen, D. Power sector asset stranding effects of climate policies. *Energy Sources, Part B: Economics, Planning, and Policy* **14**, 99–124 (2019).

64. Malik, A. *et al.* Reducing stranded assets through early action in the Indian power sector. *Environ. Res. Lett.* **15**, 094091 (2020).

65. Pan, X. *et al.* Implications of carbon neutrality for power sector investments and stranded coal assets in China. *Energy Economics* **121**, 106682 (2023).

66. von Dulong, A., Gard-Murray, A., Hagen, A., Jaakkola, N. & Sen, S. Stranded Assets: Research Gaps and Implications for Climate Policy. *Review of Environmental Economics and Policy* **17**, 161–169 (2023).

67. Meng, K. C. & Rode, A. The social cost of lobbying over climate policy. *Nat. Clim. Chang.* **9**, 472–476 (2019).

68. Marin, G. & Vona, F. Climate policies and skill-biased employment dynamics: Evidence from EU countries. *Journal of Environmental Economics and Management* **98**, 102253 (2019).

69. Carleton, T. *et al.* Valuing the Global Mortality Consequences of Climate Change Accounting for Adaptation Costs and Benefits*. *The Quarterly Journal of Economics* qjac020 (2022) doi:10.1093/qje/qjac020.

70. Ricke, K., Drouet, L., Caldeira, K. & Tavoni, M. Country-level social cost of carbon. *Nature Climate Change* **8**, 895–900 (2018).

71. IPCC. *Summary for Policymakers. In: Climate Change 2013: The Physical Science Basis. Contribution of Working Group I to the Fifth Assessment Report of the Intergovernmental Panel on Climate Change*. (Cambridge University Press, Cambridge,

United Kingdom and New York, NY, USA, 2013).

72. IPCC. Observations: Atmosphere and Surface. in *Climate Change 2013: The Physical Science Basis. Contribution of Working Group I to the Fifth Assessment Report of the Intergovernmental Panel on Climate Change* (Cambridge University Press, Cambridge, 2013).
73. RELEASE OF ENERGY INTELLIGENCE TOP 100: GLOBAL NOC & IOC RANKINGS. *Energy Intelligence* http://www.energyintel.com/pages/top100-2018.aspx.
74. Platts Top 250. https://top250.platts.com/.
75. Ekwurzel, B. *et al.* The rise in global atmospheric CO2, surface temperature, and sea level from emissions traced to major carbon producers. *Climatic Change* **144**, 579–590 (2017).
76. Taylor, M. & Watts, J. Revealed: the 20 firms behind a third of all carbon emissions. *The Guardian* (2019).
77. U.S. Securities and Exchange Commission. https://www.sec.gov/.
78. Andrew, R. M. & Peters, G. P. The Global Carbon Project's fossil CO2 emissions dataset. Zenodo https://doi.org/10.5281/zenodo.5569235 (2021).
79. O'Brien, K., Selboe, E. & Hayward, B. Exploring youth activism on climate change: dutiful, disruptive, and dangerous dissent. *Ecology and Society* **23**, (2018).
80. Marris, E. Why young climate activists have captured the world's attention. *Nature* **573**, 471–472 (2019).
81. Page, E. Intergenerational Justice and Climate Change. *Political Studies* **47**, 53–66 (1999).
82. Greta Thunberg tells world leaders 'you are failing us', as nations announce fresh

climate action. *United Nations Youth* https://www.un.org/development/desa/youth/news/2019/09/greta-thunberg/ (2019).

83. Thunberg, G. 'You did not act in time': Greta Thunberg's full speech to MPs. *The Guardian* (2019).
84. Corner, A. *et al.* How do young people engage with climate change? The role of knowledge, values, message framing, and trusted communicators. *WIREs Climate Change* **6**, 523–534 (2015).
85. White, J. Climate change and the generational timescape. *The Sociological Review* **65**, 763–778 (2017).
86. Graham, H. & Bell, S. de. The representation of future generations in newspaper coverage of climate change: A study of the UK press. *Children & Society* **35**, 465–480 (2020).
87. Karp, L. & Rezai, A. The Political Economy of Environmental Policy with Overlapping Generations. *International Economic Review* **55**, 711–733 (2014).
88. Andersen, T. M., Bhattacharya, J. & Liu, P. Resolving intergenerational conflict over the environment under the Pareto criterion. *Journal of Environmental Economics and Management* **100**, 102290 (2020).
89. Page, E. A. *Climate Change, Justice and Future Generations*. (Edward Elgar Publishing, Cheltenham, United Kingdom, 2006).
90. Schuppert, F. Climate change mitigation and intergenerational justice. *Environmental Politics* **20**, 303–321 (2011).
91. Brown, P. T., Moreno-Cruz, J. & Caldeira, K. Break-even year: a concept for understanding intergenerational trade-offs in climate change mitigation policy. *Environ.*

*Res. Commun.* **2**, 095002 (2020).

92. IPCC. *Climate Change 2014: Mitigation of Climate Change. Contribution of Working Group III to the Fifth Assessment Report of the Intergovernmental Panel on Climate Change*. vol. 6 (Cambridge University Press, Cambridge, United Kingdom and New York,USA, 2014).
93. Nikas, A., Doukas, H. & Papandreou, A. A Detailed Overview and Consistent Classification of Climate-Economy Models. *Understanding Risks and Uncertainties in Energy and Climate Policy: Multidisciplinary Methods and Tools for a Low Carbon Society* 1–54 (2019).
94. The common Integrated Assessment Model (IAM) documentation. *IAMC wiki*.
95. Kahn, M. E. *et al.* Long-term macroeconomic effects of climate change: A cross-country analysis. *International Monetary Fund* (2019).
96. Newell, R. G., Prest, B. C. & Sexton, S. E. The GDP-Temperature relationship: Implications for climate change damages. *Journal of Environmental Economics and Management* **108**, 102445 (2021).
97. Ueckerdt, F. *et al.* The economically optimal warming limit of the planet. *Earth System Dynamics* **10**, 741–763 (2019).
98. United Nations, Department of Economic and Social Affairs, Population Division. World Population Prospects 2019. (2019).
99. World Bank Open Data. https://data.worldbank.org/.
100. OECD. OECD Income Distribution Database (IDD): Gini, poverty, income, Methods and Concepts. https://www.oecd.org/social/income-distribution-database.htm.
101. CMIP5 - Coupled Model Intercomparison Project Phase 5 - Overview. *Program for*

*Climate Change Model Diagnosis & Intercomparison* https://pcmdi.llnl.gov/mips/cmip5/.

102. Ramsey, F. P. A Mathematical Theory of Saving. *The Economic Journal* **38**, 543–559 (1928).

103. Yang, H. Data for paper Economic disparity among generations under Paris Agreement. Zenodo https://doi.org/10.5281/zenodo.5103739 (2021).

104. Yang, H. Data and code for the shiny app of the paper Economic disparity among generations under Paris Agreement. Zenodo https://doi.org/10.5281/zenodo.5104877 (2021).

105. Meinshausen, M. *et al.* Greenhouse-gas emission targets for limiting global warming to 2 °C. *Nature* **458**, 1158–1162 (2009).

106. IEA. Data & Statistics. https://www.iea.org/data-and-statistics.

107. International Renewable Energy Agency. Renewable Power Generation Costs in 2020. https://www.irena.org/publications/2021/Jun/Renewable-Power-Costs-in-2020.

108. REN21. *The Renewables 2020 Global Status Report*. (2020).

109. International Energy Agency, Nuclear Energy Agency & Organisation for Economic Co-operation and Development. *Projected Costs of Generating Electricity 2020*. (IEA, Paris, 2020).

110. Lu, X., McElroy, M. B. & Kiviluoma, J. Global potential for wind-generated electricity. *Proc Natl Acad Sci USA* **106**, 10933 (2009).

111. Zhou, Y., Luckow, P., Smith, S. J. & Clarke, L. Evaluation of Global Onshore Wind Energy Potential and Generation Costs. *Environ. Sci. Technol.* **46**, 7857–7864 (2012).

112. Köberle, A. C., Gernaat, D. E. H. J. & van Vuuren, D. P. Assessing current and

future techno-economic potential of concentrated solar power and photovoltaic electricity generation. *Energy* **89**, 739–756 (2015).

113. Hoes, O. A. C., Meijer, L. J. J., Ent, R. J. van der & Giesen, N. C. van de. Systematic high-resolution assessment of global hydropower potential. *PLOS ONE* **12**, e0171844 (2017).

114. Deng, Y. Y. *et al.* Quantifying a realistic, worldwide wind and solar electricity supply. *Global Environmental Change* **31**, 239–252 (2015).

115. U.S. Energy Information Administration (EIA). https://www.eia.gov/international/data/world/electricity/electricity-consumption.

116. Shaner, M. R., Davis, S. J., Lewis, N. S. & Caldeira, K. Geophysical constraints on the reliability of solar and wind power in the United States. *Energy Environ. Sci.* **11**, 914–925 (2018).

117. Tong, D. *et al.* Geophysical constraints on the reliability of solar and wind power worldwide. *Nat Commun* **12**, 6146 (2021).

118. Oakleaf, J. R. *et al.* Mapping global development potential for renewable energy, fossil fuels, mining and agriculture sectors. *Scientific Data* **6**, 101 (2019).

119. UNFCCC. https://unfccc.int/news/global-energy-interconnection-is-crucial-for-paris-goals (2018).

120. International Energy Agency. *Electricity Market Report - July 2021*. https://www.iea.org/reports/electricity-market-report-july-2021 (2021).

121. Brinkerink, M., Gallachóir, B. Ó. & Deane, P. A comprehensive review on the benefits and challenges of global power grids and intercontinental interconnectors. *Renewable and Sustainable Energy Reviews* **107**, 274–287 (2019).

122. International Energy Agency. *Electricity Market Report-December 2020*. https://www.iea.org/reports/electricity-market-report-december-2020/2020-global-overview-trade (2020).

123. Guo, F. *et al.* Implications of intercontinental renewable electricity trade for energy systems and emissions. *Nat Energy* 1–13 (2022) doi:10.1038/s41560-022-01136-0.

124. Zhao, X. *et al.* Technical and economic demands of HVDC submarine cable technology for Global Energy Interconnection. *Global Energy Interconnection* **3**, 120–127 (2020).

125. Child, M., Kemfert, C., Bogdanov, D. & Breyer, C. Flexible electricity generation, grid exchange and storage for the transition to a 100% renewable energy system in Europe. *Renewable Energy* **139**, 80–101 (2019).

126. Barasa, M., Bogdanov, D., Oyewo, A. S. & Breyer, C. A cost optimal resolution for Sub-Saharan Africa powered by 100% renewables in 2030. *Renewable and Sustainable Energy Reviews* **92**, 440–457 (2018).

127. Bogdanov, D. & Breyer, C. North-East Asian Super Grid for 100% renewable energy supply: Optimal mix of energy technologies for electricity, gas and heat supply options. *Energy Conversion and Management* **112**, 176–190 (2016).

128. Aghahosseini, A., Bogdanov, D. & Breyer, C. Towards sustainable development in the MENA region: Analysing the feasibility of a 100% renewable electricity system in 2030. *Energy Strategy Reviews* **28**, 100466 (2020).

129. IEA. *World Energy Outlook 2019*. https://www.iea.org/reports/world-energy-outlook-2019 (2019).

130. Bogdanov, D. *et al.* Radical transformation pathway towards sustainable electricity

via evolutionary steps. *Nature Communications* **10**, 1077 (2019).

131. Interagency Working Group. *Technical Support Document: Social Cost of Carbon, Methane, and Nitrous Oxide Interim Estimates under Executive Order 13990*. https://www.whitehouse.gov/wp-content/uploads/2021/02/TechnicalSupportDocument_SocialCostofCarbonMethaneNitrousOxide.pdf (2021).

132. Ji, L., Jia, X., Chiu, A. S. F. & Xu, M. Global Electricity Trade Network: Structures and Implications. *PLOS ONE* **11**, e0160869 (2016).

133. Battaglini, A., Lilliestam, J., Haas, A. & Patt, A. Development of SuperSmart Grids for a more efficient utilisation of electricity from renewable sources. *Journal of Cleaner Production* **17**, 911–918 (2009).

134. Zickfeld, F., Wieland, A., Blohmke, J., Sohm, M. & Yousef, A. *Perspectives on a Sustainable Power System for EUMENA*. https://dii-desertenergy.org/wp-content/uploads/2016/12/DPP_2050_Study.pdf (2012).

135. Gulagi, A., Bogdanov, D., Fasihi, M. & Breyer, C. Can Australia Power the Energy-Hungry Asia with Renewable Energy? *Sustainability* **9**, 233 (2017).

136. Ralph, N. & Hancock, L. Energy security, transnational politics, and renewable electricity exports in Australia and Southeast Asia. *Energy Research & Social Science* **49**, 233–240 (2019).

137. Wu, G. C. *et al.* Strategic siting and regional grid interconnections key to low-carbon futures in African countries. *PNAS* **114**, E3004–E3012 (2017).

138. Protected Planet. Marine Protected Areas. https://www.protectedplanet.net/en/thematic-areas/marine-protected-areas.

139. National Snow and Ice Data Center. Data. *National Snow and Ice Data Center* https://nsidc.org/data.

140. Denholm, P., Hand, M., Jackson, M. & Ong, S. *Land Use Requirements of Modern Wind Power Plants in the United States*. (2009).

141. Ong, S., Campbell, C., Denholm, P., Margolis, R. & Heath, G. *Land-Use Requirements for Solar Power Plants in the United States*. (2013).

142. Gagnon, P., Margolis, R., Melius, J., Phillips, C. & Elmore, R. *Rooftop Solar Photovoltaic Technical Potential in the United States. A Detailed Assessment*. (2016).

143. Akbari, H., Menon, S. & Rosenfeld, A. Global cooling: increasing world-wide urban albedos to offset CO2. *Climatic Change* **94**, 275–286 (2009).

144. Global Solar Atlas. https://globalsolaratlas.info/map.

145. Global Wind Atlas. https://globalwindatlas.info.

146. Chowdhury, A. F. M. K. *et al.* Enabling a low-carbon electricity system for Southern Africa. *Joule* **6**, 1826–1844 (2022).

147. Energy Information Administration (EIA). https://www.eia.gov/international/data/world/electricity/electricity-capacity.

148. Brinkerink, M., Gallachóir, B. Ó. & Deane, P. Building and Calibrating a Country-Level Detailed Global Electricity Model Based on Public Data. *Energy Strategy Reviews* **33**, 100592 (2021).

149. NREL. 2022 Annual Technology Baseline. https://atb.nrel.gov/electricity/2022/data.

150. Hall, O., Bustos, M. F. A., Olén, N. B. & Niedomysl, T. Population centroids of the world administrative units from nighttime lights 1992-2013. *Sci Data* **6**, 235 (2019).

151. Monthly Electricity Statistics - Data product. *IEA* https://www.iea.org/data-and-

statistics/data-product/monthly-electricity-statistics.

152. IEA. World Energy Outlook 2020. www.iea.org/reports/world-energy-outlook-2020 (2020).

153. IRENA. *Innovation Landscape: Regional Markets*. (2019).

154. Medgrid. http://www.medgrid-psm.com/en/.

155. European Union. The North Seas Energy Cooperation. *European Commission* https://ec.europa.eu/energy/topics/infrastructure/high-level-groups/north-seas-energy-cooperation_en.

156. Patterson, W. Why an Asian super grid is a political fantasy. https://chinadialogue.net/en/energy/8973-why-an-asian-super-grid-is-a-political-fantasy/.

157. IRENA. *Innovation Landscape Brief: Supergrids*. https://www.irena.org/-/media/Files/IRENA/Agency/Publication/2019/Sep/IRENA_Supergrids_2019.pdf (2019).

158. Ueckerdt, F. *et al.* Potential and risks of hydrogen-based e-fuels in climate change mitigation. *Nat. Clim. Chang.* **11**, 384–393 (2021).

159. Odenweller, A., Ueckerdt, F., Nemet, G. F., Jensterle, M. & Luderer, G. Probabilistic feasibility space of scaling up green hydrogen supply. *Nat Energy* **7**, 854–865 (2022).

160. Vandewalle, J., Bruninx, K. & D'haeseleer, W. Effects of large-scale power to gas conversion on the power, gas and carbon sectors and their interactions. *Energy Conversion and Management* **94**, 28–39 (2015).

161. Yilmaz, H. Ü., Kimbrough, S. O., van Dinther, C. & Keles, D. Power-to-gas: Decarbonization of the European electricity system with synthetic methane. *Applied*

*Energy* **323**, 119538 (2022).

162. Fogel, S. *et al.* SNG based energy storage systems with subsurface CO 2 storage. *Energy Advances* **1**, 402–421 (2022).

163. Neumann, F., Zeyen, E., Victoria, M. & Brown, T. The potential role of a hydrogen network in Europe. *Joule* (2023) doi:10.1016/j.joule.2023.06.016.

164. Crippa, M. *et al.* GHG emissions of all world countries–2021 Report. *Publication Office of the European Union, Luxembourg* (2021).

165. Wu, R. *et al.* Air quality and health benefits of China's emission control policies on coal-fired power plants during 2005–2020. *Environ. Res. Lett.* **14**, 094016 (2019).

166. Tong, D. *et al.* Health co-benefits of climate change mitigation depend on strategic power plant retirements and pollution controls. *Nat. Clim. Chang.* 1–7 (2021) doi:10.1038/s41558-021-01216-1.

167. He, G. *et al.* Enabling a Rapid and Just Transition away from Coal in China. *One Earth* **3**, 187–194 (2020).

168. National Bureau of Statistics. National Data. https://data.stats.gov.cn.

169. Abhyankar, N. *et al.* Achieving an 80% carbon-free electricity system in China by 2035. *iScience* **25**, 105180 (2022).

170. Zhang, X. *et al.* Immediate actions on coal phaseout enable a just low-carbon transition in China's power sector. *Applied Energy* **308**, 118401 (2022).

171. Pai, S., Emmerling, J., Drouet, L., Zerriffi, H. & Jewell, J. Meeting well-below 2°C target would increase energy sector jobs globally. *One Earth* **4**, 1026–1036 (2021).

172. Zhou, S. *et al.* China's power transformation may drastically change employment patterns in the power sector and its upstream supply chains. *Environ. Res. Lett.* **17**,

065005 (2022).

173. Carley, S. & Konisky, D. M. The justice and equity implications of the clean energy transition. *Nat Energy* **5**, 569–577 (2020).

174. Kime, S., Jacome, V., Pellow, D. & Deshmukh, R. Evaluating equity and justice in low-carbon energy transitions. *Environ. Res. Lett.* **18**, 123003 (2023).

175. Larson, E. *Net-Zero America: Potential Pathways, Infrastructure, and Impacts*. (Princeton University, 2020).

176. Bao, C. & Fang, C. Geographical and environmental perspectives for the sustainable development of renewable energy in urbanizing China. *Renewable and Sustainable Energy Reviews* **27**, 464–474 (2013).

177. Wang, C. *et al.* Mapping potentials and bridging regional gaps of renewable resources in China. *Renewable and Sustainable Energy Reviews* **134**, 110337 (2020).

178. Wu, R. *et al.* Reduced-complexity air quality intervention modeling over China: the development of InMAPv1.6.1-China and a comparison with CMAQv5.2. *Geoscientific Model Development* **14**, 7621–7638 (2021).

179. van Soest, H. L., den Elzen, M. G. J. & van Vuuren, D. P. Net-zero emission targets for major emitting countries consistent with the Paris Agreement. *Nat Commun* **12**, 2140 (2021).

180. NDRC. Promoting Supply-side Structural Reform, Preventing Over Capacity of Coal-fired Power Generation (in Chinese). http://nea.gov.cn/136525062_15026980991471n.pdf.

181. National Bureau of Statistics. Classification of regions in China. http://www.stats.gov.cn/ztjc/zthd/sjtjr/dejtjkfr/tjkp/201106/t20110613_71947.htm.

182. Linking Climate and Development Policies – Leveraging International Networks and Knowledge Sharing. www.cd-links.org.

183. Mileva, A. *et al.* blue-marble/gridpath: GridPath v0.14.1. Zenodo https://doi.org/10.5281/zenodo.6678436 (2022).

184. Luo, Q. *et al.* The Health and Climate Benefits of Economic Dispatch in China's Power System. *Environ. Sci. Technol.* **57**, 2898–2906 (2023).

185. He, G. *et al.* SWITCH-China: A Systems Approach to Decarbonizing China's Power System. *Environ. Sci. Technol.* **50**, 5467–5473 (2016).

186. Global Energy Monitor. Global Coal Plant Tracker. *Global Energy Monitor* https://globalenergymonitor.org/projects/global-coal-plant-tracker/.

187. He, G. *et al.* Rapid cost decrease of renewables and storage accelerates the decarbonization of China's power system. *Nat Commun* **11**, 2486 (2020).

188. Global Energy Monitor. Global Hydropower Tracker. *Global Hydropower Tracker* https://globalenergymonitor.org/projects/global-hydropower-tracker/.

189. State Grid. *2017 Corporate Social Responsibility Report.* http://www.sgcc.com.cn/html/files/2018-08/29/20180829165036376453337.pdf (2018).

190. China Southern Power Grid. *2018 Corporate Social Responsibility Report*. http://www.csg.cn/shzr/zrbg/201905/P020190522368094315882.pdf (2019).

191. China Electric Power Enterprise Federation. *2020 China Electric Power Yearbook.* (China Electric Power Press, Beijing, 2020).

192. Zhuo, Z. *et al.* Cost increase in the electricity supply to achieve carbon neutrality in China. *Nat Commun* **13**, 3172 (2022).

193. National Renewable Energy Laboratory. 2021 Annual Technology Baseline data.

https://atb.nrel.gov/electricity/2021/data.

194. Electric Power Planning Design General Institute & Water Conservancy Hydropower Planning Design General Institute. *Grid Project Construction Cost Analysis in the 12th Five-Year Period (in Chinese)*. (2017).

195. Garrett-Peltier, H. Green versus brown: Comparing the employment impacts of energy efficiency, renewable energy, and fossil fuels using an input-output model. *Economic Modelling* **61**, 439–447 (2017).

196. Zheng, H. *et al.* Regional determinants of China's consumption-based emissions in the economic transition. *Environ. Res. Lett.* **15**, 074001 (2020).

197. National Renewable Energy Laboratory. Jobs & Economic Development Impact Models. https://www.nrel.gov/analysis/jedi/.

198. Chen, Y. Renewable energy investment and employment in China. *International Review of Applied Economics* **33**, 314–334 (2019).

199. Department of Population and Employment Statistics, National Bureau of Statistics. *China Labour Statistical Yearbook*. (China Statistics Press, Beijing, 2018).

200. Ram, M., Aghahosseini, A. & Breyer, C. Job creation during the global energy transition towards 100% renewable power system by 2050. *Technological Forecasting and Social Change* **151**, 119682 (2020).

201. US Bureau of Labor Statistics. Quarterly Census of Employment and Wages. https://www.bls.gov/cew/.

202. Tessum, C. W., Hill, J. D. & Marshall, J. D. InMAP: A model for air pollution interventions. *PLOS ONE* **12**, e0176131 (2017).

203. Yang, H. *et al.* Air quality and health impacts from the updated industrial emission

standards in China. *Environ. Res. Lett.* **14**, 124058 (2019).

204. Dockery, D. W. *et al.* An Association between Air Pollution and Mortality in Six U.S. Cities. *New England Journal of Medicine* **329**, 1753–1759 (1993).

205. Yin, P. *et al.* Long-term Fine Particulate Matter Exposure and Nonaccidental and Cause-specific Mortality in a Large National Cohort of Chinese Men. *Environmental Health Perspectives* **125**, 117002.

206. Institute for Health Metrics and Evaluation. Global health data exchange. https://ghdx.healthdata.org/gbd-results-tool.

207. Center for International Earth Science Information Network - CIESIN - Columbia University. *Gridded Population of the World, Version 4 (GPWv4): Population Count, Revision 11*. (NASA Socioeconomic Data and Applications Center (SEDAC), Palisades, NY, 2018).

208. US EPA. Mortality Risk Valuation. https://www.epa.gov/environmental-economics/mortality-risk-valuation (2014).

209. Departmental Guidance on Valuation of a Statistical Life in Economic Analysis | US Department of Transportation. https://www.transportation.gov/office-policy/transportation-policy/revised-departmental-guidance-on-valuation-of-a-statistical-life-in-economic-analysis.

210. Tang, R. *et al.* Air quality and health co-benefits of China's carbon dioxide emissions peaking before 2030. *Nat Commun* **13**, 1008 (2022).

211. China National Coal Association. A short analysis of coal production at the provincial level in 2022 (in Chinese). http://www.coalchina.org.cn/index.php?m=content&c=index&a=show&catid=10&id=1

45621.

212. UNFCCC. Nationally Determined Contributions Registry. https://unfccc.int/NDCREG.

213. Hertwich, E. G. *et al.* Integrated life-cycle assessment of electricity-supply scenarios confirms global environmental benefit of low-carbon technologies. *Proceedings of the National Academy of Sciences* **112**, 6277–6282 (2015).

214. State Council. Notice of the State Council on Issuing the '14th Five-Year Plan' Employment Promotion Plan. http://www.gov.cn/zhengce/content/2021-08/27/content_5633714.htm (2021).

215. Hu, J. *et al.* Premature Mortality Attributable to Particulate Matter in China: Source Contributions and Responses to Reductions. *Environ. Sci. Technol.* **51**, 9950–9959 (2017).

216. Gao, M. *et al.* The impact of power generation emissions on ambient PM2.5 pollution and human health in China and India. *Environment International* **121**, 250–259 (2018).

217. REN21. *The Renewables 2020 Global Status Report*. (2020).

218. Sepulveda, N. A., Jenkins, J. D., de Sisternes, F. J. & Lester, R. K. The Role of Firm Low-Carbon Electricity Resources in Deep Decarbonization of Power Generation. *Joule* **2**, 2403–2420 (2018).

219. Safaei, H. & Keith, D. W. How much bulk energy storage is needed to decarbonize electricity? *Energy Environ. Sci.* **8**, 3409–3417 (2015).

220. Shaner, M. R., Davis, S. J., Lewis, N. S. & Caldeira, K. Geophysical constraints on the reliability of solar and wind power in the United States. *Energy Environ. Sci.* **11**,

914–925 (2018).

221. Sepulveda, N. A., Jenkins, J. D., Edington, A., Mallapragada, D. S. & Lester, R. K. The design space for long-duration energy storage in decarbonized power systems. *Nat Energy* **6**, 506–516 (2021).

222. Le, T. S., Nguyen, T. N., Bui, D.-K. & Ngo, T. D. Optimal sizing of renewable energy storage: A techno-economic analysis of hydrogen, battery and hybrid systems considering degradation and seasonal storage. *Applied Energy* **336**, 120817 (2023).

223. Dowling, J. A. *et al.* Role of Long-Duration Energy Storage in Variable Renewable Electricity Systems. *Joule* **4**, 1907–1928 (2020).

224. Gawlick, J. & Hamacher, T. Impact of coupling the electricity and hydrogen sector in a zero-emission European energy system in 2050. *Energy Policy* **180**, 113646 (2023).

225. Lin, H. *et al.* Economic and technological feasibility of using power-to-hydrogen technology under higher wind penetration in China. *Renewable Energy* **173**, 569–580 (2021).

226. Pan, G. *et al.* Cost and low-carbon competitiveness of electrolytic hydrogen in China. *Energy & Environmental Science* **14**, 4868–4881 (2021).

227. Li, J., Zou, W., Yang, Q. & Bao, H. Towards net-zero smart system: An power synergy management approach of hydrogen and battery hybrid system with hydrogen safety consideration. *Energy Conversion and Management* **263**, 115717 (2022).

228. Wang, J. *et al.* Role of electrolytic hydrogen in smart city decarbonization in China. *Applied Energy* **336**, 120699 (2023).

229. Zhang, D. *et al.* Spatially resolved land and grid model of carbon neutrality in China. *Proceedings of the National Academy of Sciences* **121**, e2306517121 (2024).

230. Fan, J.-L. *et al.* A net-zero emissions strategy for China's power sector using carbon-capture utilization and storage. *Nat Commun* **14**, 5972 (2023).

231. Wang, Y. *et al.* Accelerating the energy transition towards photovoltaic and wind in China. *Nature* **619**, 761–767 (2023).

232. National Development and Reform Commission & National Energy Agency. 14th Five-year plan for renewable energy development (in Chinese). https://www.nea.gov.cn/1310524241_16479412513081n.pdf.

233. Zhu, S. *et al.* Site selection evaluation for salt cavern hydrogen storage in China. *Renewable Energy* **224**, 120143 (2024).

234. Fan, J.-L. *et al.* Carbon reduction potential of China's coal-fired power plants based on a CCUS source-sink matching model. *Resources, Conservation and Recycling* **168**, 105320 (2021).

235. Chowdhury, A. F. M. K. *et al.* Enabling a low-carbon electricity system for Southern Africa. *Joule* **6**, 1826–1844 (2022).

236. Yang, H., Deshmukh, R. & Suh, S. Global transcontinental power pools for low-carbon electricity. *Nat Commun* **14**, 8350 (2023).

237. Data | Electricity | 2023 | ATB | NREL. https://atb.nrel.gov/electricity/2023/data.

238. The Danish Energy Agency. Technology Catalogues. https://ens.dk/en/our-services/projections-and-models/technology-data.

239. Irlam, L. *Global Costs of Carbon Capture and Storage*. https://www.globalccsinstitute.com/archive/hub/publications/201688/global-ccs-cost-updatev4.pdf (2017).

240. International Energy Agency & Administrative Center for China's Agenda 21.

*Opportunities for Hydrogen Production with CCUS in China*. (OECD, 2022). doi:10.1787/78fc9e85-en.

241. Peng, T. *et al.* Choice of hydrogen energy storage in salt caverns and horizontal cavern construction technology. *Journal of Energy Storage* **60**, 106489 (2023).

242. Wei, X. *et al.* Carbon and energy storage in salt caverns under the background of carbon neutralization in China. *Energy* **272**, 127120 (2023).

243. Caglayan, D. G. *et al.* Technical potential of salt caverns for hydrogen storage in Europe. *International Journal of Hydrogen Energy* **45**, 6793–6805 (2020).

244. Huang, L. *et al.* Effect of the Fukushima nuclear accident on the risk perception of residents near a nuclear power plant in China. *Proceedings of the National Academy of Sciences* **110**, 19742–19747 (2013).

245. Yang, H. *et al.* Regional disparities in health and employment outcomes of China's transition to a low-carbon electricity system. *Environ. Res.: Energy* **1**, 025001 (2024).

246. China - Countries & Regions. *IEA* https://www.iea.org/countries/china/natural-gas.

247. Kuriqi, A., Pinheiro, A. N., Sordo-Ward, A., Bejarano, M. D. & Garrote, L. Ecological impacts of run-of-river hydropower plants—Current status and future prospects on the brink of energy transition. *Renewable and Sustainable Energy Reviews* **142**, 110833 (2021).

248. Brown, P. H. & Xu, K. Hydropower Development and Resettlement Policy on China's Nu River. in *China's Search for Energy Security* (Routledge, 2013).

249. Zhao, X., Wu, L. & Qi, Y. The energy injustice of hydropower: Development, resettlement, and social exclusion at the Hongjiang and Wanmipo hydropower stations in China. *Energy Research & Social Science* **62**, 101366 (2020).

250. Ren, M. *et al.* Enhanced food system efficiency is the key to China's 2060 carbon neutrality target. *Nat Food* **4**, 552–564 (2023).

251. McPherson, M., Johnson, N. & Strubegger, M. The role of electricity storage and hydrogen technologies in enabling global low-carbon energy transitions. *Applied Energy* **216**, 649–661 (2018).